Chapter 2. Part A: Synthesis and Study of Symmetrical aza[7] and aza[9]helicenes

2.1 Photocyclization: Useful strategy for the synthesis of aza[*n*]helicenes with regioselectivity challenge

Photocyclization is one of the most well-known and useful methods for the synthesis of different poly-nuclear hydrocarbons.[1] Under UV irradiation, stilbene and its derivatives undergo intramolecular cyclization to form dihydro phenanthrenes. In the presence of an oxidant the dihydro phenanthrene aromatizes to give polycyclic compounds. During the studies of photochemical isomerization of stillbene, the oxidative photocyclization method was developed.[2] Some unknown product was observed at the time of photo chemically induced *cis-trans* isomerization, which was later identified as phenanthrene by Parker and Spoerri.[3] Although the reaction is known in literature since 1934 but was not synthetically useful until Mallory and co workers[4] in 1962 discovered that iodine as an oxidant can catalyze the reaction better than O_2. The key step in the mechanism of the Mallory photocyclization is the formation of a trans dihydrophenanthrene (DHP) intermediate[5] **2** by an orbital symmetry allowed conrotatory electrocyclic closure. (**Scheme 2.1**) The intermediate dihydrophenanthene **2** is subsequently converted to phenanthrene by the abstraction of hydrogen by iodide radical generating HI.

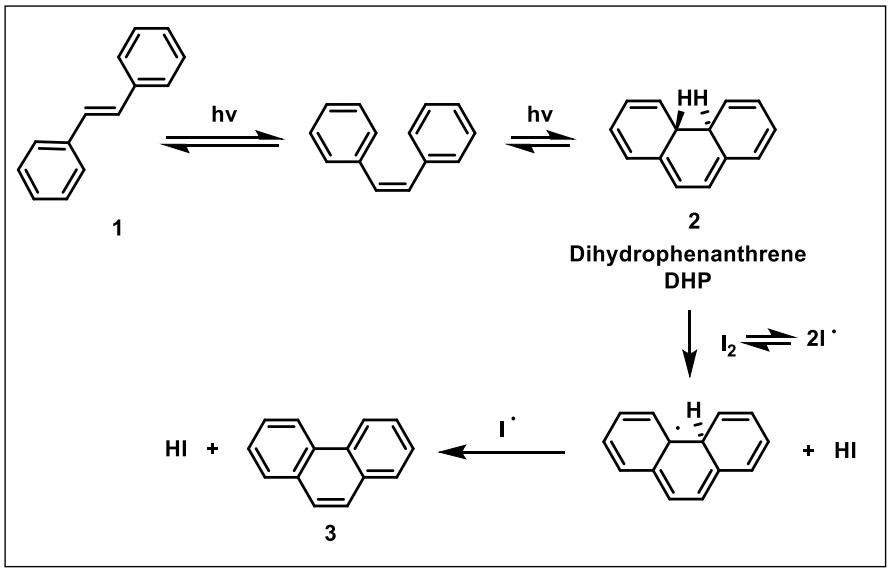

Scheme.2.1: Mechanism of Mallory photocyclization.

Although this procedure has been successfully applied to variety of substrates, its use has been limited by the formation of several byproducts, including hydrogen peroxide and hydrogen iodide, which can cause undesired side reactions, leading to poor yields.

To avoid these side reactions, Katz proposed the use of an excess of propylene oxide which can trap troublesome HI by-product.[6] Our lab has been actively involved in the chemistry of photocyclization and we have reported a cheaper alternative of propylene oxide by demonstrating the use of THF as acid scavenger. [7] This method has an added advantage of higher boiling point of THF than propylene oxide which proved to be more practical in the photocyclization reactions which require longer time. Recently an improved methodology has been reported where potassium iodide was used instead of iodine to mediate oxidative photocyclization.[8] The first example for the synthesis of helical molecules using oxidative photo cyclodehydrogenation was reported in 1967 by Martin *et al.*[9] and even today photocyclization is considered to be the method of choice for the preparation of helicenes ranging from 4 to 16 rings.[10]

2.2 Regioselectivity of photocyclization:

Regioselectivity is a crucial factor in the photocyclization of helical molecules. Naturally every molecule has a favorable choice among planar less sterically hindered aromatic hydrocarbon over the sterically more demanding non planar helical isomers. In order to get the desired outcome from the photocyclization experiments it becomes very important to understand the factors that control the regioselectivity. Martin *et al.*[9] carried out photocyclization of compound **4** in presence of iodine and observed only the angular regiomer **6** was formed during this reaction and no linear compound **7** was observed (**Scheme 2.2**). Laarhoven *et al.*[11] studied photocyclization of various stillbene precursors. In order to predict the regioselectivity, he carried out simple Huckel calculations and determined free valence electron of the excited state. Laarhoven has calculated reactivity parameters like free valence numbers ($\sum F^* rs$) and localization energies ($\sum L^* rs$) for a large number of examples. He found a good correlation between these two parameters, but the free valence numbers are more convenient and are enough to predict all the cyclization modes of a particular compound. Three rules for cyclization were determined:

1. Photocyclization do not occur when $\sum F^* rs < 0.1$.
2. When two or more cyclization are possible in a particular compound, only one product arises if $\Delta(\sum F^* rs) > 0.1$; more products are formed if the differences are smaller.

3. The second rule holds when only planar or non-planar products (penta or higher helicenes) can arise. When planar as well as non-planar products can be formed, the planar aromatic in general is the main product, provided that for its formation $\sum F * rs > 1.0$.

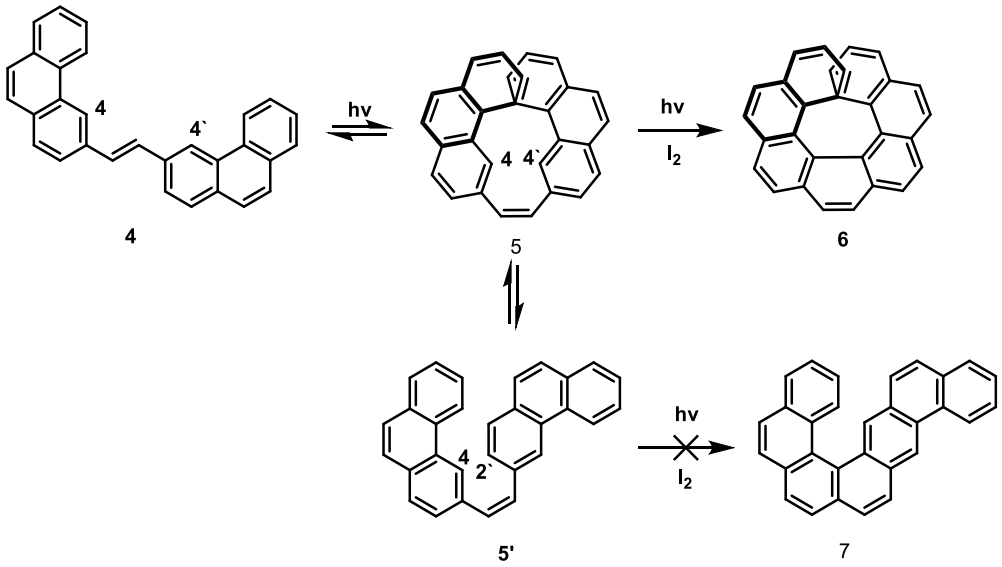

Scheme 2.2: Regioselectivity in the synthesis of [7]helicene by photocyclization.

These rules suggest that the control of regioselectivity depends on the two contradicting forces, steric effects and electronic factors. Provided the steric factors are not very severe; the electronic factors (stability of the free radicals at the site of cyclization or the stability of the intermediate) control the fate of cyclization, predominantly gives the angularly cyclized products.

Many synthetic schemes were tested on the basis of these relationships; the strategies of the syntheses may be optimized when the substitution at the alkene double bond is chosen in the right way. When compound **8** having multiple sites for possible photocyclization is irradiated, the [6]helicene **9** is obtained in low yields (22%) while compound **10** is isolated as major product (55%) (**Scheme 2.3**).[11b] The helicene **9** resulted from C-C bond formation in positions 4 and 1' while **10** is generated by the formation of a C-C bond in positions 2 and 1'. Compounds **11** and **12** resulting from C-C formation in positions 2–3`and 4–3` are not formed during photocyclization. Only position 1 of the naphthalene moiety is reactive enough. The corresponding sums of the free valence numbers for the excited state have the following values $\sum F^*_{2,3'} = 0.916$; $\sum F^*_{4,3'} = 1.020$; $\sum F^*_{2,1'} = 1.083$; $\sum F^*_{4,1'} = 1.187$.

Helicene **9** is obtained in high yield when the structure of starting alkene **13** is modified and subjected to the reaction under the same conditions. Only position 1 of the benzophenanthrene moiety is reactive. In this case, the sums of the free valence numbers for the excited state have the following values $\sum F^*_{3,2'} = 0.955$; $\sum F^*_{1,2'} = 1.117$. Often a simple phenyl moiety on one end of the alkene is favorable for helicene synthesis. One of the reasons for this is the symmetrical nature of that portion of alkene.

Despite these rules of Laarhoven it is still difficult to predict and control the regiochemical outcome of the photocyclization reactions. Hence researchers have developed different approaches to produce products with desired regioslectivity. Some of the strategies to control the regioselective product formation in photocyclization are outlined here.

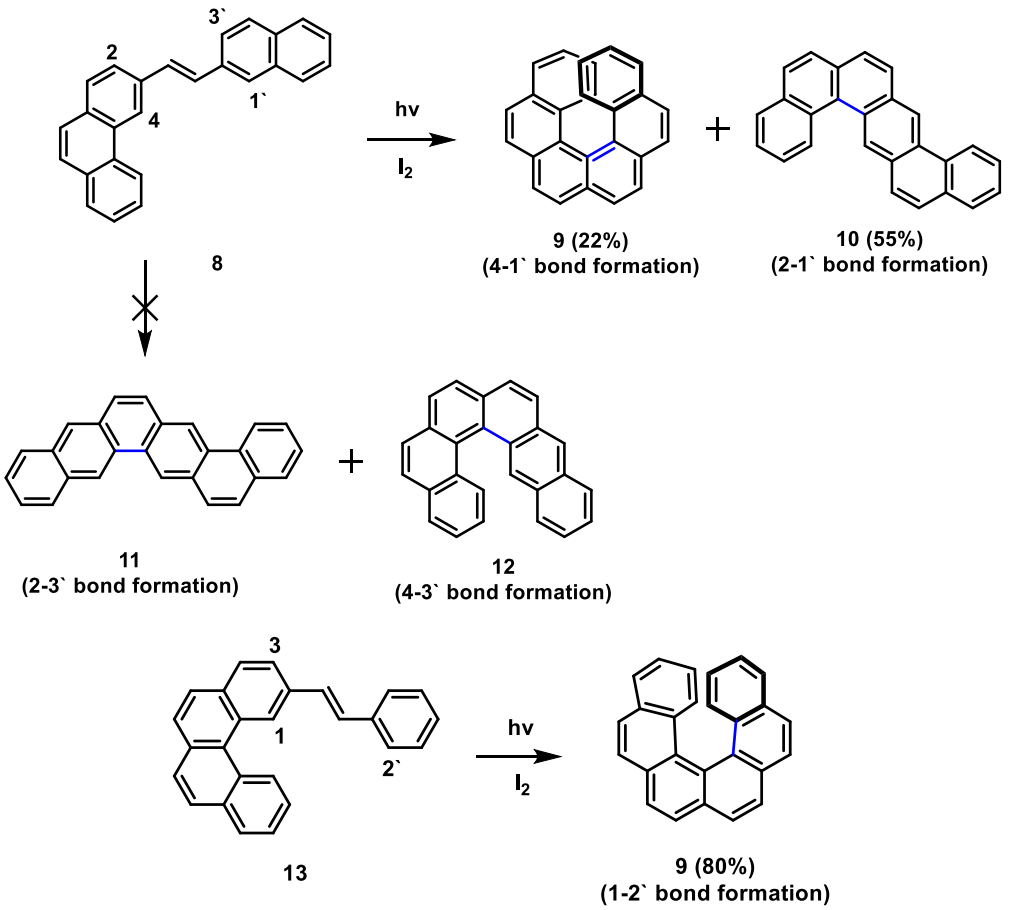

Scheme 2.3: Synthesis of [6]helicene by structural modification.

2.2.1 Controlling angular product formation using blocking groups:

Laarhoven rules predict accurately while synthesizing smaller helical molecules (Up to five membered helicenes due to their planar nature). Larger helicene (> 5 membered) no longer remain planar and linear S shaped molecule becomes the main side product of photocyclization To overcome this problem Katz *et al.*[12] developed a method in which bromo substituent act as blocking agent or as a directing group for the synthesize of angularly cyclized product. This is a very effective strategy and successfully used for many of the synthetic schemes to overcome the regioselectivity problems. When compound **14** was subjected to photocyclization the bulky bromo group directs the photocyclization giving exclusively angularly cyclized product.

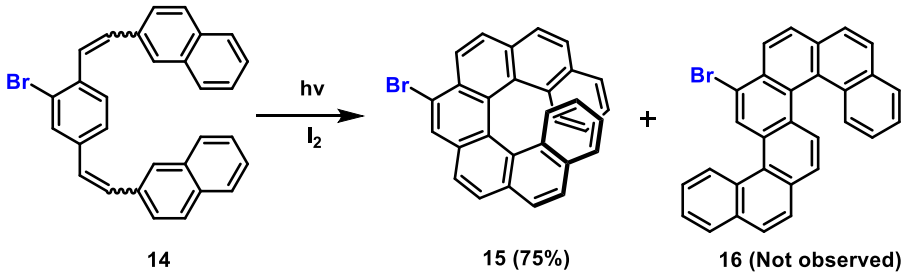

Scheme 2.4: Synthesis of angularly cyclized [7]helicene using bromo as blocking group (Katz strategy)

2.2.2 By choosing proper olefin precursor:

This strategy is based on the Laarhoven's concept of free valence electron count. A representative example is already discussed in **scheme 2.3**. Mostly the strategy is very effective in smaller helicenes. The final outcome depends on the balance between steric and electronic factors. Recently a very striking example of choosing the correct olefin precursor has been beautifully shown by Fujita *et al.*[10]. By careful selection of olefin they were able to synthesize largest ([16]helicene) in a single step. The success of the strategy relies on the thorough literature review which suggests the kind of fragments in the precursor and their photochemical output.

They, avoided the simple [1]+[1]+[1] and [2]+[2] sequences in the precursor to eliminate the possible formation of an unfavorable [5]helicene framework that is very well known to furhur oxidize into benzoperylene (**Scheme 2.5a**).[14] The [2]+[1]+[2] sequence was also avoided because it has been known to give predominantly planar dinaphthanthracene rather than the expected [7]helicene (**Scheme 2.5c**).[15]

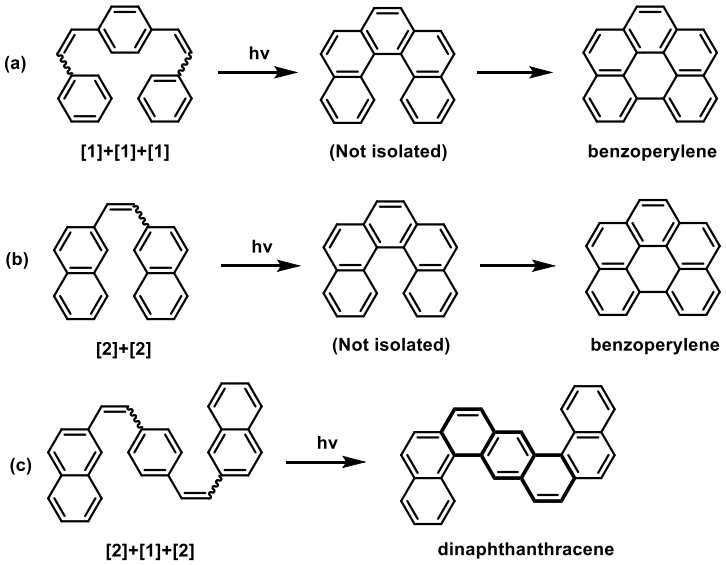

Scheme 2.5: Major unfavorable side reactions during different combinations of starting olefin precursor

Based on these considerations, they designed the following guideline for the synthesis of the precursor olefins: [2] units must be separated by two [1] units. Namely, only [2]+[1]+[1]+[2]+[1]+[1]+[2]sequences can undergo multiple oxidative photocyclizations without undesirable formation of benzoperylene or anthracene. (**Scheme 2.6**)

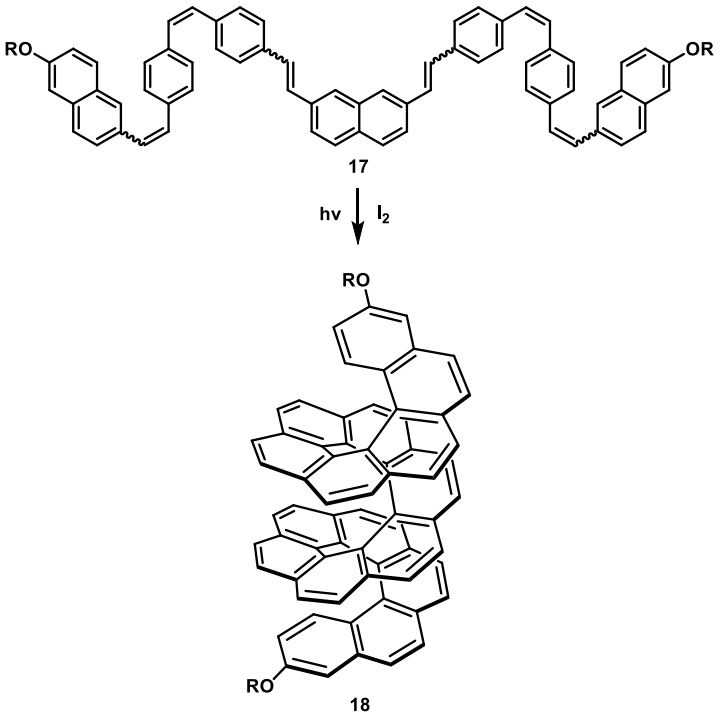

Scheme 2.6: Synthesis of [16]helicene by careful design of olefin precursor.

2.2.3 Effect of temperature:

Clennan *et al.*[16] carried out a detailed computational and experimental study to understand role of temperature on the regioselectivity of bis styryl derivatives. They synthesized four bis styryl derivatives and observed the outcome of photocyclization at different temperatures. They observed that at high temperature, thermodynamically more stable planar **23** product was the major product while at the lower temperature helicenes **21** are the major products (**Scheme 2.7**).

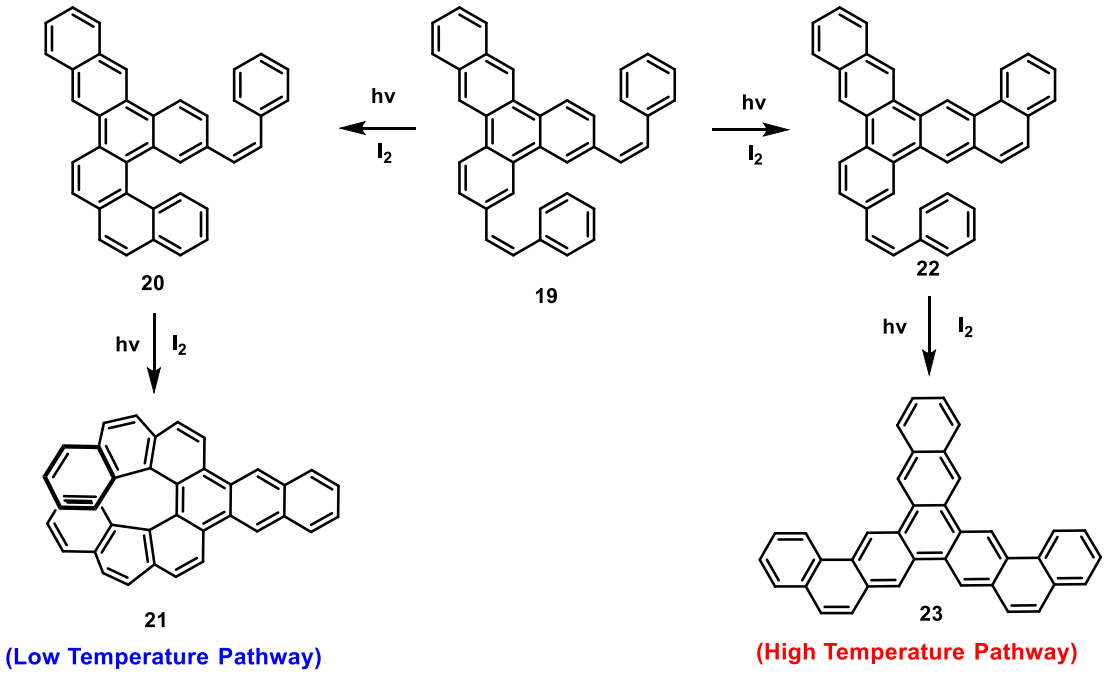

Scheme 2.7: Effect of temperature on the regioselectivity of photocyclization.

These explained observations on the basis of stability of intermediate dihydrophenanthrenes (DHP) and the magnitude of their extinction coefficients. Calculations suggest that the extinction coefficient of DHP precursor of helicenes was smaller than the planar regiomers also the thermal decomposition of the intermediates was suppressed at the low temperature. These combined effects cause higher population of helicene intermediate at lower temperature giving higher angularly cyclized product. By carefully choosing the precursor and optimizing temperature, the yield of desired angularly cyclized product can be increased.

Some other experimental parameters which can influence the extent of regioselectivity includes, the concentrations of the oxidant (e.g. I_2, O_2) and substrate, wavelength distribution of the incident light, choice of the solvent and temperature.[17] Majority of

these studies were carried out on simple substituted stillbene, and therefore it is very important to understand the role of these variables on the synthesis of larger helical molecules. By controlling these, the shortcoming of Mallory reaction can be addressed. Any contribution in this direction will surely be of very high value in photocyclization chemistry.

2.3 Synthesis and study of mono aza[7]helicenes:

2.3.1 Strategies for incorporation of *N* in helicene framework and properties:

2.3.1.i. Oxidative photocyclization:

The oxidative photocyclization is among the most general methods to prepare aza[*n*]helicenes. In 2005, Caronna *et al.* used the classical oxidative photocyclization of stillbene derivatives using to obtain aza or diaza[5]helicenes.[18] The hetero nuclei nitrogen was placed at different positions of helical backbone; reactions were highly regioselective and of good yields. (**Scheme 2.8**)

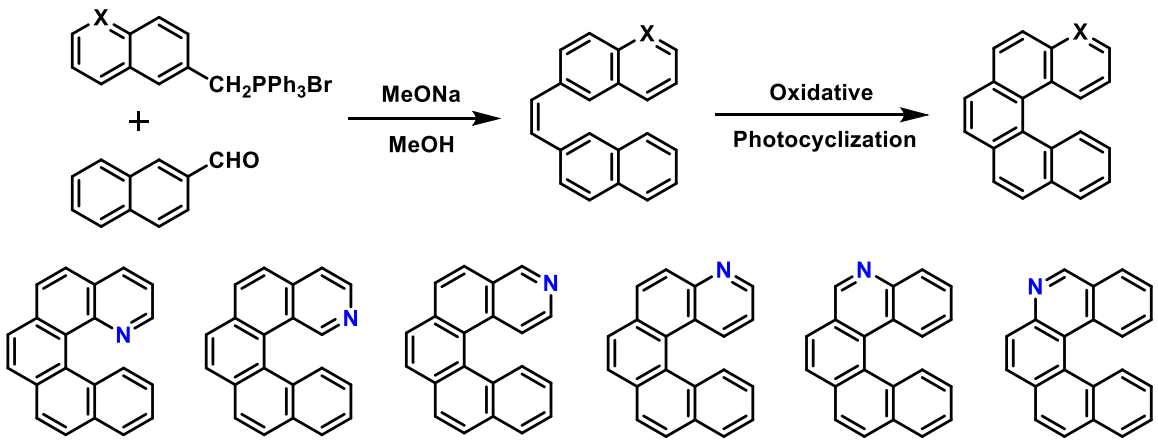

Scheme 2.8: Synthesis of various Mona aza[5]helicenes using oxidative photocyclization.

Aza[5]helicenes are good models to study racemization barrier, crystal structures and photo physical studies. Corrona *et al.* studied the racemization barriers of these aza[*n*]helicenes, their measurement confirms the lower activation barriers of aza[5]helicenes as compared to carbo[5]helicene. Similar conclusions were made by Stary and Stara group.[19] Daehen and co-workers also failed to resolve penta aza helicenes as they rapidly racemizes under ambient conditions.[20] The same oxidative photocyclization strategy was extended by Hassine for the synthesis of

aza[6]helicene.[21] (**Scheme 2.9**) HPLC separation of enantiomers was also carried out and the chiroptical properties of compound **25** were reported.

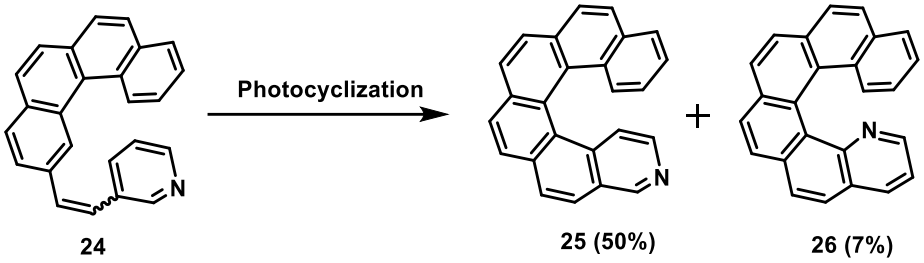

Scheme 2.9: Photochemical synthesis of aza[6]helicene.

Racemization barriers of **25** and **26** were also studied. Their racemization process was followed by HPLC over a Chiralcel OD-H column;[22] data show that 2-aza[6]helicene **25** behaves similarly to the parent [6]helicene , while 1-aza[6]- helicene **26** behaves in a different way. The considerably lower energy barrier to racemization of **26** reflects the smaller steric repulsion between the lone pair of electrons on *N*(1) and the proton attached to C-16. The proton affinities (PAs) of **25** and **26**, respectively, were determined using mass spectrometry and DFT calculations.[23] PAs around 1000 kJ mol^{-1} showing that these azahelicenes are chiral superbases with affinities similar to "proton sponge" The unique helical topology and high proton affinities of are ideal qualities for using these molecules as enantioselective ligands. The synthesis of functionalised azahelicenes by photodehydrocyclisation of stilbene-type precursors points to the strength and versatility of this methodology even though not many examples of that have been published. Many derivatives of aza[n]helicenes have been prepared ranging from five membered to larger analogues.

2.3.1.ii. Non photochemical strategies:

The transition metal catalysed [2+2+2] cycloisomerisation of aromatic triynes represents a new paradigm for the highly versatile nonphotochemical synthesis of helicenes.[24] It relies on a facile, convergent and modular assembly of aromatic triynes that can easily be cyclised to helicenes. Utilising this methodology, Stará, Starý *et al.* reported the practical syntheses of 1-aza[6]helicene **26** and 2-aza[6]helicene **31** (**Scheme 2.10**).[25] The Co(I) catalysed [2+2+2] cyclotrimerisation of aromatic pyridotriynes allowed building the helical scaffolds. Moreover, they succeeded in resolving racemates of **26** and **31** into enantiomers, assigning their absolute

configuration, determining the energy barriers to racemisation and obtaining X-ray structures of their corresponding silver complexes.

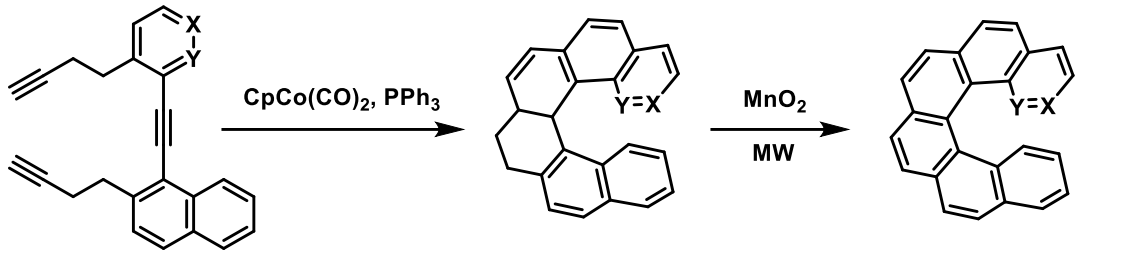

27 X=H, Y=N
28 X=N, Y=H

29 X=H, Y=N (82%)
30 X=N, Y=H (89%)

26 X=H, Y=N (65%)
31 X=N, Y=H (53%)

Scheme 2.10: Synthesis of aza helicenes using [2+2+2] cyclotrimerization.

Takenaka *et al.* devised a modular synthetic route to a series of 1-aza[5]- and [6]helicenes that is based on the key Stille-Kelly reaction to form an internal benzene ring of the helical backbone (**Scheme 2.11**).[26] Combining the benzo[*h*]quinoline-derived aldehyde **32** with the complementary benzyl-type phosphonium salt **33** allowed performing a highly *Z*-selective Wittig olefination to the aromatic dibromide **34**. Its reaction with hexamethyl ditin under Pd-catalysis led first to a monostannylated intermediate that underwent a spontaneous intramolecular Stille cross-coupling (the overall Stille-Kelly reaction) resulting in a benzo derivative of 1-aza[6]helicene **35** Two more derivatives aza[5]oxide and a variant of aza[6]oxides have also been synthesized in good yields. Racemic helicenes were subsequently transformed to *N*-oxides **36** using *m*-CPBA and their enantiomers were separated using chiral HPLC.

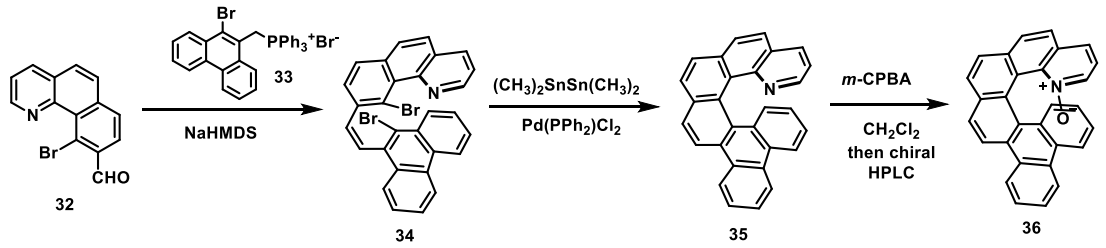

Scheme 2.11: Synthesis of enantiopure aza[n]oxide.

The helicene-*N*-oxides were tested as catalysts in the desymmetrization of *meso* epoxides with chlorosilanes, cis-stilbene epoxide reacted with $SiCl_4$ and gave the corresponding (*R,R*)-chlorohydrin with high ee values.

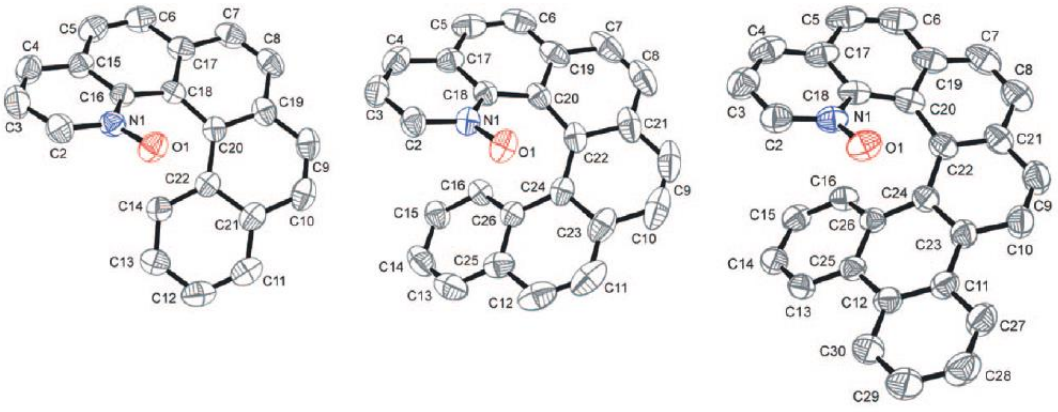

Figure 2.1: ORTEP view of different aza[*n*]oxides.[26]

Fuchter *et al.* developed a scalable and expedient route to 1-aza[6]helicene derivatives employing a Pt-catalysed alkyne-arene cycloisomerisation (Scheme 10).[27] It represents both the shortest and most practical synthesis of 1-aza[6]helicene. The conversion of alkyne-arene **37** to 1- aza[6]helicene **26** was found difficult but a successful protocol was finally developed employing $PtCl_4$ at elevated temperature (120 ^oC) to obtain **26** in good yield.

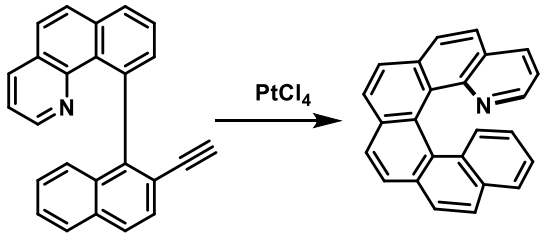

Scheme 2.12: Synthesis of 1 aza[6]helicene using alkene-alkyne-arene cycloisomerisation.

1-aza[6]helicene **26** has attracted many researcher to explore its applications in various fields. Fuchter, Campbell *et al.* prepared an organic field-effect transistor (OFET) based on 1-aza[6]helicene **26**.[28] Chiral transistor based on enantiopure **26** capable of discriminating right-handed and left-handed CP-light. It also showed excellent hole transporting properties. Interesting coordination behavior of compound **26** with different transition metal has been explored and showed some unusual properties which are useful for the development of light-emitting devices, chemosensors, photovoltaic dye-sensitized devices, etc. Stary *et al*. used racemic aza[6]helicenes **26** as *N* ligands for coordination, and 1:2 Ag(I) aza[6]helicene complexes were prepared and characterized by X-ray crystallography. They made with unique arrangement in solid

state.[29] Same group also observed preferential formation of homochiral Ag^+ complexes in gas phase. Their Pt complexes has been prepared and thoroughly studied showing unexpected reactivity difference between racemic and enantiopure Pt complexes.[30]

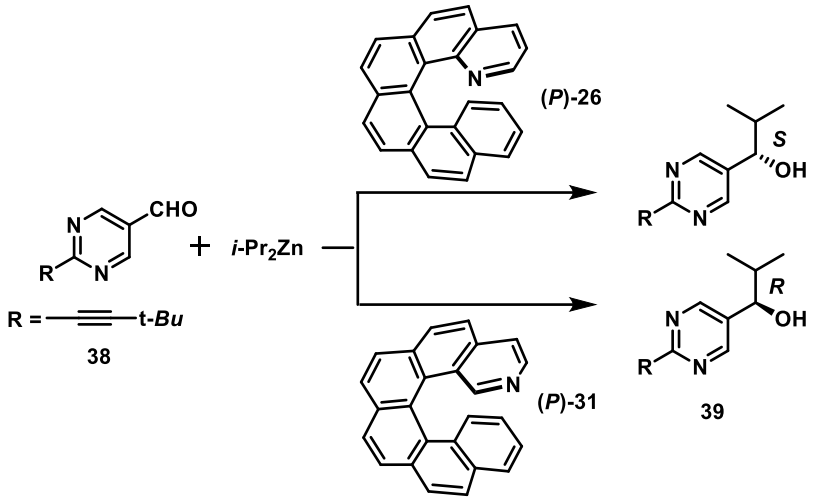

Scheme 2.13: Asymmetric autocatalysis with the reversal of enantioinduction.

In 2017, Soai reported the reversal of the sense of enantioselectivity between 1-aza[6]helicene **26** and 2-aza[6]helicenes **31**, used as chiral inducers of asymmetric autocatalysis during the addition of diisopropyl-zinc to pyrimidine aldehyde **38**, yielding secondary alcohols, either (*R*)- or (*S*)-**39**. (**Scheme 2.13**)[31]

Asymmetric synthesis of azahelicenes is so far uncommon but the first significant achievements in this direction were already accomplished. Nozaki *et al.* took advantage of availability of enantiopure 4,4'-biphenanthryl- 3,3'-diol whose nonaflate derivative (*S*)-**40** was used in the stereospecific synthesis of the enantiopure carbazol-derived aza[7]helicene (*P*)-**41** (**Scheme 2.14**).[32] Employing the Buchwald-Hartwig amination methodology, Pd-catalysed double arylation proceeded in a stereoconservative way.

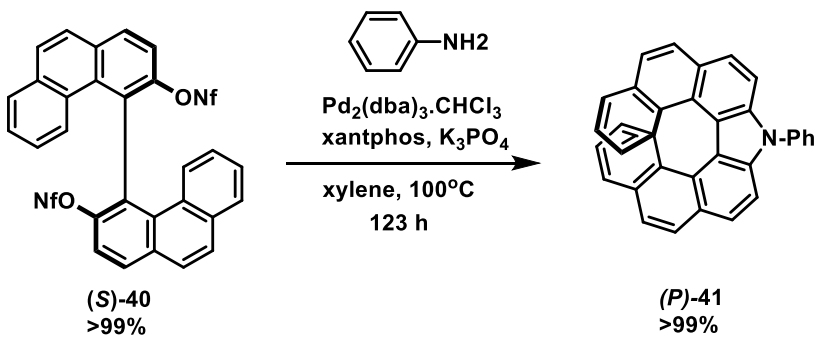

Scheme 2.14: Enantioselective synthesis of aza[7]helicene using Buchwald-Hartwig amination.

Using a similar concept, Kamikawa *et al.* transformed an enatiopure biaryl building block (*R*)-**42**) into enantiopure 6-aza[6]helicene (*P*)-**44** in good yield by utilising a palladium-catalyzed C-H annulation reaction (**Scheme 2.15**).[33]

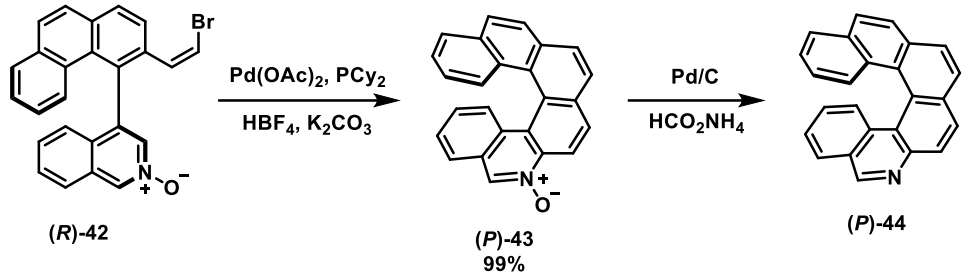

Scheme 2.15: Asymmetric synthesis of 6-aza[6]helicene using Pd-catalyzed C-H annulation reaction.

List *et al.* reported an innovative asymmetric organocatalytic approach to indole/carbazole-derived azahelicenes (**Scheme 2.16**).[34] It employed enantioselective Fischer indolisation reaction catalysed by a chiral SPINOL-derived phosphoric acid (*S*)-**145** to form the helical backbone in good yield.

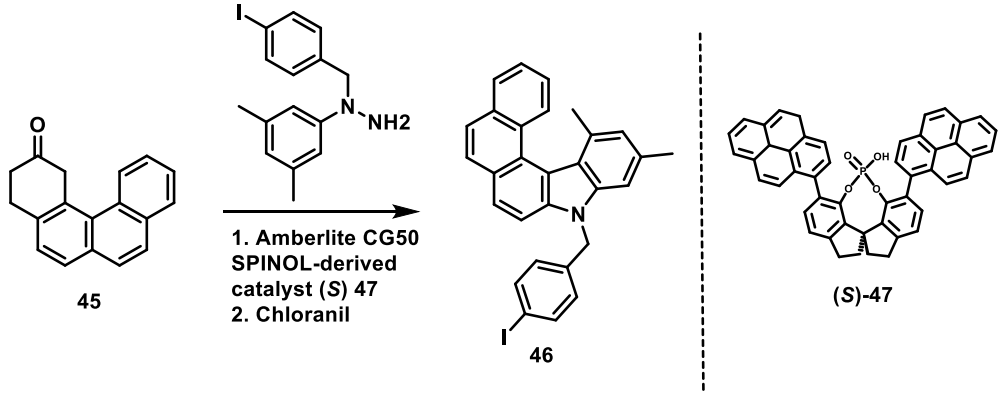

Scheme 2.16: Asymmetric synthesis of aza helicene using enantioselective Fischer Indolisation reaction.

The last decade highlighted carbohelicenes[35] as helical dominating frameworks, but heterohelicenes,[36] such as, aza- and thiahelicene, have also emerged as interesting class of molecules. Azahelicenes belongs to a subgroup of heterohelicenes, with possible applications in fields such as light-emitting devices and chemosensors.[37] Azahelicene derivatives have also been reported to have applications in enantioselective transformations, as chiral inducers, in the fields of asymmetric catalysis, self-assembly, and metal coordination complexes. Which are already discussed above in the

introduction portion of this chapter. Classical photochemical cyclization is one of the most utilized methods for the synthesis of azahelicenes. Reports for the synthesis of aza[*n*]helicenes derived from carbazoles are relatively less.

As discussed in the introduction of the thesis; various properties of carbazole attracted us for taking up this as major starting point for the synthesis of aza[*n*]helicenes. Some of the advantages include easy availability, cheap starting material, many reported for its functionalization, three inbuilt rings and well explored in the field of material science (good emission behavior). Throughout this chapter oxidative photocyclization strategy is adopted for the synthesis purpose. Primary aim was to synthesize different aza[*n*]helicenes and to study their properties. Secondary goal was to synthesize or optimize the conditions for synthesis with higher regioselectivity by minimizing the other products during photocyclization.

2.4 RESULTS AND DISCUSSION

2.4.1 Synthesis of aza[7]helicenes:

The retrosynthetic plan to access symmetrical aza[7]helicenes is based on to the oxidative double photocyclization of stilbene type analogues of carbazole (**Figure 2.2**). The required olefin precursor material for the photoreaction can be easily prepared by Mizoroki-Heck reaction of 3,6-diiodo-9-alkyl-9*H*-carbazole with suitable styrene. By choosing an appropriate styrene one can introduce different functional groups on the aza[7]helicenes and this can be a general preparative method.

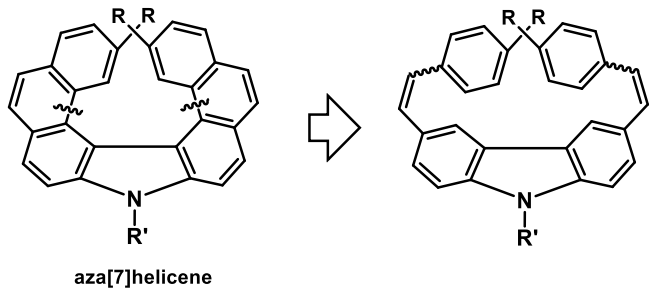

Figure 2.2: Retrosynthetic analysis of symmetrical aza[7]helicene.

The required starting material 3,6-diiodo-9-butyl-9*H*-carbazole **50** was prepared from carbazole **48** by the known literature procedures.[38] In order to overcome solubility issues; n-*Bu* group was attached to carbazole.[39] The Diiodo *N*-butyl carbazole **50** was then subjected to double Mizoroki-Heck reaction in presence of palladium catalyst,

dppp, K_2CO_3 and styrene to obtain corresponding 3,6-distyryl-9-butyl-9*H*-carbazole **51** in excellent yields. Similarly dimethyl bis-styryl derivative **52** was prepared using 4-methyl styrene. (**Scheme 2.17**).

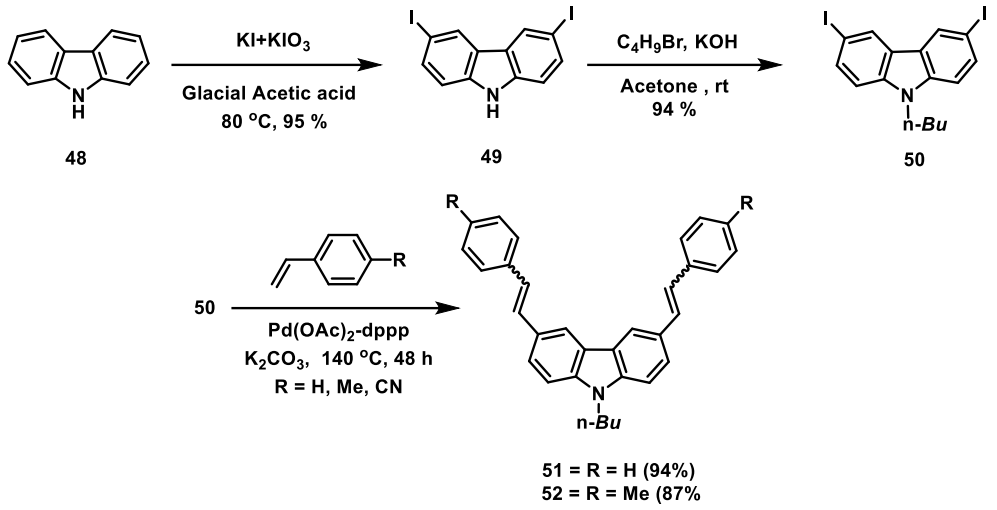

Scheme 2.17: Synthesis of 3,6-distyryl-9-butyl-9*H*-carbazoles by Mizoroki-Heck reaction.

However, this strategy of using Mizoroki-Heck reaction has a limitation of availability and stability of some styrene derivatives. To overcome this problem we have developed a protocol of making styrenes *in situ* for a one-pot reaction.[40] In this process an aromatic aldehyde with required substituent is subjected to Wittig reaction with a one carbon phosphonium salt (Ph_3PCH_3I) to generate the desired styrene derivative, which was then subjected to Mizoroki-Heck condition in the same flask to give the stilbene derivative. This method has an advantage of availability of substituted aldehydes to compensate the poor accessibility of certain styrenes. The process was applied for the synthesis of two more derivatives of the present distyryl carbazoles. In this way a method can be developed to prepare any type of 3, 6-distyryl-9-alkyl-9*H*-carbazole required for the synthesis of aza[7]helicene. Two derivatives starting from 4-methoxy benzaldehyde **53** and 4-fluoro benzaldehyde **54** were utilized to *in situ* prepare 4-methoxy styrene and 4-fluoro styrene, respectively, which were subjected to one-pot Mizoroki-Heck reaction with **50** to get two more bis styryl derivatives **55** and **56**. (**Scheme 2.18)**.

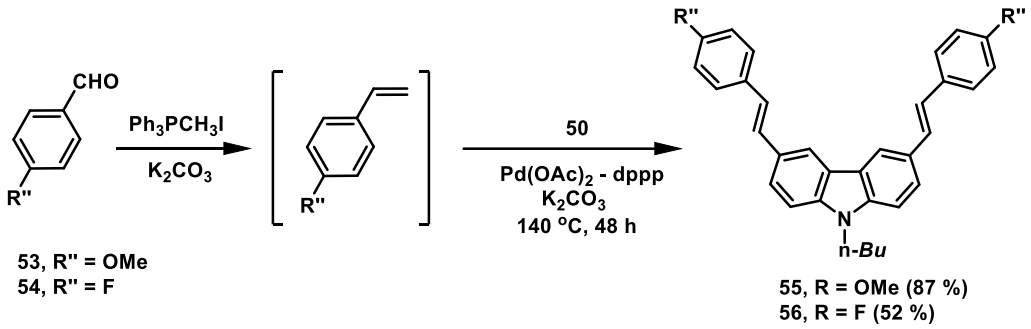

Scheme 2.18: Synthesis of 3,6-distyryl-9-butyl-9*H*-carbazoles by One pot Wittig-Heck reaction.

The distyryl derivative of carbazole **51** was then subjected to photocyclization in toluene under the high pressure mercury vapor lamp. The reaction was assisted by stoichiometric amount of iodine as an oxidizing agent and THF as a scavenger of the hydrogen iodide formed. Careful analysis of the reaction mixture revealed consumption of the starting material and formation of a major product, which was isolated by column chromatography over silica gel. The ^{1}H-NMR analysis of **57** clearly established the double angular cyclization (**Scheme 2.19**). The photocyclization was extended for the other three derivatives **52**, **55** and **56** to afford similarly cyclized aza[7]helicenes **58**, **59** and **60** respectively in moderate isolated yield. In all the cases the double angularly fused systems were isolated and characterized by ^{1}H-NMR analysis, supported by other spectral techniques. The hydrogen attached to C4 (& C5) of **5** appeared at 8.3 δ as a singlet, disappeared in **57** on cyclization. This is a clear evidence of angular cyclization. In the compound **57** the inside protons attached to C2 (& C16) appeared most upfield in the aromatic region at 6.21-6.28 δ, followed by signal at 7.16-7.20 δ for the protons attached to C3 (& C15). The other two protons attached on C1 (& C17) and C4 (& C14) of the terminal rings appeared at 7.43-7.45 and 7.81-7.83 δ.

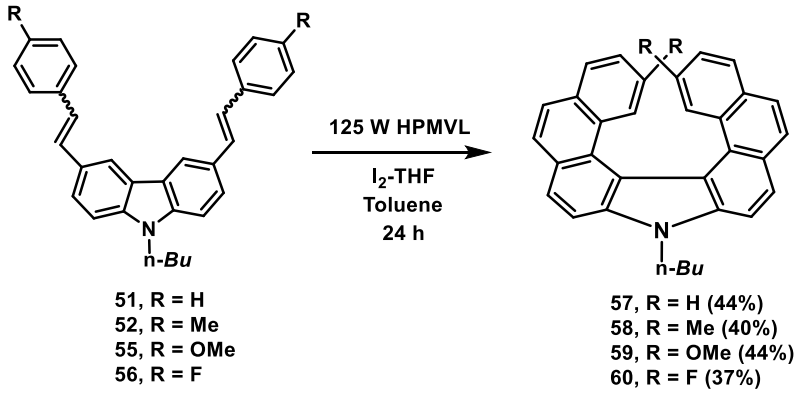

Scheme 2.19: Photocyclization of bis styryl derivatives for the synthesis of aza[7]helicenes.

2.4.2 Regioselectivity of the photocyclization:

In order to investigate regioselectivity of the photocyclization of aza[7]helicene, we recorded the ^{1}H-NMR for the crude reaction mixture of compound **57**. The ^{1}H NMR analysis indicated the reaction is highly regioselective for the double angularly cyclized product,. Importantly, the linear derivatives **61** and **62** were not formed during the cyclization step, as these regiomers would be expected to display characteristic singlet signals in the downfield region of ^{1}H-NMR. (**Figure 2.3**)

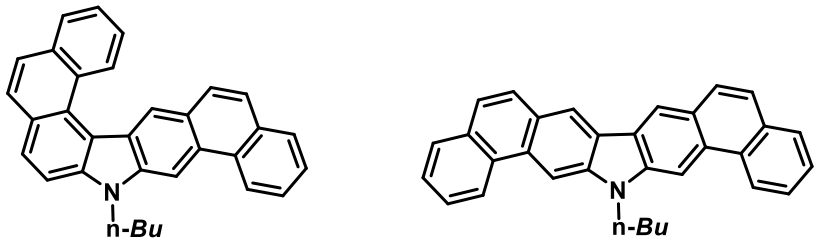

61 **62**

Figure 2.3: Structures of linear products **61** and **62**.

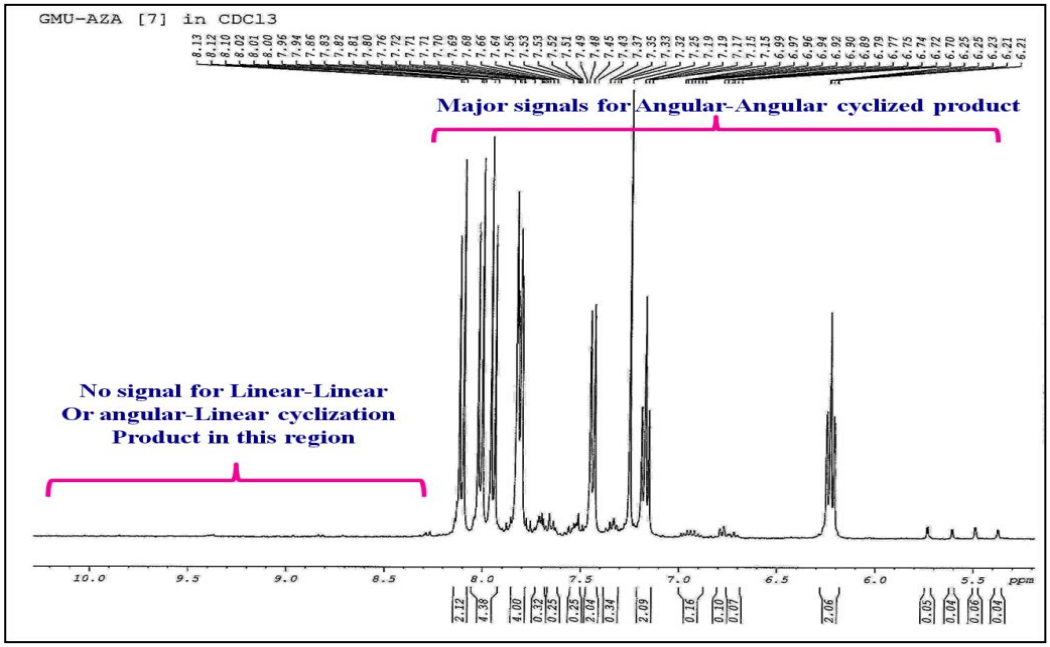

Figure 2.4: ^{1}H NMR of crude reaction mixture of aza[7]helicene **57**. (Aromatic region).

2.4.3 X-Ray Structure analysis:

All the four derivatives of aza[7]helicenes were quite soluble in organic solvents such as toluene, dichloromethane, chloroform, acetone, ethyl acetate etc. A pale yellow crystal of **60** was obtained from ethyl acetate-hexane and analyzed by single crystal X-

ray diffraction (**Figure 2.5**). Selected bond lengths, distances of non-bonded atoms, torsion angles are presented in **Table 2.1**. Some of the bonds of the outer side C19-C20, C22-C23 and C28-C29 were of the order of 1.332 – 1.358 Å, much shorter compared to the average bond of benzene (1.39 Å). Similarly as expected for helicene structure the inside bond lengths were elongated in the range of 1.403 to 1.455 Å. The distance between the non-bonded atoms of the last two terminal rings of this compound clearly indicate that they are separated by about 4 Å. The two carbon atoms bearing fluorine (C13-C27) were seen to be separated by 3.913 Å and the fluorine atom is located almost beneath the last aromatic ring of aza[7]helicene structure. This results in its upfield shift in the ^{19}F-NMR spectra due to the shielding effect of the last ring. The torsion angle along the inner frame of the aza[7]helicene varied from 14.83 to 17.27, a characteristic measure of helicity. The sum of the three dihedral angles φ 1, φ 2, φ 3 was observed to be 49.13°, which is considered to be quite pronounced and offers good rigidity to the isomers. The analysis of **16** on chiral phase HPLC supported this observation where the two well separated peaks for the helical isomers were detected [Chiralcel OD-H; IPA in hexane (10 %), 1.0 mL/min., 6.5 and 8.3 min].

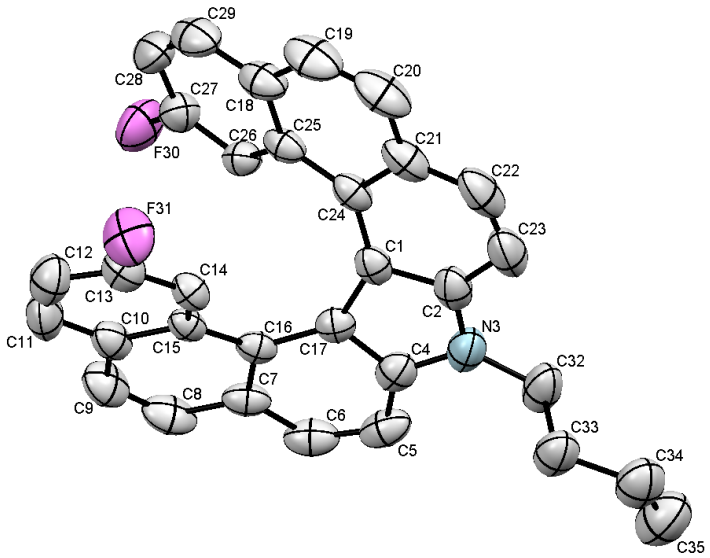

Figure 2.5: ORTEP plot of compound **60**. (CCDC No. **1004161**)

Inner carbon-carbon bond lengths (Å)	Distance between non bonded atoms (°)

C17-C1	1.455	F30-F31	5.432
C1-C24	1.424	C12-C28	4.446
C24-C25	1.440	C13-C27	3.913
C25-C26	1.403	C14-C26	3.003
Outer carbon-carbon bond length (Å)		C16-C24	3.559
C22-C23	1.342		
C19-C20	1.332		
C28-C29	1.358		
Torsion angle (°)		Distortion of the molecular structure (°)	
φ 1 = C26-C25-C24-C1	14.83	φ 1 + φ 2 + φ 3	49.13
φ 2 = C25-C24-C1-C17	17.03		
φ 3 = C24-C1-C17-C16	17.27	Dihedral angle θ (°)[a]	35.84

[a] Angle between planes passing through C10-C11-C12-C13-C14-C15 & C18-C25-C26-C27-C28-C29 rings.

Table 2.1: Selected X-ray crystallographic data of the compound **60**.

2.4.4 Photophysical properties:

The aza[7]helicene derivatives were investigated using UV–Vis absorption study performed in methanolic solution (5.0 $X10^{-5}$ mol). Spectra of these compounds exhibited a strong absorption in the region of 257–414 nm (**Figure 2.6**). Absorption maxima appears around 257 to 261 nm region, followed by few medium peaks around 315 to 335 nm and two minima 385 to 414 nm. The absorption bands in the region 250 to 350 nm ranges are associated with the π–π* and n-π* electronic transitions. Some of the prominent absorption peaks are listed in **Table 2.2**.

Compound	Wavelength (nm)				
57	260	326	335	385	401
58	261	326	333	388	404
59	260	318	330	394	414
60	257	315	327	390	408

Table 2.2: Prominent UV-Vis bands of compound **57** to **60**.

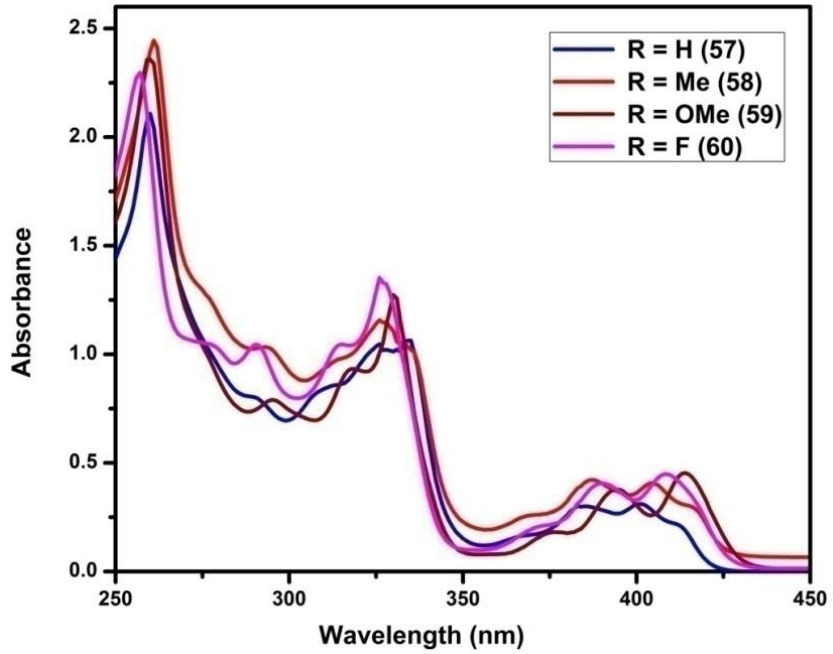

Figure 2.6: UV-Vis spectra of aza[7]helicenes.

2.4.5 Thermal properties:

Thermal behavior of aza[7]helicenes was investigated by means of differential scanning calorimetry (DSC) where the sample was heated at the rate of 10 °C/min from 25 to 300 °C, under the inert atmosphere of nitrogen (**Figure 2.7**).

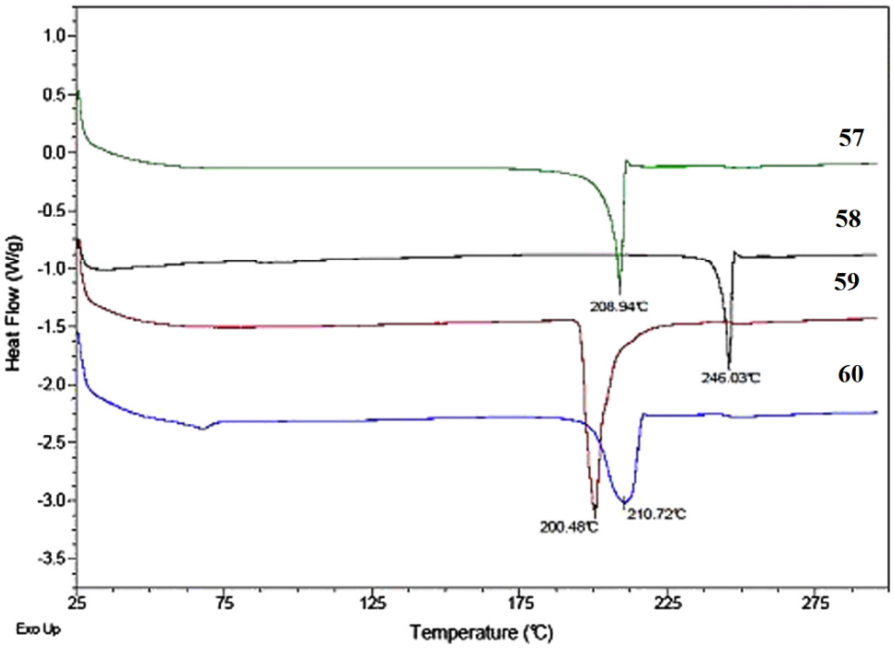

Figure 2.7: DSC Thermogram of **57** to **60**.

The analysis indicated the melting point of compounds to be in the range of 200–246 ^{o}C. The glass transition temperatures (Tg) of aza[7]helicenes lie in 147–197 ^{o}C (**Table 2.3**), which point toward high thermal stability of the helical system.

Compound	Melting Point (^{o}C)
57	208.9
58	246.0
59	200.5
60	210.7

Table 2.3: Thermal behavior of **57** to **60** by DSC analysis.

2.5 Synthesis and study of aza[9]helicenes:

In this work, we have successfully synthesized series of aza[7]helicenes using oxidative photocyclization. The reaction was highly regioselective, as only the angularly cyclized product was formed during photocyclization. We have studied its photophysical properties, and it also shows good thermal stability. The optical properties can be attributed to the extended conjugation created by the *ortho*-fused aromatic rings; hence its analogue aza[9]helicene is expected to further enhance the conjugation and the photophysical response and may also affect the thermal properties. However, the construction of such a large helicene consisting of nine rings making almost one and half turn of the helix is a challenging task, and its synthesis is not reported in the literature. Although structurally similar, the two helical compounds substantially differ in the internal strain caused by the steric crowding and offer different degree of challenge in their synthesis.

2.6 RESULTS AND DISCUSSION

2.6.1 Synthesis of aza[9]helicene:

The synthesis of the desired aza[9]helicene was achieved by following similar strategy to that of aza[7]helicene. Accordingly, the 3, 6- diiodo-*N*-butylcarbazole **50** was converted to 3,6-bis(2-(naphthalen-2-yl)vinyl)carbazole **64** by its Mizoroki−Heck reaction with vinylnaphthalene **63**. A solution of **64** in toluene was subjected to photochemical reaction (125 W HPMV lamp) in a standard immersion well reactor (**Scheme 2.20**).

The initial analysis of the reaction mixture indicated the formation of a complex mixture of the products, contrary to the earlier observation of aza[7]helicene. This is probably due to the different possible modes of cyclization of the intermediate species in the stilbenoid derivative.

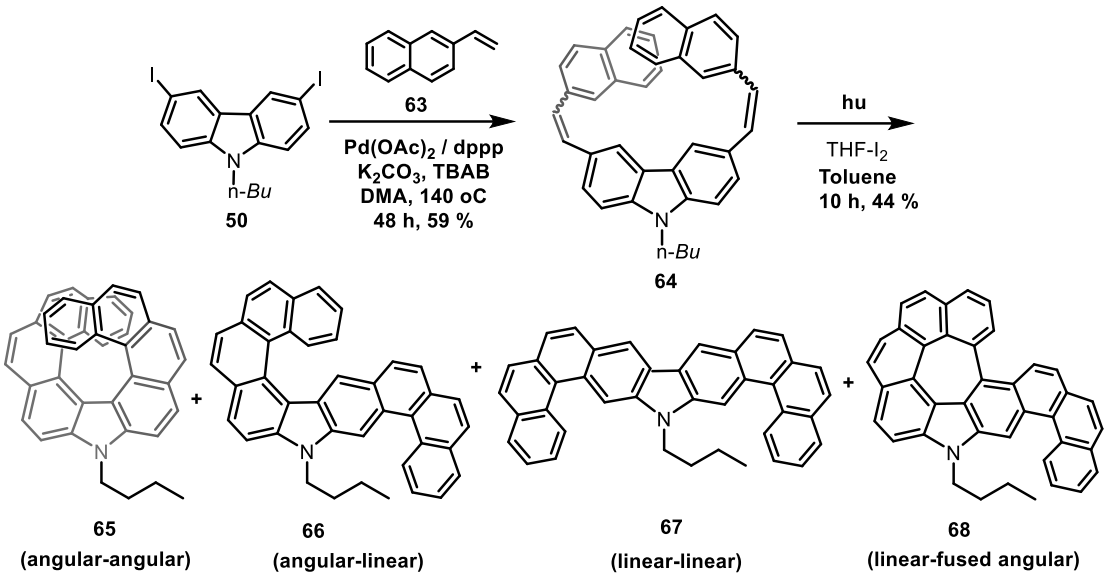

Scheme 2.20: Synthesis of aza[9]helicene.

2.6.2 Regioselectivity of aza[9]helicene:

In cases where the photocyclization can occur at two different sites of a polynuclear system, the regiochemistry is controlled by two major considerations, the electronic and steric factors.[11b] If steric hindrance is not very severe then the product is usually formed through the intermediate, which will lead to greater aromatic resonance stabilization. When the electronically favorable pathway is considerably sterically hindered, then the less hindered alternative pathway is preferred.[17] In some cases, the regioselectivity in such photocyclizations can be predicted by molecular orbital calculations of the difference in excited-state free-valence indices and Mulliken electronic overlap populations at the two sets of carbon atoms involved in ring closure. However, in some cases, even though the favorable theoretical predictions are made, the actual photocyclization may result in different outcome.[41] In the analogous case of photocyclization of carbazole based stillbene derivatives, the two available sites may direct the photocyclization leading to either angular or linear isomer. This type of the two modes of cyclization has also been discussed in a previous study,[42] explaining the formation of the two isomers resulting at electrocyclization at the a or b position (**Scheme 2.21**). The position a is electronically more favorable for electrocyclization compared to position b. The two possible dihydro intermediates IIa and IIb would on oxidation give aromatized angular product IIIa and linear product IIIb. In the angular case, the intermediate IIa retains the aromatic character of the pyrrole ring of the

carbazole moiety, while it is compromised in the intermediate IIb in linear mode. This case is analogous to the intermediates proposed by Katz *et al.*[42] for the Diels–Alder cycloaddition of vinyl carbazole, where the intermediate for the angular reaction was calculated to be 8.6 kcal/mol more stable than the corresponding linear intermediate. The electronic effects of retaining the aromatic character of the pyrrole ring in IVa direct the cyclization in an angular manner. However, this effect is partially balanced by the steric effect created by an additional aromatic ring of naphthalene unit favoring the formation of intermediate IVb, leading to the linear mode of cyclization.

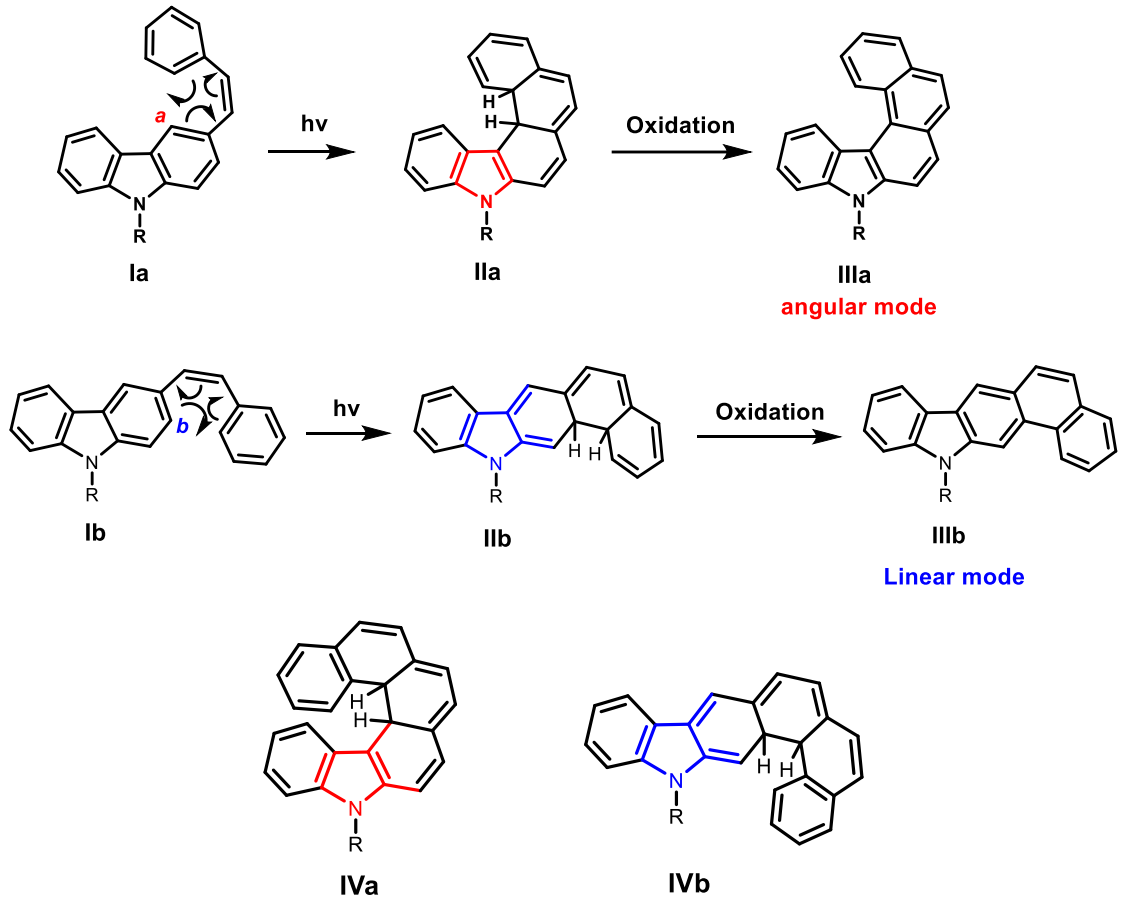

Scheme 2.21: Possible modes of photocyclization in aza[n]helicenes.

Based on this hypothesis, we anticipate the formation of product resulting in a linear mode of cyclization. The cyclization in the present bis-stilbenoid derivative **64** may follow in a stepwise manner; the regiochemistry of the second cyclization will be controlled by the first reaction. If the initial cyclization follows the angular path, an intermediate Va will be formed that may give two possible regioisomers (angular–angular **65** and angular–linear **66**) during the second reaction. On the other hand, if the

initial cyclization gives linear isomer Vb, the second cyclization can result in the formation **67** or **68**.

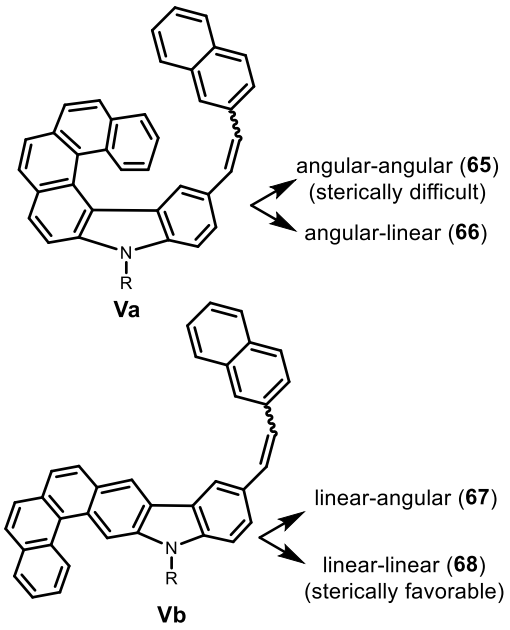

Scheme 2.22: possible product formation paths.

2.6.3 Characterization of regiomers:

Careful purification of the reaction mixture furnished four distinct products, which were adequately characterized by spectroscopic and analytical techniques (**Figure 2.8**). The structures **65** to **68** were assigned by ^{1}H NMR spectra. The compound **65** showed a symmetrical pattern without any singlet. The hydrogen attached to C1 appeared in upfield aromatic region due to being in the ring current of last aromatic ring and showed as a doublet at δ 6.12 ppm; while the hydrogen attached to C2 appeared most upfield in aromatic region at δ 5.60 ppm as a multiplet. The angular-linear isomer **66** shows unsymmetrical pattern resulting in more number of signals. Typically the hydrogen attached to C1 of the aza[6]helicene part of the molecule appeared in upfield region at δ 7.32 ppm as a doublet and hydrogen at C2 as a multiplet at δ 7.11 ppm. The linear part of the molecule is established by observing the hydrogen attached to C20 as a doublet at δ 9.47 ppm and the corresponding two singlets for hydrogens attached to C12 and C21 at δ 7.14 and 9.13 ppm respectively. The linear-linear isomer **67** also showed a symmetrical pattern in ^{1}H and ^{13}C NMR. The hydrogens attached to C9 and C21 appeared as singlets at δ 8.91 and 9.13 respectively. The hydrogen attached to C1 appeared as doublet at δ 9.41 ppm. The fourth product showed two less hydrogens and

we concluded that further oxidation has taken place similar to the formation of benzo[*ghi*]perylene. This compound **68** also showed an unsymmetrical pattern. The absence of hydrogens at C1 and C12 of the aza[6]helicene part of **66** was clearly noted. The only singlet appeared δ 8.87 ppm, corresponding to hydrogen attached to C21 The fourth product **68** appears to be formed, where the portion on the angular cyclization part of **67** (aza[6]helicene unit) undergoes further oxidation, resulting in a fused system similar to benzo[*ghi*]perylene.[43] It was observed that although the four compounds were detected in the crude sample, their separation proved to be difficult and challenging. Separation of regiomers was done by enrichment of respective compound using column chromatography followed by fractional crystallization in different solvents. The angular-angular isomer **65** was found to be slightly different in polarity, while the other three were of almost similar nature on TLC.

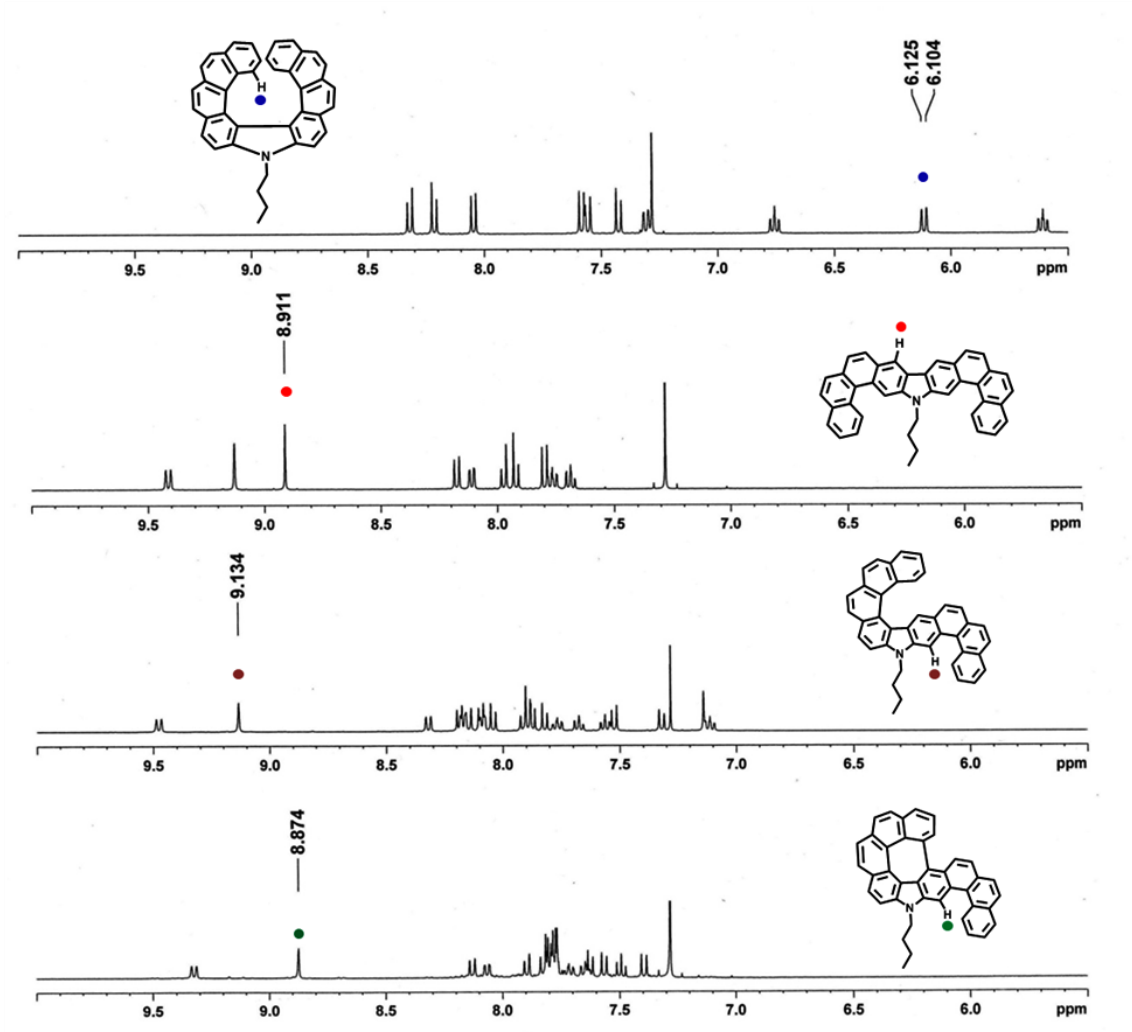

Figure 2.8: Comparison of ^{1}H NMR of regiomer **65** to **68**.

2.6.4 X-Ray Structure analysis:

All four compounds were further characterized by single crystal X-ray diffraction to determine the shape of the molecules arising due to the strain created by building up of the aromatic rings. The crystal structure of **65** indicates a high degree of distortion of the molecular structure, which is a sum of torsion angles (φ1 + φ2 + φ3 + φ4) equal to 74.22° while the dihedral angle θ was measured to be 41.01° (**Figure 2.10**).

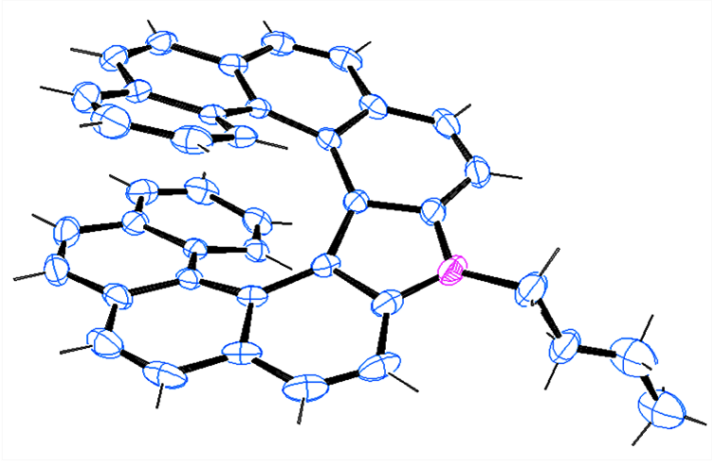

Figure 2.9: ORTEP diagram of **65**. (CCDC 1025231)

The two terminal rings were almost parallel to each other; the planes passing through them bisected at an angle of only 7.92°, and the pitch of outer helix was observed to be 3.97 Å. As expected for such helical structures, the outer C−C bonds were slightly reduced in length (1.329 to 1.398 Å) while the inside ones were bit elongated (1.407−1.449 Å) and the inner C−C bond of the pyrrole ring was 1.455 Å.

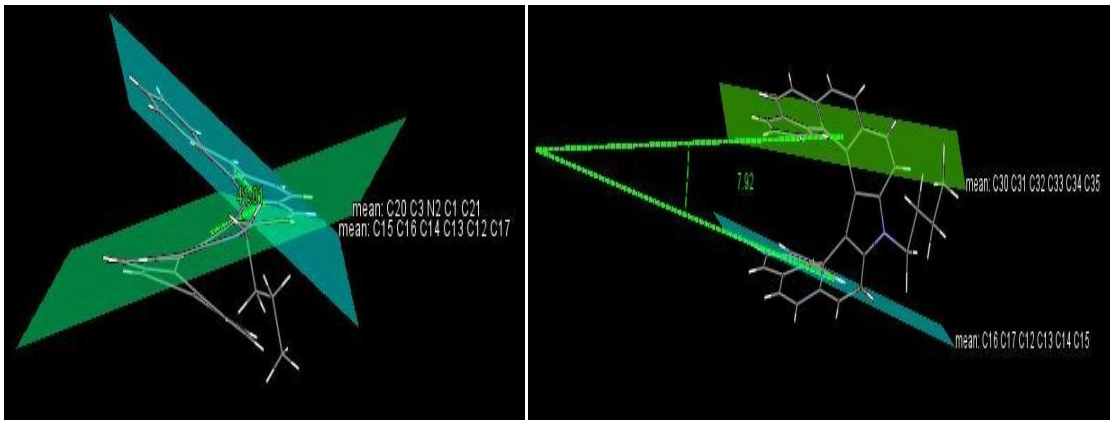

Figure 2.10: Dihedral angle and interplanar angle of compound **65**.

The other isomer **66** due to angular−linear cyclization has two components; one is the aza[6]helicene fused with the other [4]helicene. Its crystal structure indicates a distortion of the molecular structure on the former side, which is a sum of torsion angles, to be 66.77°, while the dihedral angle θ was measured to be 54.18° (**Figure 2.11**).

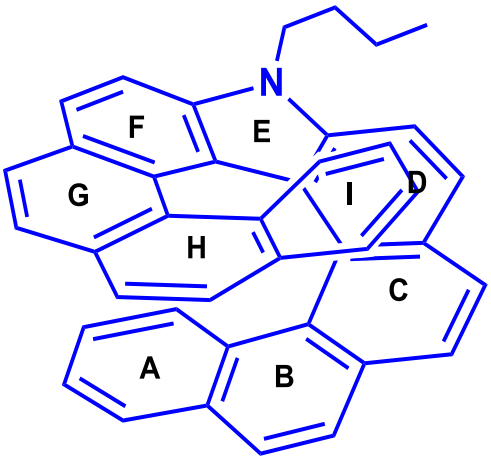

Interplanar angle
A-H: 14.59°
B-I: 4.74°

Pitch of inner helix (Å)
A-H: 3.31
B-I: 3.78
Average: 3.54

Pitch of outer helix (Å)
A-H: 4.15
B-I: 3.80
Average: 3.97

Table 2.3: Few important crystallographic parameters of target molecule **65**.

It is generally observed that the dihedral angle of smaller helical structures often tend to be larger compared to the more elongated helices.[44]

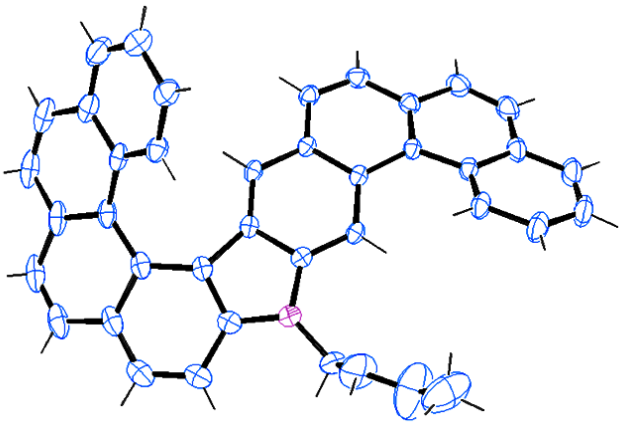

Figure 2.11: ORTEP diagram of **66**. (CCDC 1439548).

The next isomer isolated in the cyclization is due to the linear−linear mode and also shows an interesting crystal structure (**Figure 2.12**). The structure of this molecule closely resembles[45] diphenanthro[4,3-a;3′,4′-o]picene, which was almost simultaneously synthesized by Martin[46a] and Laarhoven. [46b] Molecule **67** also crystallized in the monoclinic space group of P21/c and showed a relatively small

torsion angle of about 38° and a dihedral angle of 29.7°.The molecule is like a wing of a bird, and when fully spread measures 16.67 Å in length and about 8.95 Å in width.

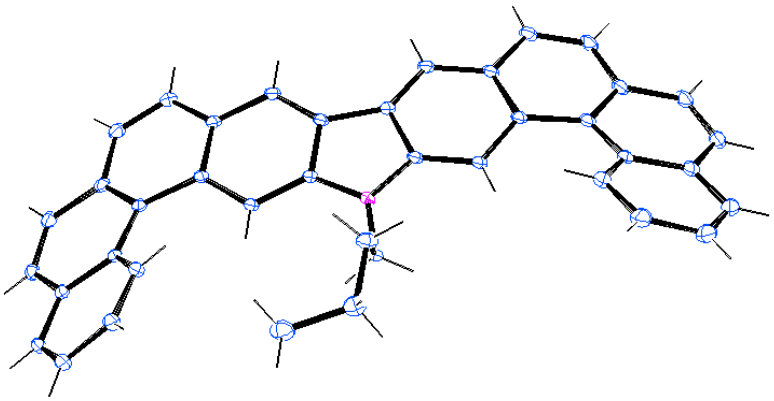

Figure 2.12: ORTEP diagram of **67**. (CCDC 1025232).

The angular−linear product **66** could undergo further oxidation reaction because the two terminal rings of the aza[6]helicene portion fall in close proximity. Hence, a much longer extended conjugation is seen in compound **68** compared to the other three molecules. As a result, the dihedral angle of the aza[6]helicene portion reduced to 33.8° as compared to **66** (**Figure 2.13**). This molecule appears to acquire a relatively flat shape as compared to the angular−linear derivative.

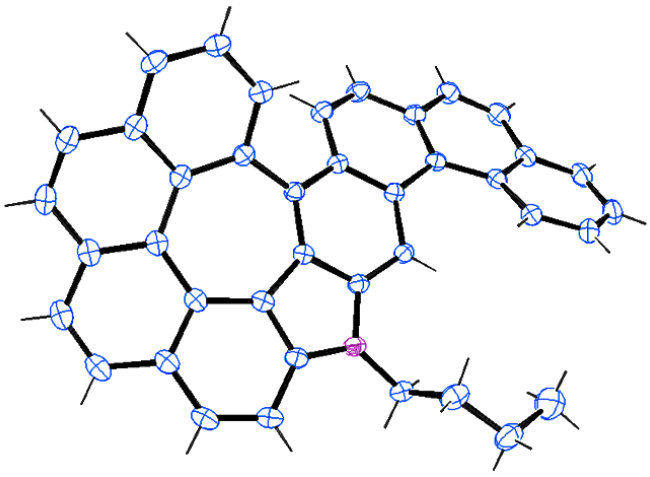

Figure 2.13: ORTEP diagram of **68**. (CCDC 1036685).

2.6.5 Effect of concentration of regiomer formation:

As already discussed, the regiomer formation in photocyclization reactions depends mainly on two considerations: steric and electronic factors. Some other factors have been studied to understand the regiomer formation. The composition of regiomers depends on various factors such as wavelength distribution of the incident light, the

reaction temperature,[47] the nature of oxidant, and concentration.[1a] One side reaction is cyclobutane formation by photochemical 2+2 cycloaddition of stilbenes. It is believed that the dimer formation is considerably reduced at much higher dilution suppressing the photodimerization process. Hence, it is recommended to carry out photolysis experiments at very high dilution to prevent the dimerization processes (10^{-2} M or less). However, the effect of concentration on the distribution of possible regioisomeric products is rarely investigated.[48] In the exploratory stage of our current investigation, the ^{1}H NMR analysis of the crude reaction mixture (**Figure 2.14**) indicated that the distribution of four observed products was concentration dependent, prompting us to investigate this further. As discussed previously, a few signals in the ^{1}H NMR for the four compounds appeared at distinctly different positions, helping us to determine the ratio in crude samples by measuring their quantity (**Table 2.4**). It was established from the above study that the desired angular−angular isomer **65** formed predominantly at higher dilution (lower concentration) while the other regiomer formed at higher concentration. The observed ratio can be attributed to the population of excited state intermediates, their stabilities, and their relative rates for the electrocyclization reactions. This observation of the correlation of concentration and the product distribution may help researchers in planning the synthesis of similar fused systems.

Entry	Concentration Moles/Liter	**65** δ = 6.12 (d)	**66** 9.13 (s)	**67** 8.91 (s)	**68** 8.87 (s)
1	150 mg in 1L ($2.86X10^{-4}$)	60.97	4.87	24.39	9.75
2	250 mg in 1L ($4.78X10^{-4}$)	38.46	14.61	22.30	24.61
3	500 mg in 1L ($9.56X10^{-4}$)	18.66	44.77	27.98	8.58
4	800 mg in 1L ($1.52X10^{-3}$)	14.32	45.27	31.80	8.59
5	1.0 g in 1L ($1.91X10^{-3}$)	ND	48	52	ND

[a]ND = not detected. Ratios in percent. Ratio determined after normalization, and the overall yield was between 43 and 45%.

Table 2.4: Effect of Concentration on the Distribution of Products.[a]

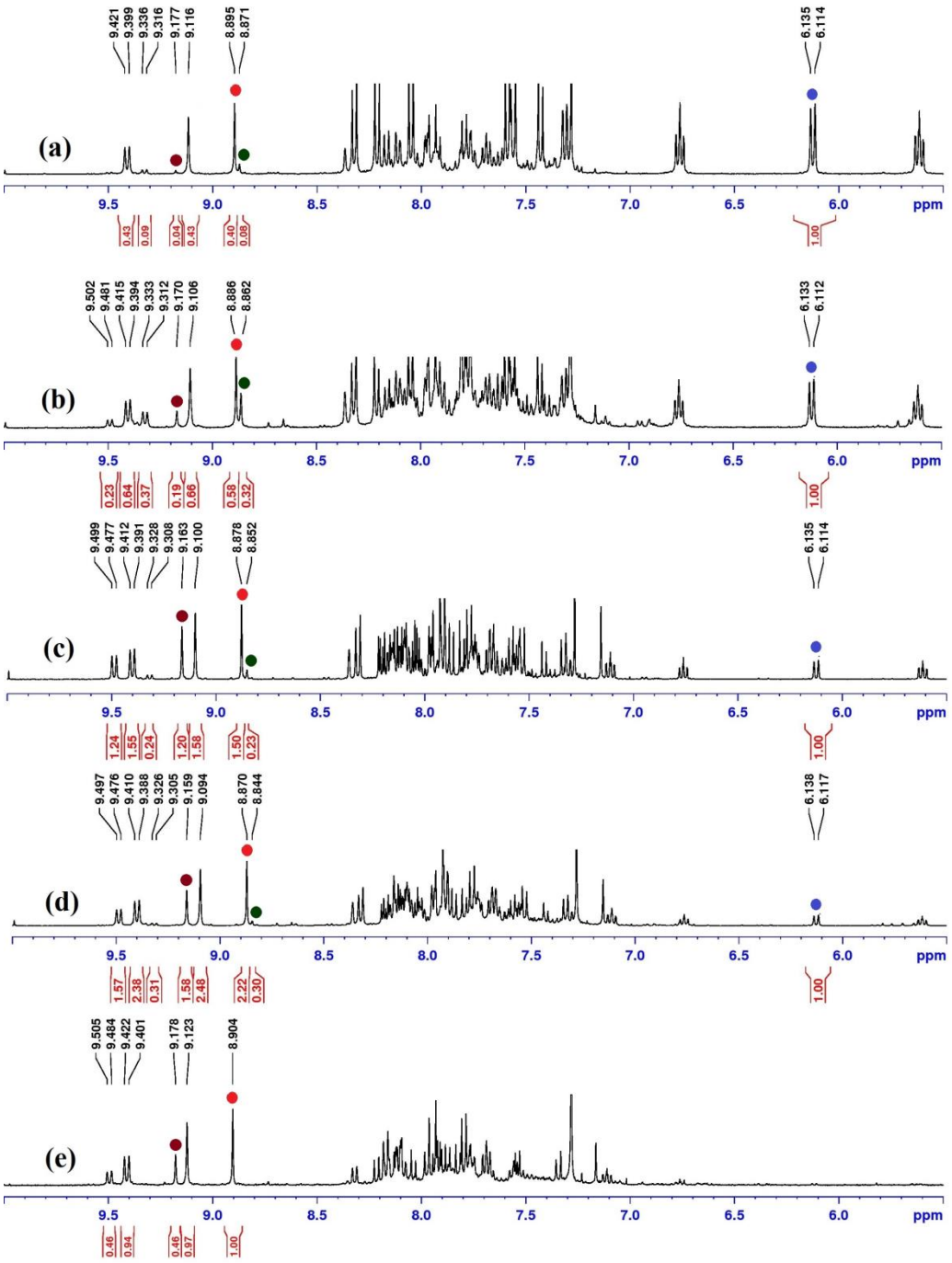

Figure 2.14: The comparison of ^{1}H NMR spectra of crude reaction mixture after photocyclization at different concentration of compound **3**. ● Angular-Angular, ● Linear-Linear, ● Angular-Linear, ● Angular-Linear (Fused) Concentrations (Moles/L) are- (a)150 mg in 1 L (2.86×10^{-4}) (b) 250 mg in 1 L (4.78×10^{-4})(c) 500 mg in 1 L (9.56×10^{-4})(d) 800 mg in 1 L 1.52×10^{-3})(e) 1.0 g in 1L (1.91×10^{-3})**# All the reactions were performed in 350 mL of toluene**

2.6.6 Optical properties:

The absorption and emission spectra of all of the compounds were recorded in dilute solutions of dichloromethane at room temperature (**Figure 2.15**). The π conjugation length is almost similar for all four isomers (65−68), so the shifts in both the absorption and emission spectra can be explained on the basis of effective spread of the π resonance system over the entire molecule.

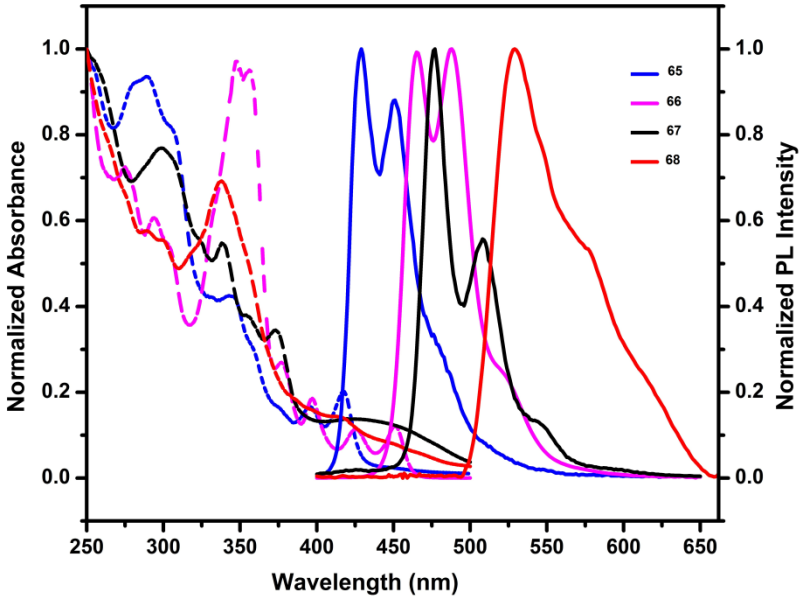

Figure 2.15: Absorption (dotted line) and emission (solid line) spectra of **65−68** in dichloromethane (abs 1 × 10^{-5} M; em 1 × 10^{-6} M).

The angular−angular compound **65** exhibited a deep blue emission peak at 429 nm and a shoulder peak at 451 nm. It appeared to show the most blue shift in the emission spectra, reinforcing the highly distorted structure created by helical twist. Such a shape contributes to the non-coplanar geometry, resulting in the reduction of effective π conjugation causing a blue shift in the fluorescence spectra of aza[6]helicene.[49] Interestingly, the emission maximum for aza[9]helicene was almost similar to the corresponding aza[7]helicene probably due to combination of contradictory effects of distorted geometry (leading to more blue shift) and extended conjugation (resulting in red shift). The angular−linear compound **66** showed a blue shift compared to the more linear π molecular systems **67** and **68**; this phenomenon might be attributed to the high dihedral angle which limits the delocalization of electrons throughout the molecule to some extent. The compound **67** showed a red shift due to effective delocalization as well as better π−π stacking. The compound **68** showed the maximum bathochromic

shift in emission spectra, indicating more effective delocalization of π electrons due to annulation.

The fluorescence quantum yields of four isomers were recorded in dilute dichloromethane solution (10^{-6} M) at room temperature; data are summarized in **Table 2.5**.

Compound	λ_{abs}/nm	λ_{em}/nm (λ_{exc}/nm)	Stokes shift/nm	Φ_{FL} (λ_{exc}, nm)
57	262, 329, 337	430, 448 (262)	186	0.17 (366)
65	289	429, 451 (289)	140	0.20 (313)
66	348	465, 488 (348)	117	0.19 (306)
67	299	477, 508 (299)	178	0.21 (363)
68	338	529, 578 (338)	191	0.07 (338)

Table 2.5: Photophysical properties of **65** to **68**.

The Φ (fluorescence quantum yield) of all regiomers were found to be low to moderate (0.07−0.21), which probably indicates that the excitons were not confined to the whole backbone of these molecules due to its nonplanar molecular structure. The reason for moderate quantum yields can be attributed to the marginal loss of energy during the exciton migrations.[50a] The quantum yield of the compound **65** was higher than the similar carbo analogue, [9]helicene[50b] (Φ = 0.014) and pentathia[9]- helicene[50c] (Φ = 0.02) and also approximately three times higher than compound **68**, which can be explained by greater steric hindrance in compound **65**. The greater strain and rigidity of **65** also reduces the availability of nonradiative deactivation pathways, forcing the molecule to relax via photon emission.[50d] Fluorescence quantum yields were determined using a solution of quinine sulfate in H_2SO_4 (0.5 M) as a reference standard (ΦFL = 0.546).

2.7 Chapter 2 part B Synthesis and study of functionalized mono aza[*n*]helicenes

Generally, two methods can be employed for the synthesis of functionalized helicene molecules: a suitable substituent can be introduced to the molecule of a helicene precursor before the final cyclization step or the appropriate helicene-based compound can be functionalized after cyclization. Functionalization of helicenes can be easily achieved by electrophilic aromatic substitution including nitration, halogenation, and acylation. For heterohelicenes, some C–H bonds can be activated by themselves. The transformations of bromohelicenes and hydroxyl helicenes can conveniently produce various functionalized helicene derivatives.

2.8 Post Functionalization or transformation of helical skeleton:

2.8.1 Direct C–H Functionalization

Early studies[51] established that for electrophilic aromatic substitution reactions including nitration, halogenation, and acylation (**Scheme 2.23**), the first functionalization takes place at the C(5) position being the most reactive site. Then the second functionalization takes place at C(7). This conclusion was also demonstrated by other groups. Chen group,[52] prepared benzo[5]helicene **69**, and the subsequent bromination occurred at C(5) and C(5′) positions (**Scheme 2.23**).

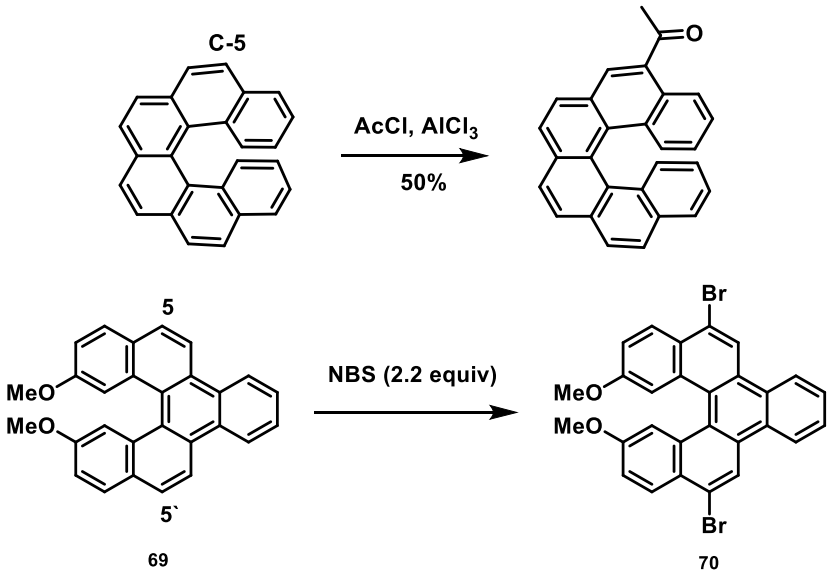

Scheme 2.23: Few examples of functionalization of helicenes with the preference of reaction site.

This reactivity trend is applicable for the simple helicenes. If helicene is multifunctionalized, the chemoselectivity will change accordingly. For example, Katz group prepared the substrates for bromination, and the products varied as the functionalities changed. Helicenebisquinone **71** gave the bromide at C(2) and C(2′) **72** and not at C(5) position.[53a] Similar reactivity was observed with tetramethoxy-substituted helicene.[53b] (**Scheme 2.24**)

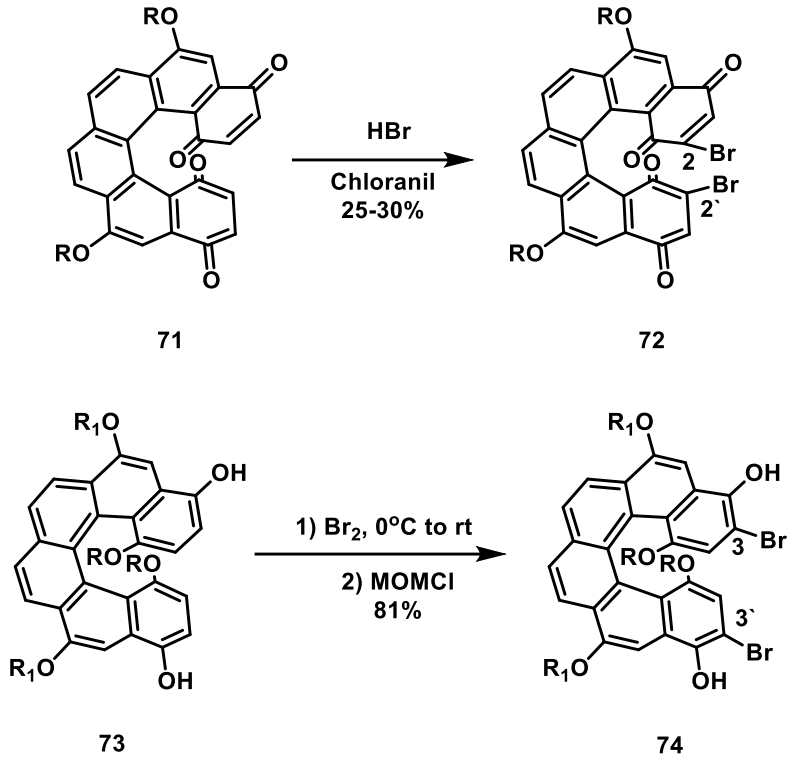

Scheme 2.24: Bromination of multifunctionalized helicenes.

Additionally, for heterohelicenes, some C–H bonds can be activated themselves by the heteroatom. Maiorana and colleagues examined the direct formylation of thiahelicene **75** via Vilsmeier–Haack reaction to afford 2-formyl helicene **76**[54a] (**Scheme 2.25**).

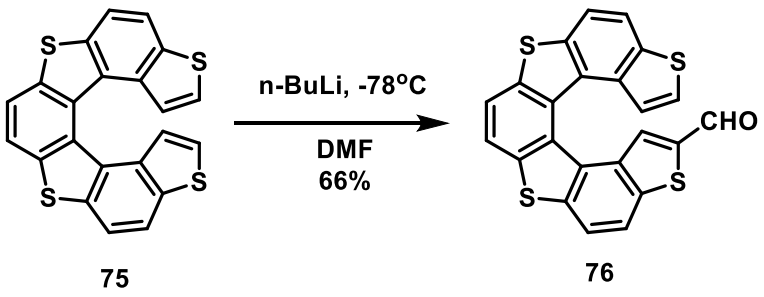

Scheme. 2.25: Formylation of thiahelicenes **75**.

Stephenson and Doulcet described a new approach for the asymmetric synthesis of formylated helicenes via kinetic resolution (**Scheme 2.26**)[54b]. By the weak interaction between the helicene anion and chiral formamide, enantioenriched 2-formyl helicene **76** was prepared in 30% yield and 40 % ee.

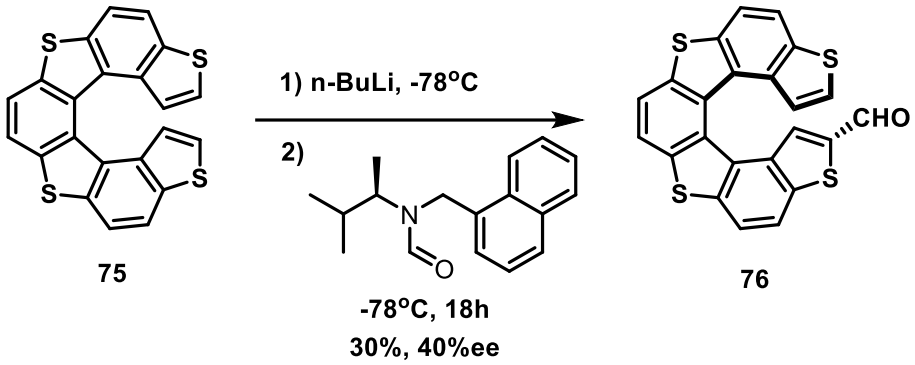

Scheme 2.26: Asymmetric formylation of thiahelicenes **75**.

2.8.2 Transformations of Functional groups:

The transformation of bromohelicenes and hydroxyl helicenes is most common, because most of other functional groups could be embedded on Br and hydroxyl groups. The Br atom could be incorporated to the substrates or via bromination of helicenes, while the hydroxyl groups should be embedded into the precursors, usually as methoxy group. Storch group[55] and Gingras group[56] had extensively studied the reactivity of bromohelicene. Recently Sakora and co workers[57] improved and revised the synthesis of 2-bromo [6]helicene and prepared 17 different derivatives from it. Herein, we would like to use Storch's results as an example (**Scheme 2.27**). By Suzuki–Miyaura cross-coupling reaction, phenyl group could be incorporated. In some cases, the substituent on aryl group would reduce the solubility of the helicene greatly. Helicene-embedded phosphine **79** could be prepared by direct Pd-catalyzed *P*-arylation, which could be further oxidized as a stable species **80**. As an alternative strategy, phosphine could also be prepared via Li/Br exchange and quenched by $ClPPh_2$ or $ClP(O)Ph_2$. Helicene nitrile **81** could be obtained via nucleophilic substitution of CuCN, and alkynyl-substituted helicene **82** was synthesized via Sonogashira reaction. In addition, Pd-mediated *N*-arylation afforded helical amine **83** in excellent yield. Also, thioether **84** could be obtained via Pd-catalyzed reaction, which is converted into thiol **85** with the help of t-BuSNa at high temperature. Thioether could be prepared via Pd-

catalyzed reaction between bromide and organotin reagent. Besides the reactions mentioned above, after Li/Br exchange, the substrate could be transformed into aldehyde if quenched by DMF or converted into acid in the presence of CO_2.

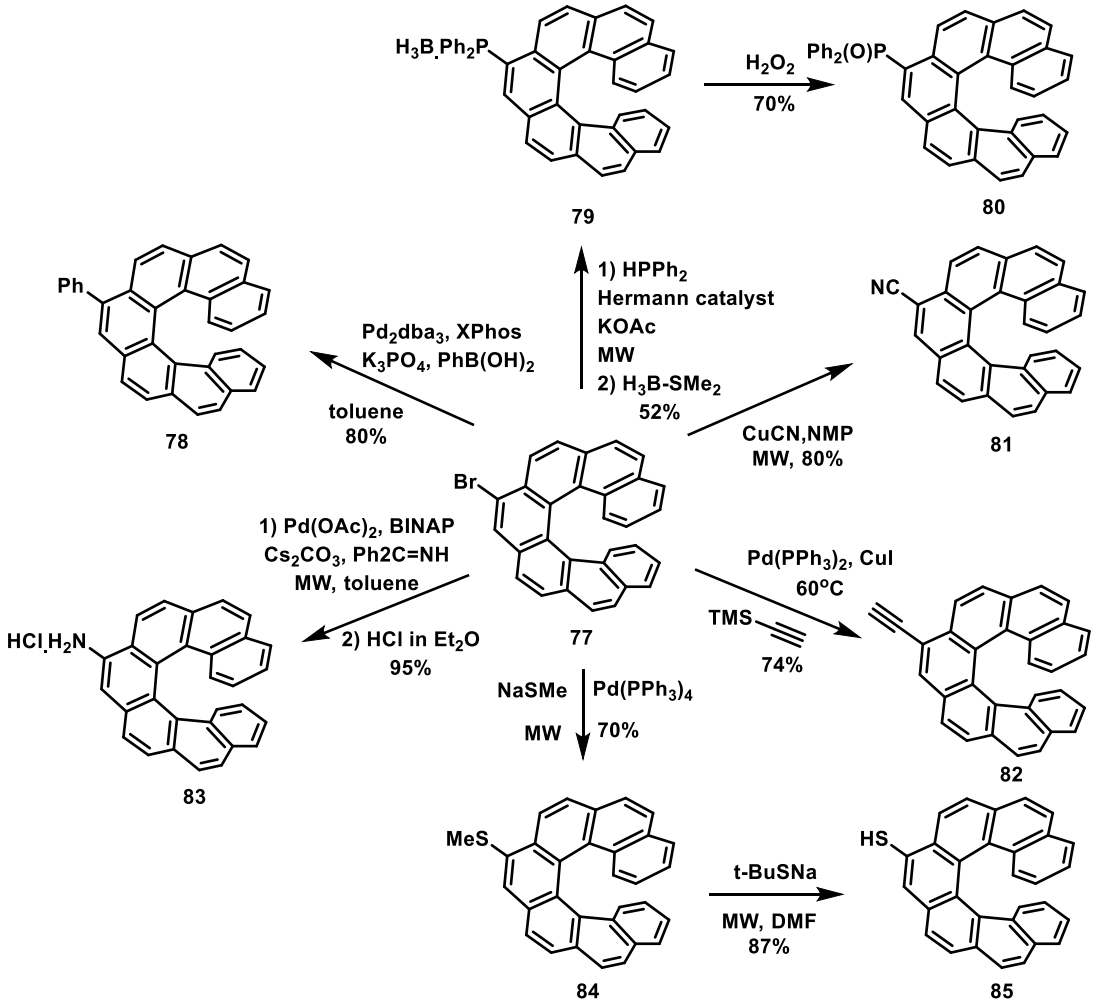

Scheme 2.27: Functionalization of bromohelicene **77**.

In a slightly different approach, Starý and Stará reported the functionalization of 3-hydroxy[*6*]helicene into various heteroatom containing helicenes,[24b] and Crassous explored the reactivity of [*6*]helicene pinacolboronate for the synthesis of amines and amino acids with a helical scaffold.[58] Recently an interesting visible light photochemical approach for the late stage functionalization of helicenes is reported by Storch *et.al*.[59]

2.8.3 Functionalization of aza helicenes:

Functionalization of already synthesized azahelicenes was less explored in the past. However, recently there has been an increase in research activity in this regard. There are several challenges that have to be faced: a problem of regioselectivity of the functionalisation, diminished reactivity in innermost positions of the heterohelicene backbone and the fact that some reactions at (hetero)helicenes as electron rich substrates are slowed down (for example oxidative addition in cross-coupling chemistry). Nevertheless, the range of reactions allowing the functionalization of existing azahelicenes is steadily growing. Takenaka *et al*. presented a facile conversion of enantiopure 1-aza[6]helicene *N*-oxides **36** and **86** to the corresponding 2-amino and 2-alkylamino derivatives **87a-f** (**Scheme 2.28**).[60] On reaction with the lithiated pyridine, the enantiopure 1-aza[6]helicene *N*-oxide was also transformed to the helical 2,2'-bipyridine *N*-monoxide **88** in high yield. (**Scheme 2.29**)

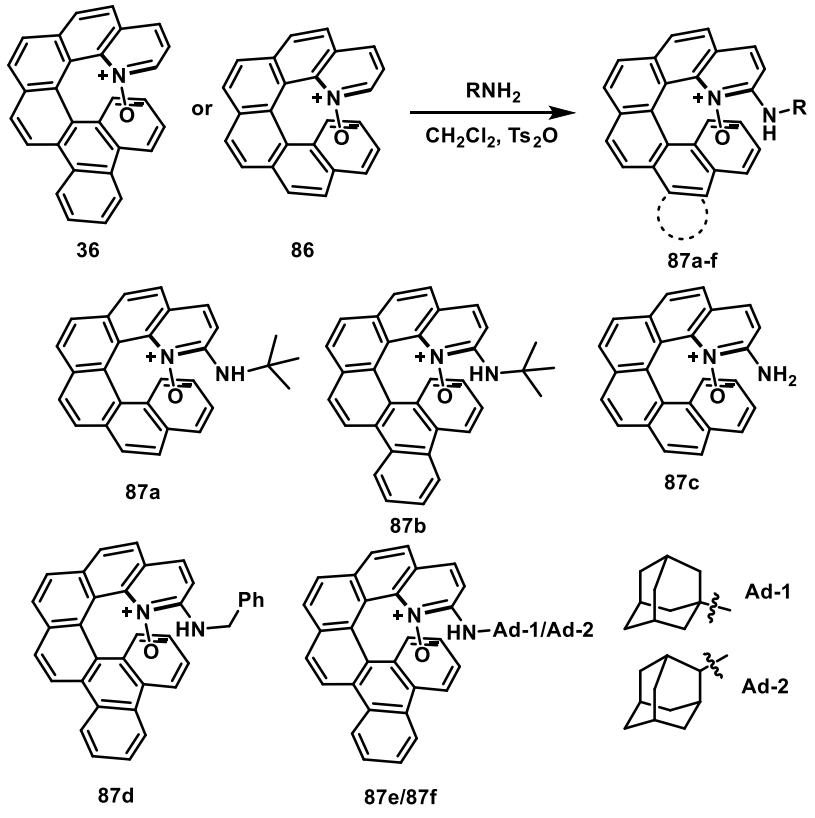

Scheme 2.28: Synthesis of amino, alkylamino *N*-oxide derivatives of aza[6]helicene.

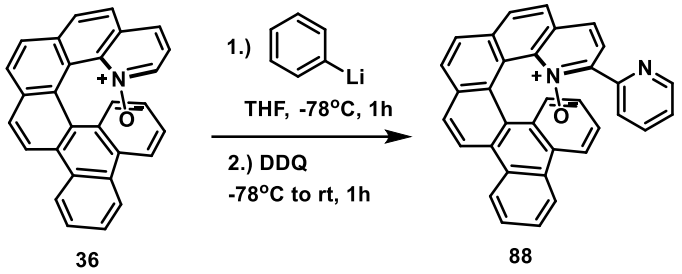

Scheme 2.29: Synthesis of helical 2,2'-bipyridine *N*-monoxide **88.**

Fuchter *et al.* demonstrated the first successful Suzuki-Miyaura cross-coupling, Buchwald–Hartwig amination and Heck reaction performed on (trifluoromethanesulfonyl)oxy derivatives of 1-aza[6]helicene **89** (**Scheme 2.30**).[27] While the cross-coupling reaction of triflate **89** with boronic acid proceeded without any difficulty to give the functionalized 1-aza[6]helicene **90**, amination with pyrrolidine delivered the product **91** and reaction of **89** with *n*-butylvinylether gave the acetyl derivative **92**.

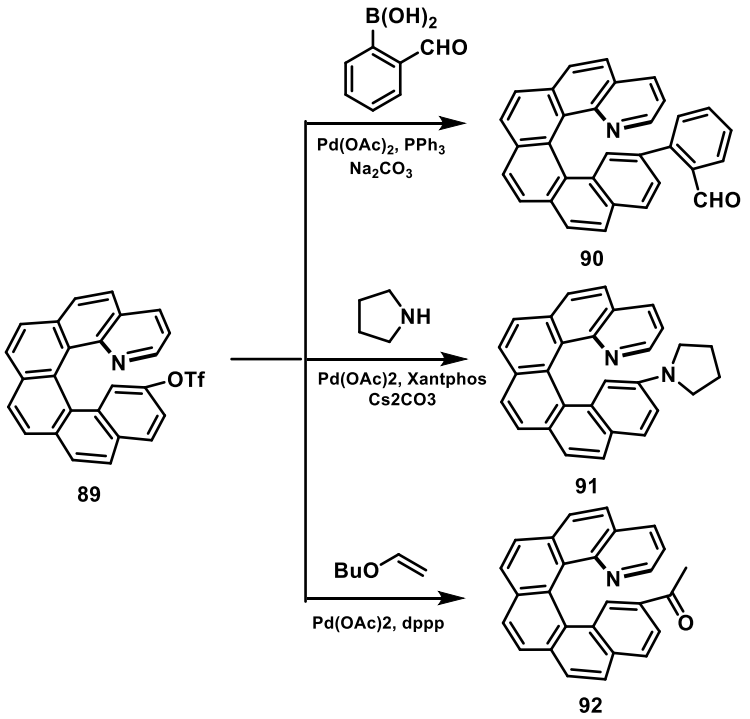

Scheme 2.30: Functionalization of compound **89**.

The carbazole-derived aza[7]helicene **41** can be transformed into its dibromo or tetrabromo derivative **93** or **94**, respectively, simply by changing the amount of *N*-bromosuccinimide as reported by Nozaki *et al.* (**Scheme 2.31**).[32] On lithiation and

subsequent reaction with methyl chloroformate, the tetrabromide **94** was converted into tetraester **95**.

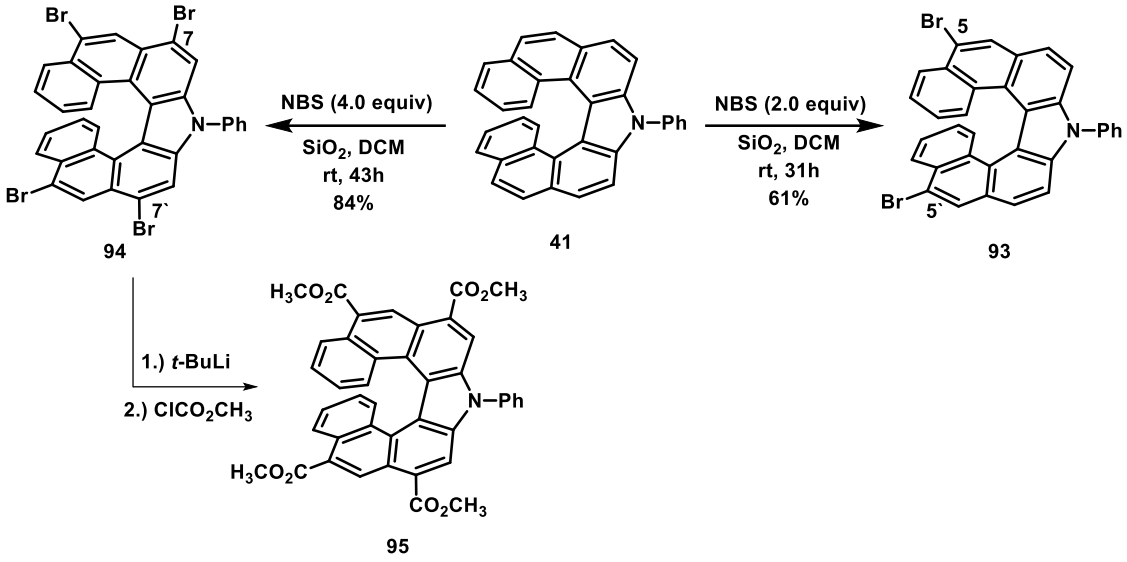

Scheme 2.31: Functionalization of aza[7]helicene **41**.

Shinokubo *et al.* performed double Sonogashira reaction of dibromo azahelicene **96** with trimethylsilylacetylene (**Scheme 2.32**). [61]

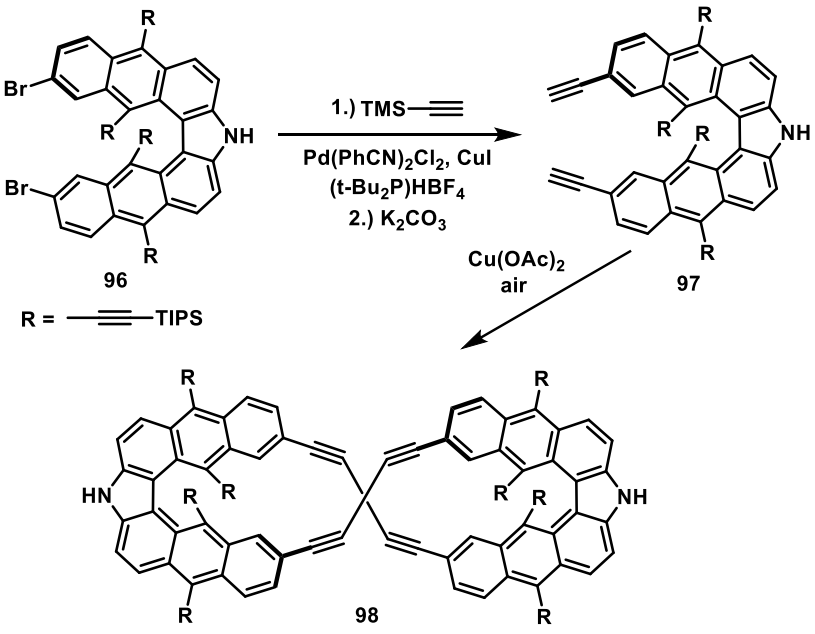

Scheme 2.32: Synthesis of bridged aza helicene dimer **98**.

After desilylation and resolution of racemate by HPLC on a chiral column, the enantiopure diyne (*P*)-**97** was subjected to Eglinton oxidative coupling of terminal

alkynes to undergo macrocyclisation delivering the bisbutadiyne bridged azahelicene dimer (*P*,*P*)-**98**.

The C-H functionalization and functional group transformation is very important for the conversion of helical molecules into some useful derivative. These derivatives can be explored for various applications and can provide useful handles to separate the enantiomers.

Owing to the benefits of CN group such as ease of introduction and availability of methods of functional group conversions, we decided to introduce cyano group in helical molecules. One of the easiest methods to incorporate cyano group is by Knovenagel condensation where a compound containing carbonyl group can be condensed with a compound having active methylene group (activated by a nearby cyano functional group) in alkaline media. Cyano group is a strong electron withdrawing group thereby can alter the electronic properties of helical molecules specially when conjugation with electron releasing group, giving the opportunity to undergo electron pull and push phenomenon. Cyano group can be transformed to many other functional groups such as $–CH_2NH_2$ (by reduction), -COOH (by hydrolysis) and many other possibilities.

2.9 Results and Discussion:

2.9.1 Synthesis of cyano aza[*n*]helicenes:

Our synthetic approach is based on the utilization of benzyl cyanide and its derivatives as a source to introduce cyano group on the helical backbone. For the synthesis of Cyano aza[5]helicenes, the key reaction in the sequence is Knovenagel reaction, providing stilbene-like precursor **101** by the reaction between 3-formyl *N*-butyl carbazole **99** and of benzyl cyanide **100** with sodium ethoxide as a base at room temperature to get olefin **101** in 89% yield. The aldehyde derivative was prepared from *N*-butyl carbazole by Vilsmeier-Haack reaction using phosphorous oxychloride and dimethyl formamide in an excellent yield using reported literature procedure. The photocyclization of olefin precursor **101** using 250 W high-pressure mercury vapor lamp in toluene with the presence of stoichiometric amount of iodine and excess of THF gives compound **102** in 83% yield, no linear isomer formed during the photocyclization. (**Scheme 2.23**)

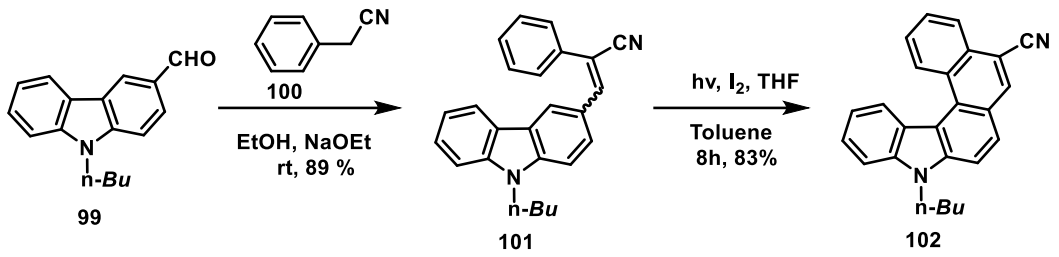

Scheme 2.33: Synthesis of 5-Cyano aza[5]helicene **102**.

The cyano functional group serves here to increase the solubility and also act as a suitable starting point for further structural modifications. After the successful synthesis of compound **102** we tested its configurational stability at ambient conditions by chiral phase HPLC analysis. No separation of peaks was observed over various chiral HPLC columns confirming their dynamic behavior. Compound **102** was also investigated for functionalization reactions. We carried out Vilsmier Haack formylation reaction on compound **102** in presence of dry DMF and $POCl_3$ to get compound **103** in 81% yield. Compound **103** was then subjected to hydrogen peroxide mediated rearrangement reaction in presence of acid catalyst gave the hydroxy derivative **104** of aza[5]helicene in excellent yield of 86%. (**Scheme 2.34**)

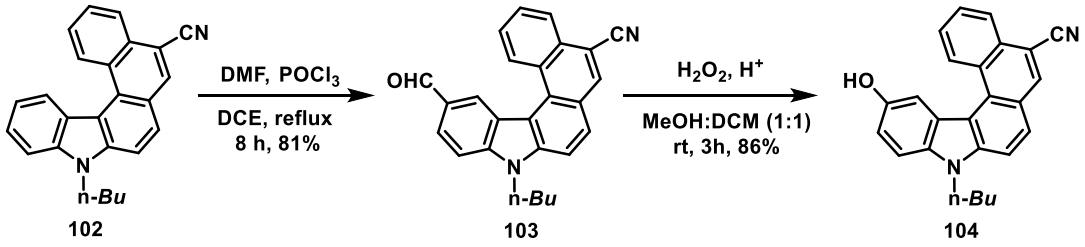

Scheme 2.34: Post functionalization of compound **102**.

With the compound **104** in hand; we began to develop conditions for homo coupling reaction. Different coupling conditions were tried such as $(t\text{-}BuO)_2$, $(PhCO_2)_2$, $CuSO_4/Al_2O_3$, $CuCl_2$/TMEDA, $FeCl_3$, H_2O_2 and $VO(acac)_2$. Instead of getting the desired polar dihydroxy coupling product **105**, in majority of cases we observed decomposition or formation of a non polar unidentifiable spot.

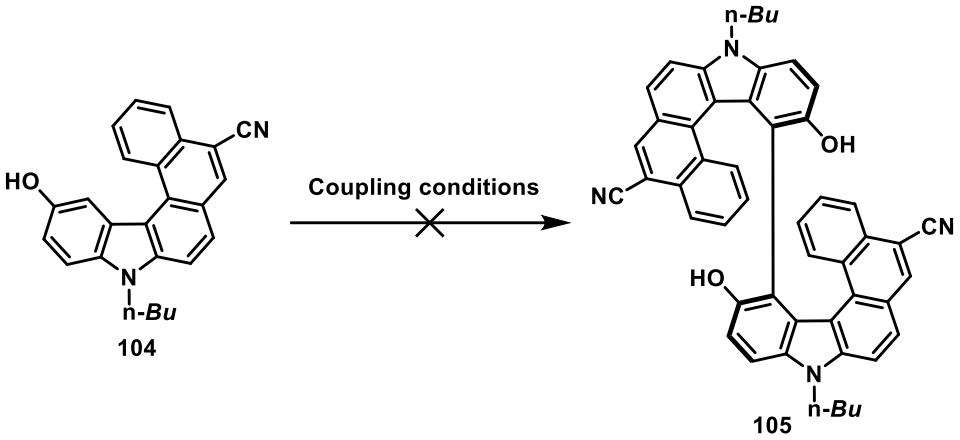

Scheme 2.35: Attempted synthesis of dihydroxy aza[5]helicene **105**.

In order to increases the configurational stability of helical molecules we decided to introduce one more aromatic ring. One of the starting materials **99** remains same while the second counterpart (derivative of benzyl cyanide) was synthesized by following the sequence of bromination of 2-methyl naphthalene **106** with *N*-bromosuccinimide in the presence of light using benzoyl peroxide as an initiator which gave 2-(bromomethyl)naphthalene **107**. This 2-(bromomethyl) naphthalene was converted to 2-(cyanomethyl) naphthalene **108** using potassium cyanide in toluene water (9:1) mixture using 20 mol % TBAB (tetrabutylammoniumbromide) as a phase transfer catalyst.

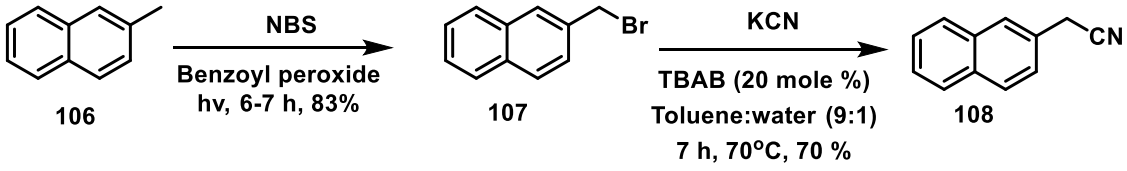

Scheme 2.36: Synthesis of compound **108**.

Both the reactant 3-formyl *N*-butyl carbazole **99** and 2-(cyanomethyl)naphthalene **108** was then subjected to Knovenagel reaction in dry ethanol in presence of sodium ethoxide as base, reaction proceed smoothly in 6-7 hour with a good yield (83 %) of olefin **109** (Precursor for photocyclization). The olefin was subjected to standard photocyclization conditions using iodine and tetrahydrofuran in toluene as solvent, careful analysis of the product revealed the formation of helicene within 7-8 hours. The reaction was carried out in routine immersion well photo reactor using 250 W High

pressure mercury vapor lamp (HPMV). The product formed was separated and identified using NMR, mass and single crystal analysis.

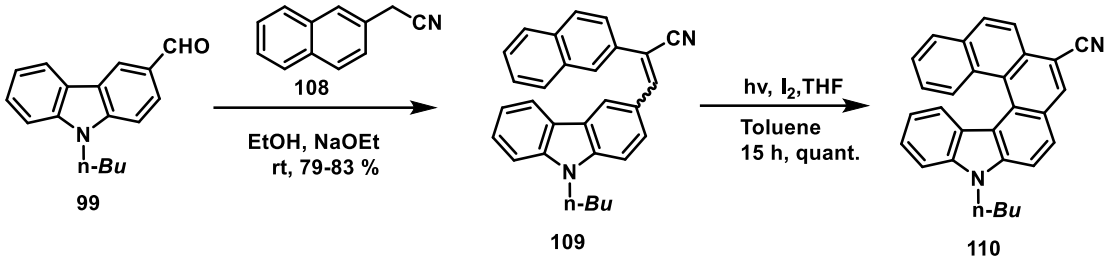

Scheme 2.37: Synthesis of 7-Cyano aza[6]helicene **110**.

The HPLC analysis of **110** shows two well separated peaks at 20.9 and 22.6 (10 % IPA:hexane, Daicel make Chiralpak IC Column, 1.0 mL/min flow rate) which indicates good configurational stability at room temperature; so we decided to synthesize this compound in large quantity and explore its resolution and applications. Before we tried the synthesis of compound **110**, we also attempted the synthesis of aza[6]helicene **112** without having cyano group attached to the alkene. This compound **111** was then subjected to photocyclization, TLC of reaction mixture suggested disappearance of starting material within 5 hours.

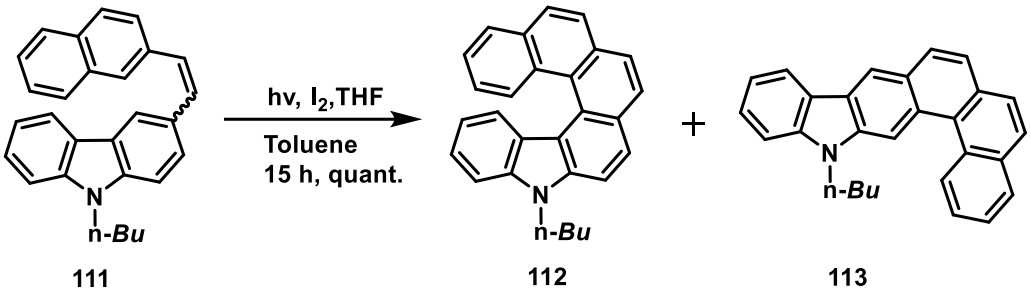

Scheme 2.38: Photocyclization of compound **111**.

A comparative study for the photocyclization of compound **110** and **112** was carried out. The photocyclization of precursor olefins **109** (having CN group) and **111** (without CN) group were subjected to photocyclization under identical conditions. The ^{1}H-NMR of crude reaction mixture was recorded. We observed significant difference in the regioselectivity of two substrates. Although in both the conditions we observed mixture of angular and linear isomers, but the ratio of angular, linear product for the photocyclization of **109** was 1:0.19 while for compound **111** it was 1.0:0.57 (**Figure 2.16**). Quantitative yield was found for olefin **109** while for olefin **111**, 83% yield was

observed. Moreover, the separation of regiomers having CN could be accomplished by simply crystallizing in $CHCl_3$ and pet ether giving 71% of pure angularly cyclized product **110**. On the other hand the regiomer mixture of compounds **112** and **113** could not be separated by column chromatography or by crystallization technique. So presence of CN serves two purposes it provides improvement in the regioselectivity of photocyclization[62] and ease of separation of regiomers.

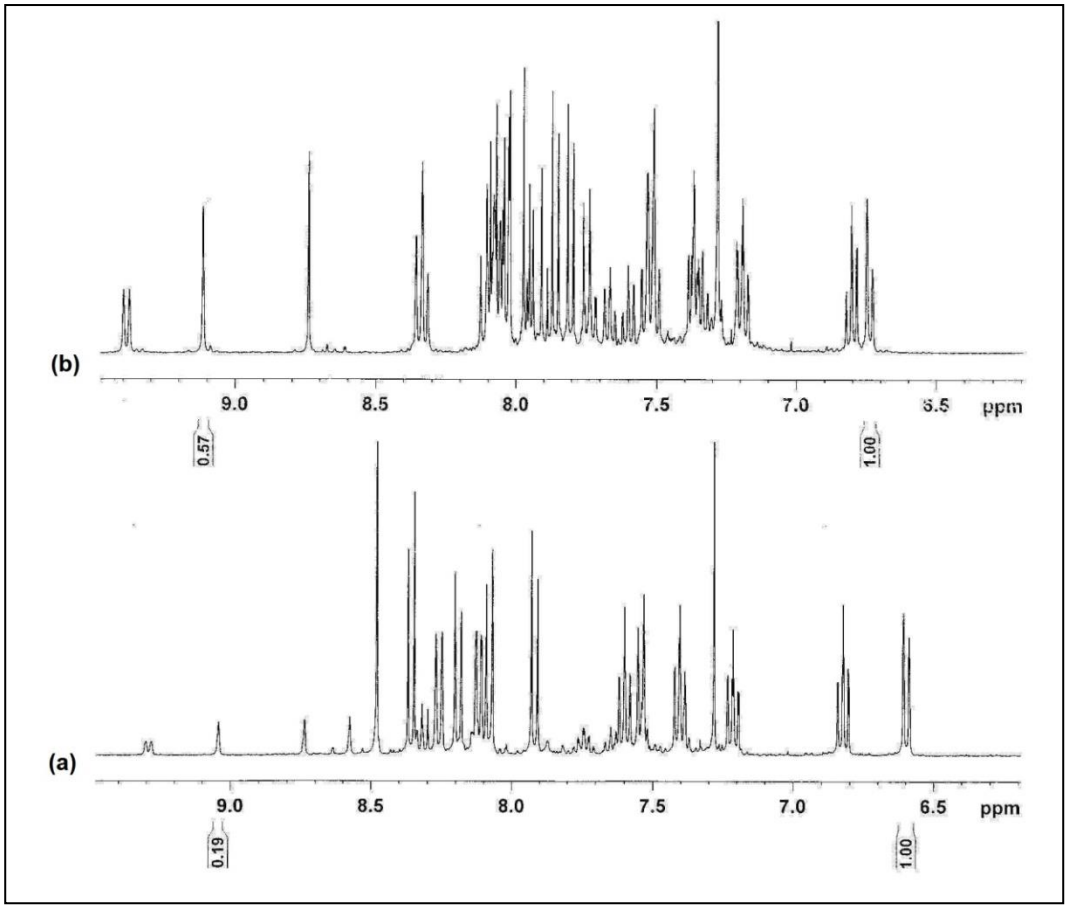

Figure 2.16: Effect of CN on the regioselectivity of photocyclization. (a) with CN (b) without CN.

We further attempted to extend this strategy for even larger helicene (aza[7]helicene). The counterpart for aldehyde was cyano methyl phenanthrene **119**; which was synthesized by few simple operations. The Heck reaction between *p*-methyl styrene **114** and iodo benzene **115** gave stilbene derivative **116** in 91% yield which was then subjected to photocyclization, the reaction was monitored by ^{1}H-NMR. Side chain bromination was performed on compound **117** with NBS. This conversion was found to be low yielding in tungsten lamp bulb (22%), but under thermal conditions yield slightly improved to 41%. This was the limiting step of this synthesis, for unknown reasons this step was low yielding in our hands. The compound **118** was then treated

with KCN in ethanol water (9:1 mixture) to get cyano methyl derivative **119** in 80% yields with an overall yield of 25% from **114**.

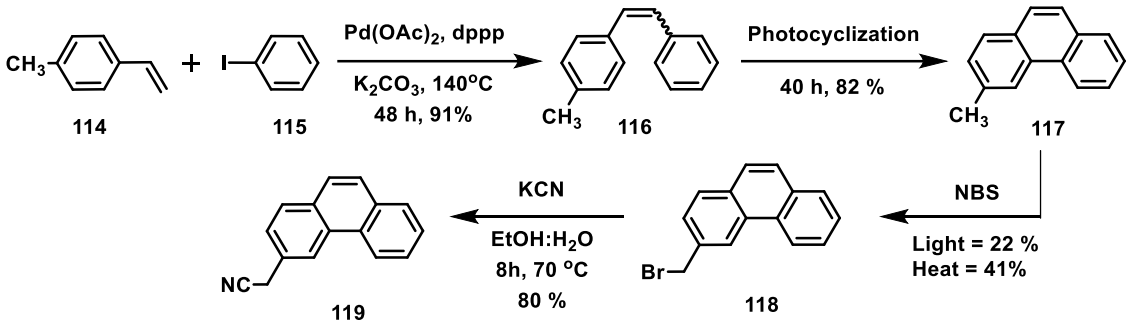

Scheme 2.39: Synthesis of Cyano methyl phenanthrene **119**.

To solve the low yield problem another approach was adopted; styrene **120** was treated with *p*-bromo benzyl cyanide **121** under Heck reaction conditions at slightly lower temperature of 90°C to get stilbene derivative **122** in good yield (83%). The stilbene **122** was then subjected to standard photocyclization conditions to get desired phenanthrene **119** in 78% yield. The overall yield for this approach was much improved (60%).

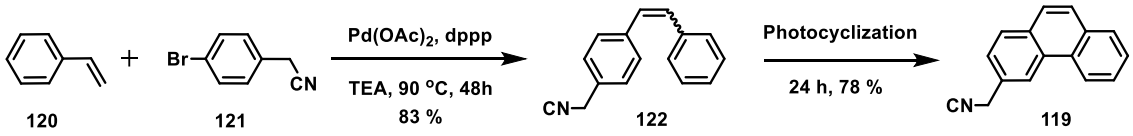

Scheme 2.40: A different approach for the synthesis of cyano methyl naphthalene **119**.

Both the reactants 3-formyl *N*-butyl carbazole **99** and (cyanomethyl) phenanthrene **119** were then subjected to Knovenagel reaction in presence of sodium ethoxide as base, reaction goes smoothly within 6-7 hours with a good yield (71%) of olefin **123**. The olefin was then subjected to standard photocyclization conditions. Careful analysis of the product revealed the formation of mixture of products. The products formed were separated and identified by NMR, mass and single crystal analysis. Unlike in the photocyclization of cyano aza[6]helicene, even the presence of cyano could not control the regioselectivity and we got the mixture of angular **124** (35%) and **125** linear (30%) products. The linear compound **125** was found to be highly fluorescent. Formation of

both the regiomers on the photocyclization of **123** suggests the electronic favorable factors were compromised by the presence of larger steric hindrance (**Scheme 2.41**).

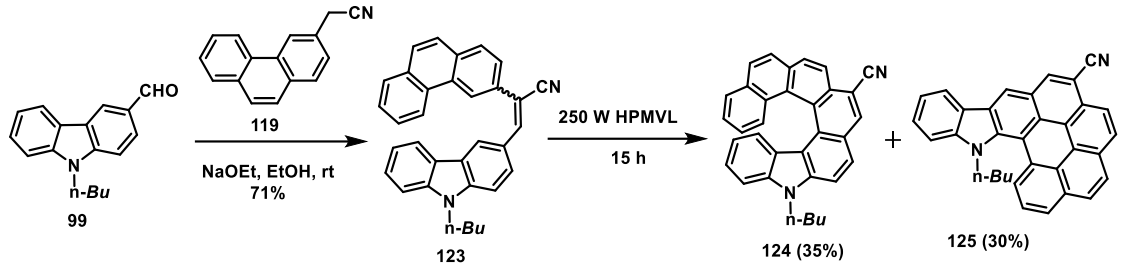

Scheme 2.41: Synthesis of Cyano aza[7]helicene **124**.

After the successful synthesis of penta **102**, hexa **110** and hepta **124** cyano aza[n]helicenes, we found that penta helicene is configurationally not stable at room temperature and hence its enantiomers cannot be separated. Hepta helicene proved to be difficult to synthesize in large quantities as mixture of regiomers were formed during photocyclization which were difficult to separate. Hexa helicene was undoubtedly the best intermediate for the purpose of post functionalization, functional group transformation and for the separations of enantiomers because of their high configurational stability and ease of scalability.

2.9.2 Functional group transformation of cyano aza[6]helicene (110):

Besides high yielding reactions, imparting good crystalline nature and controlling the regioselectivity of photocyclization reaction, the presence of cyano functionality can be utilized for modifications in to different important functional groups. In this direction we attempted to convert cyano to carboxylic acid by base catalyzed hydrolysis. Initial approaches were based on routinely available methods to reflux the compound in ethanol in presence of NaOH or KOH as base was failed possibly due to poor solubility of compound **110** in ethanol. We also attempted the similar reaction in mixed solvent system such as ethanol-THF, but without any success. High boiling solvent 2-methoxy ethanol with base was also tried under refluxing conditions for 5 days but result remains same. Lastly we decided to use high boiling alcoholic solvent such as diethylene glycol with KOH as base; to our satisfaction reaction gave a clean quantitative conversion to carboxylic acid **126** in 24 hours.

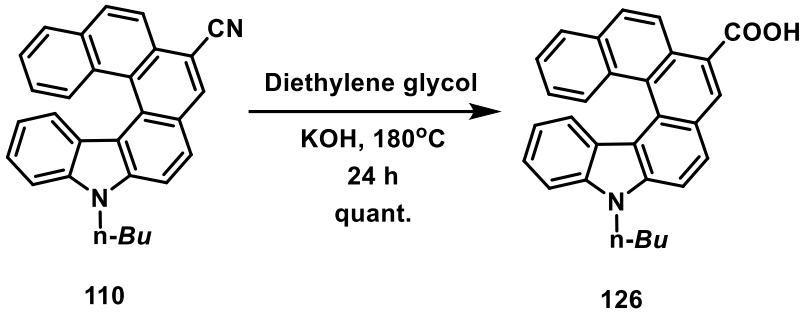

110 126

Scheme 2.42: Synthesis of compound **126**.

We also attempted to reduce cyano functionality to amine by reduction. We tried different methods for reduction such as $LiAlH_4$, (multiple products formed), $NaBH_4$ + I_2, palladium on charcoal, under hydrogen atmosphere but the desired conversion could not be achieved. The desired transformation could be achieved by $NiCl_2$+$NaBH_4$ in ethanol **127**. The amine **127** was not purified and directly converted in to *N*, *N*-dimethyl amine **128** using formaldehyde and sodium cyanoborohydride. The overall yield for this transformation was 17% only. The limiting factor was incomplete conversion of cyano group to amine. We observed that the reduction reaction in $NiCl_2$ strictly needs to be perform at room temperature; at elevated temperature complete disappearance of cyano aza[6]helicene was observed and unexpected ethyl group insertion in the product was observed although the actual structure could not be confirmed by ^1H NMR. We believe the source of ethyl group might be the solvent (ethanol) itself.

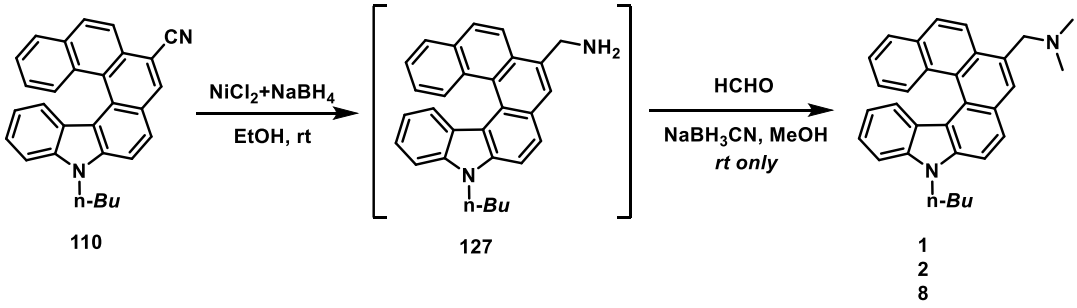

110 127 128

Scheme 2.43: Synthesis of compound **128**.

Attempts to carry out transformation of cyano to aldehyde using DIBAL-H and Ni-Al alloy/HCOOH failed, while the Grignard reaction on the compound **110** gave mixture of products in very low yield to proceed any further in this direction.

2.9.3 Functionalization of cyano aza[6]helicene (110) via electrophilic aromatic substation and post functionalization:

As carbazole is very susceptible to electrophilic aromatic substitution reaction, carbazole derived helicene can be converted to various useful helical skeletons.

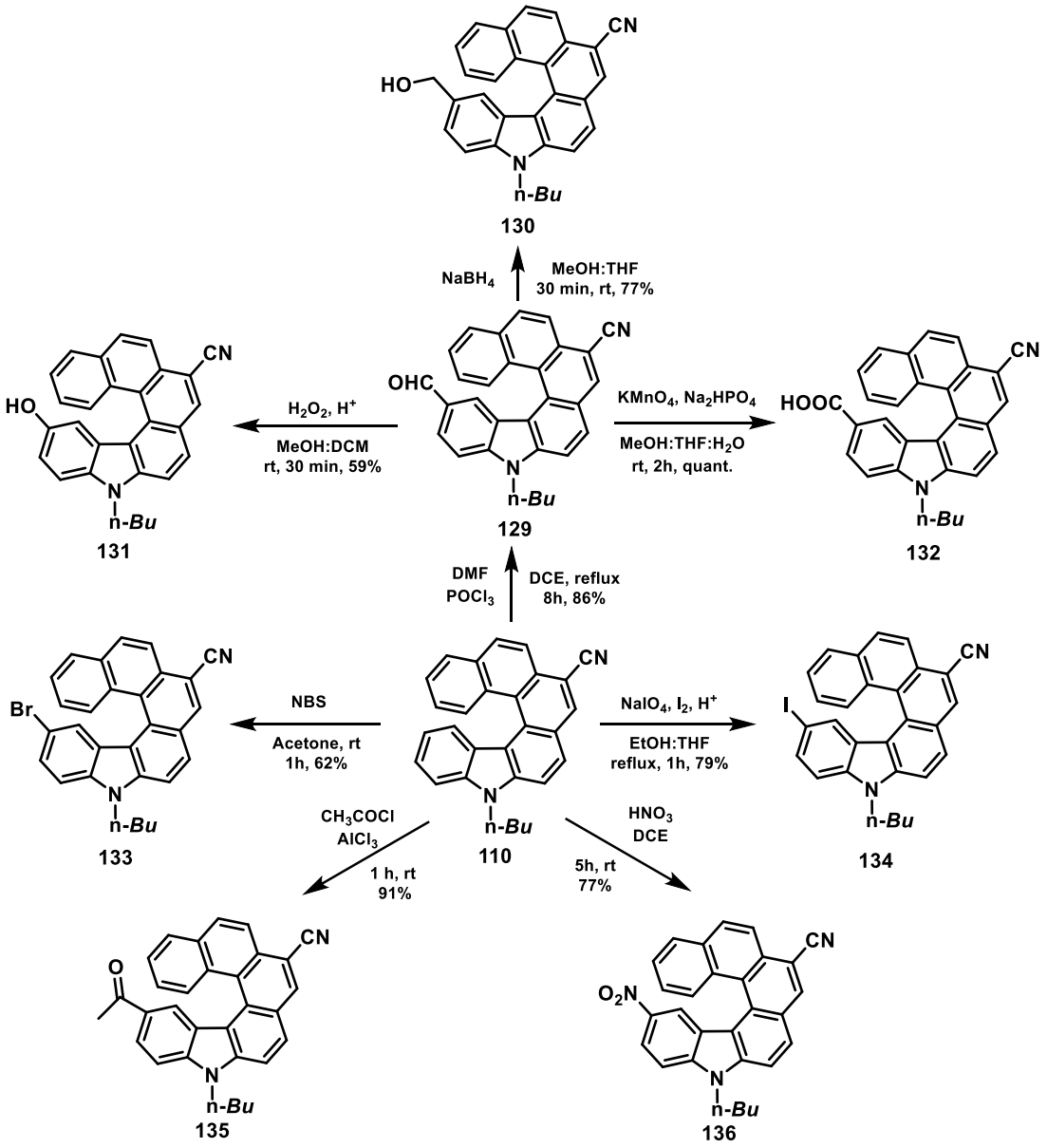

Scheme 2.44: Functionalization of compound **110**.

Firstly we carried out Vilsmier Haack formylation reaction on compound **110** in presence of dry DMF and $POCl_3$ to get compound **129** in 86% yield. The aldehyde derivative **129** was then reduced to primary alcohol **130** using $NaBH_4$ in 77% yield; aldehyde **129** was also oxidized to carboxylic acid **132** using $KMnO_4$ in quantitative

yield. The compound **132** was confirmed using ^{1}H NMR and IR spectroscopy, the compound **132** shows poor solubility in all common organic solvents. One more transformation of aldehyde to phenolic hydroxyl group **131** was also performed using H_2O_2 in presence of catalytic amount of H_2SO_4 to get 59% yield. Electrophilic aromatic halogenation of compound **110** using NBS gave bromo helicene **133** in 62% yield and iodination was achieved using $NaIO_4$, I_2 in presence of acid catalyst. Other transformations such as Friedel Crafts acylation using acetyl chloride and $AlCl_3$ gave the desired target molecule **135** in excellent yield of 91%, nitrations was easily done using HNO_3 to get compound **136**. All the above reactions resulted in formation of expected products and can offer generally useful methods to access functionalized aza[6]helicenes.

2.9.4 Attempted enzymatic resolution of compound (130):

The alcohol **130** is a perfect synthon to attempt separation of isomers by kinetic resolution. This strategy can easily open up possibility to screen suitable bio catalyst to selectively convert one of the isomers into acetyl derivative **137**, in enantioselective manner (**Scheme 2.45**).

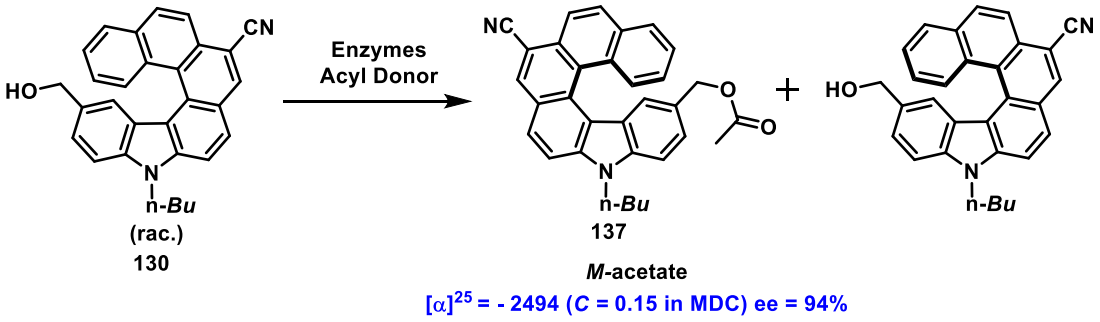

Scheme 2.45: Attempted enzymatic resolution of compound **130**.

The reaction course was monitored by chiral HPLC (Chiral OD-H column). The results of the kinetic resolutions are summarized in **Table 2.6**. Acetylation of rac-**130** in the presence of Lipase proceeded to give no enantioselectivity (entry 1). Furthermore, even the longer reaction time with higher equivalents of enzymes and acyl donors did not change the outcome of reaction. Amano PS also showed very low reactivity and low enantioselectivity (entry 2). The best results were seen when we used Novozyme enzyme. With 2.0 w/w equivalents of vinyl acetate in dichloromethane at room temperature gave acetate **137** in 33% yield with 72% ee (entry-3). Acetate **137** on

crystallization in chloroform and pet ether gave material with 94% ee in 24% yield. The specific optical rotation value of acetate was -2494 (*C* = 0.15 in dichloromethane). Although the product was obtained in less quantity, this method gave us a way to resolve isomers of helical alcohol **130**

Sr. No.	Enzyme	Acyl Donor	Solvent	Acetate	Alcohol	Time	Remarks
1.	Lipase (1:1 w/w to (1:3)	Vinyl acetate/ isopropenyl acetate (up to 10 equiv.)	THF/MDC	Poor conversion on TLC	---	1 to 10 days	---
2.	Amano PS	Vinyl acetate/ IPA (1-2 equiv.)	THF/MDC	Poor conversion on TLC	---	1 to 6 days	*P* Acetate enriched Yield = 23 % ee = 70.5 %
3	Novozyme (1:1 w/w)	Vinyl acetate (2 equiv.)	MDC	ee =72 %, Yield = 33 %	ee = 13.41% Yield= 47%	3 days 16 h	After crystallization ee of acetate increases up to 94% Yield = 24 %
4.	Novozyme (1:1 w/w)	IPA (2 equiv.)	MDC	ee = 87 % Yield = 23 %	ee = 16 % Yield = 59%	5 days 15 h	

Table 2.6: Enzymatic resolution of compound **130**.

2.9.5 Synthesis and Resolution of aza[6]helicene based amine ligands:

The ease of synthesis and configurational stability of compound **110** prompted us to synthesize and resolve amino substituted aza[6]helicene. The method of choice for the resolution was diastereomeric separation using a chiral amine utilizing the Buchwald−Hartwig amination reaction. Amination reaction of **110** with S-(−)-α-methyl benzylamine using Cs_2CO_3, as the base, 10 mol % $Pd(OAc)_2$, 5.0 mol % XPhos, and toluene as the solvent gave desired product in 59% yield (1.0:0.6 mixture of diastereomers) (**Scheme 2.46**). The major side product was the dehalogenation product **110**. The ratio was determined by chiral HPLC. The obtained diastereomers were readily separated using standard column chromatography.

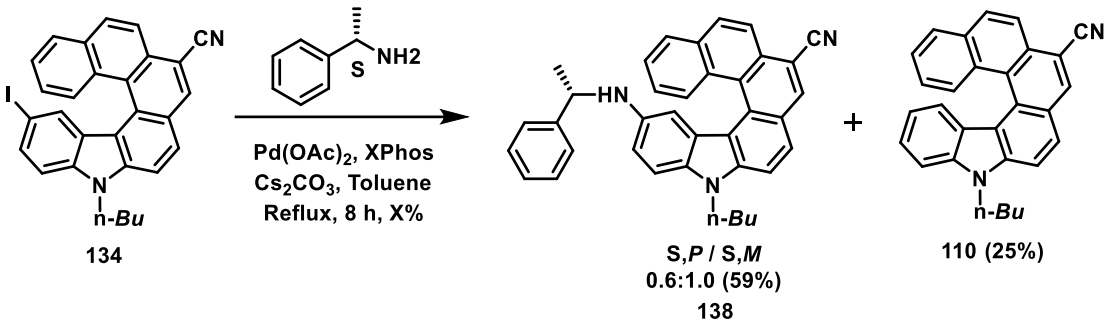

Scheme 2.46: Synthesis of ligand 1 (**Compound 138**).

The aim was to synthesize various amino helicenes and test their applications as chiral sensors, chiral solvating agents or to study their biological binding properties. In order to study the effects of distance of additional chiral centre apart from helicene chirality another amino ligand was synthesized having additional methylene group. Initial attempts to synthesize amino ligand **139** using conventional technique of refluxing aldehyde **129** with S-(−)-α-methyl benzylamine in presence of acid catalyst with Dean Stark apparatus did not gave the desirable conversion. A different method of reductive amination using titanium(IV) isopropoxide-sodium borohydride was used. To our satisfaction the reaction worked well and the product was obtained in good yield (68%). Surprisingly reaction was highly diastereoselective 90% > d.e.; which may be attributed to bulky nature of the helicene framework.

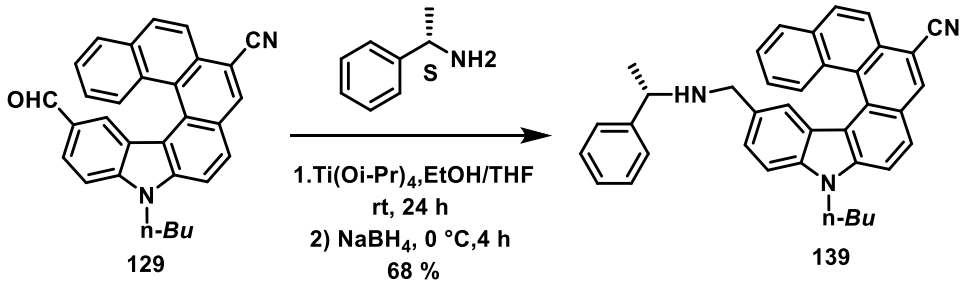

Scheme 2.47: Synthesis of ligand 2 (Compound **139**).

Using similar approach third amino ligand containing *N*,*N*-dimethyl amino side chain has been synthesized. The yield of the reaction was 48%. Attempts to resolve compound **140** are currently under progress.

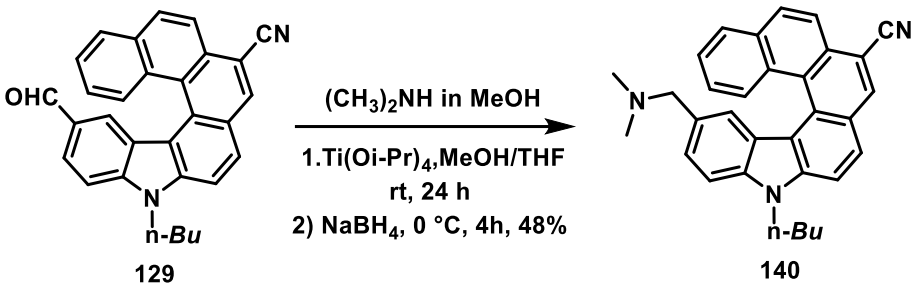

Scheme 2.48: Synthesis of ligand 3. (**Compound 140**)

2.10 Synthesis of dicyano aza[9]helicene:

The encouraging regiocontrol of photocyclization for compound **110** in the presence of CN prompted us to test this hypothesis on symmetrical dicyano aza[9]helicene. As previously discussed the photocyclization for the preparation of aza[9]helicene dramatically gave us mixture of four product and separation of them is quite challenging task. We decided to put CN group near the olefinic site in compound **141** to check whether it can improve the regiocontrol. Compound **141** was subjected to standard photocyclization conditions at high concentration. (250 mg in 350ml toluene) (**Figure 2.17**) The ^{1}H-NMR of crude reaction mixture was recorded which shows the presence of two sets of signals indicating the ratio of angular:linear isomers to be 2.08:0.13.

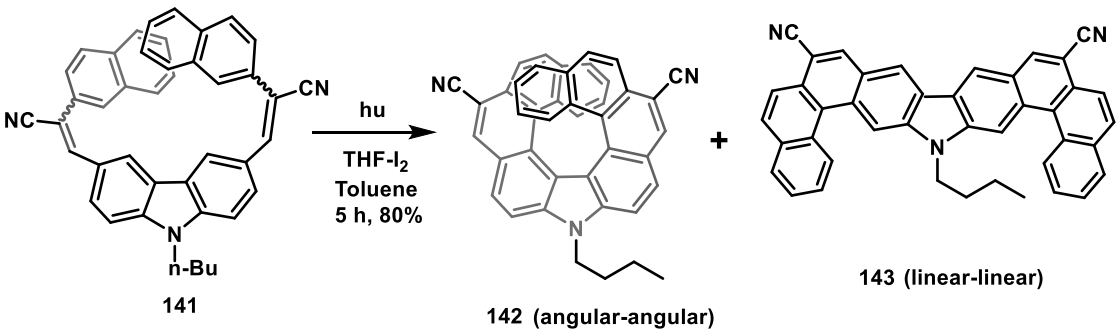

Scheme 2.49: synthesis of dicyano aza[9]helicene **142**.

During the synthesis of [9]helicene we have observed the formation of several products, to overcome this difficulty we were required to carry out phochemical cyclization under a dilute condition. The above result with suitably placed cyano group, helped in achieving a better selectivity in favour of angular isomer even at moderate

concentration. This is an interesting and important conclusion of this work. This result confirms the presence of CN improves the regioselectivity of photocyclization reaction.

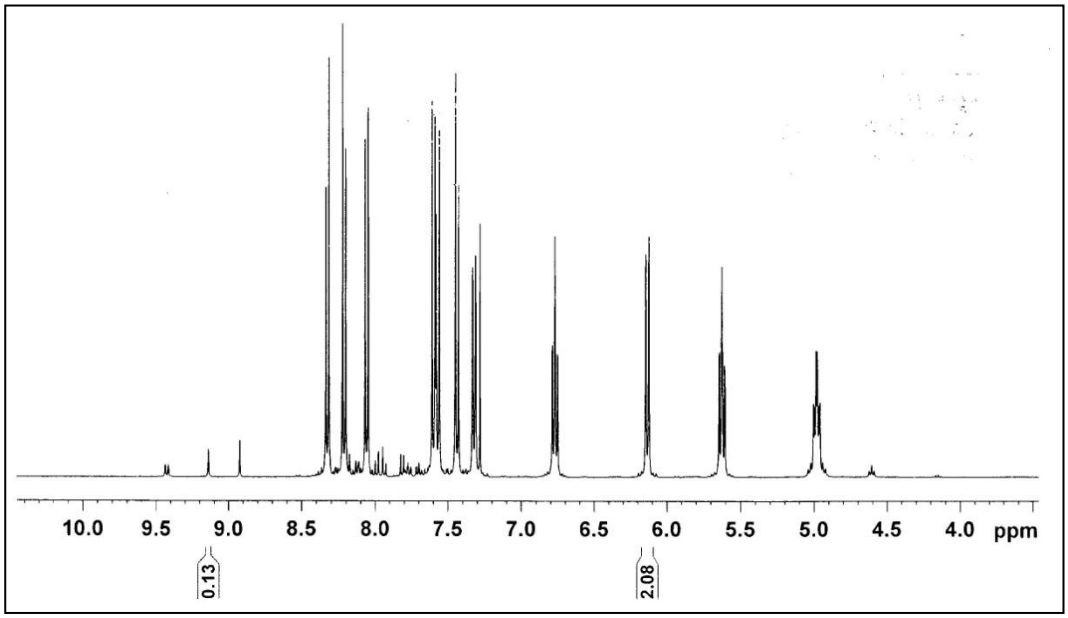

Figure 2.17: Influence of CN on the photocyclization of compound **142**.

2.11 Conclusion

In summary synthesis of symmetrical aza[7]helicenes have been achieved using oxidative photocyclization. Their photophysical and thermal properties were studied.

The same strategy was applied for the synthesis of larger aza[9]helicene and various regioisomers were carefully separated and their crystal structures and photophysical properties were studied.

Various CN group containing aza helicenes ([5], [6] and [7]). have been successfully synthesized. Configurationally stable aza[6]helicenes was then successfully tested for post functionalization and functional group conversion. Three different ligands have been prepared from aza[6]helicene. Two ligands were resolved and attempts to resolve third ligand is currently under process. Detailed investigations of these amino ligands as fluorescence sensors are currently under progress.

Two important observations were made during this course of study for regioselective photocyclization of carbazole based aza[*n*]helicene.

1. Higher dilution not only prevent the dimerization process but also controls the formation of angularly cyclized product for larger helicenes.
2. Presence of CN group near the olefinic site not only drasitically improves regioselectivity but also simplifies the purification from undesired products.

2.12 Experimental procedures:

3,6 -Diiodo carbazole (49):

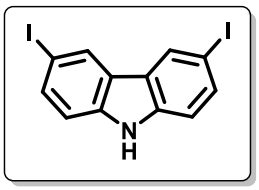

To a round bottom flask (250 mL, two-neck), equipped with a condenser, was loading a solution of carbazole (5.0 g, 29.90 mmol), KI (6.45 g, 38.87 mmol), KIO_3 (6.39 g, 29.90 mmol), acetic acid (100 mL) and deionized water (10 mL). The iodination reaction was continued at 80°C for 24 h. After cooling to room temperature, the mixture was filtered, washed with deionized water, saturated sodium carbonate solution, and methanol to afford a white light grey solid (11.91 g, 95%). The analytical data were in complete agreement with the previously published data.[63a]

^{1}H-NMR ($CDCl_3$, 400 MHz): δ 830 (s, 1H), 8.10 (s, 1H), 7.66 (d, *J* = 7.8 Hz), 7.20 (d, *J* = 7.6 Hz, 2H)

9-Butyl-3,6-diiodo-9*H*-carbazole (50):

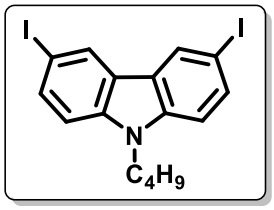

3,6-Diiodocarbazole **49** (2.0 g, 4.77 mmol), powdered potassium hydroxide (1.60 g, 28.65 mmol) were mixed in a flask containing acetone (25 mL). After stirred for 30 minutes, 1-bromobutane (0.98 g, 0.77 mL, 7.16 mmol) was added slowly. The solution was stirred for 5 h at room temperature. After the completion of the reaction, the mixture was poured in ice-cold water and extracted with ethyl acetate (3 x 100 mL). The combined organic phase was washed with water, brine and dried over anhydrous sodium sulfate. The solvent was removed under reduced pressure and the crude product was purified by column chromatography on silica gel using petroleum ether as an eluent to afford white solid (2.13 g, 94%). The analytical data were in complete agreement with the previously published data.[63a]

^{1}H-NMR ($CDCl_3$, 400 MHz): δ 8.34 (s, 2H), 7.72 (d, *J* = 8.4 Hz, 2H), 7.19 (d, *J* = 8.4 Hz, 2H), 4.24 (t, *J* = 7.2 Hz, 2H), 1.81 (m, 2H), 1.36-1.34 (m, 2H), 0.93 (t, *J* = 7.2 Hz, 3H).

General procedure for the synthesis of di-styryl derivative by Mizoroki-Heck reaction:

3,6-Distyryl-9-butyl-9*H*-carbazole (51):

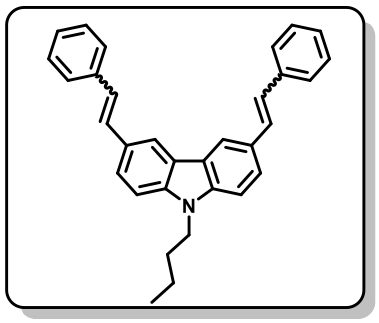

A solution of palladium acetate (0.009 g, 0.042 mmol, 2 mol %) and 1,3- bis(diphenylphosphinopropane) (0.034 g, 0.084 mmol, 4 mol %) was prepared in *N*,*N*-dimethylacetamide (5 mL) under nitrogen atmosphere. The mixture was stirred at room temperature until a homogeneous solution was obtained. This catalyst solution was repeatedly purged by N_2 prior to use.

A two-necked round bottom flask was charged with 3, 6-diiodo-*N*-butylcarbazole **50** (1.0 g, 2.1 mmol), dry potassium carbonate (1.16 g, 8.4 mmol), TBAB (0.135 g, 0.42 mmol, 20 mol %), and *N*,*N*-dimethylacetamide (10 mL). The solution was repeatedly purged with N_2. Styrene (0.546 g, 5.25 mmol) was added at 60 ºC and the mixture was heated up to 100 ºC. At 100 ºC, the previously prepared Pd catalyst solution was added drop wise and the mixture was further heated to 140 ºC for 48 h. After the completion of the reaction, the mixture was poured into ice-cold water and extracted with dichloromethane (3 x 100 mL). The combined organic phase was washed with water, brine, and dried over anhydrous sodium sulfate. The solvent was removed under reduced pressure and the crude product was purified by column chromatography on silica gel using petroleum ether–ethyl acetate (98:2) as eluent to afford predominantly *trans* isomer of 3,6-distyryl-*N*-butylcarbazole **51** as light yellow solid (0.845 g (94 %), m.p. = 152–156 ºC.

^{1}H-NMR (400 MHz, $CDCl_3$): δ 8.29 (s, 2H), 7.70 (dd, *J* = 8.8 and 1.6 Hz, 2H), 7.62 (d, *J* = 7.6 Hz, 4H), 7.45–7.38 (m, 6H), 7.32-7.28 (m, 4H), 7.21 (d, *J* = 16.4 Hz), 4.29 (t, *J* = 7.2, 2H), 1.90–1.85 (m, 2H), 1.48–1.40 (m, 2H), 0.99 (t, *J* = 7.2 Hz, 3H).

^{13}C-NMR (100 MHz, $CDCl_3$): δ 140.6, 137.9, 129.5, 128.7, 127.1, 126.2, 126.1, 124.6, 123.2, 118.7, 109.1, 43.0, 31.2, 20.5, 13.9

MS (EI): m/z, (%) 428 (83), 427 (24), 426 (100), 385 (55).

IR (KBr): 3438, 3023, 2954, 2867, 1623, 1592, 1484, 1382, 1341, 1244, 1208, 1153, 1130, 1070, 959, 881, 802, 751, 690 $cm.^{-1}$

9-Butyl-3,6-bis(4-methylstyryl)-9*H*-carbazole (52):

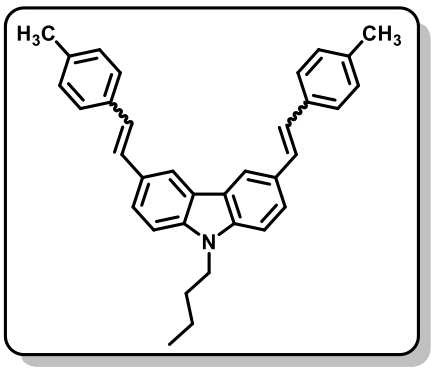

Yield = 87%, Physical state = Light yellow solid
m.p. = 182–186 °C.
^{1}H-NMR (400 MHz, $CDCl_3$): δ 8.27 (d, *J* = 1.2 Hz), 7.68 (dd, *J* = 8.4 and 1.2 Hz), 7.49 (d, *J* = 8.0 Hz), 7.39 (d, *J* = 8.4 Hz), 7.32-7.14 (m, 6H), 4.32 (t, *J* = 7.2 Hz, 2H), 2.40 (s, 6H), 2.07-1.85 (m, 2H), 1.45-1.37 (m, 2H), 0.97 (t, *J* = 7.6 Hz, 3H).
IR (KBr): 3439, 3003, 2951, 2877, 1725, 1623, 1592, 1484, 1382, 1341, 1244, 1208, 1153, 1130, 1070, 959, 881, 802, $cm.^{-1}$

General procedure for the synthesis of di-styryl derivative by one pot Wittig-Heck reaction:

3,6-di(4-methoxystyryl)-9-butyl-9*H*-carbazole (55):

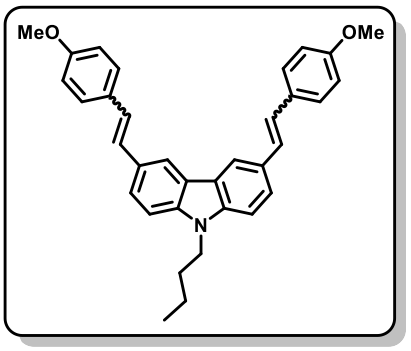

A solution of palladium acetate (0.010g, 0.042 mmol, 2 mol%) and 1.3-bis(diphenylphosphinopropane) (0.034 g, 0.084 mmol, 4 mol%) was prepared in *N,N*-dimethylacetamide (5 mL) under nitrogen atmosphere. The mixture was stirred at room temperature until a homogeneous solution was obtained. This catalyst solution was repeatedly purged by N_2 prior to use.

A two neck round bottom flask was charged with 3, 6-diiodo-*N*-butylcarbazole **50** (1.0 g, 2.10 mmol), 4-methoxy benzaldehyde (0.715 g, 5.26 mmol), methyltriphenylphosphonium iodide (2.56 g, 6.31mmol), dry potassium carbonate (2.18g, 15.7 mmol), TBAB (0.135 g, 0.42 mmol, 20 mol%) and *N,N*-dimethylacetamide (10 mL) and the mixture was heated up to 100 °C. When the temperature reached 100 °C, the previously prepared Pd catalyst solution was added drop wise and the mixture was heated to 140 °C for 48 h. After the completion of the reaction, the mixture was poured in ice-cold water and extracted with dichloromethane (3 x 100 mL). The combined organic phase was washed with water, brine and dried over anhydrous sodium sulfate. The solvent was removed under reduced pressure and the crude product was purified by column chromatography on silica gel using

petroleum ether:ethyl acetate (95:5) as eluent to afford predominantly *trans* isomer of 3,6-bis-(4-methoxystyryl)-*N*-butylcarbazole **55** as light yellow solid (0.887 g, 87%).

m.p. = 201-203 °C

^{1}H-NMR (400 MHz, $CDCl_3$): δ 8.22-8.21 (d, *J* = 1.2 Hz, 2H), 7.63-7.61 (dd, *J* = 8.4 Hz and 1.2 Hz, 2H), 7.51-7.48 (broad d, 4H), 7.34-7.32 (d, *J* = 8.4 Hz, 2H), 7.20-7.16 (d, *J* = 16.4 Hz), 7.12-7.08 (d, *J* = 16.4 Hz, 2H), 6.93-6.91 (broad d, 4H) 4.27-4.23 (t, *J* = 7.2, 2H), 3.83 (s, 6H), 1.87-1.80 (m, 2H), 1.42-1.33 (m, 2H), 0.98-0.91 (t, *J* = 7.2 Hz, 3H).

^{13}C-NMR (100 MHz, $CDCl_3$): δ 158.8, 140.4, 130.8, 129.0, 127.5, 127.4, 125.6, 124.4, 123.2, 118.3, 114.1, 109.0, 55.3, 43.0, 31.2, 20.5, 13.9.

MS (EI): *m/z*, (%) 489 (10), 488 (29), 487 (100), 486 (42), 485 (47), 445 (10), 444 (13), 443 (16), 428 (08), 341 (06), 243 (10), 136 (12), 95 (16).

IR (KBr): 3429, 3020, 2957, 1872, 1604, 1482, 1383, 1344, 1301, 1246, 1175, 1109, 1033, 961, 851, 818, 760 $cm.^{-1}$

9-Butyl-3,6-bis(4-fluorostyryl)-9*H*-carbazole (56):

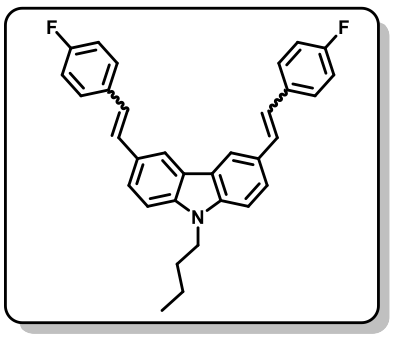

Yield = 52%, Physical State = Light yellow solid.

m.p. = 200-204 °C

^{1}H-NMR ($CDCl_3$, 400 MHz): δ 8.26 (d, *J* = 1.6 Hz, 2H), 7.67 (dd, *J* = 8.4 Hz, *J* = 1.6 Hz, 2H), 7.56-7.53 (m, 4H), 7.40 (d, *J* = 8.4 Hz, 2H), 7.26 (d, *J* = 16.4 Hz, 2H), 7.14 (d, *J* = 16.4 Hz, 2H), 7.08 (d, *J* = 8.8 Hz, 4H), 4.32 (t, *J* = 7.2 Hz, 2H), 1.93-1.86 (m, 2H), 1.46-1.40 (m, 2H), 0.97 (t, *J* = 7.2 Hz, 3H).

General procedure for photocyclization of aza[7]helicenes

***N*-butyl aza[7]helicene (57):**

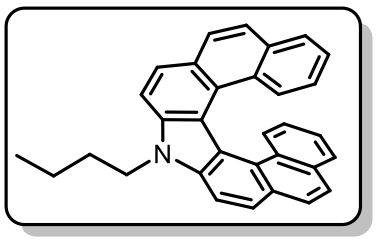

A solution of 3, 6-distyryl-*N*-butylcarbazole **51** (0.350 g, 0.82 mmol), iodine (0.457 g, 1.80 mmol), dry THF (2.95 g, 3.32 mL, 41.3 mmol), and toluene (1.2 L) was irradiated using a 125W HMPV lamp (24 h monitored by TLC). After the completion of the reaction, the excess of iodine was removed by washing the solution with aqueous $Na_2S_2O_3$ and

water. The organic layer was concentrated under reduced pressure to obtain the crude product. The crude product was purified by column chromatography over silica gel using petroleum ether– ethyl acetate (98:2) as eluent to obtain title compound **57** as light brown solid (0.151 g, 44 %), m.p. = 206-208 ºC.

^{1}H-NMR (400 MHz, $CDCl_3$): δ 8.11 (d, *J* = 8.4 Hz, 2H), 8.02 (d, *J* = 8.4 Hz, 2H), 7.95 (d, *J* = 8.4 Hz, 2H), 7.83–7.81 (m, 4H), 7.44 (d, *J* = 8.4 Hz, 2H), 7.25-7.15 (m, 2H), 6.25–6.21 (m, 2H), 4.76 (t, *J* = 7.2 Hz, 2H), 2.10–2.04 (m, 2H), 1.57–1.51(m, 4H signal merged with water peak), 1.01 (t, *J* = 7.2 Hz, 3H).

^{13}C-NMR (100 MHz, $CDCl_3$): δ 139.3, 131.2, 130.2, 128.2, 127.0, 126.7, 126.6, 126.6, 126.2, 125.9, 124.2, 122.6, 116.7, 109.6, 43.4, 31.9, 20.7, 13.9.

MS (EI): m/z, (%) 423 (100), 380 (34), 379 (15), 378 (04), 377 (06), 366 (13), 364 (08), 363 (08), 211 (03).

IR (KBr): 3427, 3042, 2952, 2927, 2867, 1725, 1660, 1588, 1522, 1495, 1450, 1339, 1283, 1218, 795, 746, 645 cm^{-1}.

HRMS (TOF MS ES+): *m/z* calculated for $C_{32}H_{24}NNa$ [M+Na]: 446.1879; observed 446.1879.

2,16-Dimethyl-*N*-butyl[7]azahelicene (58):

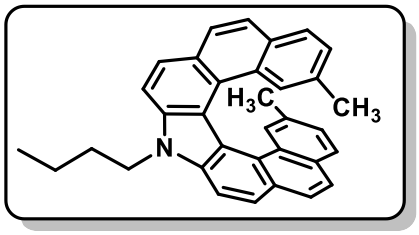

Yield = 40%, Physical state = Light yellow solid

m.p. = 245-248 ºC.

^{1}H-NMR (400 MHz, $CDCl_3$): δ 8.13 (d, *J* = 8.4 Hz, 2H), 8.0 (d, *J* = 8.4 Hz, 2H), 7.97 (d, *J* = 8.8 Hz, 2H), 7.86 (d, *J* = 8.4 Hz, 2H), 7.71 (d, *J* = 8.0 Hz, 2H), 7.15 (d, *J* = 0.8 Hz, 2H), 7.05 (dd, *J* = 8.0 and 1.2 Hz, 2H), 4.79 (t, *J* = 7.6 Hz, 2H), 2.15-2.07 (m, 2H), 1.59-1.54 (m, 2H), 1.54 (s, 6H), 1.04 (t, *J* = 7.6 Hz, 3H).

^{13}C-NMR (100 MHz, $CDCl_3$): δ 139.1, 132.3, 129.8, 129.6, 127.7, 127.6, 126.75, 126.70, 126.3, 126.0, 125.8, 123.7, 116.7, 109.4, 43.4, 31.9, 20.8, 20.7, 13.9

IR (KBr): 3435, 3042, 2957, 2917, 1722, 1584, 1508, 1339, 1155, 891, 831, 772, 647, 556 cm^{-1}

HRMS: calculated for $C_{34}H_{29}N$ 452.2371; observed 452.2372.

2,16-Dimethoxy-*N*-butyl[7]azahelicene (59):

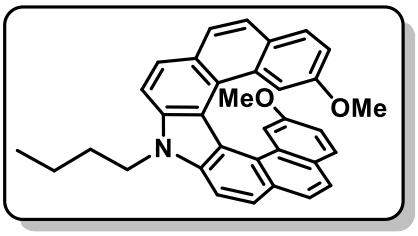

Yield = 44%, Physical State = Light yellow solid.

m.p. = 199-203 ºC

^{1}H-NMR (400 MHz, $CDCl_3$): δ 8.06 (d, *J* = 8.4 Hz, 2H), 7.93 (d, *J* = 8.4 Hz, 2H), 7.89 (d, *J* = 8.8 Hz, 2H), 7.79 (d, *J* = 8.4 Hz, 2H), 7.79 (d, *J* = 8.4 Hz, 2H), 7.73 (d, *J* = 8.4 Hz, 2H), 6.89-6.85 (m, 4H), 4.74 (t, *J* = 7.6 Hz, 2H), 2.47 (s, 6H), 2.12-2.04 (m, 2H), 1.60-1.51 (m, 2H), 1.02 (t, *J* = 7.2 Hz, 3H).

^{13}C-NMR (100 MHz, $CDCl_3$): δ 139.3, 131.2, 130.2, 128.2, 127.0, 126.7, 126.69, 126.61, 126.2, 125.9, 124.2, 122.6, 116.7, 109.6, 43.4, 31.9, 20.7, 13.9

MS (EI): m/z, (%) 423 (100), 380 (34), 379 (15), 378 (04), 377 (06), 366 (13), 364 (08), 363 (08), 211 (03).

IR (KBr): 3427, 3042, 2952, 2927, 2867, 1725, 1660, 1588, 1522, 1495, 1450, 1339, 1283, 1218, 795, 746, 645 cm^{-1}.

HRMS: Calculated for $C_{34}H_{29}NO_2Na$ 506.2091; Observed 506.2090.

2,16-Difluoro-*N*-butyl[7]azahelicene (60):

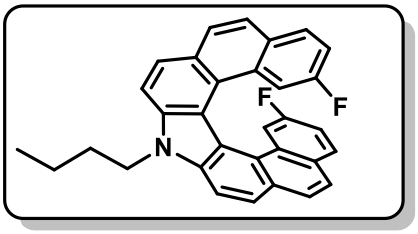

Yield = 37 %, Physical state = Light yellow solid.

m.p. = 244-248 ºC.

^{1}H-NMR (400 MHz, $CDCl_3$): δ 8.14 (d, *J* = 8.4 Hz, 2H), 8.02 (d, *J* = 8.8 Hz, 2H), 7.99 ((d, *J* = 8.4 Hz, 2H), 7.90-7.84 (m, 4H), 7.07 (dd, *J* = 7.6 and 2.8 Hz, 2H), 7.03-6.99 (m, 2H), 4.78 (t, *J* = 7.2 Hz, 2H), 2.13-2.06 (m, 2H), 1.57-1.54 (m, 2H), 1.03 (t, *J* = 7.6 Hz, 3H).

^{13}C-NMR (100 MHz, $CDCl_3$): δ 159.8, 157.4, 139.2, 131.1, 131.0, 128.5, 128.4, 127.0, 126.6, 126.18, 126.16, 123.9, 116.1, 114.9, 114.7, 112.3, 112.1, 110.3, 43.5, 31.9, 20.6, 13.9.

^{19}F-NMR (376 MHz, $CDCl_3$): δ –117.38.

IR (KBr): 3019, 2960, 1684, 1599, 1504, 1215, 832, 757, 668 cm^{-1}

HRMS: calculated for $C_{32}H_{23}NF_2$: 460.1874; observed 460.1871.

9-Butyl-3,6-bis (-2-(naphthalen-2-yl) vinyl)-9*H*-carbazole (64):

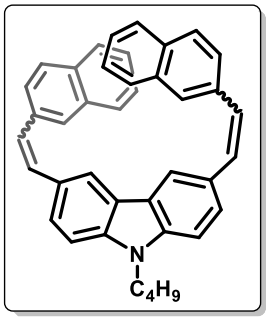

A solution of palladium acetate (0.004g, 0.021 mmol, 2 mol%) and 1,3-bis(diphenylphosphinopropane) (0.017 g, 0.042 mmol, 4 mol%) was prepared in *N,N*-dimethylacetamide (5 mL) under nitrogen atmosphere. The mixture was stirred at room temperature until a homogeneous solution was obtained. This catalyst solution was repeatedly purged by N_2 prior to use.

A two neck round bottom flask was charged with 3,6-diiodo-*N*-butylcarbazole **50** (0.5 g, 1.05 mmol), 2-vinyl naphthalene **63** (0.357 g, 2.31 mmol) dry potassium carbonate (0.581g, 4.21 mmol), TBAB (0.067 g, 0.21 mmol, 20 mol%) and *N,N*-dimethylacetamide (10 mL) and the mixture was heated up to 100 °C. When the temperature reached 100 °C, the previously prepared Pd catalyst solution was added drop wise and the mixture was heated to 140 °C for 48 h. After the completion of the reaction, the mixture was poured in ice-cold water and extracted with dichloromethane (3 x 100 mL). The combined organic phase was washed with water, brine and dried over anhydrous sodium sulfate. The solvent was removed under reduced pressure and the crude product was purified by column chromatography on silica gel using petroleum ether:ethyl acetate (90:10) to (60:40) as eluent to afford *cis-trans* mixture of 9-butyl-3,6-bis(-2-(naphthalen-2-yl)vinyl)-9*H*-carbazole **64** as light yellow amorphous solid (0.328 g, 59 %), m.p. = 204-205 ^{o}C

^{1}H-NMR (400 MHz, $CDCl_3$): δ 8.35 (s, 2H), 7.92-7.74 (m, 11H), 7.53-7.34 (m, 10H), 4.34 (t, *J* = 6.8 Hz, 2H), 1.93-1.89 (m, 2H), 1.47-1.42 (m, 2H), 0.99 (t, *J* = 7.2 Hz, 3H)

^{13}C-NMR (100 MHz, $CDCl_3$): 140.7, 135.4, 133.8, 132.8. 129.9, 128.8, 128.2, 127.9, 127.7,126.2, 126.0, 125.6, 124.7, 123.5, 123.3, 118.7, 109.1, 43.1, 31.2, 20.5, 13.9.

IR (KBr):

3045,2954,2859,1617,1592,1481,1428,135,1244,1148,957,888,861,811,643,584 cm^{-1}

HRMS (TOF MS ES+): *m/z* calculated for $C_{40}H_{33}N$ $[M+H]^{+}$: 528.2684; found; 528.2685

Procedure for photocyclization of aza[9]helicene

A solution of *cis*/*trans*- mixture of 9-butyl-3,6-bis(-2-(naphthalen-2-yl)vinyl)-9*H*-carbazole **64** (0.175 g, 0.33 mmol), iodine (0.185 g, 0.73 mmol), THF (2.39 g, 2.69 mL, 33.2 mmol) and toluene (350 mL) was irradiated using a 125W HPMV lamp (10 h

monitored by TLC). After the completion of reaction, the excess of iodine was removed by washing the solution with aqueous $Na_2S_2O_3$, followed by distilled water. The organic layer was concentrated under the reduced pressure to obtain the crude product. The crude product purified by column chromatography over silica gel using petroleum ether: ethyl acetate (98:2) as eluent to obtained a pale yellow solid.
Overall Yield = 0.077 g (44%, mixture of four compounds **65-68**).

Separation and purification of regioisomers:

Separation of regiomers was done by enrichment of respective compound using column chromatography followed by crystallization in different solvents. For the separation of each regiomer the reaction mixture in which they formed predominantly for example the reaction performed at lower concentrations (enriched with angular-angular cyclization product) was mixed and column chromatography was performed initial fractions was collected and crystallized using ethyl acetate and pet ether giving tiny yellow crystals of title compound **65**.Similarly the reaction mixtures in which the other isomers formed predominantly (reaction performed at higher concentrations) was mixed and purified roughly by column chromatography and dissolved in chloroform pet ether mixture and kept in refrigerator for overnight. Two types of crystals were obtained, yellow plate like (compound **67**) and dark orange crystals (compound **68**) which were separated by hand picking. The mother liquor of this is (enriched of angular linear cyclization product) concentrated and obtained solid was crystallized in ethyl acetate pet ether giving yellow crystals of compound **66**.

Angular-angular isomer (65):

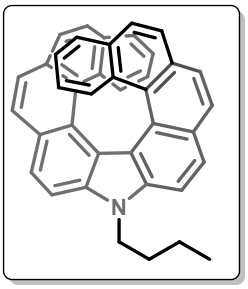

Physical State = Yellow solid, m.p. = 260-262 ^oC

^{1}H-NMR (400 MHz, $CDCl_3$): δ 8.32 (d, *J* = 8.4 Hz, 2H), 8.21 (d, *J* = 8.4 Hz, 2H), 8.04 (d, *J* = 8.4 Hz, 2H), 7.58 (d, *J* = 8.4 Hz, 2H), 7.55 (d, *J* = 8.4 Hz, 2H), 7.42 (d, *J* = 8.4 Hz, 2H), 7.31 (d, *J* = 7.6 Hz, 2H), 6.77-6.73 (m, 2H), 6.11 (d, *J* = 8.4 Hz, 2H), 5.62-5.58 (m, 2H), 5.01-4.97 (m, 2H), 2.35-2.26 (m, 2H), 1.75-1.66 (m, 2H)1.14 (t, *J* = 7.6 Hz, 3H).

^{13}C-NMR (100MHz, $CDCl_3$): δ 137.6, 129.6, 129.2, 127.8, 127.4, 126.4, 126.2, 126.1 (2C), 125.9, 125.0, 124.6 (2C), 123.9, 123.8, 121.6, 118.7, 108.9, 43.7, 32.3, 20.8, 14.1.

IR (KBr): 3042, 2956, 2928, 2868, 1619, 1577, 1527, 1490, 1463, 1439, 1360, 1335, 1287, 1251, 952, 910, 882, 777, 748, 628, 542 cm.$^{-1}$

HRMS (APCI): *m/z* calculated for $C_{40}H_{29}N$ $[M+H]^+$: 524.2373; found; 524.2372.

Angular-linear isomer (66):

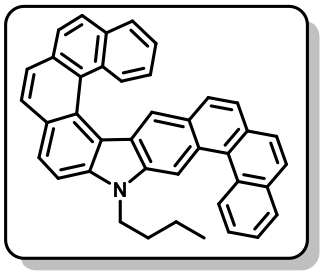

Physical State= Yellow solid, m.p. = 240 ^oC

^{1}H-NMR (400 MHz, $CDCl_3$): δ 9.47 (d, *J* = 8.4 Hz, 1H), 9.13 (s, 1H), 8.32 (d, *J* = 8.8 Hz, 1H), 8.19-8.03 (m, 6H), 7.92-7.69 (m, 5H), 7.69-7.65 (m, 1H), 7.58-7.56 (m, 1H), 7.52 (d, *J* = 8.4 Hz, 1H), 7.32 (d, *J* = 8.8 Hz, 1H), 7.14 (s, 1H), 7.13-7.09 (m, 1H), 4.62-4.58 (m, 2H), 2.14-2.09 (m, 2H), 1.68-1.58 (m, 2H), .11 (t, *J* = 7.2 Hz, 3H).

^{13}C-NMR (100MHz, $CDCl_3$):

δ 142.6, 139.6, 133.3, 132.6, 131.8, 130.7 (2C), 130.0, 129.1, 128.9, 128.7, 128.3, 128.2, 128.0, 127.9, 127.7, 127.6, 127.2, 127.0, 126.9, 126.6, 126.3 (2C), 125.9, 125.7, 125.6, 125.4, 125.3, 125.1, 125.0, 123.6, 123.5, 123.2, 117.4, 110.1, 105.2, 43.2, 31.3, 20.8, 14.1.

IR (KBr): 3045, 2956, 2928, 1619, 1577, 1527, 1463, 1441, 1360, 1337, 1287, 1251, 911, 882, 777, 748, 542 cm.$^{-1}$

HRMS (APCI): *m/z* calculated for $C_{40}H_{29}N$ $[M+H]^+$: 524.2372; found; 524.2372.

Linear-linear isomer (67):

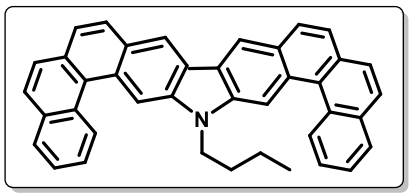

Physical State = Yellow solid , m.p. = 265 ^oC

^{1}H-NMR (400 MHz, $CDCl_3$): δ 9.41 (δ, *J* = 8.4 Hz, 2H), 9.13 (s, 2H), 8.91 (s, 2H), 8.17 (d, *J* = 8.4 Hz, 2H), 8.11 (dd, *J* = 8.0 Hz & 1.2 Hz, 2H), 7.97 (d, *J* = 8.8 Hz, 2H), 7.92 (d, *J* = 8.4 Hz, 2H), 7.79 (d, *J* = 8.8 Hz, 2H), 7.78-7.74 (m, 2H), 7.70-7.66 (m, 2H), 4.62 (t, *J* = 6.8 Hz, 2H), 2.19-2.12 (m, 2H),1.72-1.63 (m, 2H), 1.11 (t, *J* = 7.2 Hz, 3H).

^{13}C-NMR (100MHz, $CDCl_3$): δ 142.5, 133.4, 131.2, 130.7, 130.0, 128.7, 128.3, 127.7, 127.3, 127.2, 127.1, 126.9, 126.0, 125.5, 123.8, 123.5, 120.3, 105.1, 43.3, 30.9, 20.9, 14.1.

IR (KBr): 3041, 2953, 2861, 2369, 1684, 1615, 1430, 1262, 1198, 1132, 881, 829, 790, 745, 623, 539 cm.$^{-1}$

HRMS (ESI): *m/z* calculated for $C_{40}H_{29}N$ $[M+Na]^+$: 546.2190; found; 546.2192.

Angular-linear fused compound (68):

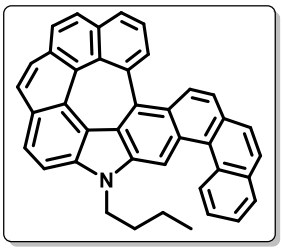

Physical State = Yellow solid, m.p. = 260 ^oC (Decomposed).

^{1}H-NMR (400 MHz, $CDCl_3$): δ 9.32 (d, *J* = 8.4 Hz, 1H), 8.87 (s, 1H), 8.12 (d, *J* = 8.8 Hz, 1H), 8.06 (dd, *J* = 8.0 Hz & 1.2 Hz, 1H), 7.89 (d, *J* = 8.4 Hz, 1H), 7.83-7.69 (m, 8H), 7.66-7.61 (m, 2H), 7.56 (d, *J* = 8.4 Hz, 1H), 7.49 (t, *J* = 7.6 Hz, 1H), 7.39 (d, *J* = 9.2 Hz, 1H), 4.48-4.34 (m, 2H), 2.07-1.93 (m, 2H), 1.55-1.54 (m, 2H merged with water peak), 1.05 (t, *J* = 7.2 Hz, 3H).

^{13}C-NMR (100MHz, $CDCl_3$): δ 144.3, 139.9, 138.6, 137.5 (2C), 136.1, 135.8, 133.3 (2C), 133.0, 132.9, 132.6, 131.6, 131.2, 130.6 (2C), 129.7, 128.7 (2C), 128.6, 128.4, 128.3, 128.0, 127.1 (2C), 126.8, 126.4 (2C), 126.0, 125.8, 125.3, 125.2, 121.9, 119.6, 109.8, 105.3, 43.0, 31.2, 20.6, 14.0.

IR (KBr): 3043, 2973, 2861, 2365, 1684, 1615, 1431, 1262, 1198, 1132, 881, 829, 790, 745, 627, 539 cm.$^{-1}$

HRMS (ESI): *m/z* calculated for $C_{40}H_{27}N$ $[M+H]^+$:522.2223; found; 522.2216.

9-Butyl -9*H* carbazole:

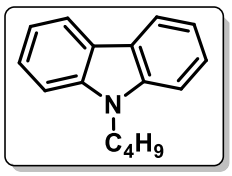

In a round bottom flask carbazole **48** (5.0 g, 29.94 mmol) was added into the solution of KOH (10.48 g, 186 mmol) in 50 mL acetone at the conditions of stirring and room temperature. After 1 h, a solution of 1- bromobutane (6.14 g, 44.0 mmol) in acetone was added to the reaction mixture and then maintained for 8 h. The final reaction mixture was concentrated under vacuum and then poured into 400 mL water. The product was extracted with ethyl acetate (50 x 3 mL). Ethyl acetate layer was washed with water twice, dried over sodium sulphate and concentrated under vacuum. The crude product was purified by column chromatography on silica gel using petroleum ether as a eluent to afford 9-butyl 9-*H* carbazole as white solid (6.26 g, 94 %). m.p.: 54 ^oC. The analytical data were in complete agreement with the previously published data.[63b]

^{1}H-NMR ($CDCl_3$, 400 MHz): δ 8.10 (d, *J* = 7.8 Hz, 2 H), 7.44(m, 4 H), 7.22(m, 2 H), 4.3(t, *J* = 7.2 Hz, 2 H), 1.80–1.90 (m, 2 H), 1.34–1.46 (m, 2 H), 0.94 (t, *J* = 7.4 Hz, 3 H).

3-Formyl *N*-butyl carbazole (99):

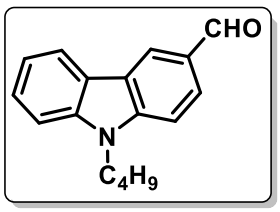

In a dry two neck round bottom flask phosphoryl chloride (13.76 g, 8.36 mL, 89.0 mmol) was added slowly in DMF (16.36 g, 17.22 mL, 224 mmol) which was purged with nitrogen and cooled to 0 °C. The reactant was warmed to room temperature and stirred for 1 hour and cooled again to 0 °C. To this mixture was added *N*-butyl carbazole (10.0 g, 44.8 mmol) in 1, 2-dichloroethane (50 mL). In 1 hour, the reaction temperature was raised to 90 °C and then kept for 8 hours. The cooled solution was poured in to ice water and extracted with dichloromethane (3X100 mL). The organic layer was washed with water, dried over anhydrous sodium sulfate and concentrated at reduced pressure. The purification of compound was performed by column chromatography over silica gel using 10 % ethyl acetate pet ether as eluent to obtain **99** as viscous liquid which solidify as brown solid (10.g, 89%) on standing at low temperature. m.p.: 60 °C. The analytical data were in complete agreement with the previously published data.[63c]

^{1}H-NMR (400 MHz, $CDCl_3$): δ 10.11 (s, 1H), 8.62 (d, *J* = 1.2 Hz, 1H), 8.14 (d, *J* = 8.8 Hz, 1H), 8.03-8.01 (m, 1H), 7.57-7.55 (m, 1H), 7.53-7.47 (m, 1H), 7.46-7.32 (m, 2H), 4.35 (t, *J* = 7.2 Hz, 2H), 1.91-1.87 (m, 2H), 0.98 (t, *J* = 7.2 Hz, 3H).

2-(Bromomethyl) naphthalene (107):

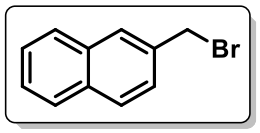

In round bottom .flask equipped with a magnetic stirrer and reflux condenser 2-methyl naphthalene **106** was (2.0 g, 14.0 mmol) dissolved in carbon tetrachloride (25 mL). To this solution, the mixture of *N*-bromo succinimide (2.62g, 14.7 mmol) and benzoyl peroxide (0.169g, 0.7 mmol) was added. The mixture was stirred in presence of tungsten filament domestic light for 5-6 hrs. After the completion of reaction (TLC), succinimide was filtered and the solvent was removed under the reduced pressure. Solid material after distillation was recrystallised from petroleum ether as brown solid (2.44 g, 83%). m.p. = 50-52 °C. The analytical data were in complete agreement with the previously published data.[63d]

^{1}H-NMR (400 MHz, $CDCl_3$): δ 7.81-7.78 (m, 4H), 7.49-7.46 (m, 3H), 4.64 (s, 2H).

2-(Cyanomethyl) naphthalene (108):

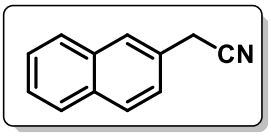

2-(Bromomethyl)naphthalene **107** (1.0 g, 4.5 mmol) potassium cyanide(0.588 g, 9.05 mmol) and tetrabutylammoniumbromide (0.291g, 0.9 mmol) was dissolved in toluene water mixture (9:1, 20 mL).The reaction mixture was stirred for 7-8 hours at 70 ^oC. After completion of reaction the reaction (TLC) mixture was poured in ice cold water and extracted using ethyl acetate (3X50 mL).The organic layer was washed with water (50 mL), dried over anhydrous sodium sulfate and concentrated under reduced pressure. The purification of compound was performed by column chromatography over silica gel using 10% ethyl acetate-pet ether as eluent to afford white solid (0.528 g, 70%). m.p.= 88 ^oC. The analytical data were in complete agreement with the previously published data.[63e]

^{1}H-NMR (400 MHz, $CDCl_3$): δ 7.89-7.84 (m, 4H), 7.55-7.53 (m, 2H), 7.40 (dd, *J* = 8.4 and 1.6 Hz, 3.94 (s, 2H).

3-(Bromomethyl) phenanthrene (118):

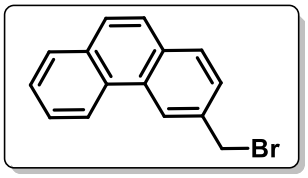

A. Light mediated bromination: The compound was prepared similarly to the procedure reported to obtain 2-(bromomethyl)phenanthrene **107** in presence of tungsten filament domestic light. Yield = 22 %

B. Thermal condition: A mixture of 3-methyl phenanthrene **117** (1.0 g, 5.2 mmol), NBS (1.39 g, 7.8 mmol), and benzoyl peroxide (0.063 g, .0.26 mmol) in 30 mL of CCl_4, was heated at reflux for 5 h. The solution was cooled and the copious precipitate was filtered off and washed with CCl_4 and concentrated at reduced pressure. The purification of compound was performed by column chromatography over silica gel using 2 % ethyl acetate pet ether as eluent to obtain white solid (0.578.g, 41 %). (Reported = 96%) The analytical data were in complete agreement with the previously published data.[63f]

^{1}H-NMR (400 MHz, $CDCl_3$): δ 8.71-8.69 (m, 2H), 7.93-7.89 (m, 2H), 7.79-7.73 (m, 2H), 7.72-7.68 (m, 1H), 7.66-7.62 (m, 2H), 4.80 (s, 2H).

2-(4-Styrylphenyl)acetonitrile (122):

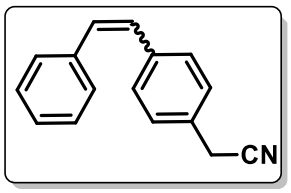

A two necked round bottom flask was charged with styrene **120** (0.318 g, 3.06 mmol), 4-bromophenylacetonitrile **121** (0.5 g, 2.55 mmol), $Pd(OAc)_2$.(0.006g, 0.0255 mmol), triphenyl phosphine (0.013g, 0.051 mmol), triethylamine (5.0 mL) and *N,N*-dimethylacetamide (25 mL), the mixture was heated to 90 °C for 48 h. After the completion of the reaction, the mixture was poured in ice-cold water and extracted with dichloromethane (3 x 50 mL). The combined organic phase was washed with water, brine and dried over anhydrous sodium sulfate. The solvent was removed under reduced pressure and the crude product was purified by column chromatography on silica gel using petroleum ether:ethyl acetate (90:10)) as eluent to afford *trans* 2-(4-styrylphenyl)acetonitrile **122** as white solid.(0.468 g, 83%); m.p. = 89-92 °C (Reported = 92 °C). The analytical data were in complete agreement with the previously published data.[63g]

2-(Phenanthren-3-yl)acetonitrile (119):

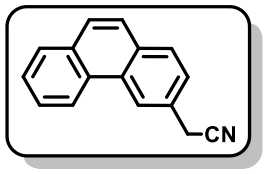

Method A (from compound 118): 3-(bromomethyl) phenanthrene **118** (0.5 g, 1.84 mmol) potassium cyanide (0.240 g, 3.69 mmol) was dissolved in ethanol water mixture (9:1, 20 mL).The reaction mixture was stirred for 7-8 hours at 70 °C. After completion of reaction the reaction (TLC) mixture was poured in ice cold water and extracted using ethyl acetate (3X50 mL).The organic layer was washed with water (50 mL), dried over anhydrous sodium sulfate and concentrated under reduced pressure. The purification of compound was performed by column chromatography over silica gel using 10% ethyl acetate-pet ether as eluent to afford **119** as white solid (0.320 g, 80%).

Method B Photocyclization: A solution of **122** (0.4 g, 1.82 mmol) and iodine (0.509 g, 2.0 mmol) in toluene (650 mL) and tetrahydrofuran (7.40 mL, 91.3 mmol, 50 equivalent) was irradiated in a standard immersion well photoreactor with 250W high pressure mercury vapor lamp for 24 hours. The reaction mixture was then washed with aqueous sodium thiosulfate and dried over anhydrous sodium sulfate. The concentrated mixture was purified on silica gel using 10% ethyl acetate-pet ether as eluent to afford **119** as white solid (0.309 g, 78%). M.p. = 81-84 °C. (Reported 84-85 °C)[63h]

^{1}H-NMR (400 MHz, $CDCl_3$): δ 8.70 (dd, *J* = 8.0 and 0.4 Hz, 1H), 8.66 (s, 1H), 7.94-7.91 (m, 2H), 7.79 (d, *J* = 8.8 Hz, 1H), 7.75 (d, *J* = 8.8 Hz, 1H), 7.73-7.63 (m, 2H), 7.54 (dd, *J* = 8.4 and 2.0 Hz, 1H), 4.03 (s, 1H)

General procedure for the synthesis of stilbene derivative by Knovenagel reaction:

3-(9-Butyl-9*H*-carbazol-3-yl)-2-phenylacrylonitrile (101):

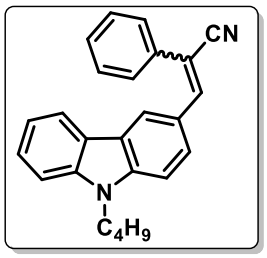

A solution of 3-Formyl *N*-butyl carbazole **99** (0.75 g, 2.98 mmol) and phenylacetonitrile **100** (0.524 g, 4.48 mmol) in dry ethanol (25 mL) was placed in a single neck R.B. flask fitted with a septum , which is degassed and purged with nitrogen. To this was added drop-wise, with stirring, a solution of (0.343 g, 14.94 mmol) sodium dissolved in 25 mL of dry ethanol and the mixture was stirred vigorously for 5 hours at room temperature. After completion of reaction the ethanol was evaporated under reduced pressure the mixture was poured into ice-cold water and extracted with ethyl acetate (3 x 50 mL). The combined organic phase was washed with water, brine, and dried over anhydrous sodium sulfate. The solvent was removed under reduced pressure and the crude product was purified by column chromatography on silica gel using petroleum ether–ethyl acetate (95:05) as eluent to afford **101** as viscous yellow oil which solidifies on cold storage (0.93 g, 89%).

^{1}H-NMR (400 MHz, $CDCl_3$): δ (*mixture of cis/trans*) 8.65 (d, *J* = 1.2 Hz, 1H), 8.19-8.15 (m, 2H), 7.75-7.73 (m, 3H), 7.56-7.38 (m, 3H), 7.33-7.24 (m, 3H), 4.34 major (t, *J* = 7.2 Hz, 2H), 4.25 minor (t, *J* = 7.2 Hz, 1H) 1.91-1.88 (m, 2H), 1.46-1.40 (m, 3H), 1.00-0.93 (m, 4H).

^{13}C-NMR (100 MHz, $CDCl_3$): δ 145.4, 143.5, 141.6, 141.1, 141.0, 140.3, 135.3, 133.6, 129.2, 129.0, 128.7, 128.4, 128.2, 127.8, 127.0, 126.4, 126.3, 125.7, 124.7, 124.2, 123.2, 122.8, 122.7, 126.6, 121.1, 120.7, 120.3, 119.7, 119.6, 119.2, 110.2, 109.1, 108.6, 107.3, 43.09, 43.01, 31.1, 31.0, 20.57, 20.53, 13.9, 13.8.

HRMS: *m/z* calculated for $C_{25}H_{22}N_2$ $[M+Na]^+$:373.1681; found; 373.1637.

3-(9-Butyl-9*H*-carbazol-3-yl)-2-(naphthalen-2-yl)acrylonitrile (109):

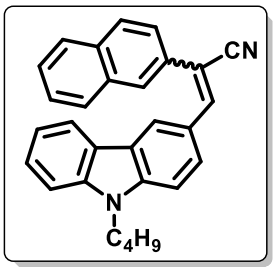

^{1}H-NMR (400 MHz, $CDCl_3$): (*trans*) δ 8.69 (d, *J* = 1.6 Hz, 1H), 8.22-8.18 (m, 3H), 7.94-7.81 (m, 5H), 7.58-7.44 (m, 5H), 7.34-7.30 (m, 1H), 4.33 (t, *J* = 6.8 Hz, 2H), 1.91-1.87 (m, 2H), 1.44-1.40 (m, 2H), 0.99 (t, *J* = 7.2 Hz, 3H)

^{13}C-NMR (100 MHz, $CDCl_3$): δ 143.5, 141.6, 141.0, 133.4, 133.0, 132.4, 128.7, 128.3, 127.6, 127.1, 126.8, 126.6, 126.4, 125.5, 124.8, 123.2, 122.8, 122.7, 122.6, 120.7, 119.8, 119.2, 109.2, 109.1, 107.3, 43.0, 31.1, 20.5, 13.9

IR (KBr): ν 2955, 2928, 2201, 1626, 1590, 1466, 1237, 802, 746, 728 cm^{-1}

3-(9-Butyl-9*H*-carbazol-3-yl)-2-(phenanthren-3-yl)acrylonitrile (123):

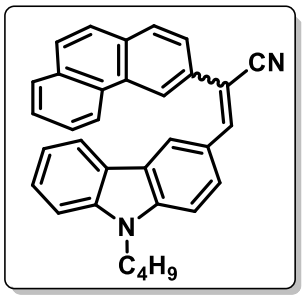

^{1}H-NMR (400 MHz, $CDCl_3$): δ 8.98 (d, *J* = 7.6 Hz, 1H), 8.83-8.80 (m, 1H), 8.68 (d, *J* = 6.4 Hz, 1H), 8.24-8.19 (m, 2H), 7.92-7.97 (m, 4H), 7.78-7.71 (m, 3H), 7.66 (t, *J* = 7.2 Hz, 1H), 7.54 (t, *J* = 7.6 Hz, 1H), 7.48-7.42 (m, 2H), 7.31 (t, *J* = 7.2 Hz, 1H), 4.29 (t, *J* = 7.6 Hz, 2H), 1.91-1.86 (m, 2H), 1.44-1.42 (m, 2H), 0.99 (t, *J* = 7.2 Hz, 3H).

^{13}C-NMR (100 MHz, $CDCl_3$): δ 143.6, 141.6, 141.0, 133.1, 132.3, 131.8, 130.4, 130.1, 129.2, 128.7, 127.7, 127.09, 127.04, 126.9, 126.4, 126.3, 124.8, 123.3, 123.2, 122.86, 122.82, 122.7, 120.7, 120.3, 119.8, 119.3, 109.2, 109.1, 107.5, 43.0, 31.1, 20.5, 13.8.

9-Butyl-3-(2-(naphthalen-2-yl)vinyl)-9*H*-carbazole (111):

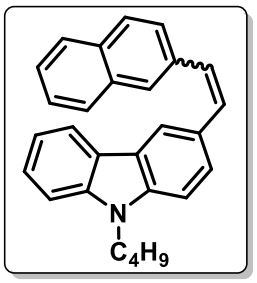

A solution of 3-Formyl *N*-butyl carbazole **99** (0.5 g, 1.99 mmol) and Bromo(naphthalen-2-ylmethyl)triphenylphosphorane (1.44 g, 2.98 mmol) in dry ethanol (25 mL) was placed in a single neck R.B. flask fitted with a septum , which is degassed and purged with nitrogen. To this was added drop-wise, with stirring, a solution of (0.228 g, 9.95 mmol) sodium dissolved in 25 mL of dry ethanol and the mixture was stirred vigorously for 5 hours at room temperature. After completion of reaction the ethanol was evaporated under reduced pressure the mixture was poured into ice-cold water and extracted with ethyl acetate (3 x 50 mL). The combined organic phase was washed with water, brine, and dried over anhydrous

sodium sulfate. The solvent was removed under reduced pressure and the crude product was purified by column chromatography on silica gel using petroleum ether–ethyl acetate (95:05) as eluent to afford light white solid (0.649 g, 87%).

^{1}H-NMR (400 MHz, $CDCl_3$): 8.32 (d, *J* = 1.2 Hz, 1H), 8.18 (d, *J* = 7.6 Hz, 1H), 7.92-7.83 (m, 5H), 7.75 (dd, *J* = 8.4 and 1.6 Hz, 1H), 7.65-7.37 (m, 7H), 7.33-7.30 (m, 2H), 4.33 (t, *J* = 7.2 Hz, 2H), 1.92-1.88 (m, 2H), 1.58-1.41 (m, 2H), 0.99 (t, *J* = 7.2 Hz, 3H)

General procedure for the photocyclization of cyano aza[*n*]helicene:

5-Cyano *N*-butyl aza[5]helicene (102):

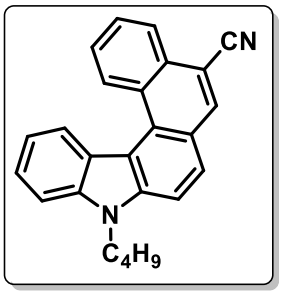

A solution of **101** (0.75 g, 2.14 mmol) and iodine (0.598 g, 2.35 mmol) in toluene (1250 mL) and tetrahydrofuran (8.69 mL, 107.14 mmol, 50 equivalent) was irradiated in a standard immersion well photoreactor with 250W high pressure mercury vapor lamp for 8 hours. The reaction mixture was then washed with aqueous sodium thiosulfate and dried over anhydrous sodium sulfate. The concentrated mixture was purified on silica gel using 5% ethyl acetate-pet ether as eluent to afford yellow solid (0.619 g, 83%).

^{1}H-NMR (400 MHz, $CDCl_3$): δ 9.38 (d, *J* = 8.4 Hz, 1H), 8.73 (d, *J* = 8.0 Hz, 1H), 8.39-8.32 (m, 2H), 7.91-7.73 (m, 4H), 7.63-7.56 (m, 2H), 7.33-7.31 (m, 1H), 4.49 (t, *J* = 7.2 Hz, 2H), 1.98-1.94 (m, 2H), 1.53-1.47 (m, 2H), 1.02 (t, *J* = 7.2 Hz, 3H).

^{13}C-NMR (100 MHz, $CDCl_3$):

δ 141.7, 140.3, 136.1, 130.0, 129.0, 128.2, 128.1, 127.4, 125.7, 125.2, 124.8, 123.3, 12 3.2, 119.0, 118.6, 116.5, 111.0, 109.6, 105.2, 43.1, 31.2, 20.5, 13.9.

HRMS: *m/z* calculated for $C_{25}H_{20}N_2Na$ 371.1519 found; 371.1519**.**

7-Cyano *N*-butyl aza[6]helicene (110):

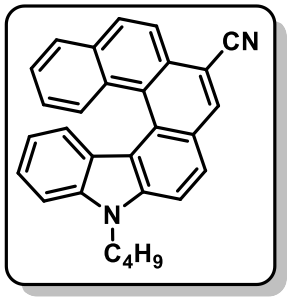

^{1}H-NMR (400 MHz, $CDCl_3$): δ 8.47 (s, 1H), 8.35 (d, *J* = 8.4 Hz, 1H), 8.25 (d, *J* = 8.4 Hz, 1H), 8.19 (d, *J* = 8.4 Hz, 1H), 8.11 (d, *J* = 7.6 Hz, 1H), 8.07 (d, *J* = 8.0 Hz, 1H), 7.91 (d, *J* = 8.8 Hz, 1H), 7.62-7.58 (m, 1H), 7.54 (d, *J* = 8.0 Hz, 1H), 7.42-7.38 (m, 1H), 7.23-7.19 (m, 1H), 6.84-6.80 (m, 1H), 6.59 (d, *J* = 8.0 Hz, 1H), 4.53 (t, *J* = 7.6 Hz, 2H), 2.03-1.99 (m, 2H), 1.58-1.53 (m, 2H), 1.05 (t, *J* = 7.6 Hz, 3H).

^{13}C-NMR (100 MHz, $CDCl_3$): δ 141.5, 139.5, 135.3, 131.8, 129.98, 129.9, 129.4, 128.4, 127.9, 127.0, 126.9, 126.6, 126.4, 126.1, 125.4, 125.0, 122.8, 122.5, 118.8, 118.3, 118.1, 111.5, 108.7, 104.7, 43.2, 31.3, 20.6, 13.9

IR (KBr): 2957, 2922, 2212, 1577, 1518, 1465, 891, 822, 794 cm^{-1}

Mass (EI): 397.98 (100 %), 354.81 (60 %)

HRMS: *m/z* calculated for $C_{29}H_{23}N_2$ 399.1855 found; 399.1856.

HPLC condition: 20.9 and 22.6 (10 % IPA: hexane, Daicel make Chiralpak IC Column, UV = 254 nm, Flow = 1.0 mL/min)

9-cyano *N*-butyl aza[7]helicene (124):

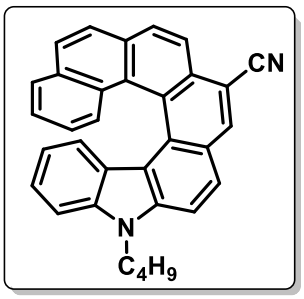

^{1}H-NMR (400 MHz, $CDCl_3$): δ 8.51 (s, 1H), 8.41 (d, *J* = 8.4 Hz, 1H), 8.19 (d, *J* = 8.8 Hz, 1H), 8.08-8.06 (m, 2H), 8.0 (d, *J* = 8.8 Hz, 1H), 7.86 (d, *J* = 8.8 Hz, 1H), 7.68 (d, *J* = 7.6 Hz, 1H), 7.39 (d, *J* = 8.4 Hz, 1H), 7.21 (d, *J* = 8.0 Hz, 1H), 7.11-7.07 (m, 1H), 7.07-7.02 (m, 1H), 6.50-6.46 (m, 1H), 6.39-6.35 (m, 1H), 5.91 (d, *J* = 8.4 Hz, 1H), 4.42 (t, *J* = 7.2 Hz, 2H), 1.91-1.87 (m, 2H), 1.42-1.40 (m, 2H), 1.0 (t, *J* = 7.6 Hz, 3H).

Linear isomer of aza[7]helicene (125):

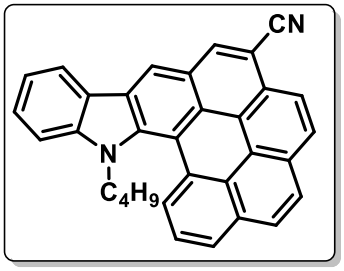

^{1}H-NMR (400 MHz, $CDCl_3$): δ 8.82 (s, 1H), 8.78 (d, *J* = 7.6 Hz, 1H), 8.75 (d, *J* = 8.4 Hz, 1H), 8.67 (s, 1H), 8.53 (d, *J* = 8.4 Hz, 1H), 8.42 (d, *J* = 7.6 Hz, 1H), 8.29-8.23 ((m, 3H), 8.06 (t, *J* = 7.6 Hz, 1H), 7.78-7.70 (m, 2H), 7.54-7.50 (m, 1H), 4.63 (s, 2H broad), 1.26-0.97 (m, 2H broad), 0.39 (s, 2H), 0.25 (t, *J* = 6.8 Hz).

^{13}C-NMR (100 MHz, $CDCl_3$): δ 145.6, 140.4, 136.1, 131.5, 129.2, 128.3, 127.8, 127.6, 127.4, 127.1, 126.3, 126.2, 125.9, 125.8, 125.7, 125.3, 124.8, 124.3, 124.0, 123.6, 122.8, 121.3, 121.1, 119.2, 118.2, 115.0, 112.5, 106.5, 47.1, 29.5, 19.4, 13.1.

Compound 103:

In a dry two neck round bottom flask phosphoryl chloride (4.41 g, 2.68 mL, 28.7 mmol) was added slowly in DMF (3.15 g, 3.31 mL, 43.10 mmol) which was purged

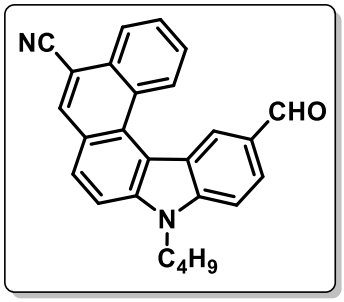

with nitrogen and cooled to 0 ºC. The reactant was warmed to room temperature and stirred for 1 hour and cooled again to 0 ºC. To this mixture was added 5-cyano *N*-butyl aza[5]helicene **102** (1.0 g, 2.87 mmol) in 1, 2-dichloroethane (30 mL). In 1 hour, the reaction temperature was raised to 90 ºC and then kept for 8 hours. The cooled solution was poured in to ice water and extracted with dichloromethane (3X50 mL). The organic layer was washed with water, dried over anhydrous sodium sulfate and concentrated at reduced pressure. The purification of compound was performed by column chromatography over silica gel using 20 % ethyl acetate pet ether as eluent to obtain yellow solid (0.875.g, 81%).

^{1}H-NMR (400 MHz, $CDCl_3$): δ 10.05 (s, 1H), 9.20 (d, *J* = 8.0 Hz, 1H), 9.11 (s, 1H), 8.27 (d, *J* = 8.0 Hz, 1H), 8.21 (s, 1H), 8.09 (dd, *J* = 8.8 and 1.2 Hz, 1H), 7.88 (d, *J* = 8.4 Hz, 1H), 7.77-7.69 (m, 3H), 7.65 (d, *J* = 8.8 Hz, 1H), 4.51 (t, *J* = 7.2 Hz, 2H), 1.99-1.92 (m, 2H), 1.54-1.47 (m, 2H), 1.02 (t, *J* = 7.2 Hz, 3H).

^{13}C-NMR (100 MHz, $CDCl_3$): δ 191.7, 143.6, 142.3, 135.6, 129.9, 129.7, 128.6, 128.5, 128.4, 127.6, 126.1, 125.9, 125.3, 125.2, 123.1, 118.2, 116.8, 111.2, 110.0, 106.0, 43.5, 31.2, 20.5, 13.8.

HRMS: *m/z* calculated for $C_{26}H_{20}N_2ONa$ 399.1476 found; 399.1468.

Compound 104:

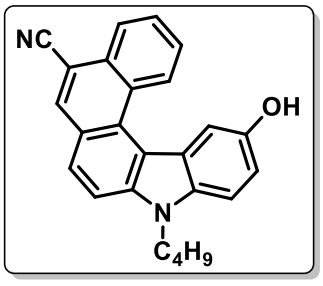

To a solution of compound **103** (0.1 g, 0.265 mmol) in CH_2Cl_2 (5 mL) and MeOH (5 mL), one drop of conc. H_2SO_4 and H_2O_2 (0.011g, 0.04 mL, 30% in water) were added, and the resultant solution was stirred for 1 h at room temperature. After completion of the reaction, the solvent was evaporated under reduced pressure, and the residue was dissolved in dichloromethane. The resultant solution was washed with water, brine, dried over anhyd. Na_2SO_4 and solvent removed in vacuo. The purification of compound was performed by column chromatography over silica gel using 20 % ethyl acetate pet ether as eluent to obtain yellow solid (0.083.g, 86%).

^{1}H-NMR (400 MHz, $CDCl_3$): δ 9.26 (d, *J* = 8.0 Hz, 1H), 8.29 (s, 2H), 8.07 (dd, *J* = 8.4 and 0.8 Hz, 1H), 7.87 (d, *J* = 8.8 Hz, 1H), 7.75 (d, *J* = 8.4 Hz, 1H), 7.66-7.62 (m,

1H), 7.49 (d, *J* = 8.8 Hz, 1H), 7.44-7.40 (m, 1H), 7.20 (dd, *J* = 8.4 and 2.0 Hz, 1H), 5.71 (s, 1H), 4.47 (t, *J* = 7.2 Hz, 2H), 1.99-1.67 (m, 2H), 1.52-1.47 (m, 2H), 1.01 (t, *J* = 7.2 Hz, 3H).

^{13}C-NMR (100 MHz, $CDCl_3$): δ 149.1, 142.3, 136.0, 135.3, 130.2, 129.9, 128.7, 128.1, 127.8, 127.3, 125.5, 124.8, 124.5, 123.8, 118.6, 115.9, 115.3, 111.2, 110.3, 108.7, 104.4, 43.3, 31.3, 20.6, 13.9.

HRMS: *m/z* calculated for $C_{25}H_{20}N_2ONa$ 387.1458 found; 387.1458.

***N*-butyl aza[6]helicene 7-carboxylic acid (126):**

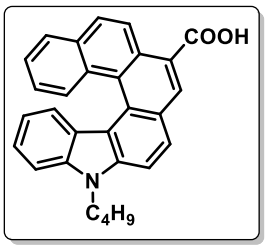

To a suspension of **110** (0.1 g, 0.25 mmol) in diethylene glycol (10 mL) was added aq. KOH (10 M, 1.0 mL). The mixture was heated at 180 ºC for 8h. The cooled solution was poured in to ice water. The solution was acidified with 1N HCl and extracted with dichloromethane (3X25 mL). The organic layer was washed with water, dried over anhydrous sodium sulfate and concentrated at reduced pressure to afford **126** (99 mg, quant) as a brown solid.

^{1}H-NMR (400 MHz, $CDCl_3$): δ 9.31 (d, *J* = 9.2 Hz, 1H), 9.0 (s, 1H), 8.28 (d, *J* = 8.0 Hz, 1H), 8.17 (d, *J* = 8.0 Hz, 2H), 8.10 (d, *J* = 7.6 Hz, 1H), 7.90 (d, *J* = 8.8 Hz, 1H), 7.58-7.51(m, 2H), 7.39 (t, *J* = 7.6 Hz, 1H), 7.17 (t, *J* = 7.6 Hz, 1H), 6.81 (t, *J* = 7.6 Hz, 1H), 6.61 (d, *J* = 8.0 Hz, 1H), 4.53 (t, *J* = 7.2 Hz, 2H), 2.05-1.97 (m, 2H), 1.58-1.53 (m, 2H), 1.05 (t, *J* = 7.2 Hz, 3H)

Compound 128:

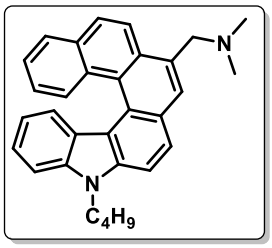

To a solution of Compound **110** (0.1 g, 0.25 mmol), anhydrous nickel chloride $NiCl_2$ (0.064 g, 0.50 mmol) in dry ethanol (5.0 mL) and THF (5.0 ml) was added $NaBH_4$ (0.028 g, 0.75 mmol) in portions while stirring the solution vigorously, black precipitates appeared during the addition of sodium borohydride. When the addition was complete, stirring was continued for 3 hour at room temperature. The progress of reaction was monitored by TLC, when no progress in the product formation was observed; the reaction mixture was filtered through a celite filter pad. The filtered precipitate was washed with THF. The combined organic solvent was removed under vacuo. The resulted dark colored solid was taken directly in the next step. Solid was dissolved in methanol (15 mL), to this turbid solution; aqueous

solution of formaldehyde (0.022 g, 0.056 mL, 40% in water) was added and stirred for 15 minutes. Sodium cyanoborohydride $NaBH_3CN$ (0.016 g, .25 mmol) was added to the reaction mixture and reaction was continued for 2 hour at room temperature. After completion of the reaction, the solvent was evaporated under reduced pressure, and the residue was dissolved in dichloromethane. The resultant solution was washed with water, brine, dried over anhyd. Na_2SO_4 and solvent removed in vacuo. The purification of compound was performed by column chromatography over alumina using 30 % ethyl acetate pet ether as eluent to obtain yellow solid (0.018 g, 17%).

^{1}H-NMR (400 MHz, $CDCl_3$): δ 8.39 (d, *J* = 8.8 Hz, 1H), 8.31 (d, *J* = 8.4 Hz, 1H), 8.08-8.04 (m, 3H), 7.92 (s, 1H), 7.84 (d, *J* = 8.8 Hz, 1H), 7.53-7.48 (m, 1H), 7.17-7.14 (m, 1H), 6.79-6.75 (m, 1H), 6.65 (d, *J* = 8.0 Hz, 1H), 4.51 (t, *J* = 7.2 Hz, 2H), 4.14 (d, *J* = 12.8 Hz, 1H), 3.81 (d, *J* = 12.8 Hz, 1H), 2.39 (s, 6H), 2.09-1.98 (m, 2H), 1.58-1.52 (m, 2H), 1.04 (t, *J* = 7.2 Hz, 3H).

^{13}C-NMR (100 MHz, $CDCl_3$): δ 139.8, 139.4, 131.5, 131.2, 130.5, 129.4, 128.8, 127.52, 127.5, 127.4, 126.6, 126.5, 125.6, 125.36, 125.3, 124.7, 124.2, 123.2, 122.5, 118.1, 117.5, 110.3, 108.2, 62.8, 45.6, 43.1, 31.4, 20.6, 13.9.

HRMS: *m/z* calculated for $C_{31}H_{31}N_2$ 431.2481 found; 3431.2482.

Compound 129:

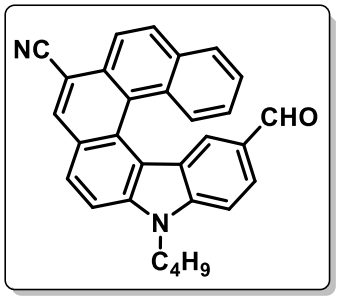

In a dry two neck round bottom flask phosphoryl chloride (3.83 g, 2.33 mL, 25.12 mmol) was added slowly in DMF (2.28 g, 2.40 mL, 31.25 mmol) which was purged with nitrogen and cooled to 0 ºC. The reactant was warmed to room temperature and stirred for 1 hour and cooled again to 0 ºC. To this mixture was added 7-cyano *N*-butyl aza[6]helicene **110** (0.5 g, 1.25 mmol) in 1, 2-dichloroethane (25 mL). In 1 hour, the reaction temperature was raised to 90 ºC and then kept for 8 hours. The cooled solution was poured in to ice water and extracted with dichloromethane (3X50 mL). The organic layer was washed with water, dried over anhydrous sodium sulfate and concentrated at reduced pressure. The purification of compound was performed by column chromatography over silica gel using 20-30 % ethyl acetate pet ether as eluent to obtain yellow solid (0.460.g, 86%).

^{1}H-NMR (400 MHz, $CDCl_3$): δ 9.39 (s, 1H), 8.48 (s, 1H), 8.35 (d, *J* = 8.8 Hz, 1H), 8.22 (d, *J* = 8.8 Hz, 1H), 8.17-8.13 (m, 3H), 7.98 (dd, *J* = 8.4 and 1.2 Hz, 1H), 7.94 (d, *J* = 8.8 Hz, 1H), 7.62-7.59 (m, 2H), 7.19-7.15 (m, 1H), 6.95 (d, *J* = 1.2 Hz, 1H), 4.56 (t, *J* = 7.2 Hz, 2H), 2.06-1.98 (m, 2H), 1.60-1.53 (m, 2H), 1.06 (t, *J* = 7.2 Hz, 3H).

^{13}C-NMR (100 MHz, $CDCl_3$): δ 191.6, 142.9, 142.1, 135.3, 132.0, 131.1, 130.1, 129.8, 129.5, 128.4, 128.2, 128.1, 127.6, 127.0, 126.7, 126.3, 125.9, 124.3, 122.5, 118.4, 118.3, 111.7, 109.4, 105.7, 43.6, 31.3, 20.6, 13.9.

IR (KBr): 3449, 2955, 2922, 2852, 2819, 2733, 2213, 1686, 1578, 1316, 1206, 902, 806 $cm.^{-1}$

HRMS: *m/z* calculated for $C_{30}H_{23}ON_2$ found; 427.1804, 427.1804.

Compound 130:

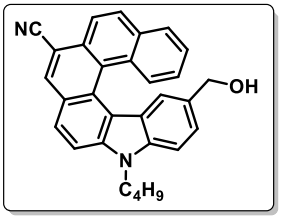

To a solution of compound **129** (0.2 g, 0.47 mmol) in methanol (5 mL) and THF (5 mL) was added $NaBH_4$ (0.018 g, 0.47 mmol), the resultant solution was stirred for 1 h at room temperature. After completion of the reaction, the solvent was evaporated under reduced pressure, and the residue was dissolved in dichloromethane. The resultant solution was washed with water, brine, dried over anhyd. Na_2SO_4 and solvent removed in vacuo. The purification of compound was performed by column chromatography over silica gel using 30 % ethyl acetate pet ether as eluent to obtain yellow solid (0.155.g, 77%)

^{1}H-NMR (400 MHz, $CDCl_3$): δ 8.48 (s, 1H), 8.34 (d, *J* = 8.8 Hz, 1H), 8.20-8.14 (m, 3H), 8.09 (d, *J* = 8.4 Hz, 1H), 7.91 (d, *J* = 8.8 Hz, 1H), 7.63-7.59 (m, 1H), 7.53 (d, *J* = 8.4 Hz, 1H), 7.42 (dd, *J* = 8.4 and 1.6 Hz, 1H), 7.22-7.18 (m, 1H), 6.47 (d, *J* = 0.8 Hz, 1H), 4.54 (t, *J* = 7.6 Hz, 2H), 4.39 (d, *J* = 6.0 Hz, 1H), 4.35 (d, *J* = 6.0 Hz, 1H), 2.04-1.96 (m, 2H), 1.58-1.51 (m, 2H), 1.13 (t, *J* = 6.4 Hz, 1H), 1.04 (t, *J* = 7.2 Hz, 3H).

^{13}C-NMR (100 MHz, $CDCl_3$): δ 141.8, 139.2, 135.4, 131.9, 130.8, 130.1, 129.8, 129.5, 128.8, 128.2, 127.2, 126.8, 126.5, 126.3, 125.9, 125.7, 124.8, 124.5, 122.7, 118.8, 117.8, 111.6, 108.9, 104.8, 65.9, 43.4, 31.4, 20.6, 13.9.

IR (KBr): ν 3386, 2957, 2858, 2215, 1618, 1578, 1521, 1355, 892, 817.

HRMS: *m/z* calculated for $C_{30}H_{24}ON_2Na$ 451.1780 found; 451.1780.

Compound 137:

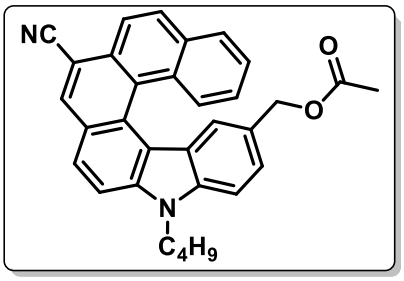

To a stirred solution of alcohol **130** (0.1 g, 0.23 mmol) and triethyl amine (0.035 g, 0.05 mL, 0.35 mmol) in dry dichloromethane (10 mL), acetyl chloride (0.055 g, 0.05 mL, 0.70 mmol) was added at 0 ^{o}C and stirring was continued for 2 hour at room temperature. After completion of the reaction, the solvent was evaporated under reduced pressure, and the residue was dissolved in dichloromethane. The resultant solution was washed with water, brine, dried over anhyd. Na_2SO_4 and solvent removed in vacuo. The purification of compound was performed by column chromatography over silica gel using 20 % ethyl acetate pet ether as eluent to obtain yellow solid (0.056.g, 51%)

^{1}H-NMR (400 MHz, $CDCl_3$): δ 8.49 (s, 1H), 8.36 (d, *J* = 8.4 Hz, 1H), 8.22-8.18 (m, 2H), 8.14-8.09 (m, 2H), 7.92 (d, *J* = 8.8 Hz, 1H), 7.62-7.58 (m, 1H), 7.53 (d, *J* = 8.4 Hz, 1H), 7.42 (dd, *J* = 8.4 Hz and 1.6 Hz, 1H), 7.22-7.19 (m, 1H), 6.50 (d, *J* = 1.2 Hz, 1H) 4.87 (d, *J* = 8.0 Hz, 1H), 4.71 (d, *J* = 7.6 Hz, 1H), 4.54 (t, *J* = 7.6 Hz, 2H), 2.06-1.98 (m, 5H signal merged), 1.57-1.27 (m, 2H), 1.05 (t, *J* = 7.2 Hz, 3H).

^{13}C NMR (100 MHz, $CDCl_3$): δ 170.8, 141.8, 139.4, 135.3, 131.8, 130.0, 129.8, 129.5, 128.4, 128.0, 127.3, 126.9, 126.6, 126.5, 126.0, 125.7, 125.4, 122.8, 122.6, 118.7, 117.9, 111.5, 108.8, 104.9, 67.0, 43.4, 31.3, 21.0, 20.6, 13.9.

IR (KBr): 3049, 2954, 2927, 2869, 2214, 1737, 1581, 1226, 803 cm.$^{-1}$

Compound 131:

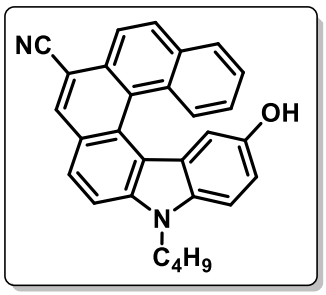

To a solution of aldehyde **129** (0.1 g, 0.24 mmol) in CH_2Cl_2 (5 mL) and MeOH (5 mL), one drop of conc. H_2SO_4 and H_2O_2 (0.009 g, 0.03 mL, 30% in water) were added, and the resultant solution was stirred for 2 hour at room temperature. After completion of the reaction, the solvent was evaporated under reduced pressure, and the residue was dissolved in dichloromethane. The resultant solution was washed with water, brine, dried over anhyd. Na_2SO_4 and solvent removed in vacuo. The purification of compound was performed by column chromatography over silica gel using 30 % ethyl acetate pet ether as eluent to obtain yellow solid (0.057.g, 57%).

^{1}H-NMR (400 MHz, $CDCl_3$): δ 8.43 (s, 1H), 8.14 (d, *J* = 8.4 Hz, 1H), 8.07-8.02 (m, 2H), 7.98 (d, *J* = 7.6 Hz, 1H), 7.89 (d, *J* = 8.8 Hz, 1H), 7.84 (d, *J* = 8.4 Hz, 1H), 7.61-7.57 (m, 1H), 7.43 (d, *J* = 8.8 Hz, 1H), 7.25-7.21 (m, 1H), 7.02 (dd, *J* = 8.8 and 2.4 Hz, 1H), 5.84 (d, *J* = 2.4 Hz, 1H), 4.69 (s, 1H), 4.52 (t, *J* = 7.6 Hz, 2H), 2.03-1.99 (m, 2H), 1.62-1.53 (m, 2H), 1.06 (t, *J* = 7.6 Hz, 3H).

^{13}C NMR (100 MHz, $CDCl_3$): δ 148.2, 142.0, 135.2, 134.5, 131.6, 129.8, 129.6, 129.1, 128.5, 127.7, 127.1, 127.0, 126.6, 126.2, 125.9, 125.6, 123.4, 122.3, 118.8, 117.4, 114.1, 111.7, 110.9, 109.4, 104.1, 43.4, 31.4, 20.6, 13.9.

HRMS: *m/z* calculated for $C_{29}H_{22}N_2ONa$ 437.1630 found; 337.1624.

Compound 132:

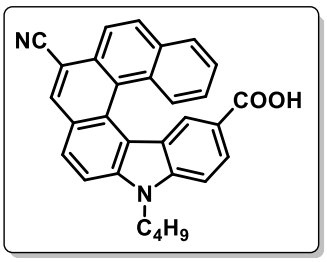

A solution of aldehyde **129** (0.025 g, 0.058 mmol) in MeOH (5 mL) and THF (5 mL) was added a solution of $KMnO_4$ (0.018 g, 0.116 mmol) and Na_2HPO_4 (0.008 g, 0.058) in water (2 mL); the resultant solution was stirred for 2 hour at room temperature. After completion of the reaction, the solvent was evaporated under reduced pressure, and the residue was dissolved in dichloromethane. The resultant solution was washed with water, brine, dried over anhyd. Na_2SO_4 sulfate and concentrated at reduced pressure to afford **132** (22 mg, quant) as a light brown solid.

^{1}H-NMR (400 MHz, DMSO-*d6*): δ 8.92 (s, 1H), 8.42-8.35 (m, 3H), 8.25 (m, 2H), 8.03 (d, *J* = 8.4 Hz, 1H), 7.97 (d, *J* = 9.2 Hz, 1H), 7.84 (d, *J* = 8.8 Hz, 1H), 7.65 (m, 1H), 7.20 (m, 1H), 7.14 (s, 1H), 4.69 (m, 2H), 1.88 (m, 2H), 1.43 (m, 2H), 0.94 (t, *J* = 7.6 Hz, 3H).

Compound 134:

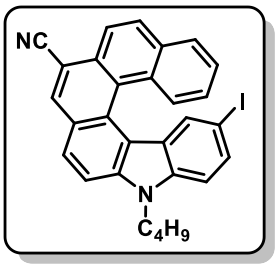

To a stirred solution of 7-cyano *N*-butyl aza[6]helicene **110** (1.0 g, 2.51 mmol) in ethanol (25 ml) and THF (25 mL), solid sodium periodate (0.538 g, 2.51 mmol) and molecular iodine (0.637 g, 2.51 mmol) were added. Then 2 to 3 drops of concentrated sulfuric acid was added gently. The reaction was stirred for 1 hour at 70° until the tlc indicated that the reaction was completed. The reaction mixture was neutralized with sodium hydroxide, extracted with dichloromethane (3 x 50 ml) and washed with water. The combined extracts were dried

over sodium sulfate, and evaporated in vacuo to give a brownish solid residue. The purification of compound was performed by column chromatography over silica gel using 20 % ethyl acetate pet ether as eluent to obtain brown solid (1.03.g, 79%).

^{1}H-NMR (400 MHz, $CDCl_3$): δ 8.48 (s, 1H), 8.35 (d, *J* = 8.8 Hz, 1H), 8.21 (d, *J* = 8.8 Hz, 1H), 8.17 (d, *J* = 7.6 Hz, 1H), 8.11 (d, *J* = 8.8 Hz, 1H), 8.06 (d, *J* = 8.4 Hz, 1H), 7.90 (d, *J* = 8.8 Hz, 1H), 7.74-7.70 (m, 1H), 7.65 (dd, *J* = 8.4 and 3.6 Hz, 1H), 7.31 (d, *J* = 8.4 Hz, 1H), 7.28-7.24 (m, 1H), 6.71 (d, *J* = 1.6 Hz, 1H), 4.50 (t, *J* = 7.2 Hz, 2H), 2.0-1.96 (m, 2H), 1.59-1.49 (m, 2H), 1.03 (t, *J* = 7.6 Hz, 3H).

Compound 133:

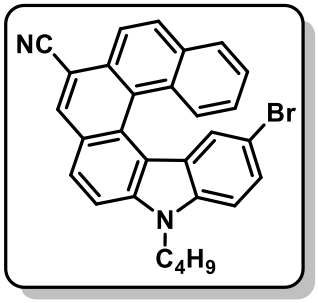

To a stirred solution of 7-cyano *N*-butyl aza[6]helicene **110** (0.5 g, 1.25 mmol) in acetone (20 mL), *N*-bromosuccinimide (0.246 g, 1.38 mmol) was added and stirring was continued for 30 minutes to 1 hour at room temperature. After completion of the reaction, the solvent was evaporated under reduced pressure. The purification of compound was performed by column chromatography over silica gel using 20 % ethyl acetate pet ether as eluent to obtain brown solid (0.37 g, 62%).

^{1}H-NMR (400 MHz, $CDCl_3$): δ 8.50 (s, 1H), 8.35 (d, *J* = 8.8 Hz, 1H), 8.22 (d, *J* = 8.8 Hz, 1H), 8.16 (d, *J* = 7.6 Hz, 1H), 8.13-8.08 (m, 2H), 7.91 (d, *J* = 8.8 Hz, 1H), 7.72-7.68 (m, 1H), 7.49 (dd, *J* = 8.4 and 1.6 Hz, 1H), 7.41 (d, *J* = 8.8 Hz, 1H), 7.29-7.24 (m, 1H), 6.54 (d, *J* = 2.0 Hz, 1H), 4.51 (t, *J* = 7.6 Hz, 2H), 2.02-1.94 (m, 2H), 1.63-1.49 (m, 2H), 1.04 (t, *J* = 7.6 Hz, 3H).

Compound 135:

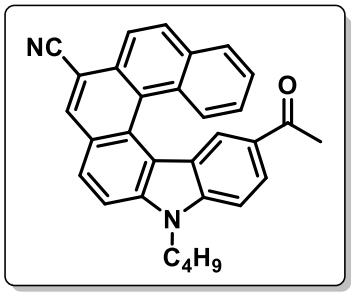

Acetyl chloride (0.078 g, 0.07 mL, 1.0 mmol) was added drop wise to a solution of compound **110** (0.2 g, 0.50 mmol) and aluminum chloride (0.134 g, 1.0 mmol) in dichloromethane (15 mL) with stirring at 0 °C and the mixture was stirred for 1 hour at room temperature. After completion of the reaction, the solvent was evaporated under reduced pressure, and the residue was dissolved in dichloromethane. The resultant solution was washed with water, brine, dried over anhyd. Na_2SO_4 and solvent

removed in vacuo. The purification of compound was performed by column chromatography over silica gel using 30 % ethyl acetate pet ether as eluent to obtain brown solid (0.201.g, 91%).

^{1}H-NMR (400 MHz, $CDCl_3$): δ 8.43 (s, 1H), 8.32 (d, *J* = 8.4 Hz, 1H), 8.19 (d, H = 8.8 Hz, 1H), 8.14-8.11 (m, 3H), 8.07 (d, *J* = 8.4 Hz, 1H), 7.90 (d, *J* = 8.8 Hz, 1H), 7.64-7.60 (m, 1H), 7.55 (d, *J* = 8.8 Hz, 1H), 7.19-7.15 (m, 2H), 4.53 (t, *J* = 7.6 Hz, 2H), 2.04-1.97 (m, 2H), 1.93 (s, 3H), 1.58-1.49 (m, 2H), 1.05 (t, *J* = 7.6 Hz, 3H).

IR (KBr): 3438, 3056, 2958, 2928, 2218, 1727, 1668, 1488, 1397, 954 cm.$^{-1}$

Compound 136:

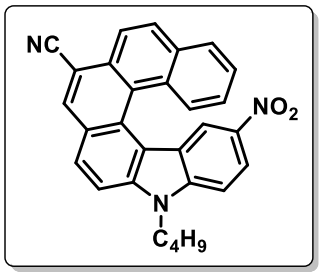

Concentrated nitric acid (0.031 g, 0.05 mL, 65%) was added drop wise to a solution of compound **110** (0.1 g, 0.25 mmol)) in 1,2- dichloroethane (10 mL) with stirring at 0 ^oC and the mixture was stirred for 5 hour at room temperature. After completion of the reaction, the solvent was evaporated under reduced pressure, and the residue was dissolved in dichloromethane. The resultant solution was washed with water, brine, dried over anhyd. Na_2SO_4 and solvent removed in vacuo. The purification of compound was performed by column chromatography over silica gel using 50 % ethyl acetate pet ether as eluent to obtain yellow solid (0.85 g, 77%).

^{1}H NMR (400 MHz, $CDCl_3$): δ 8.52 (s, 1H), 8.39 (d, J=8.8 Hz, 1H), 8.32 (dd, J=8.8 and 2.4 Hz, 1H), 8.28 (d, J=8.8 Hz, 1H), 8.22 ((d, J=8.8 Hz, 2H), 8.05 (d, J=8.4 Hz, 1H), 7.96 (d, J=8.8 Hz, 1H), 7.69-7.65 (m, 1H), 7.56 (d, J=8.8 Hz, 1H), 7.44 (d, J=2.4 Hz, 1H), 7.20-7.15 (m, 1H), 4.59 (t, J=7.2 Hz, 2H), 2.07-2.00 (m, 2H), 1.57-1.53 (m, 2H), 1.07 (t, J=7.2 Hz, 3H).

IR (KBr): 3444, 3086, 3055, 2960, 2931, 2869, 2222, 1598, 1521, 1332, 846 cm.$^{-1}$

Compound 138 (Ligand 1):

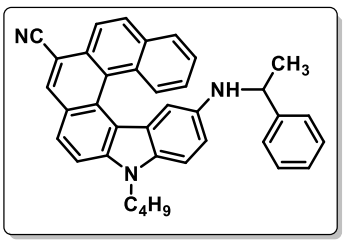

(*S*)-α-Methyl benzylamine (0.347 g, 0.37 mL, 2.86 mmol), Cs_2CO_3 (3.10 g, 9.54 mmol), Xphos (0.045 g, 0.095), and $Pd(OAc)_2$ (0.043 g, 0.190 mmol) were added to a solution of **134** (1.0 g, 1.90 mmol) in dry toluene (25 mL), and the reaction mixture was stirred at reflux for 8 h.

After completion of the reaction, the solvent was evaporated under reduced pressure, and the residue was dissolved in dichloromethane. The resultant solution was washed with water, brine, dried over anhyd. Na_2SO_4 and solvent removed in vacuo. The purification of compound was performed by column chromatography over silica gel using 10 % ethyl acetate pet ether as eluent to obtain mixture of diastereomers as yellow solid (0.581.g, 59%). These diastereomers were readily separated by silica gel column chromatography.

^{1}H-NMR (400 MHz, $CDCl_3$): (*minor diastereomer*) δ 8.44 (s, 1H), 8.37 (d, *J* = 8.8 Hz, 1H), 8.22-8.17 (m, 2H), 8.12 (d, *J* = 7.6 Hz, 1H), 7.98 (d, *J* = 8.8 Hz, 1H), 7.81 (d, *J* = 8.8 Hz, 1H), 7.63-7.59 (m, 1H), 7.33-7.21 (m, 7H), 6.70 (dd, *J* = 8.8 and 2.4 Hz, 1H), 5.80 (d, *J* = 2.4 Hz, 1H), 4.41 (t, *J* = 7.2 Hz, 2H), 4.06 (q, *J* = 6.4 Hz, 1H), 1.96-1.93 (m, 2H), 1.53-1.47 (m, 2H), 1.27 (d, *J* = 6.4 Hz, 3H), 1.02 (t, *J* = 7.6 Hz, 3H).

^{1}H-NMR (400 MHz, $CDCl_3$): (*major diastereomer*) δ 8.38 (s, 1H), 8.36 (d, *J* = 8.4 Hz, 1H), 8.24 (d, *J* = 8.4 Hz, 2H), 8.19 (d, *J* = 8.4 Hz, 1H), 7.92 (d, *J* = 8.8 Hz, 1H), 7.77 (d, *J* = 8.8 Hz, 1H), 7.69-7.66 (m, 1H), 7.32-7.30 (m, 2H), 7.07-6.91 (m, 5H), 6.79 (dd, *J* = 8.8 and 2.4 Hz, 1H), 5.55 (d, *J* = 2.4 Hz, 1H), 4.41 (t, *J* = 7.2 Hz, 2H), 3.59 (q, *J* = 6.8 Hz, 1H), 1.93-1.87 (m, 2H), 1.63-1.45 (m, 2H), 1.34 *J* = 6.4 Hz, 3H), 1.01 (t, *J* = 7.2 Hz, 3H).

Compound 139 (Ligand 2)

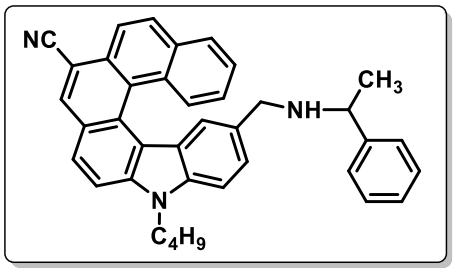

To a solution of **134** (0.1 g, 0.23 mmol) in anhydrous EtOH/THF (10 mL) was added (*S*)-α-Methyl benzylamine (0.170 g, 0.18 mL, 1.4 mmol) titanium(IV) isopropoxide (0.0.20 g, 0.20 mL, 0.7 mmol). The resulting solution was stirred at RT for 10 h. Sodium borohydride (0.017 g, 0.47 mmol) was added to the solution at 0 ^oC and was stirred at RT for 5 h before pouring into 2.0 M aqueous ammonia (10 mL). The suspension was filtered through Celite, and to the filtrate was added H_2O. Crude product was extracted with DCM, dried over anhydrous sodium sulfate. The purification of compound was performed by column chromatography over silica gel using 30 % ethyl acetate pet ether as eluent to obtain yellow solid (0.085 g, 68%).

^{1}H-NMR (400 MHz, $CDCl_3$): δ 8.45 (s, 1H), 8.37-8.35 (m, 1H), 8.20 (d, *J* = 8.8 Hz, 2H), 8.08 (d, *J* = 8.4 Hz, 1H), 8.03 (dd, *J* = 9.2 and 2.0 Hz, 1H), 7.86 (dd, *J* = 8.8 and 1.6 Hz, 1H), 7.48-7.44 (m, 2H), 7.38-7.15 (m, 7H), 6.43 (s, 1H), 4.50 (t, *J* = 6.8 Hz, 2H), 3.67 (q, *J* = 6.4 Hz, 1H), 3.7-3.34 (m, 1H signal merged), 3.28 (d, *J* = 12.4 Hz, 1H), 2.02-1.95 (m, 2H), 1.58-1.48 (m, 2H), 1.33 (t, *J* = 6.4 Hz, 3H), 1.04 (t, *J* = 7.2 Hz, 3H).

Compound 140 (Ligand 3)

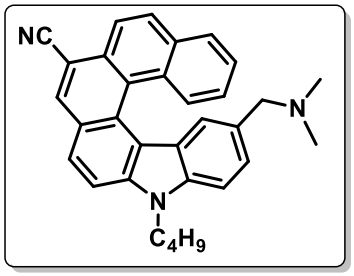

To a solution of **134** (0.1 g, 0.23 mmol) in anhydrous EtOH/THF (10 mL) was added *N*, *N*-dimethyl amine (0.106 g, 1.17 mL, 2.3 mmol, 2.0 M solution in MeOH), titanium(IV) isopropoxide (0.0.20 g, 0.20 mL, 0.7 mmol). The resulting solution was stirred at RT for 10 h. Sodium borohydride (0.017 g, 0.47 mmol) was added to the solution at 0 ^oC and was stirred at RT for 5 h before pouring into 2.0 M aqueous ammonia (10 mL). The suspension was filtered through Celite, and to the filtrate was added H_2O. Crude product was extracted with DCM, dried over anhydrous sodium sulfate. The purification of compound was performed by column chromatography over alumina gel using 30 % ethyl acetate pet ether as eluent to obtain yellow solid (0.051 g, 51%).

^{1}H-NMR (400 MHz, $CDCl_3$): δ 8.48 (s, 1H), 8.36 (d, *J* = 8.8 Hz, 1H), 8.22-8.19 (m, 2H), 8.12 (d, *J* = 7.6 Hz, 1H), 8.06 (d, *J* = 8.8 Hz, 1H), 7.91 (d, *J* = 8.8 Hz, 1H), 7.59-7.55 (m, 1H), 7.52 (d, *J* = 8.4 Hz, 1H), 7.46 (dd, *J* = 8.4 and 1.2 Hz, 1H), 7.17-7.13 (m, 1H), 6.37 (s, 1H), 4.53 (t, *J* = 7.6 Hz, 2H), 3.20 (d, *J* = 12.4 Hz, 1H), 2.91 (d, *J* = 12.4 Hz, 1H), 2.07 (s, 6H), 2.05-1.74 (m, 2H), 1.58-1.52 (m, 2H), 1.05 (t, *J* = 7.6 Hz, 3H).

Compound 141:

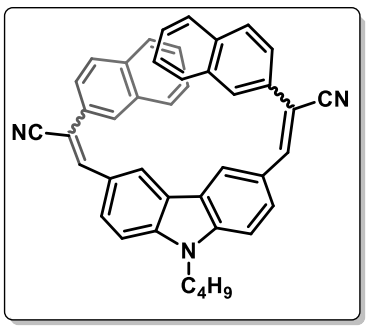

A solution of 9-butyl carbazole-3,6-dicarbaldehyde (0.2 g, 0.72 mmol) and Cyanomethyl naphthalene (0.299 g, 1.79 mmol) in dry ethanol (25 mL) was placed in a single neck R.B. flask fitted with a septum , which is degassed and purged with nitrogen. To this was added drop-wise, with stirring, a solution of (0.165 g, 7.17 mmol) sodium dissolved in 25 mL of dry ethanol and the mixture was stirred

vigorously for 6 hours at room temperature. After completion of reaction the ethanol was evaporated under reduced pressure the mixture was poured into ice-cold water and extracted with ethyl acetate (3 x 50 mL). The combined organic phase was washed with water, brine, and dried over anhydrous sodium sulfate. The solvent was removed under reduced pressure and the crude product was purified by column chromatography on silica gel using 30% ethyl acetate-pet ether as eluent to afford compound **141** as yellow solid. (0.32 g, 77%)

^{1}H-NMR (400 MHz, $CDCl_3$): δ 8.70 (d, *J* = 1.6 Hz, 2H), 8.27 (dd, *J* = 8.8 and 1.6 Hz, 2H), 8.21 (d, *J* = 1.6 Hz, 2H), 7.95 (7.82 (m, 9H), 7.58-7.52 (m, 6H), 4.35 (t, *J* = 7.2 Hz, 2H), 1.94-1.90 (m, 2H), 1.46-1.02 (m, 2H), 1.00 (t, *J* = 7.6 Hz, 3H).

^{13}C-NMR (100 MHz, $CDCl_3$): δ 142.9, 142.1, 133.3, 133.1, 132.2, 128.8, 128.4, 127.6, 127.5, 126.8, 126.7, 125.8, 125.6, 123.1, 123.0, 122.5, 119.0, 109.6, 108.1, 43.3, 31.1, 20.5, 13.8.

Compound 142:

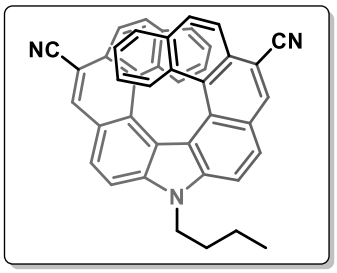

In an immersion wall photo reactor (borosilicate glass) equipped with a water cooling jacket and stir bar a solution of 3,3-(9-butyl-9*H*carbazole-3,6-diyl)-bis(2-phenylacrylonitrile) **141** (0.25 g, 0.43 mmol), iodine (0.242 g, 0.95 mmol), THF (3.12 g, 3.51 mL, 43.0 mmol) and toluene (350 mL) was irradiated using a 125W HPMV lamp for 5-7 h monitored by TLC. After the completion of reaction, the excess of iodine was removed by washing the solution with aqueous $Na_2S_2O_3$, followed by distilled water. The organic layer was concentrated under the reduced pressure to obtain the crude product. The crude product purified by column chromatography over silica gel using petroleum ether: ethyl acetate (80:20) as eluent to obtained compound **142** as yellow solid (0.198 g, 80%).

^{1}H-NMR (400 MHz, $CDCl_3$): δ 8.32 (d, *J* = 8.4 Hz, 2H), 8.21 (d, *J* = 8.4 Hz, 2H), 8.12 (d, *J* = 8.0 Hz, 2H), 7.62-7.55 (m, 4H), 7.43 (d, *J* = 8.4 Hz, 2H), 7.33-7.31 (m, 2H), 6.79-6.75 (m, 2H), 6.13 (d, *J* = 8.4 Hz, 2H), 5.64-5.60 (m, 2H), 5.02-4.94 (m, 2H), 2.32-2.28 (m, 2H), 1.74-1.57 (m, 2H), 1.12 (t, *J* = 7.2 Hz, 3H).

^{13}C-NMR (100 MHz, $CDCl_3$): δ 139.5, 133.8, 129.5, 128.3, 127.3, 127.2, 127.1, 126.37, 126.31, 126.0, 125.5, 125.1, 124.8, 122.7, 121.3, 118.8, 118.3, 110.5, 105.3, 44.1, 32.2, 20.8, 14.0.

2.13 Spectral data:

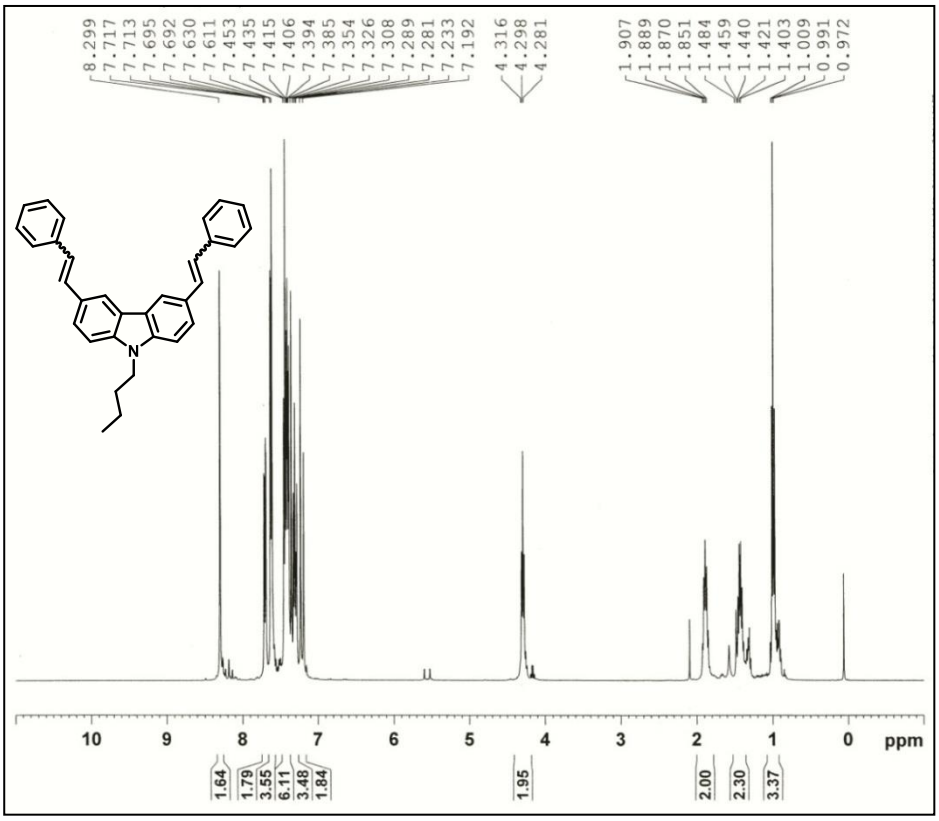

^{1}H-NMR of compound 51 ($CDCl_3$ 400 MHz

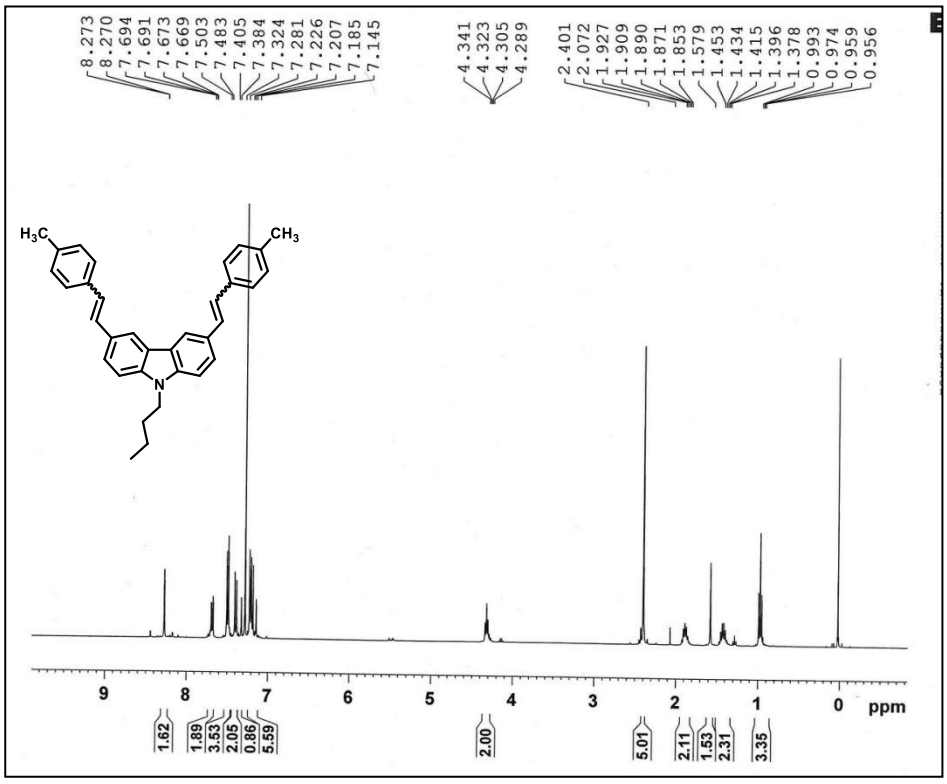

^{1}H-NMR of compound 52 ($CDCl_3$ 400 MHz

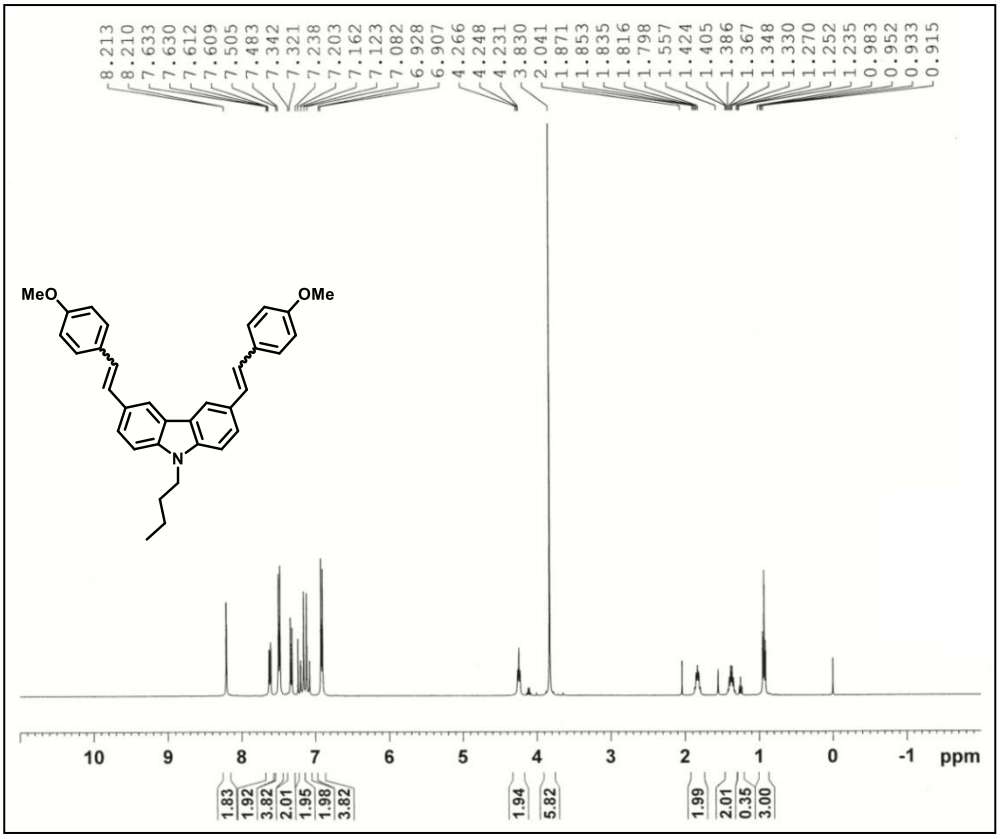

^{1}H-NMR of compound 55 ($CDCl_3$ 400 MHz)

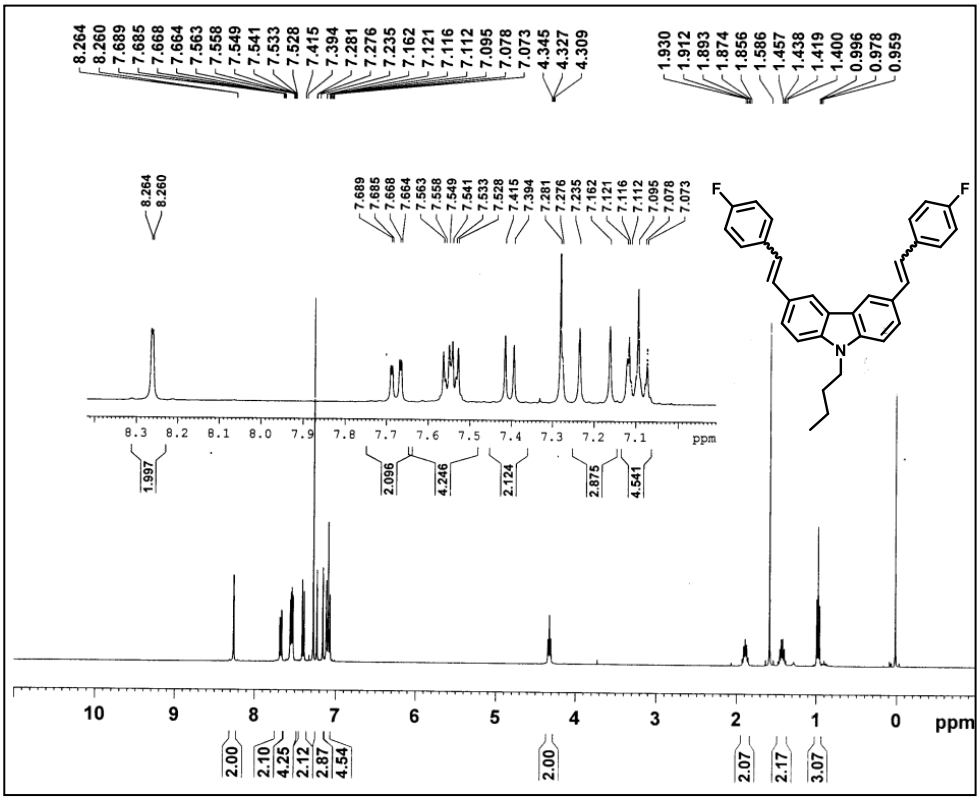

^{1}H-NMR of compound 56 ($CDCl_3$ 400 MHz)

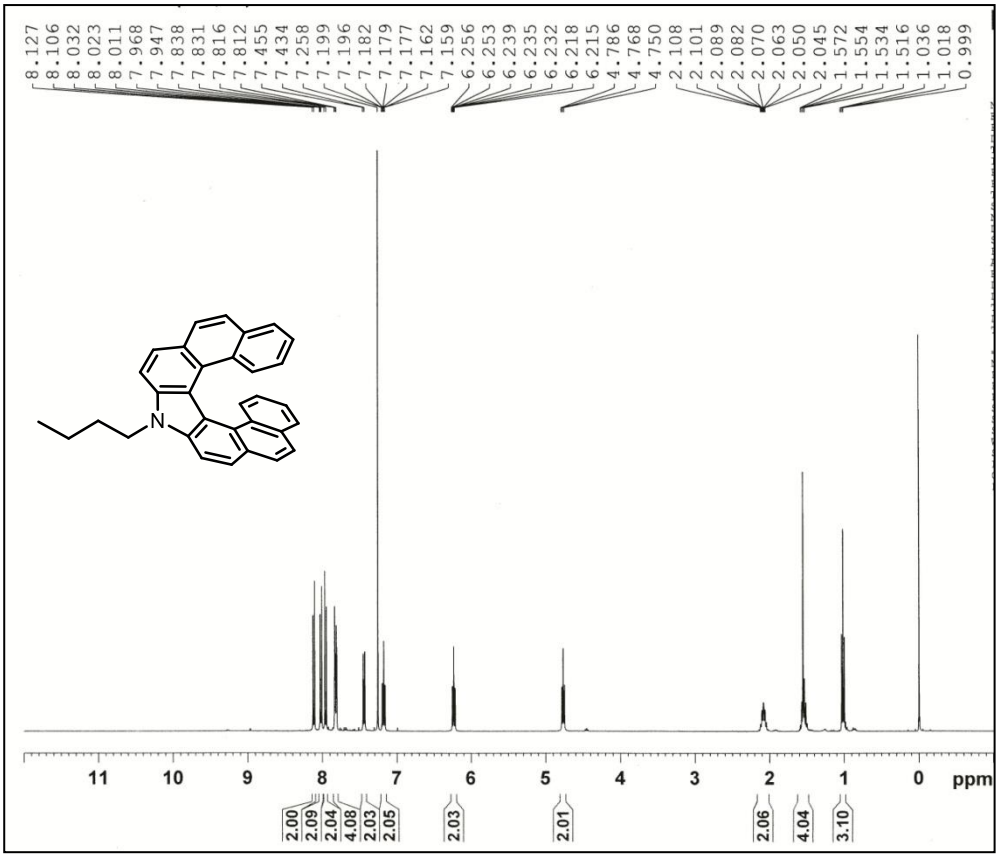

^{1}H-NMR of compound 57 ($CDCl_3$ 400 MHz)

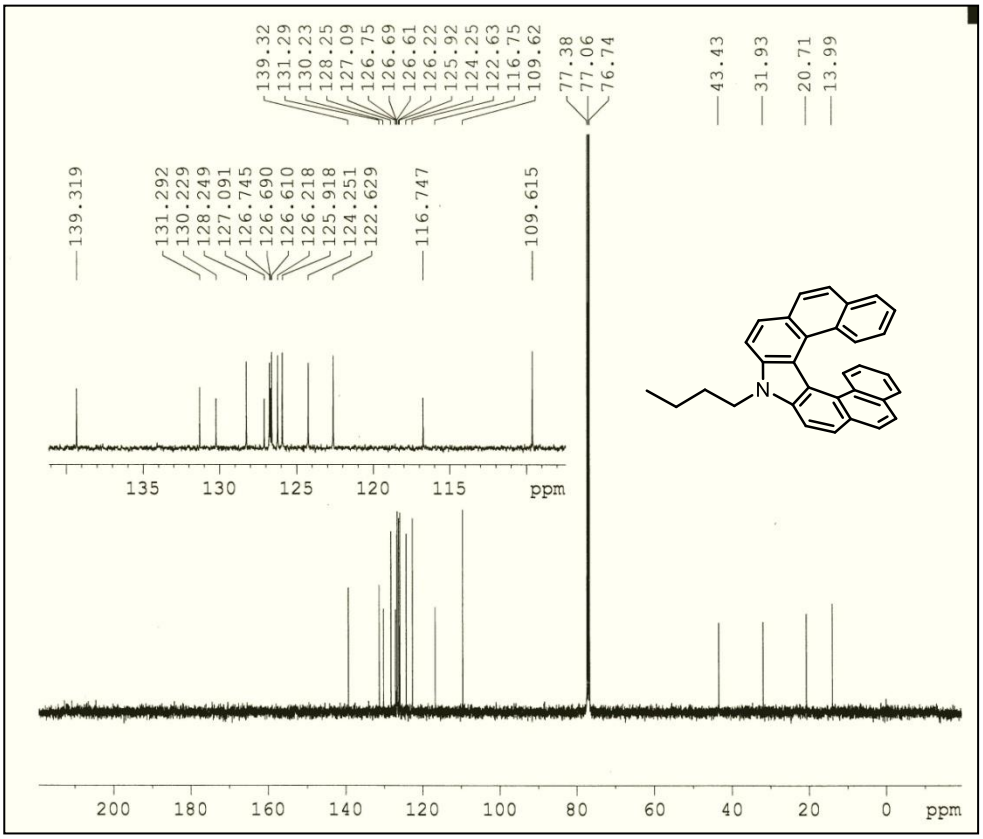

^{13}C-NMR of compound 57 ($CDCl_3$, 100 MHz)

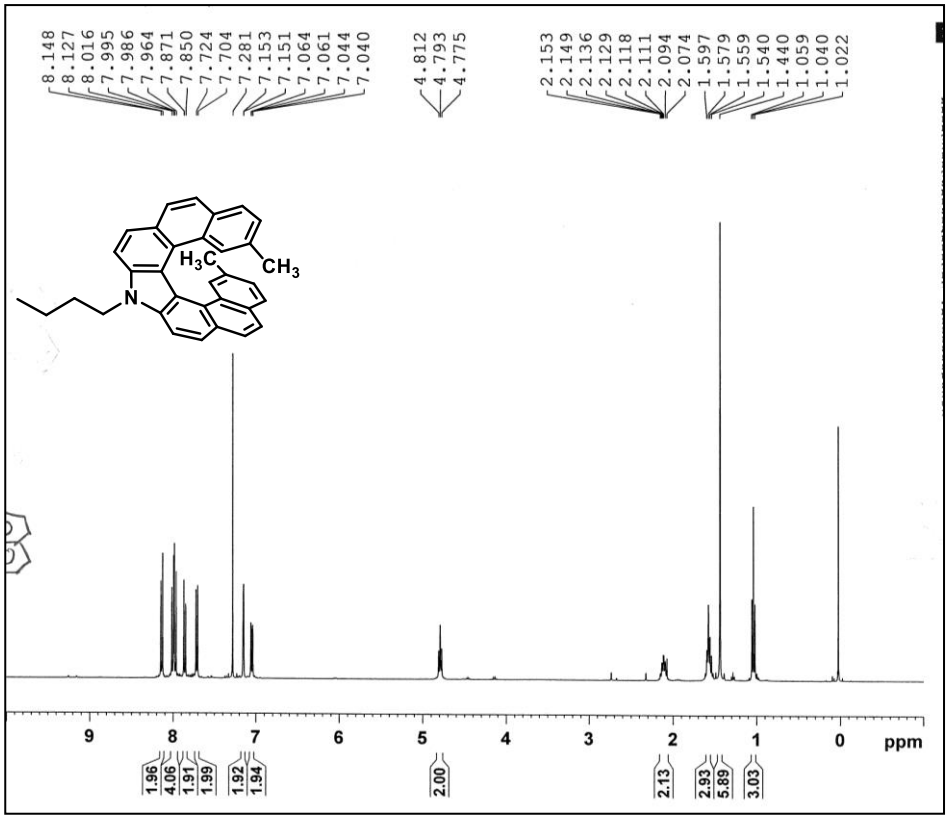

^{1}H-NMR of compound 58 ($CDCl_3$ 400 MHz)

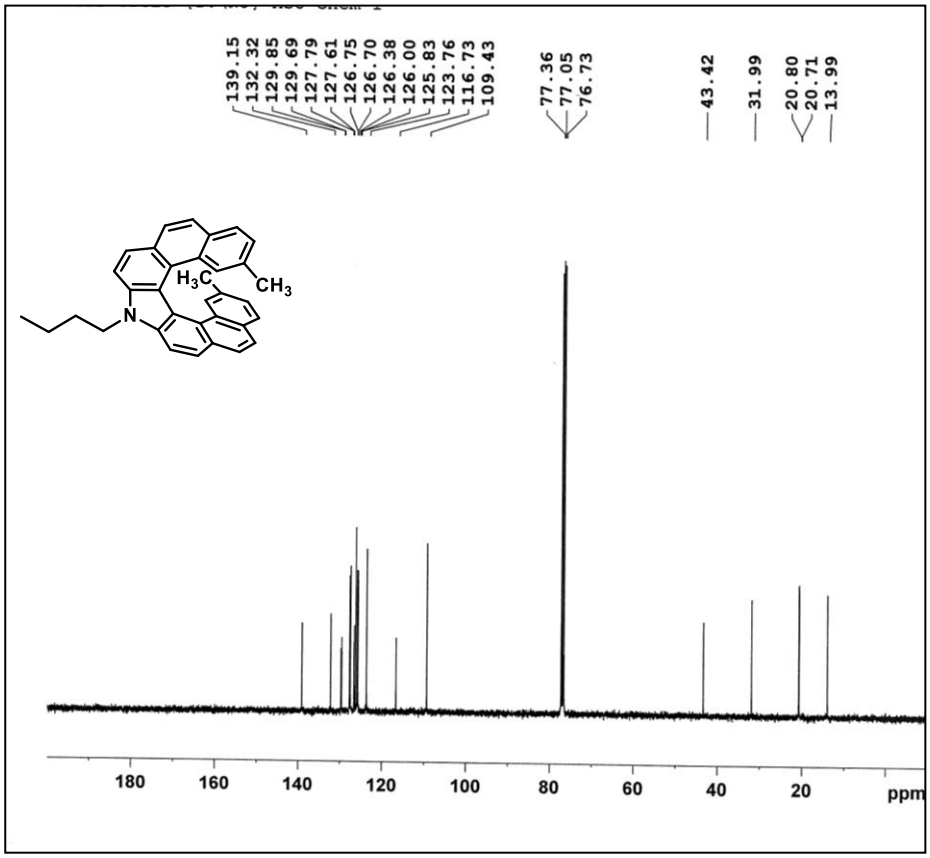

^{13}C-NMR of compound 58 ($CDCl_3$, 100 MHz)

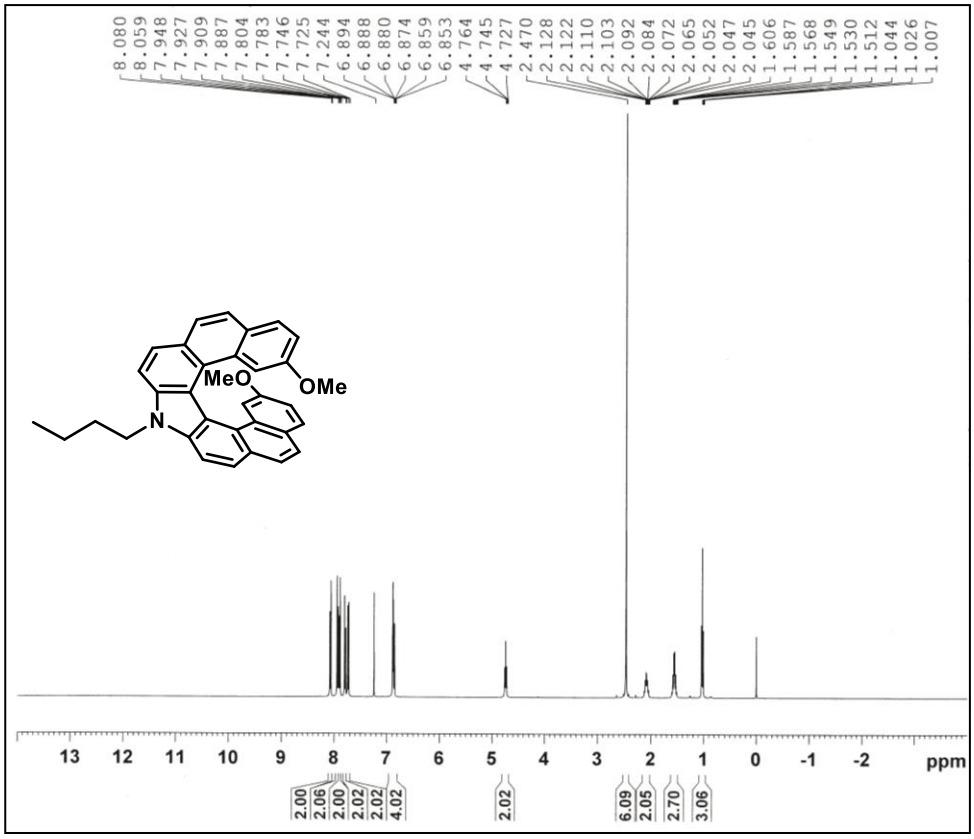

^{1}H-NMR of compound 59 ($CDCl_3$ 400 MHz)

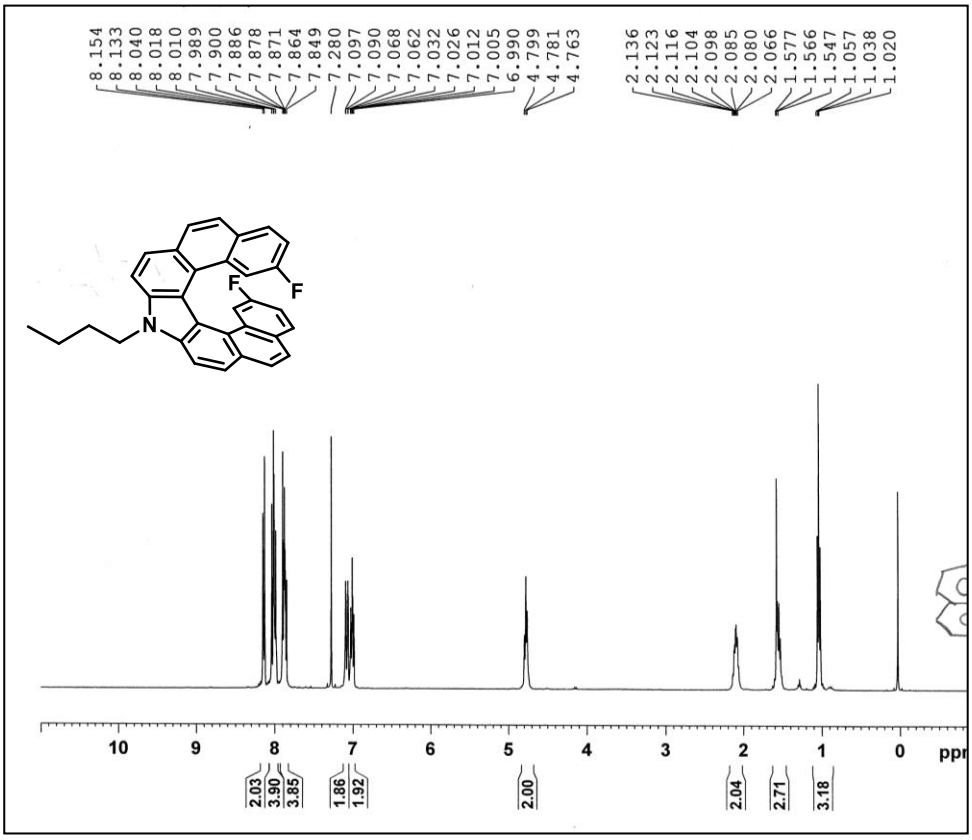

^{1}H-NMR of compound 60 ($CDCl_3$ 400 MHz)

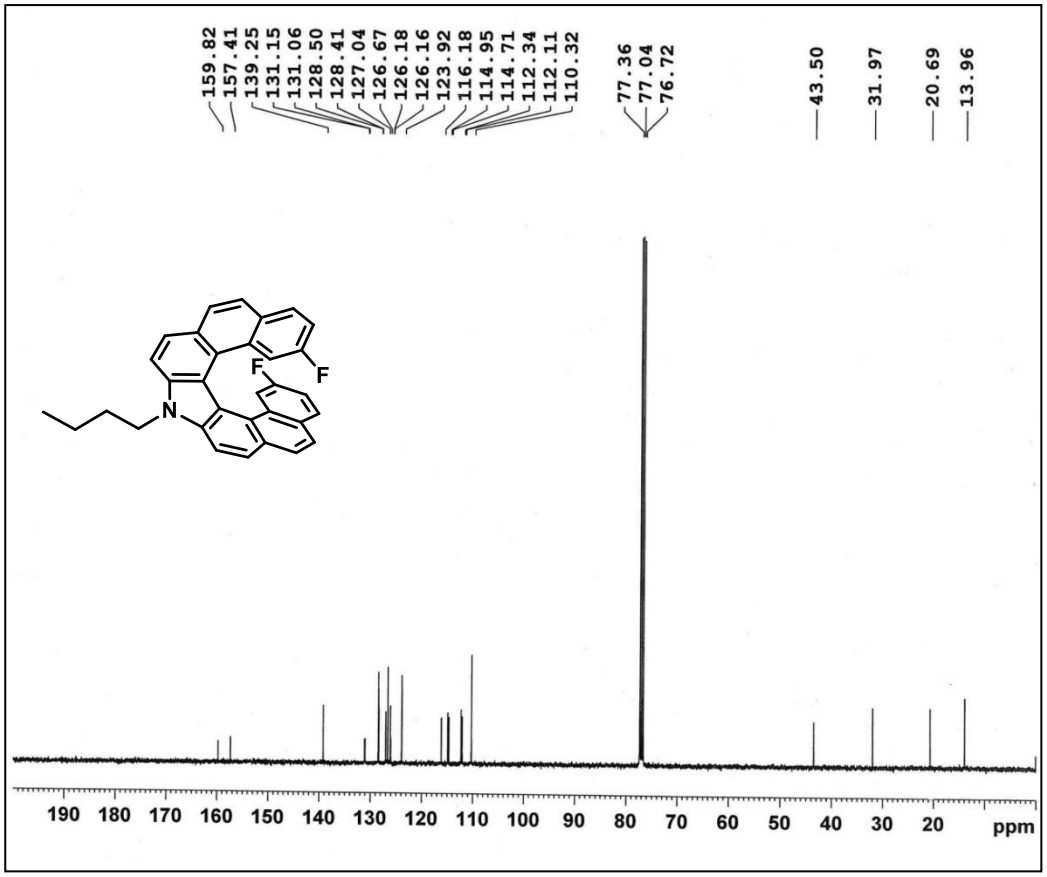

^{13}C-NMR of compound 60 ($CDCl_3$, 100 MHz)

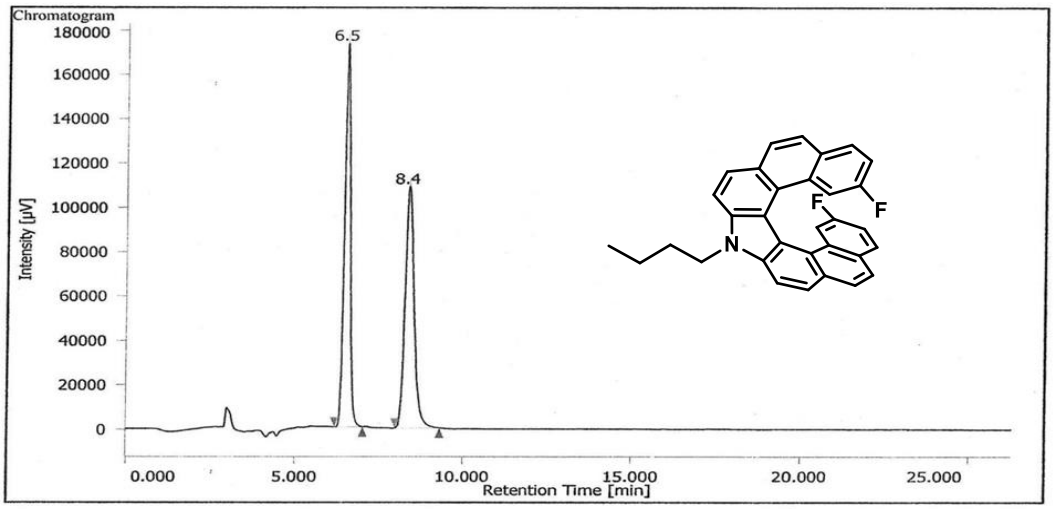

Peak Information

#	Peak Name	CH	tR [min]	Area [µV·sec]	Height [µV]	Area%	NTP	Resolution	Symmetry Factor
1	Unknown	1	6.508	2063422	172953	49.932	7011	4.657	1.160
2	Unknown	1	8.358	2069055	108912	50.068	4739	N/A	1.309

HPLC Chromatoram of compound 60

HPLC conditions: Chiralcel OD-H Column, Solvent System: Hexane: *Iso*-propanol (90:10), Flow rate: 1.0 mL/min.

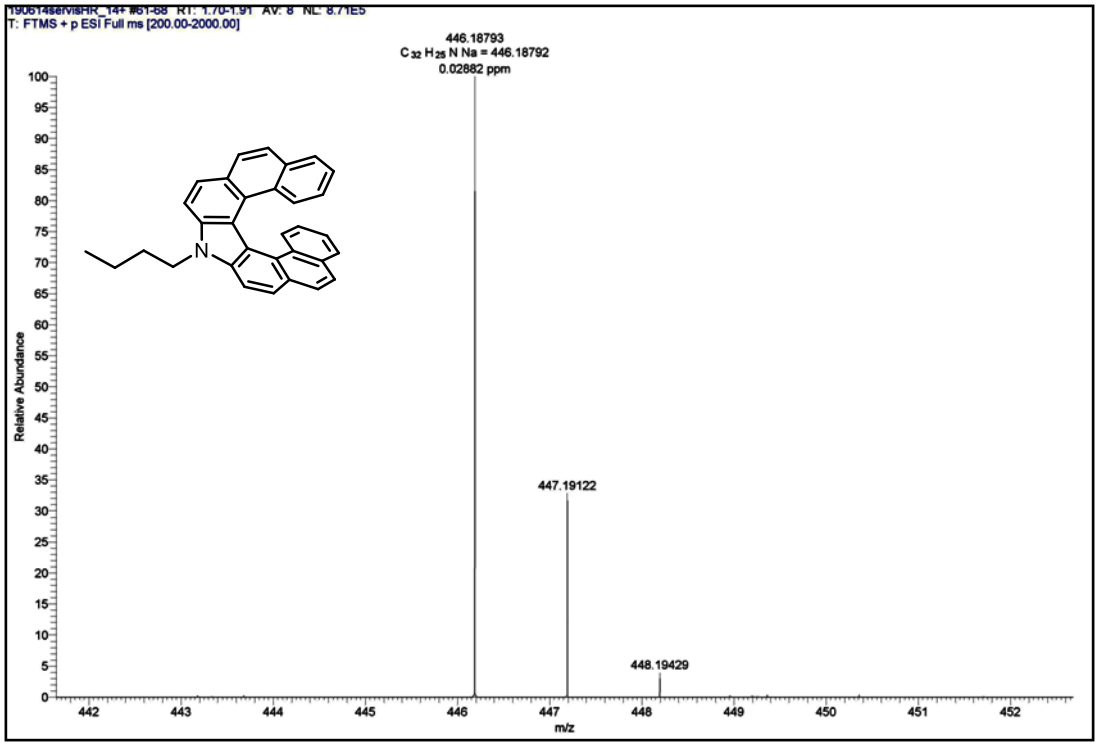

HRMS of compound 57

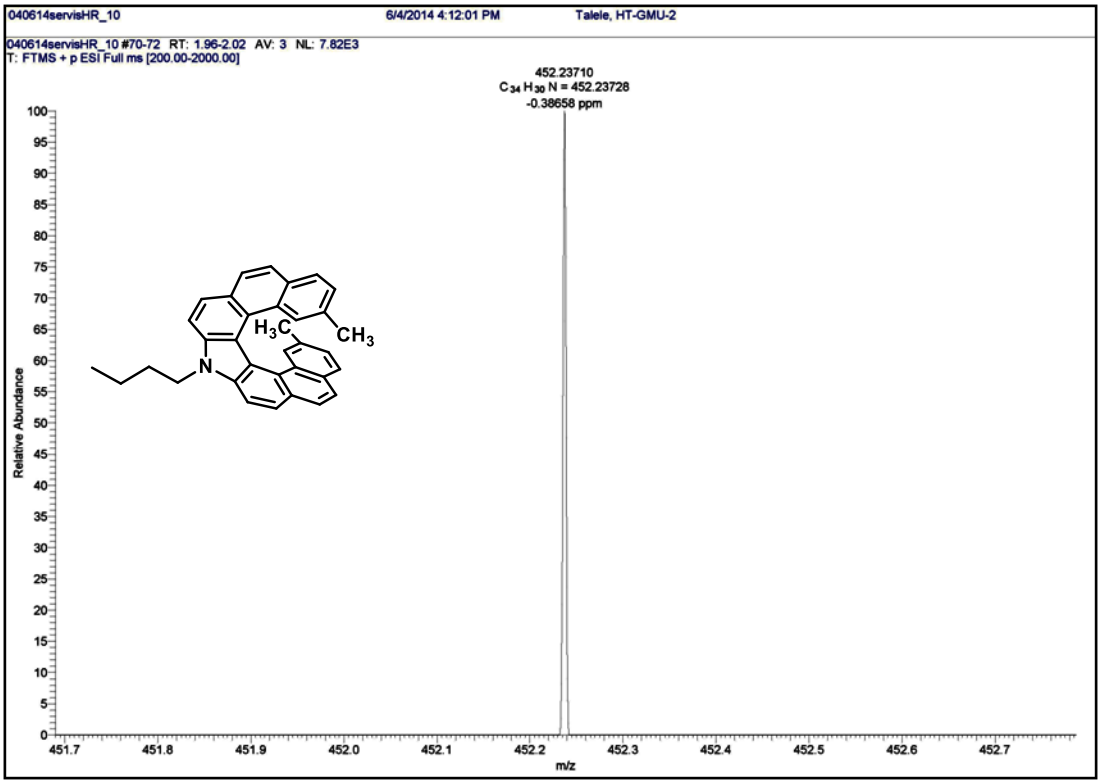

HRMS of compound 58

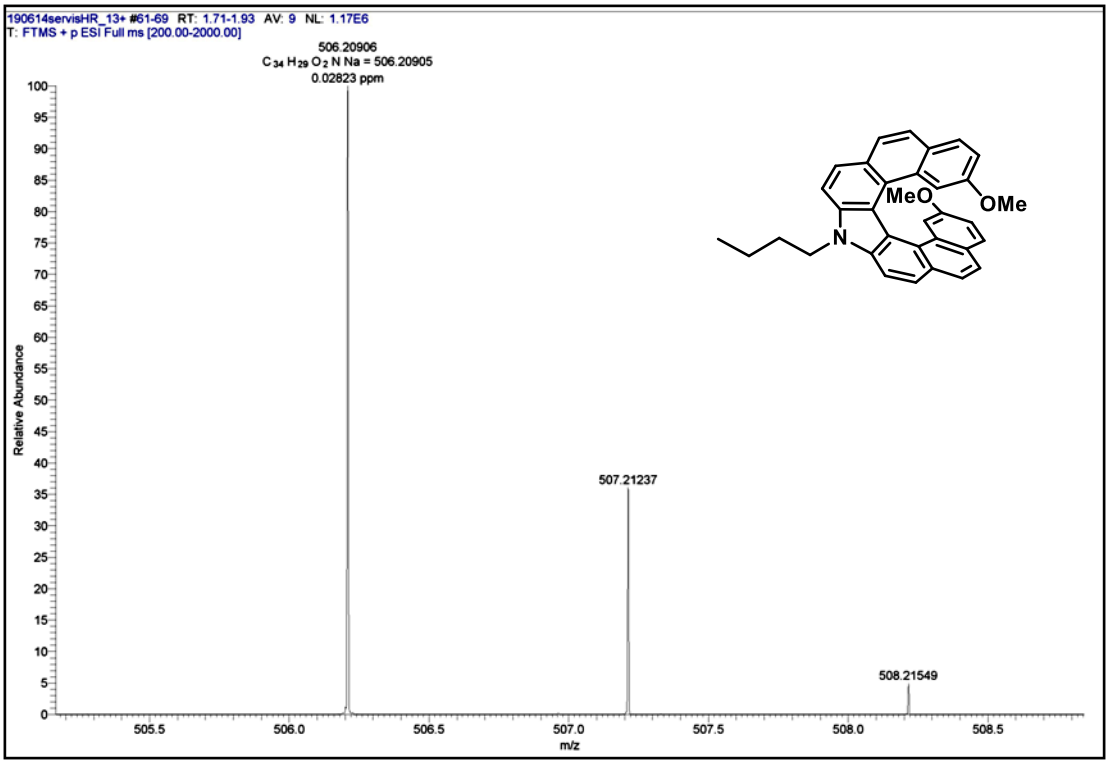

HRMS of compound 59

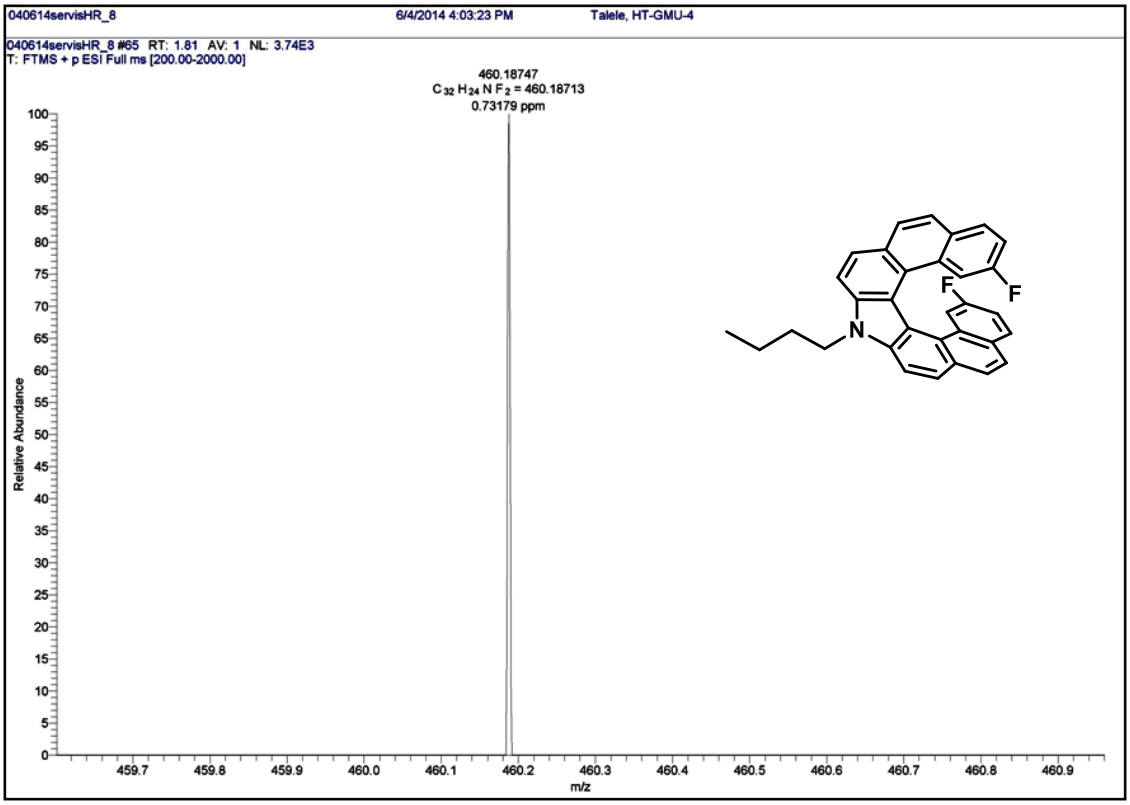

HRMS of compound 60

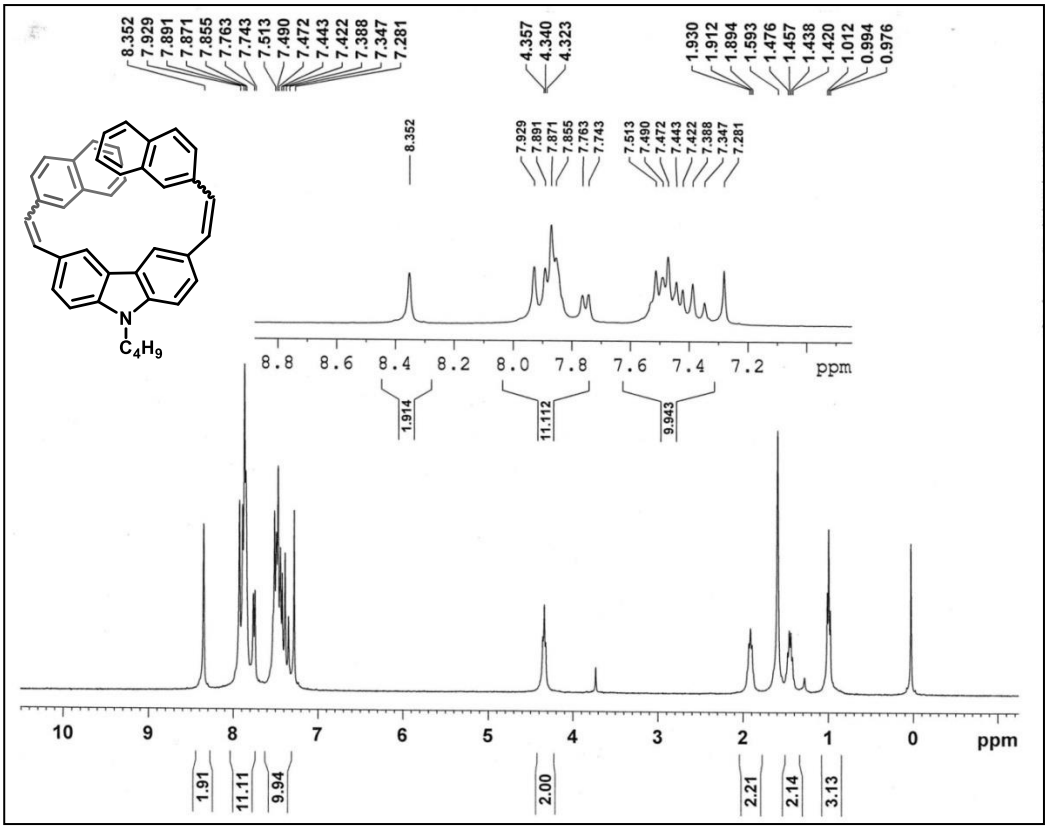

^{1}H-NMR of compound 64 ($CDCl_3$ 400 MHz)

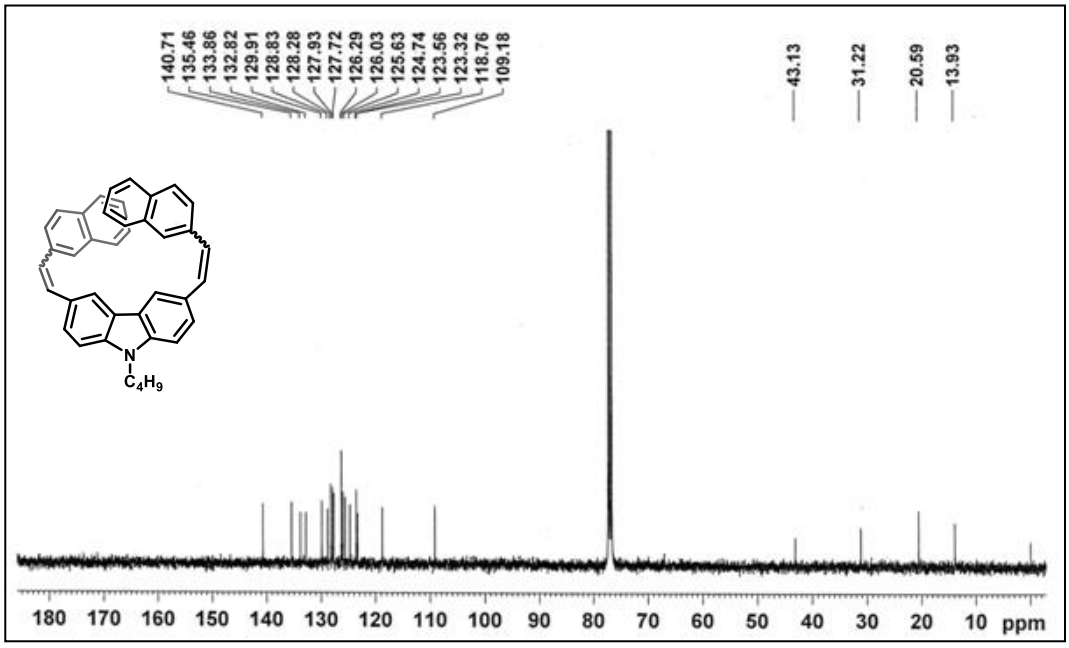

^{13}C-NMR of compound 64 ($CDCl_3$, 100 MHz)

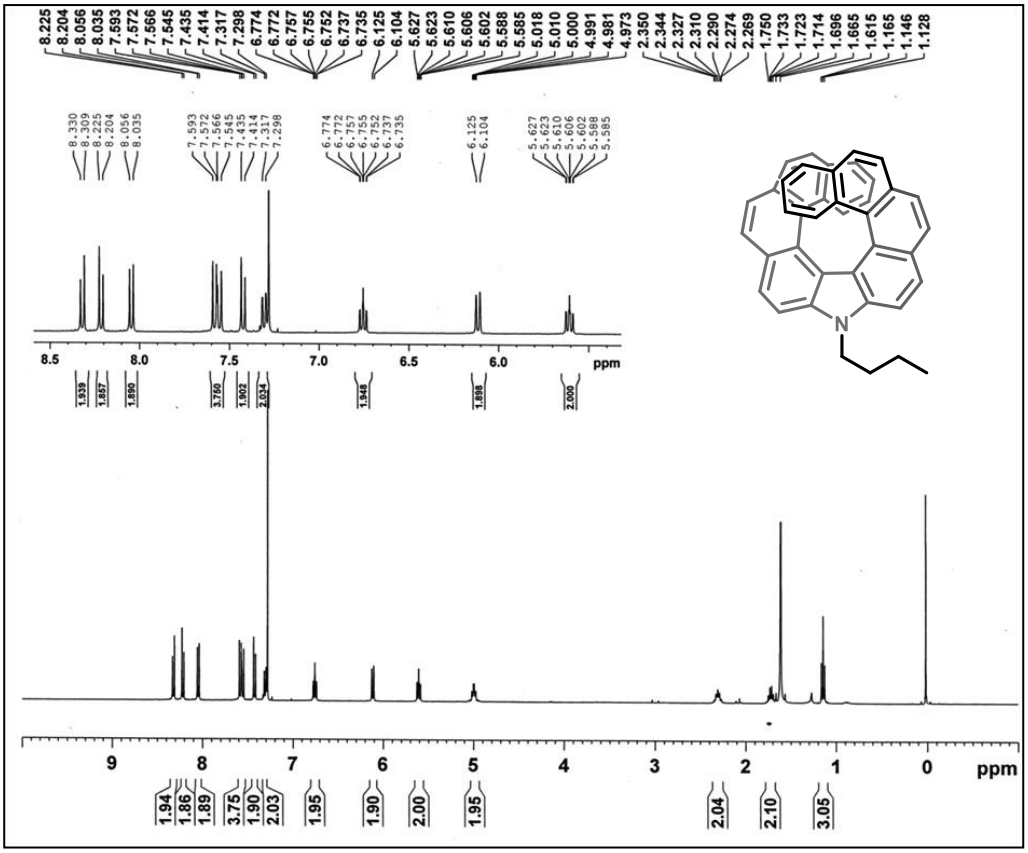

^{1}H-NMR of compound 65 ($CDCl_3$ 400 MHz)

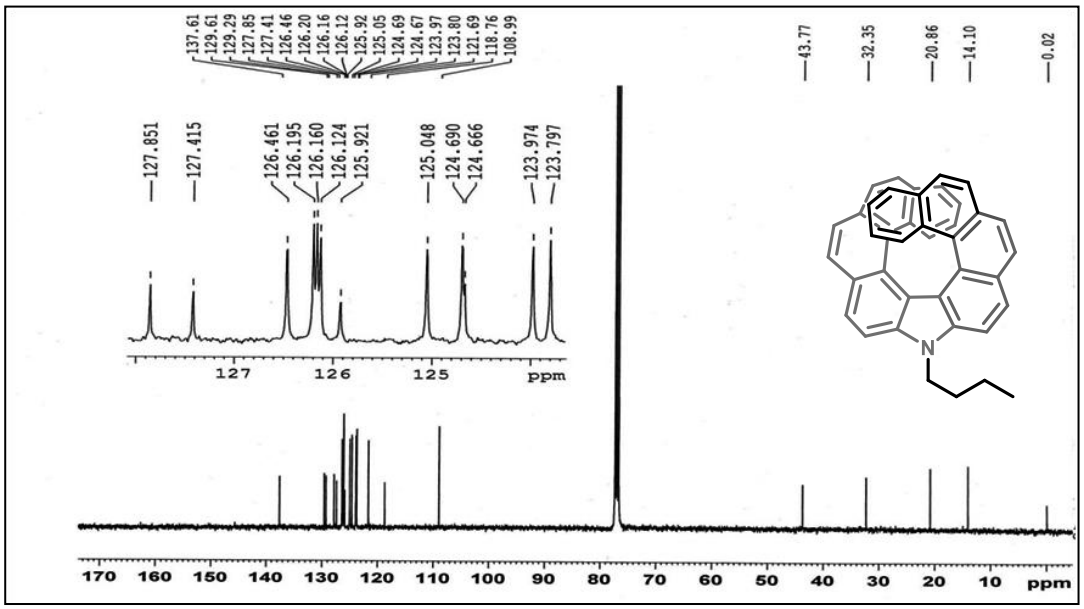

^{13}C-NMR of compound 65 ($CDCl_3$, 100 MHz)

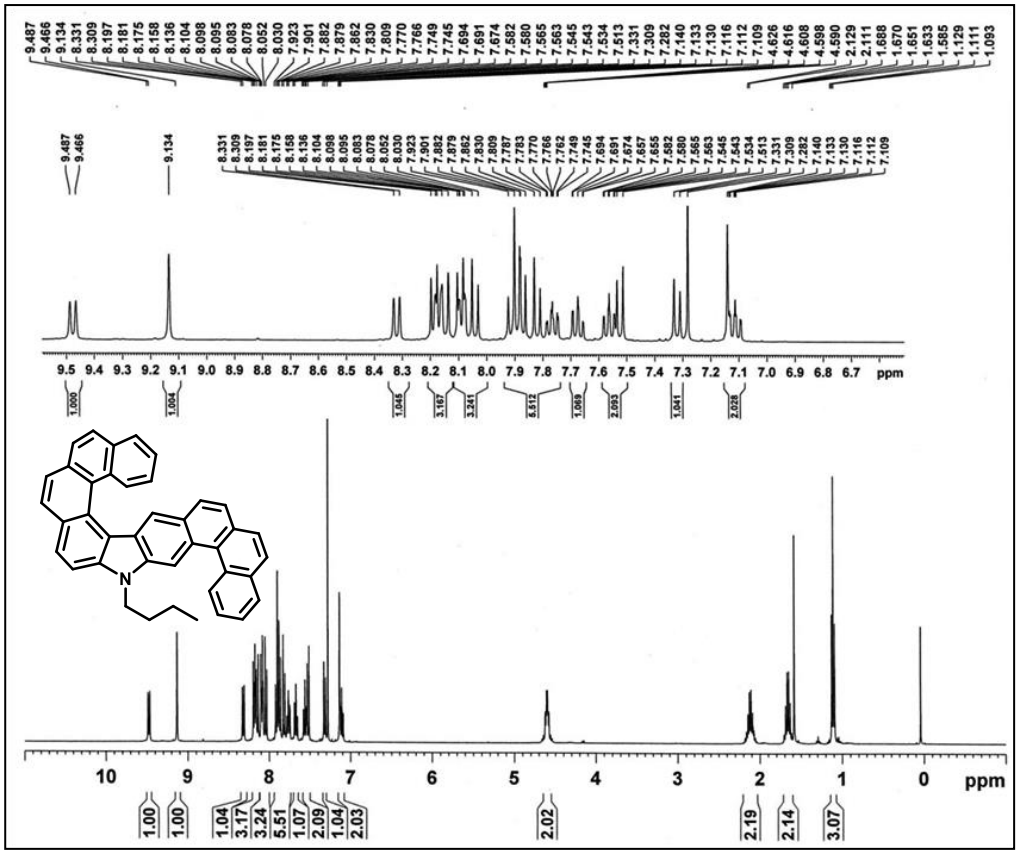

^{1}H-NMR of compound 66 ($CDCl_3$ 400 MHz)

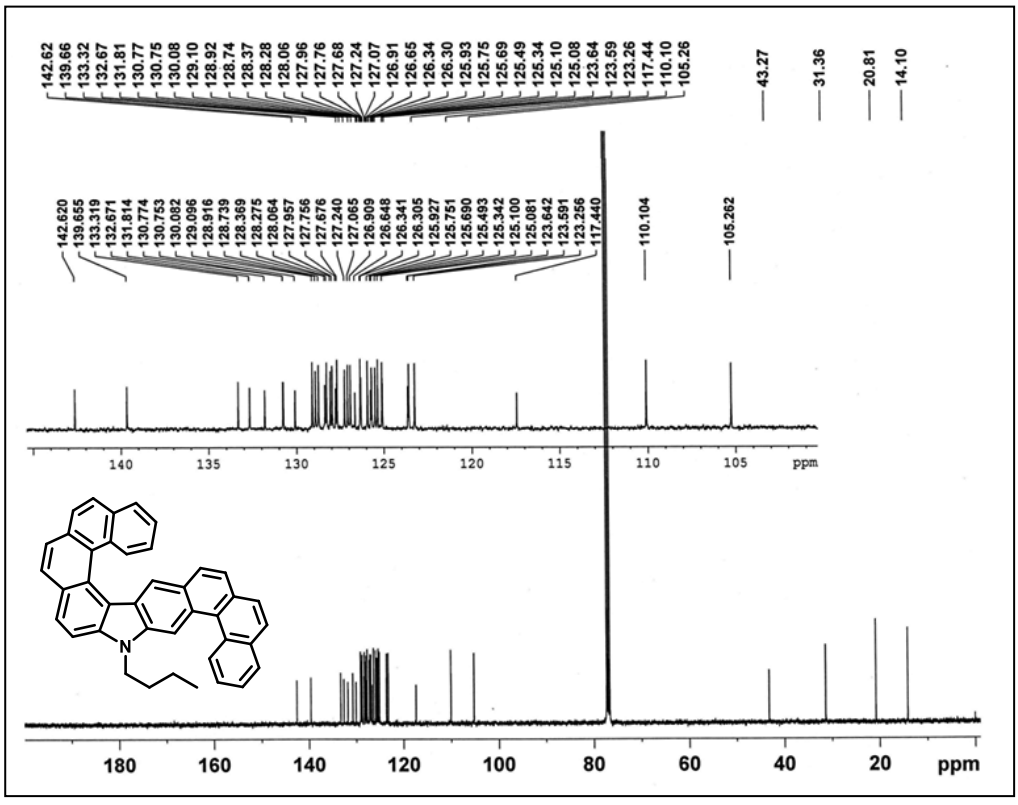

^{13}C-NMR of compound 66 ($CDCl_3$, 100 MHz)

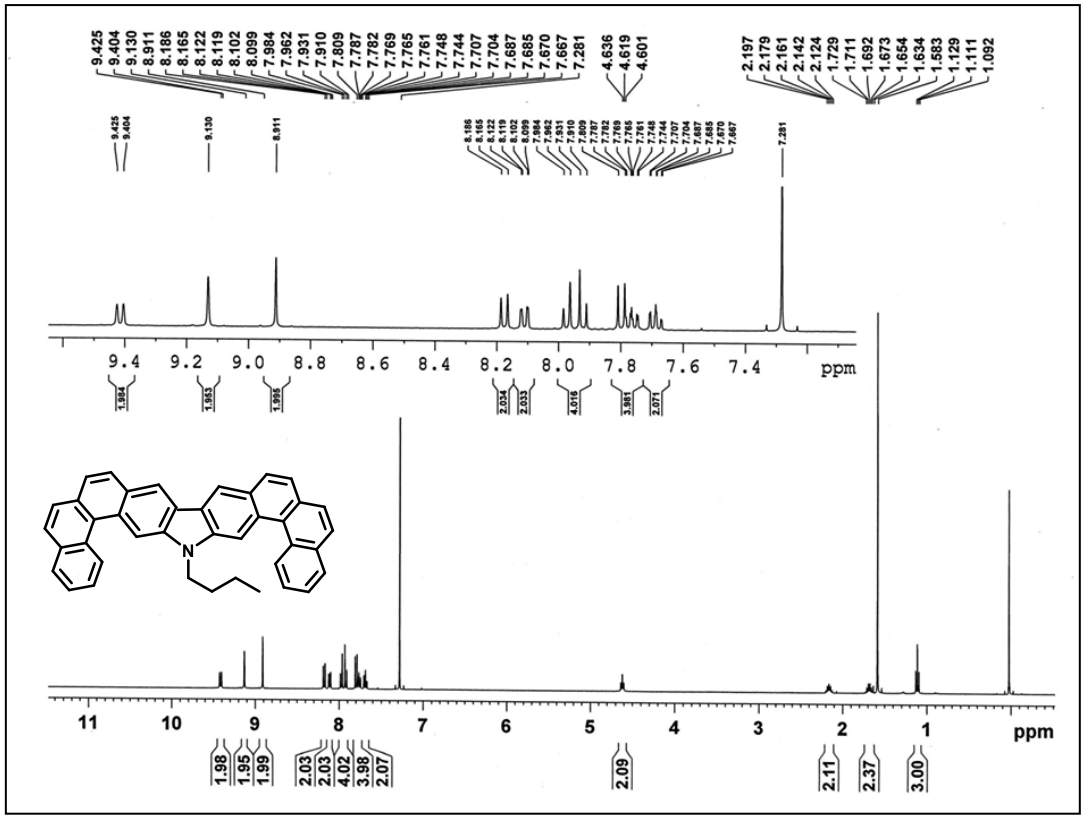

^{1}H-NMR of compound 67 ($CDCl_3$ 400 MHz)

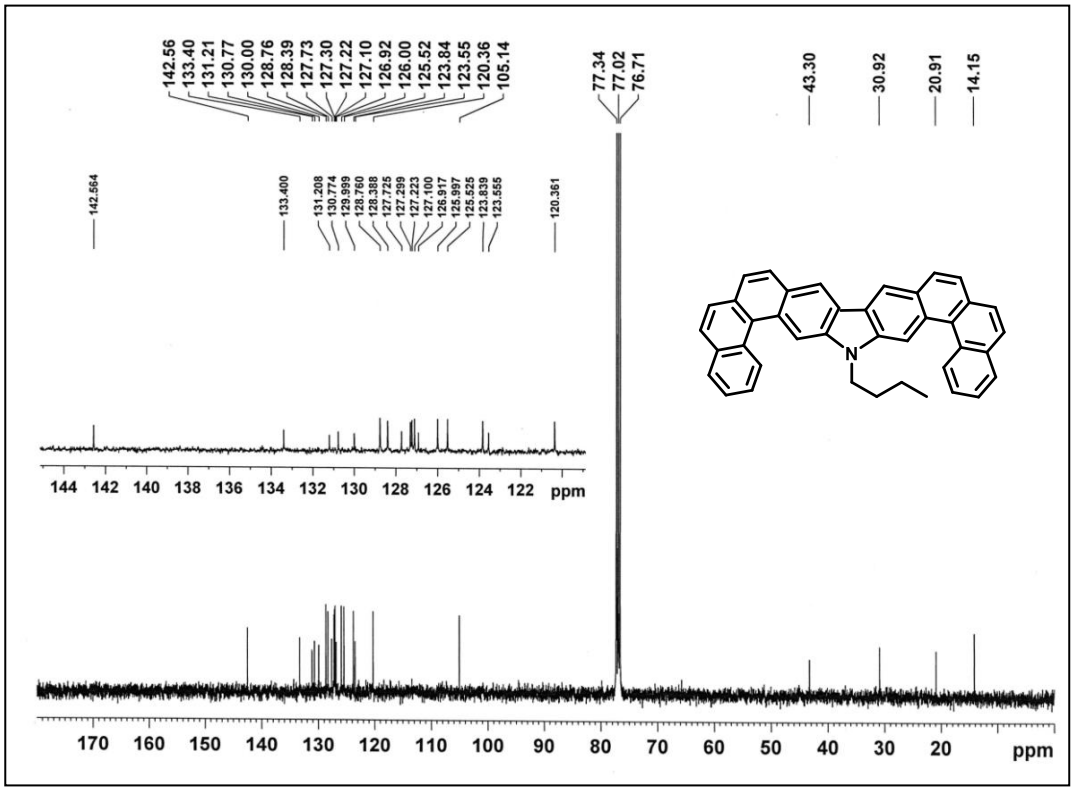

^{13}C-NMR of compound 67 ($CDCl_3$, 100 MHz)

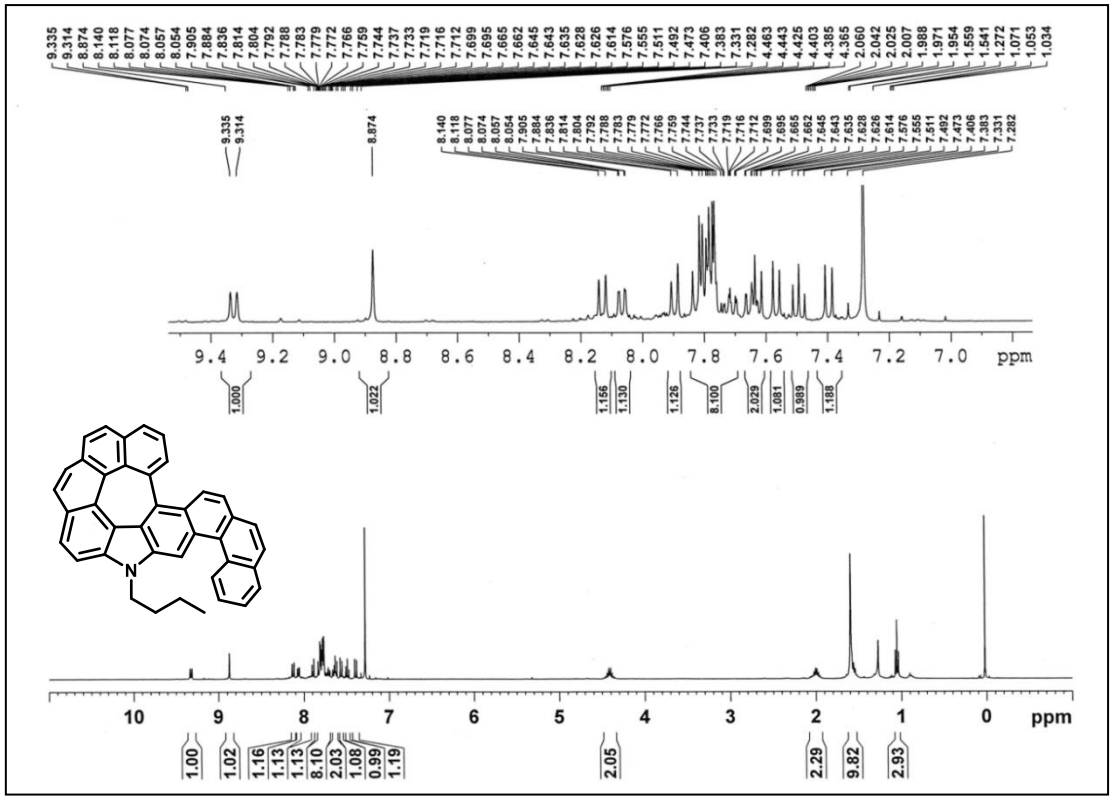

^{1}H-NMR of compound 68 ($CDCl_3$ 400 MHz)

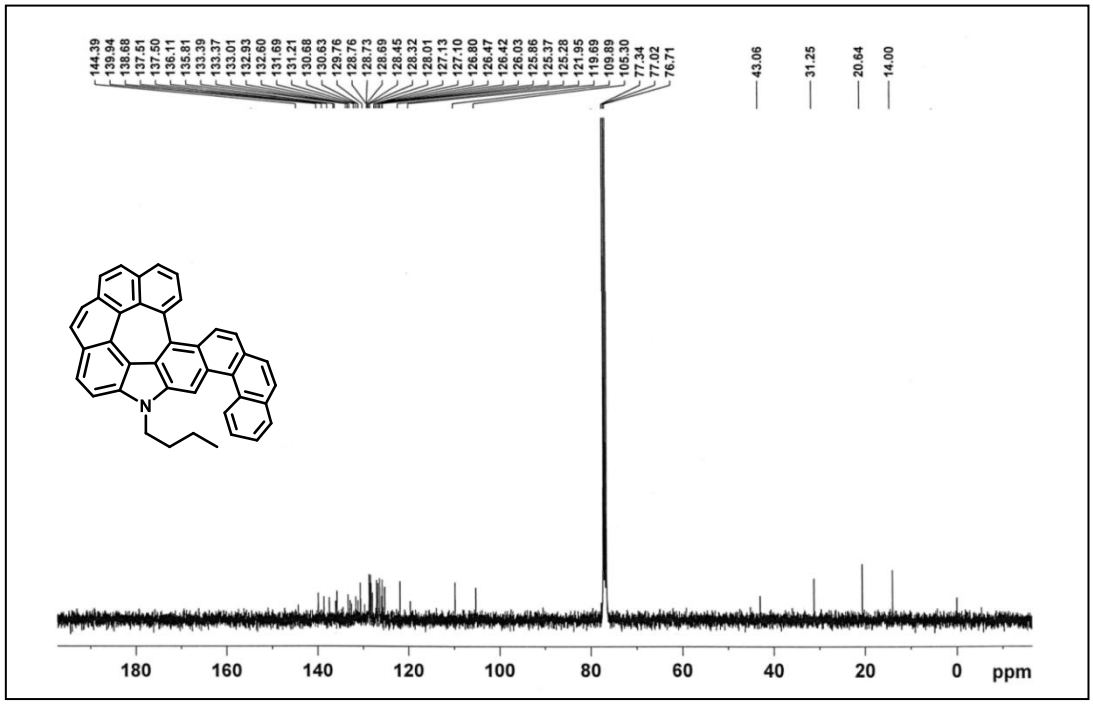

^{13}C-NMR of compound 68 ($CDCl_3$, 100 MHz)

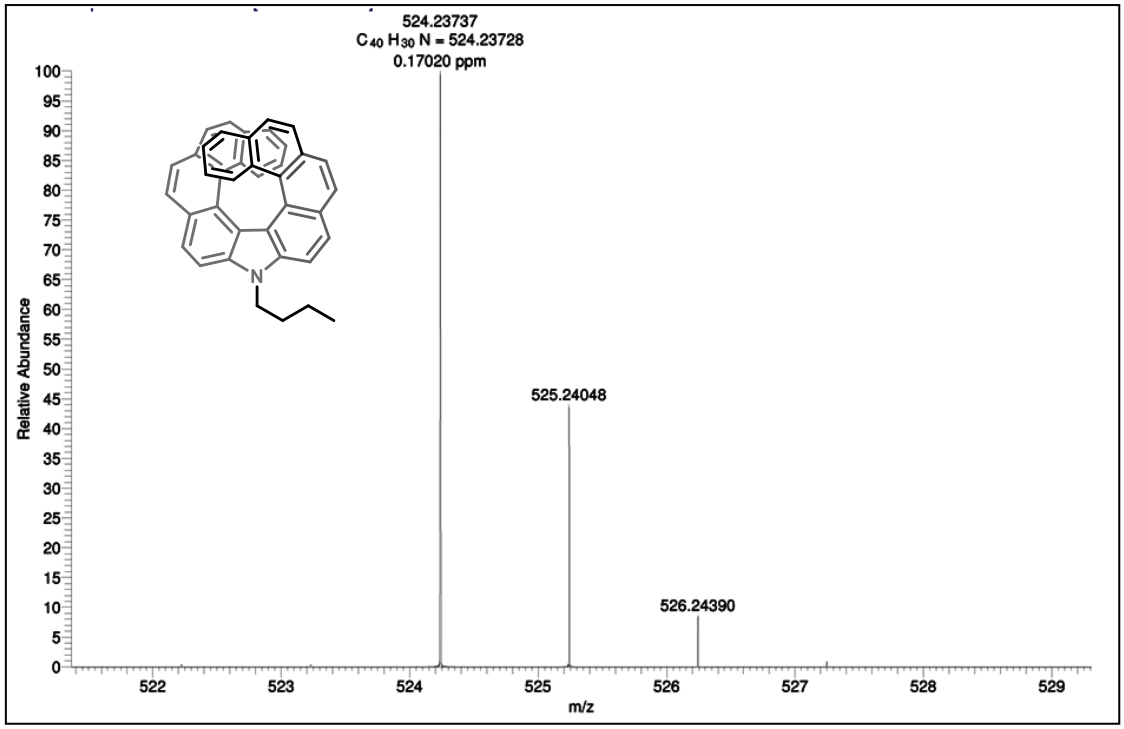

HRMS of compound 65

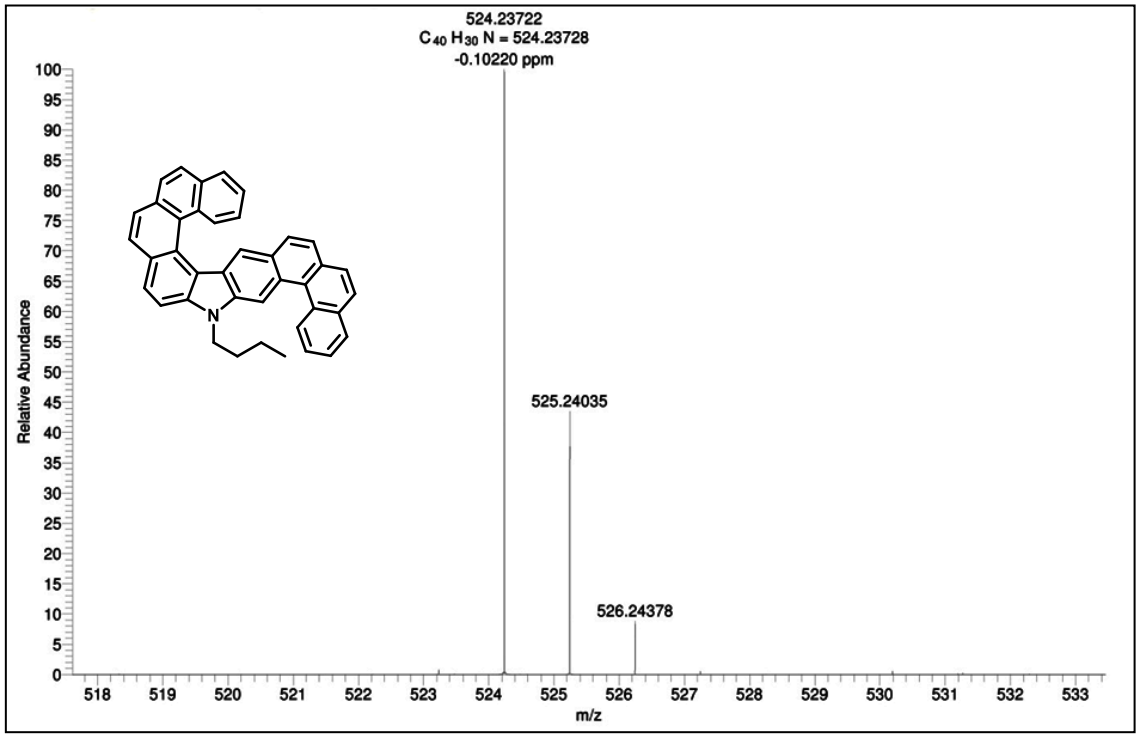

HRMS of compound 66

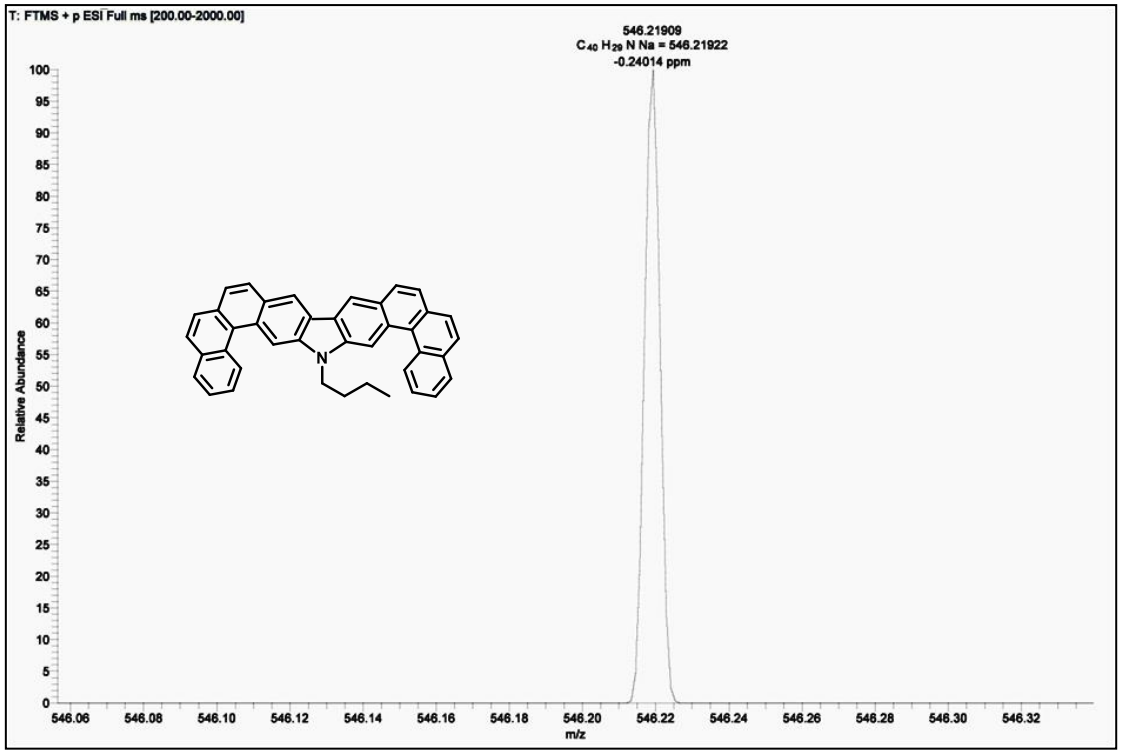

HRMS of compound 67

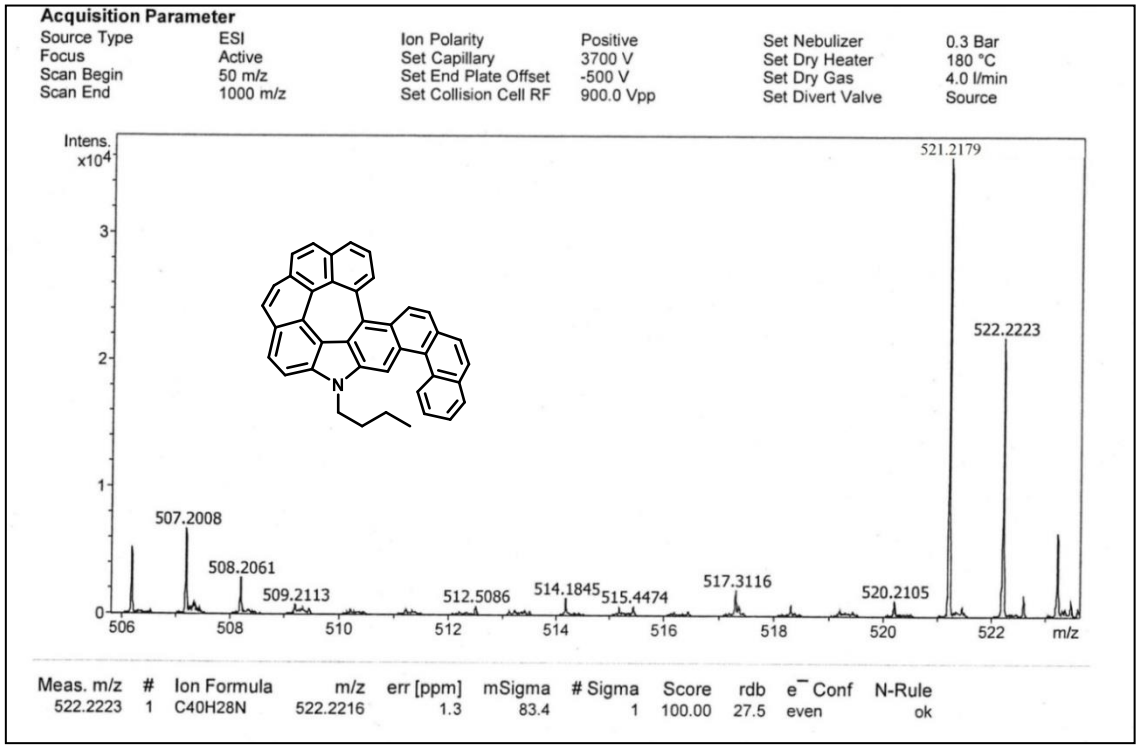

HRMS of compound 68

Spectra

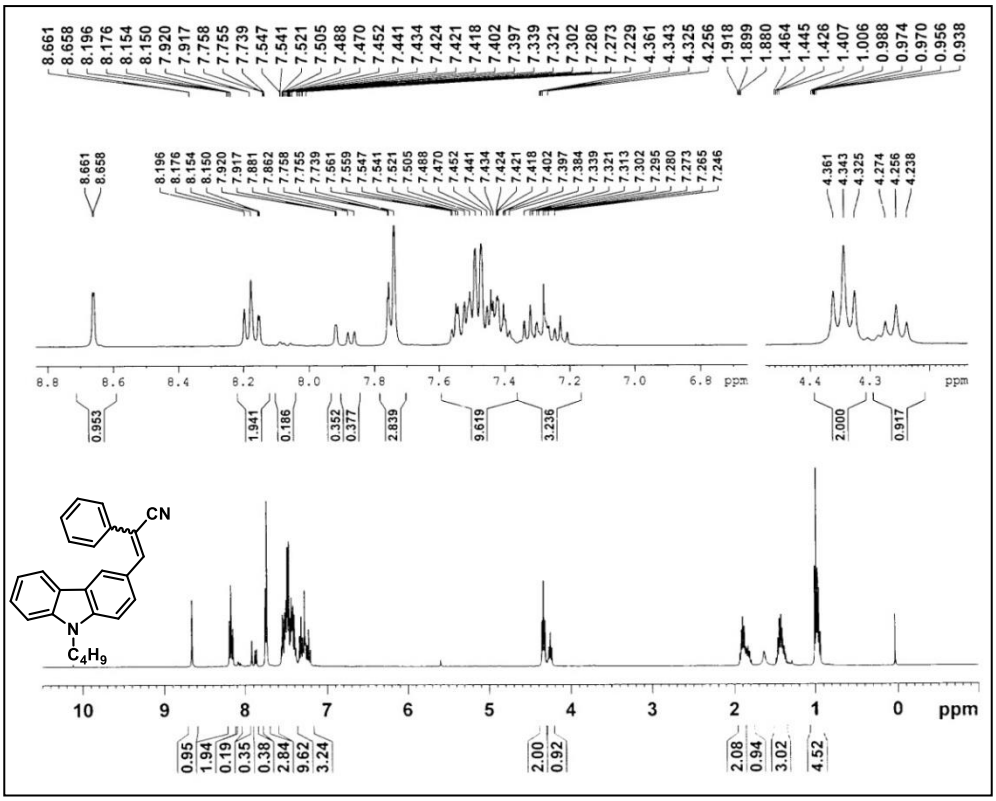

^{1}H-NMR of compound 101 ($CDCl_3$ 400 MHz)

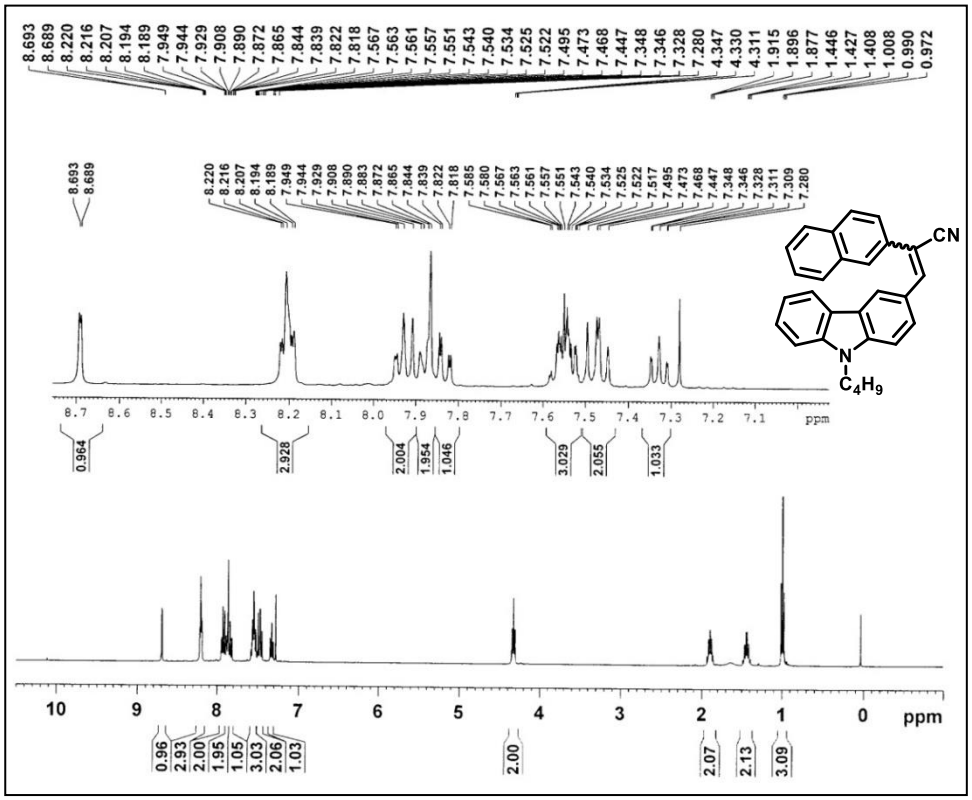

^{1}H-NMR of compound 109 ($CDCl_3$ 400 MHz)

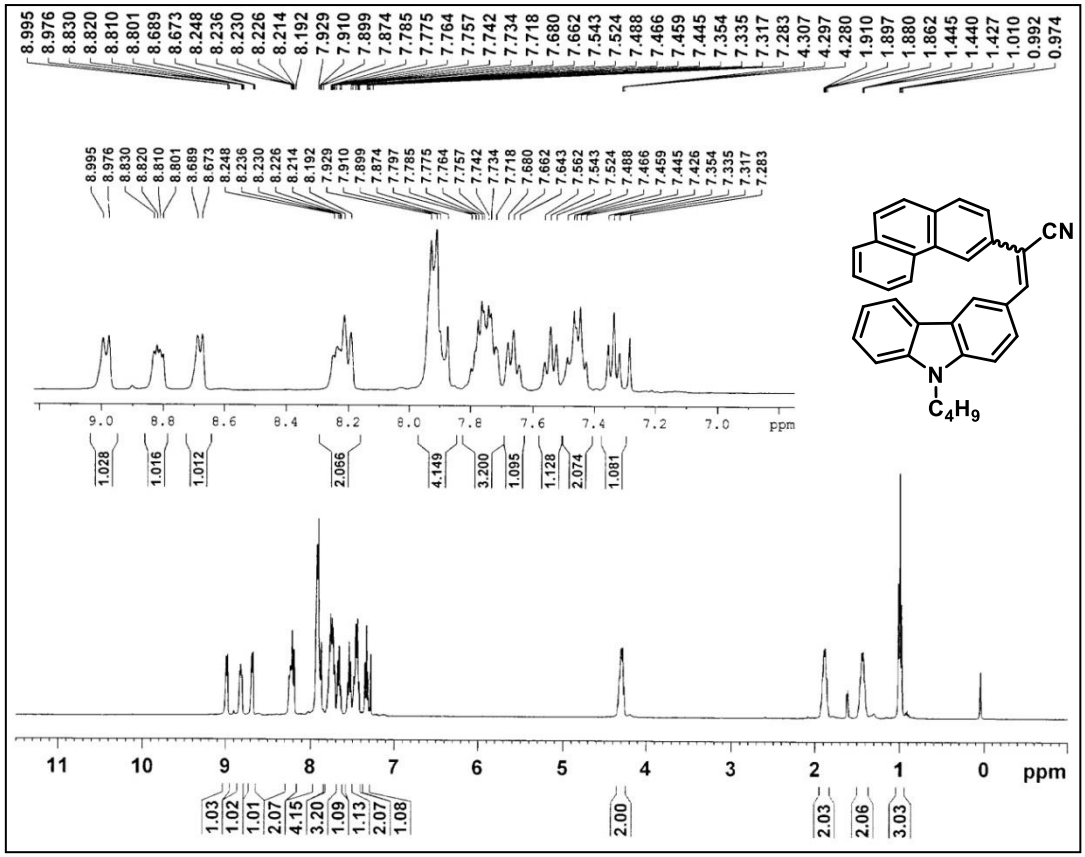

^{1}H-NMR of compound 123 ($CDCl_3$ 400 MHz)

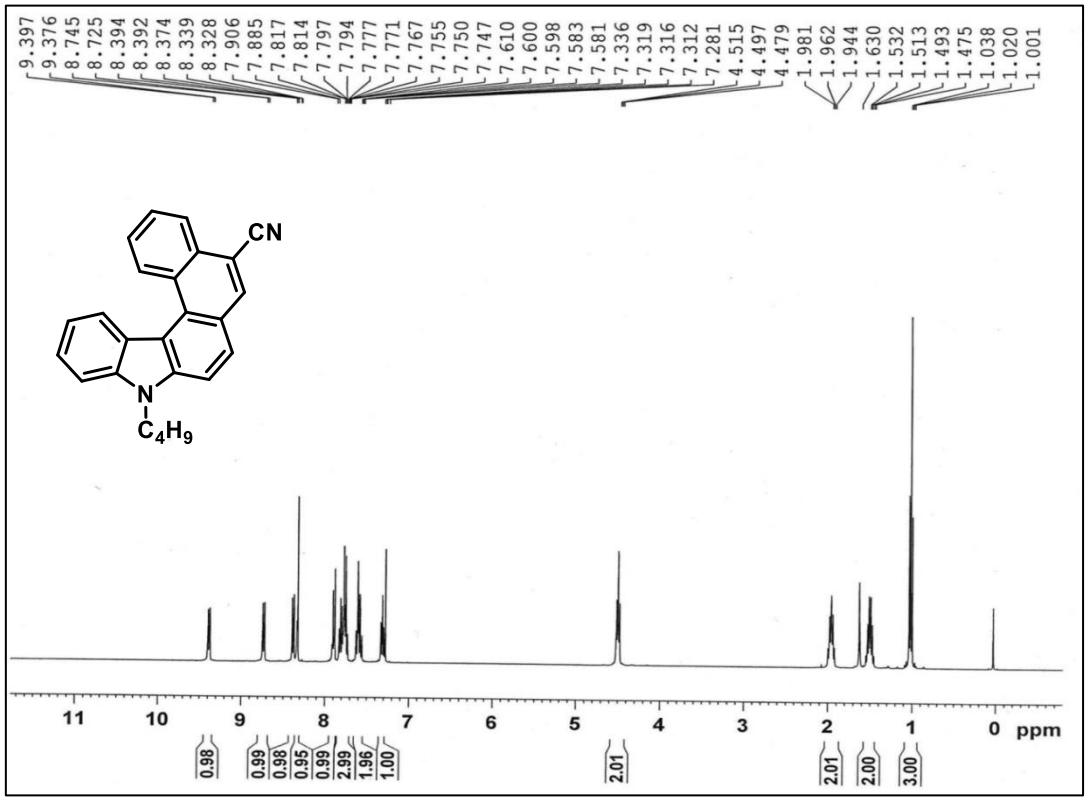

^{1}H-NMR of compound 102 ($CDCl_3$ 400 MHz)

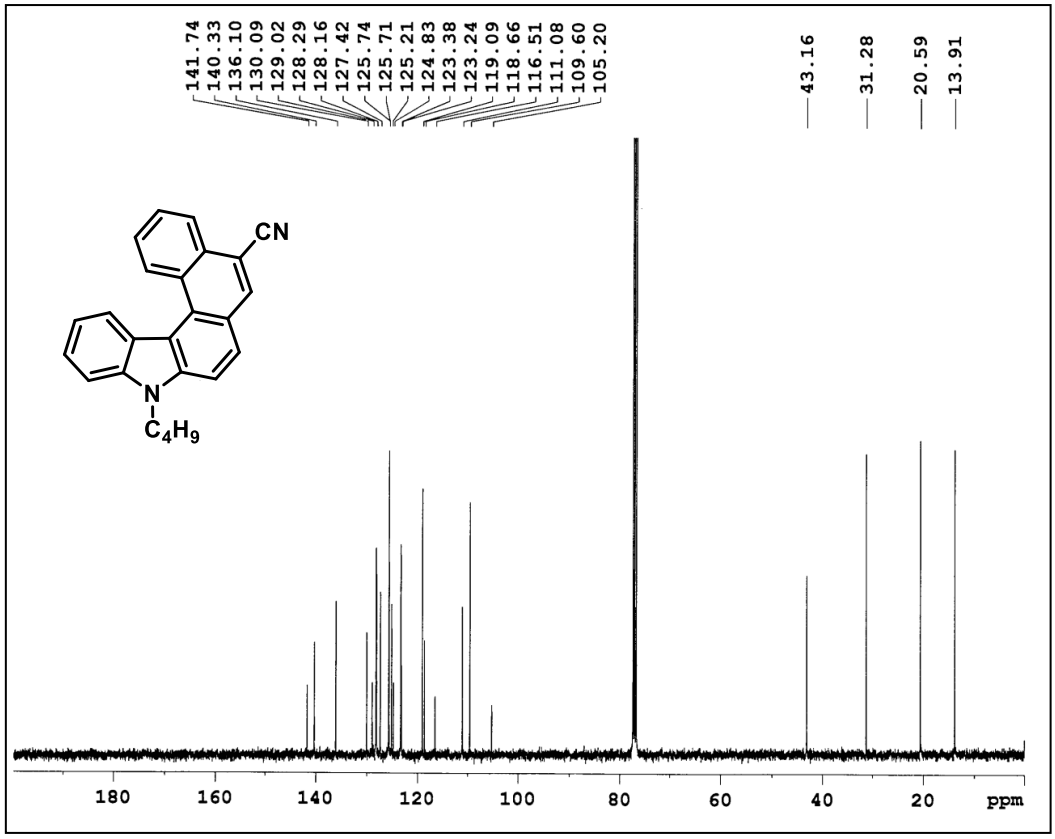

^{13}C-NMR of compound 102 ($CDCl_3$, 100 MHz)

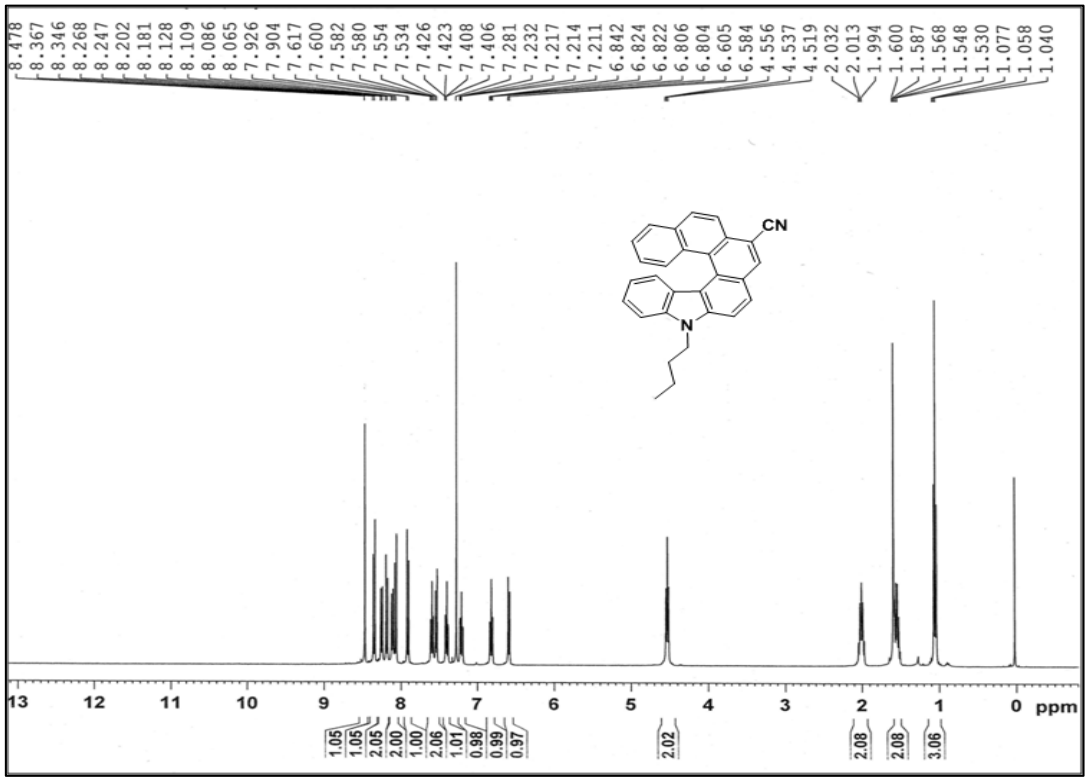

^{1}H-NMR of compound 110 ($CDCl_3$ 400 MHz

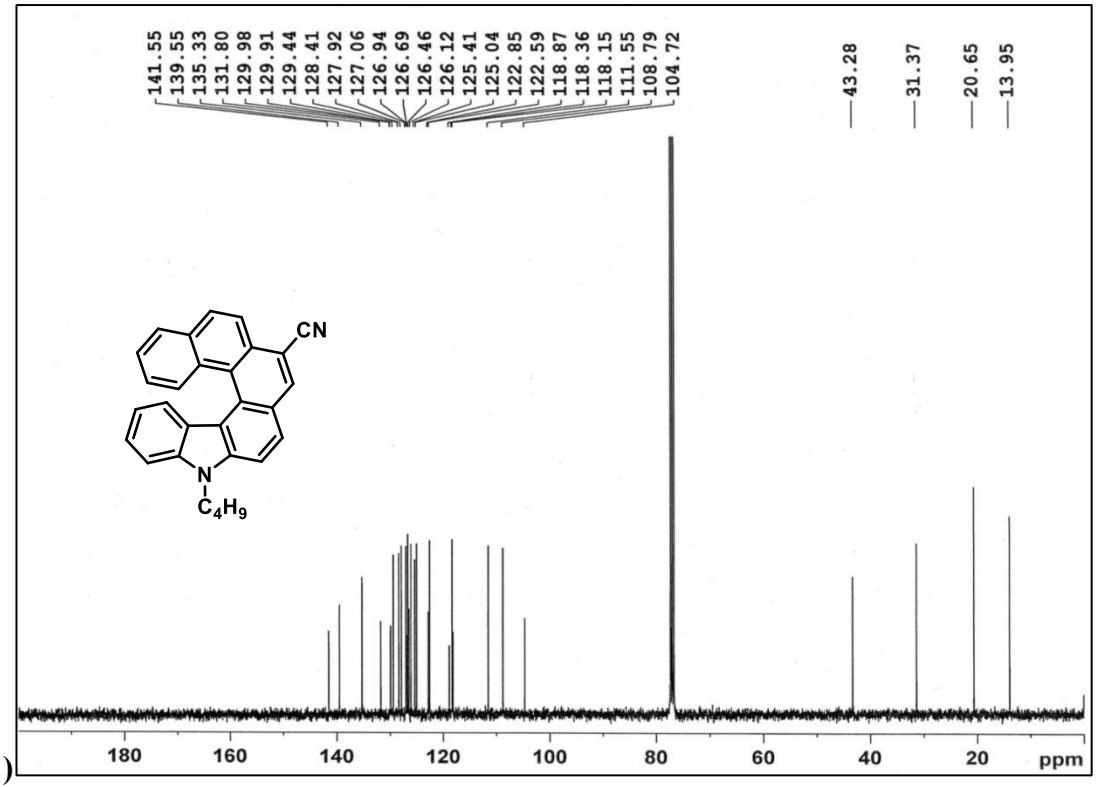

)

^{13}C-NMR of compound 110 ($CDCl_3$, 100 MHz)

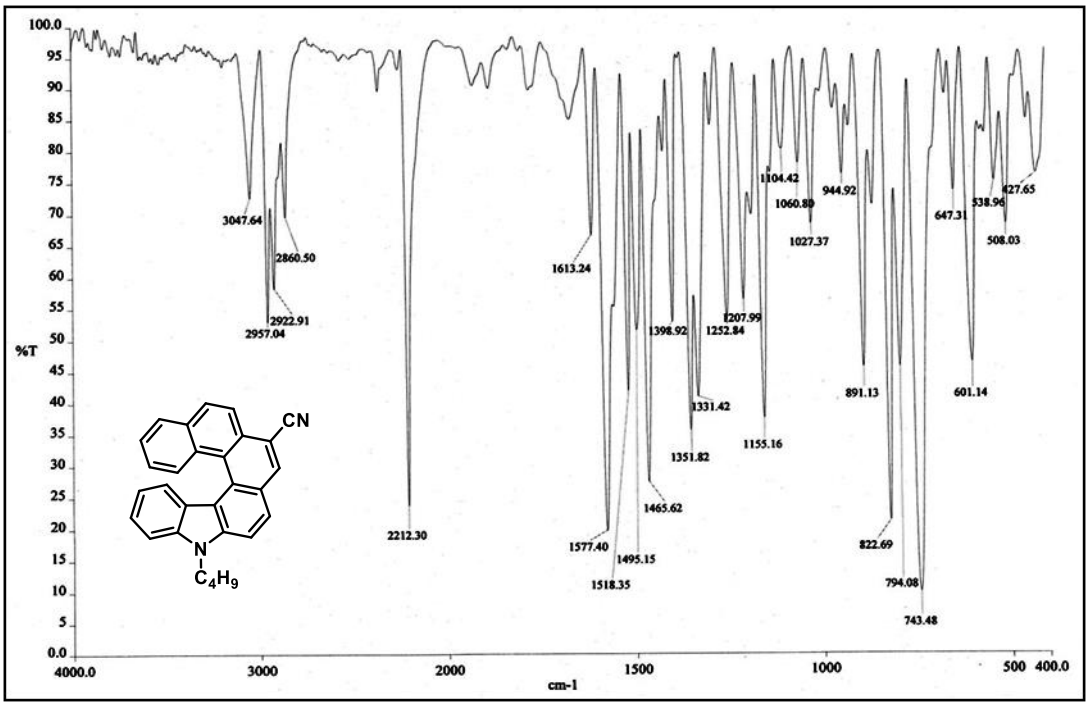

IR spectrum of compound 110

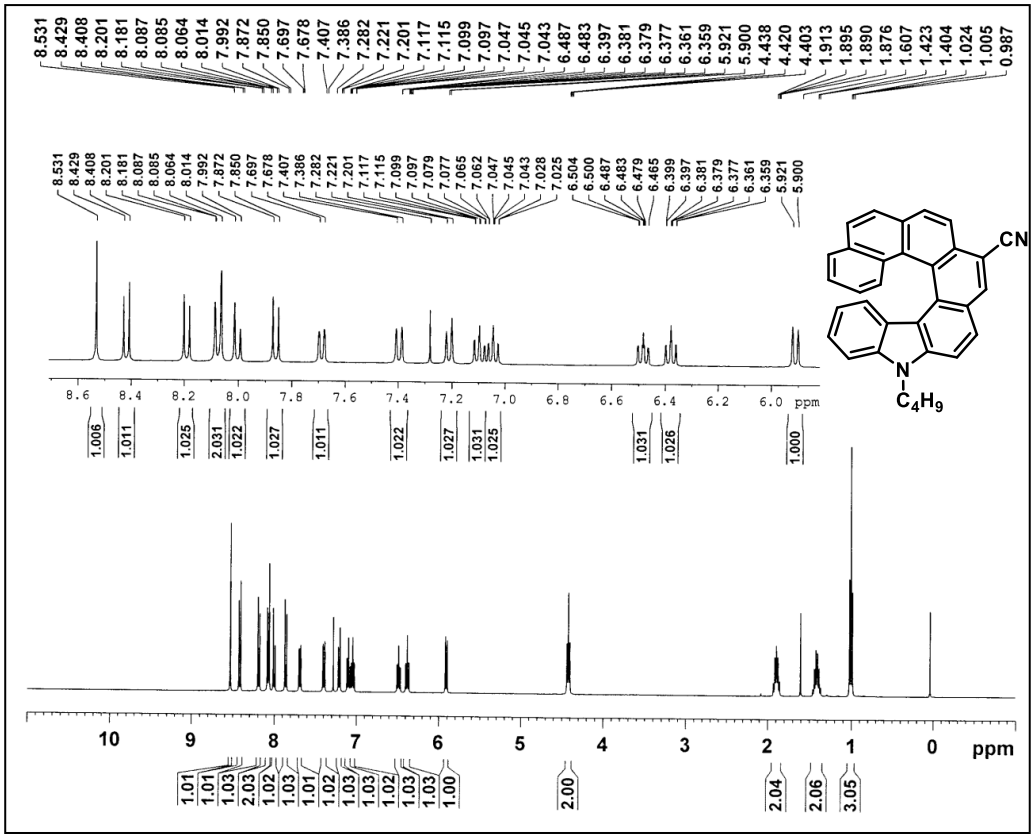

^{1}H-NMR of compound 124 ($CDCl_3$ 400 MHz

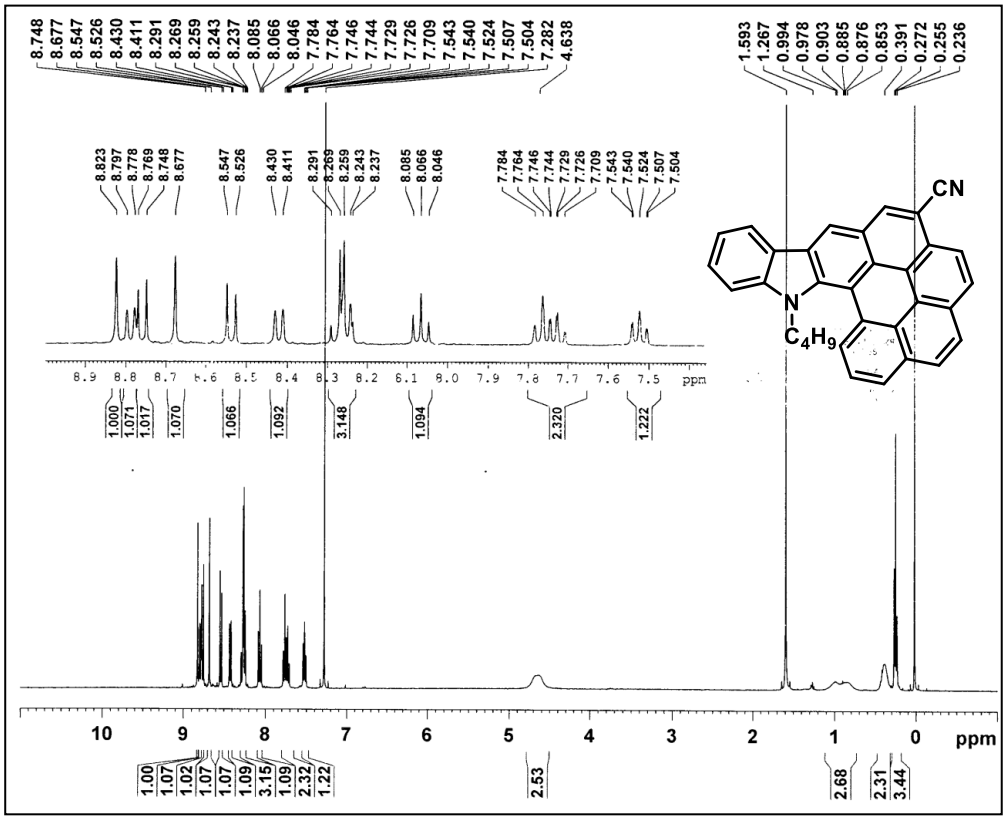

^{1}H-NMR of compound 125 ($CDCl_3$ 400 MHz

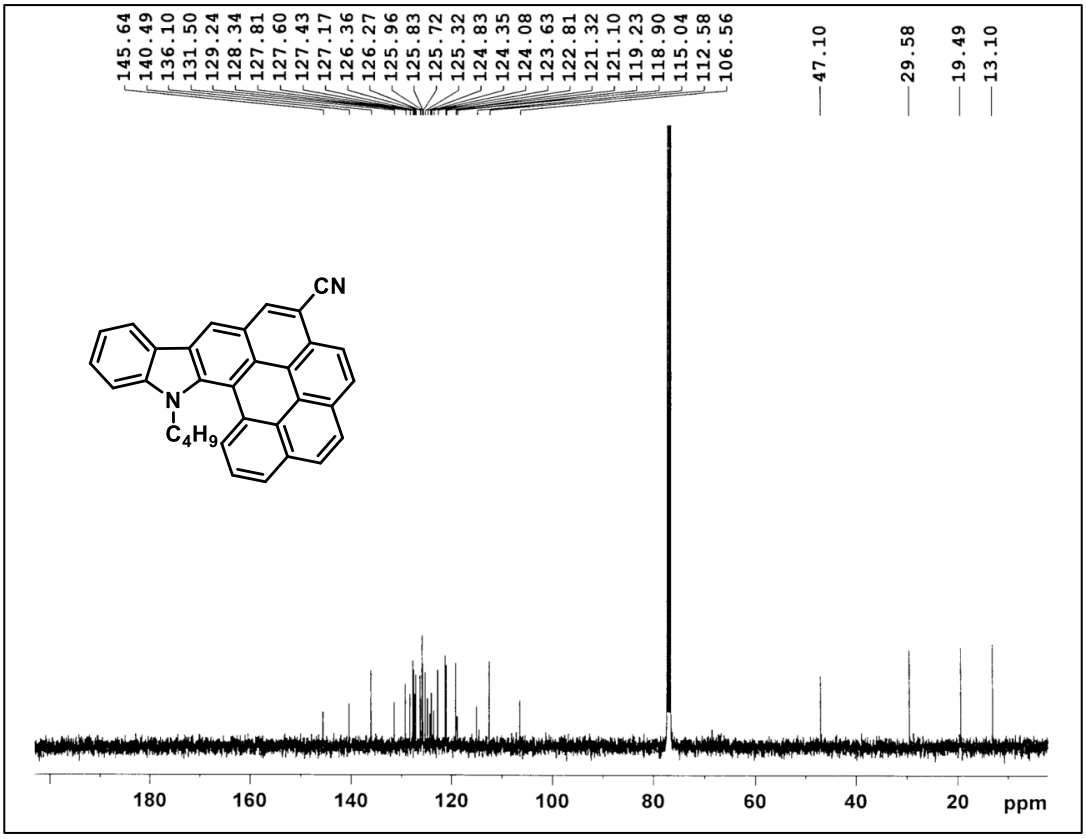

^{13}C-NMR of compound 125 ($CDCl_3$, 100 MHz)

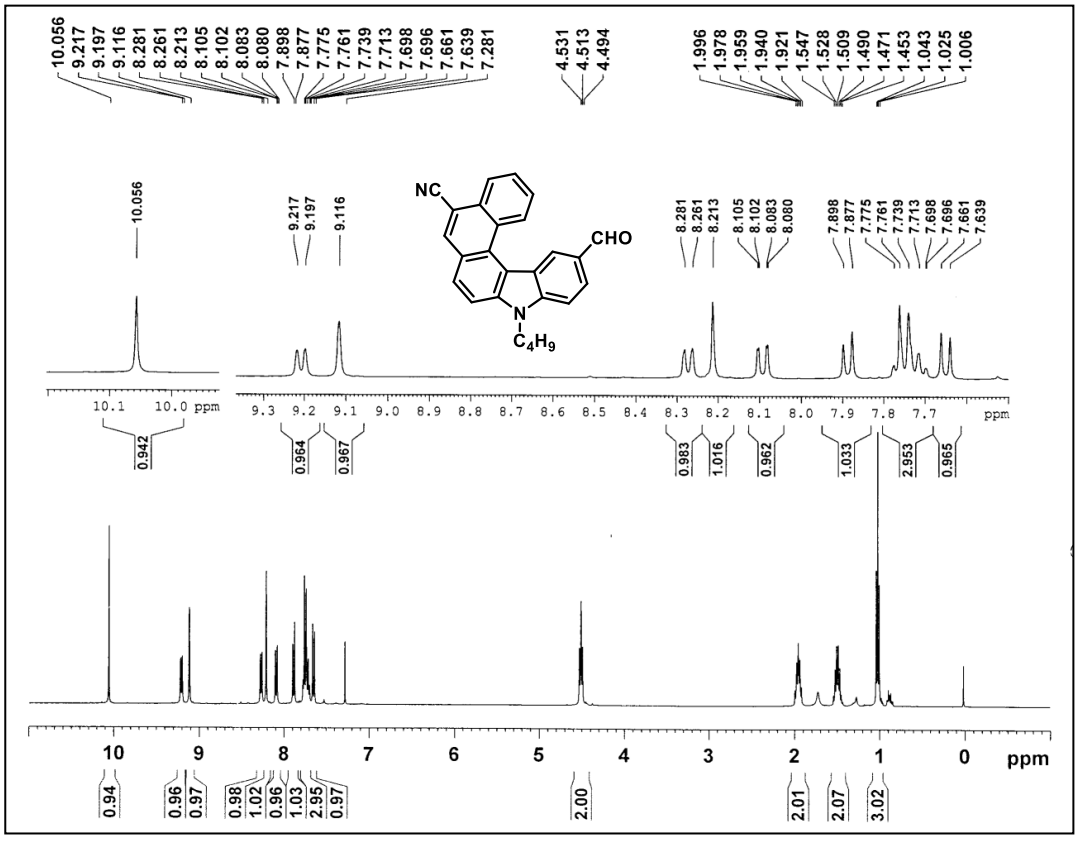

^{1}H-NMR of compound 103 ($CDCl_3$ 400 MHz)

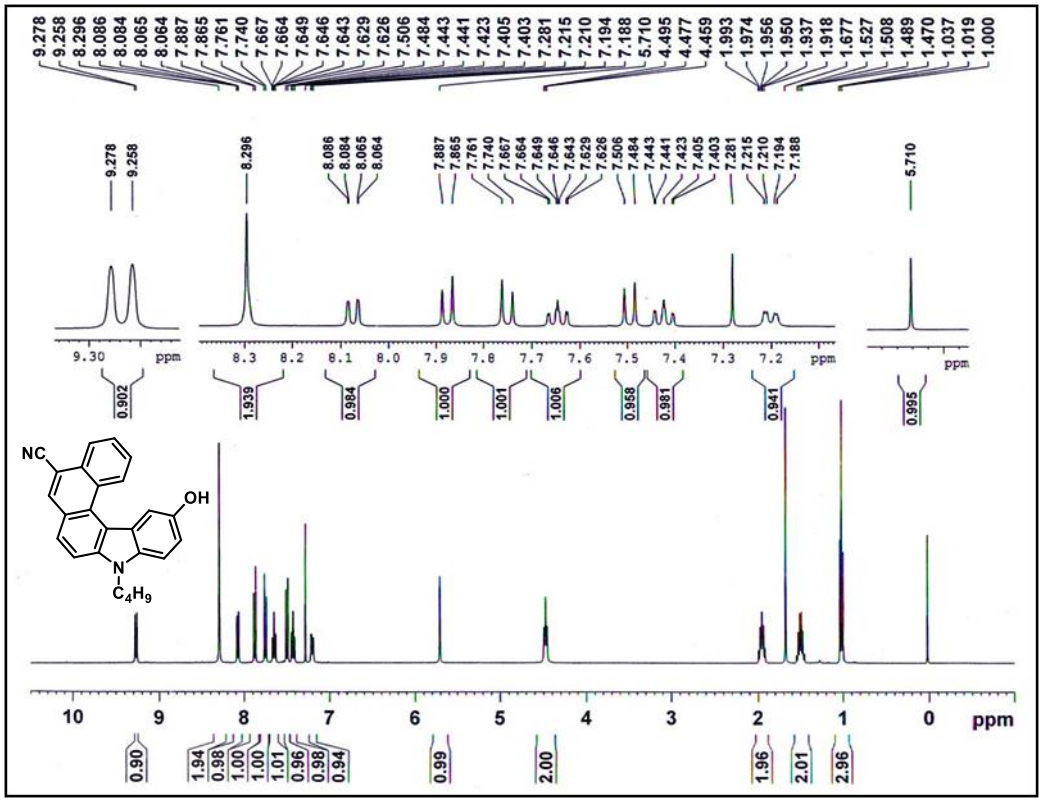

^{1}H-NMR of compound 104 ($CDCl_3$ 400 MHz)

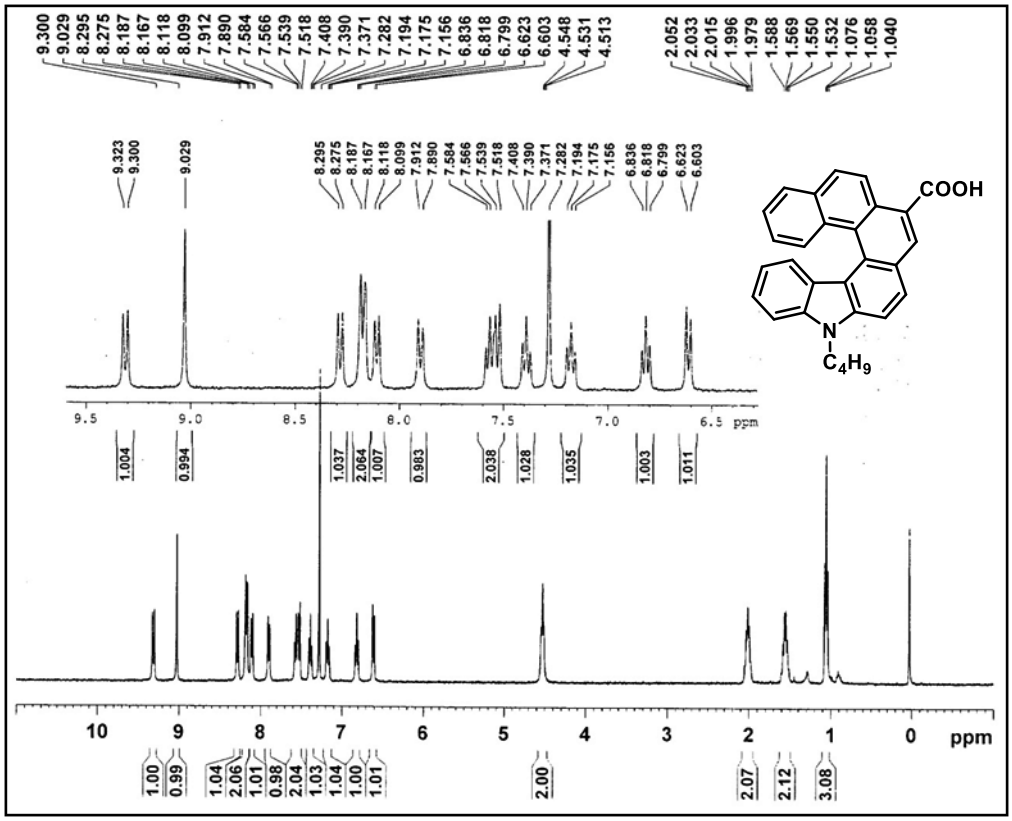

^{1}H-NMR of compound 126 ($CDCl_3$ 400 MHz)

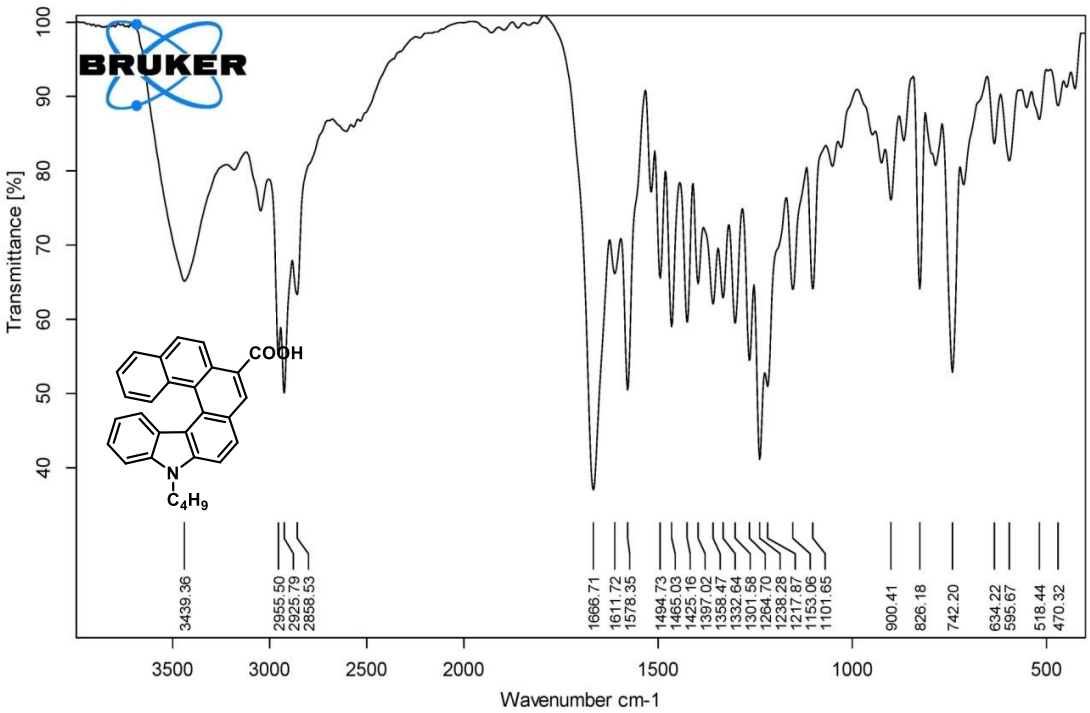

IR spectrum of compound 126

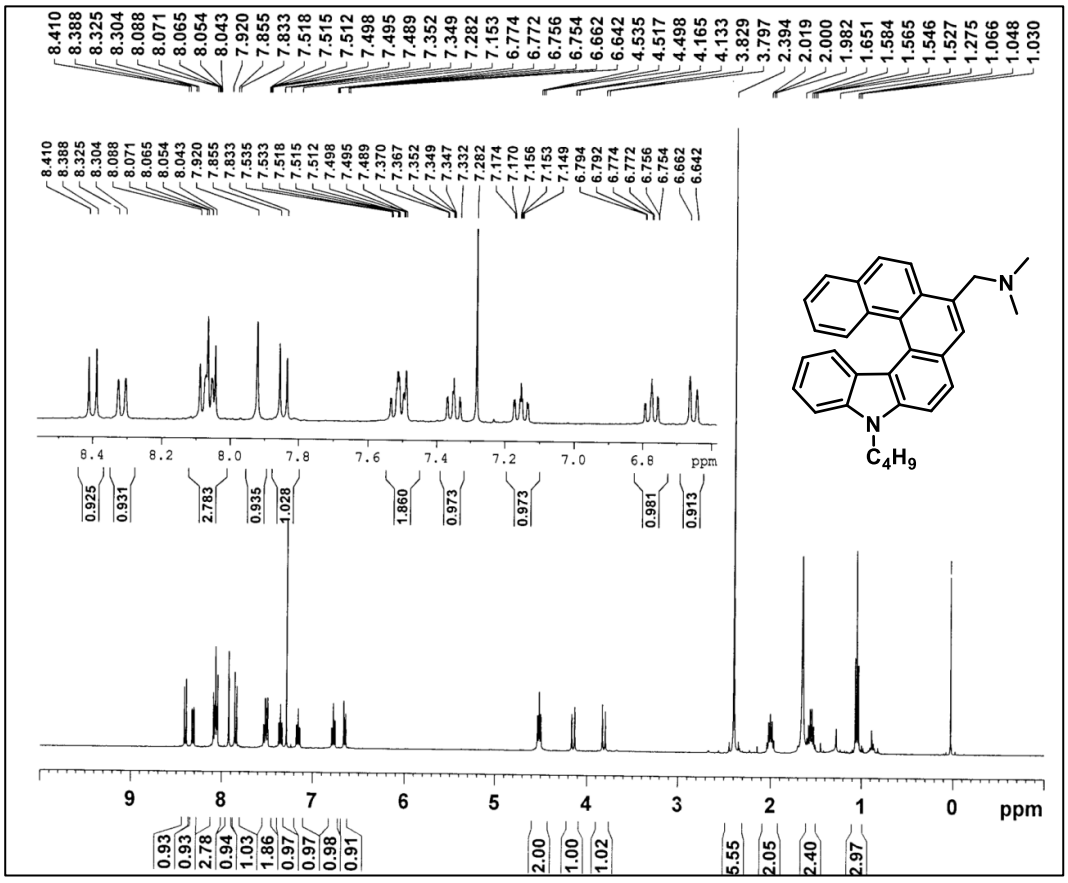

^{1}H-NMR of compound 128 ($CDCl_3$ 400 MHz)

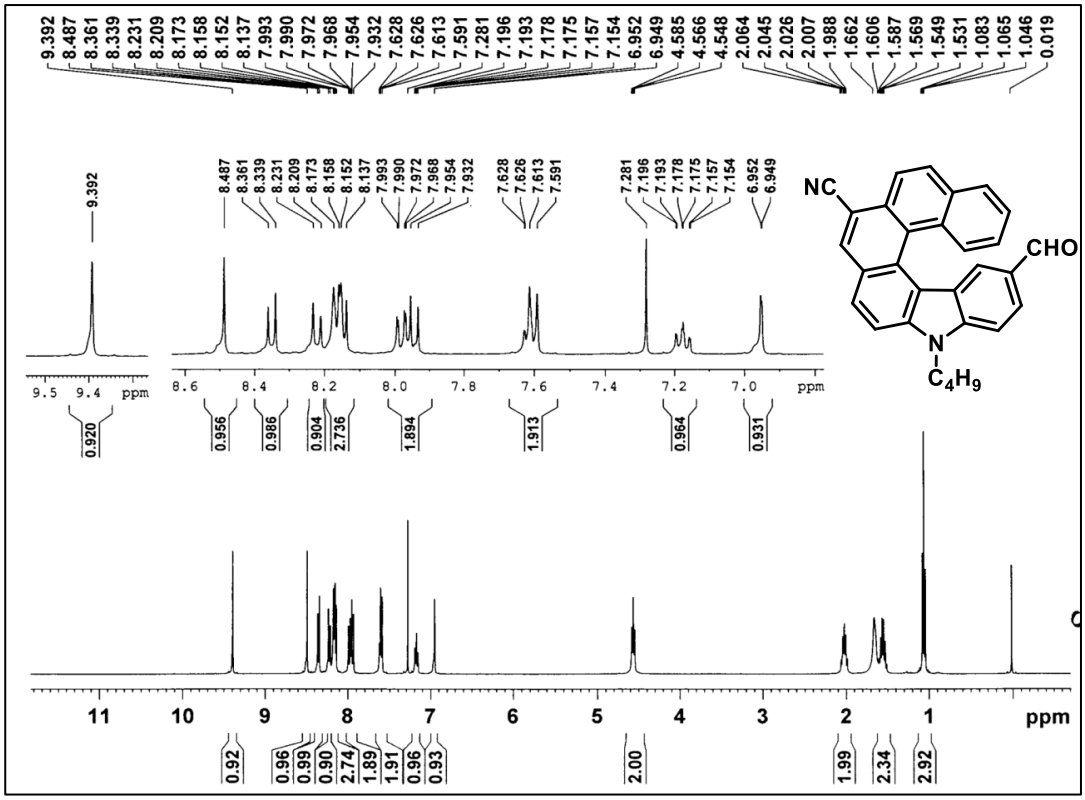

^{1}H-NMR of compound 128 ($CDCl_3$ 400 MHz)

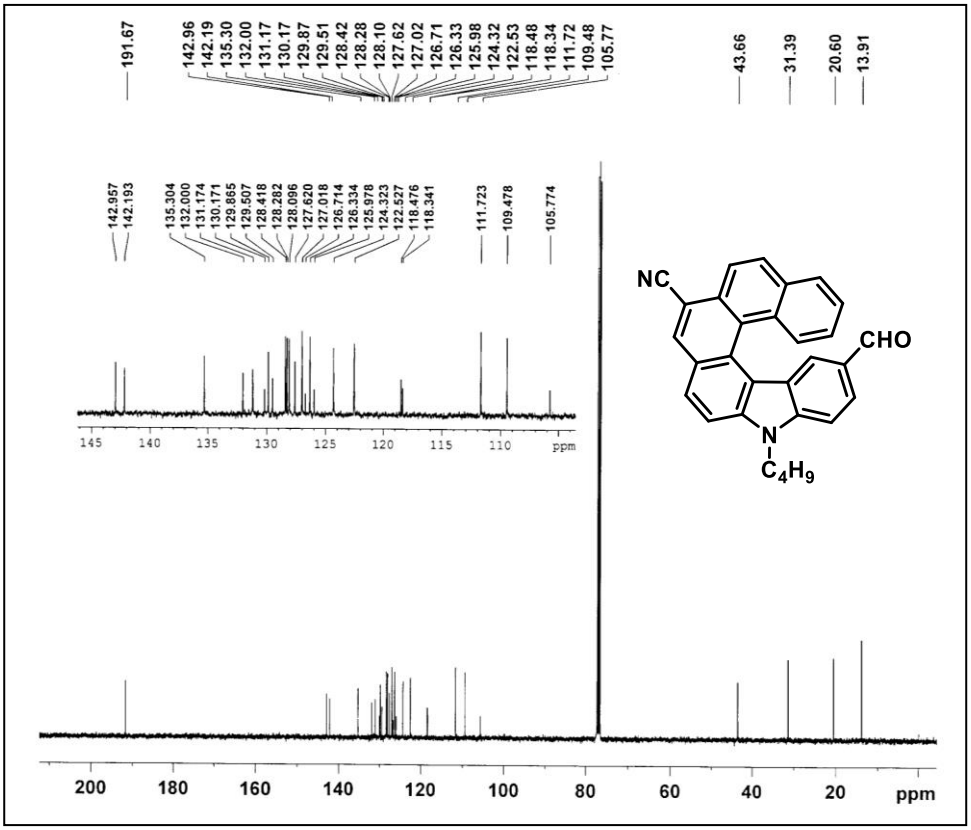

^{13}C-NMR of compound 128 ($CDCl_3$, 100 MHz)

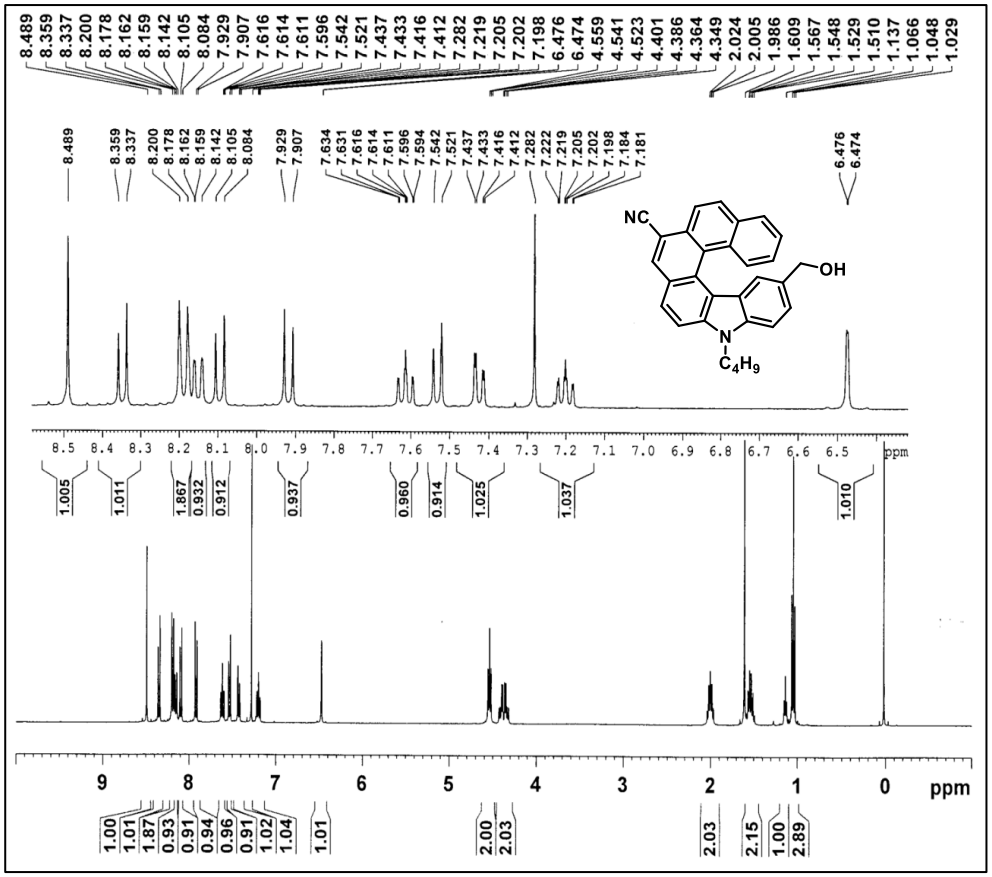

^{1}H-NMR of compound 130 ($CDCl_3$ 400 MHz)

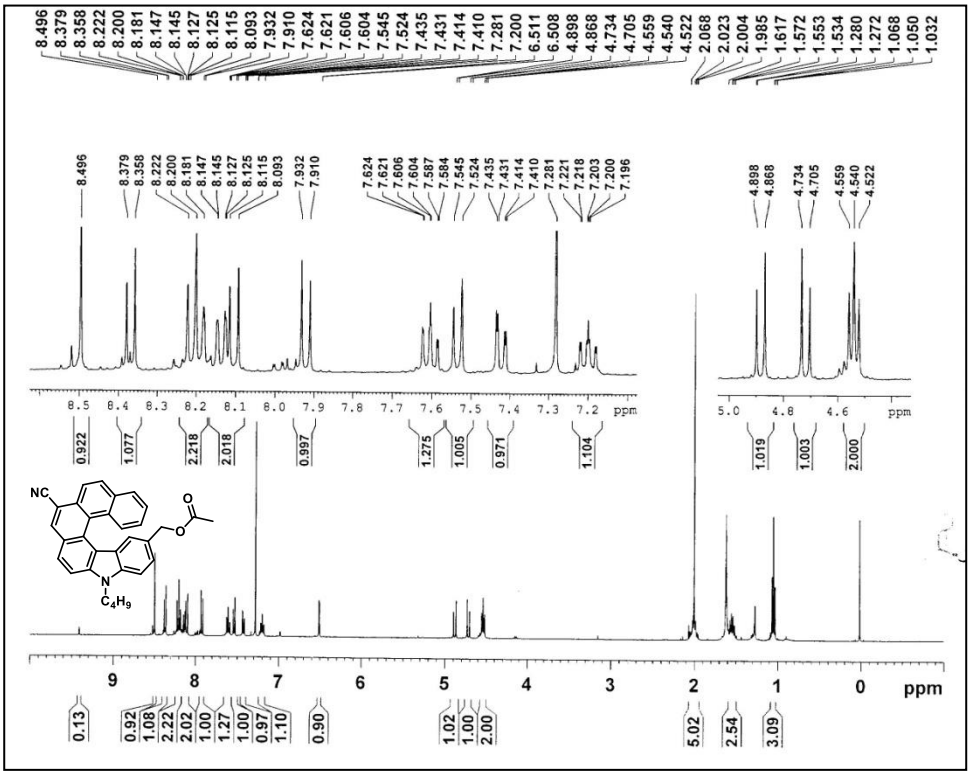

^{1}H-NMR of compound 137 ($CDCl_3$ 400 MHz)

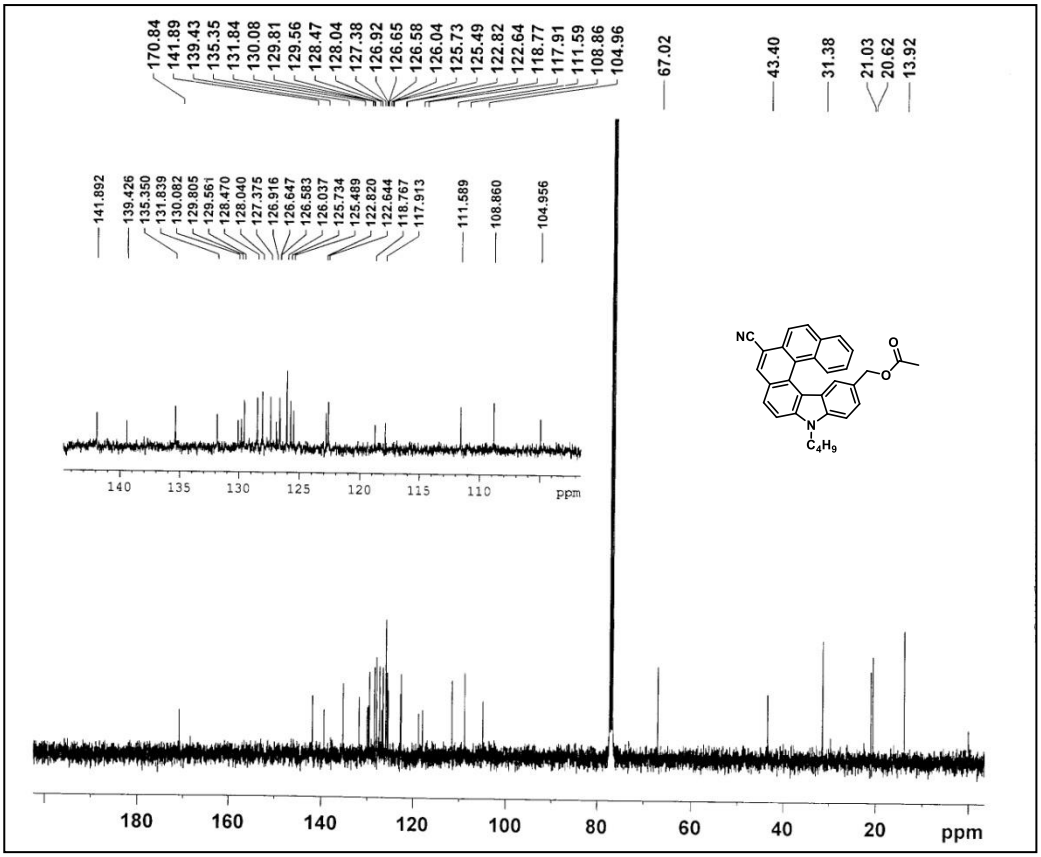

^{13}C-NMR of compound 137 ($CDCl_3$, 100 MHz)

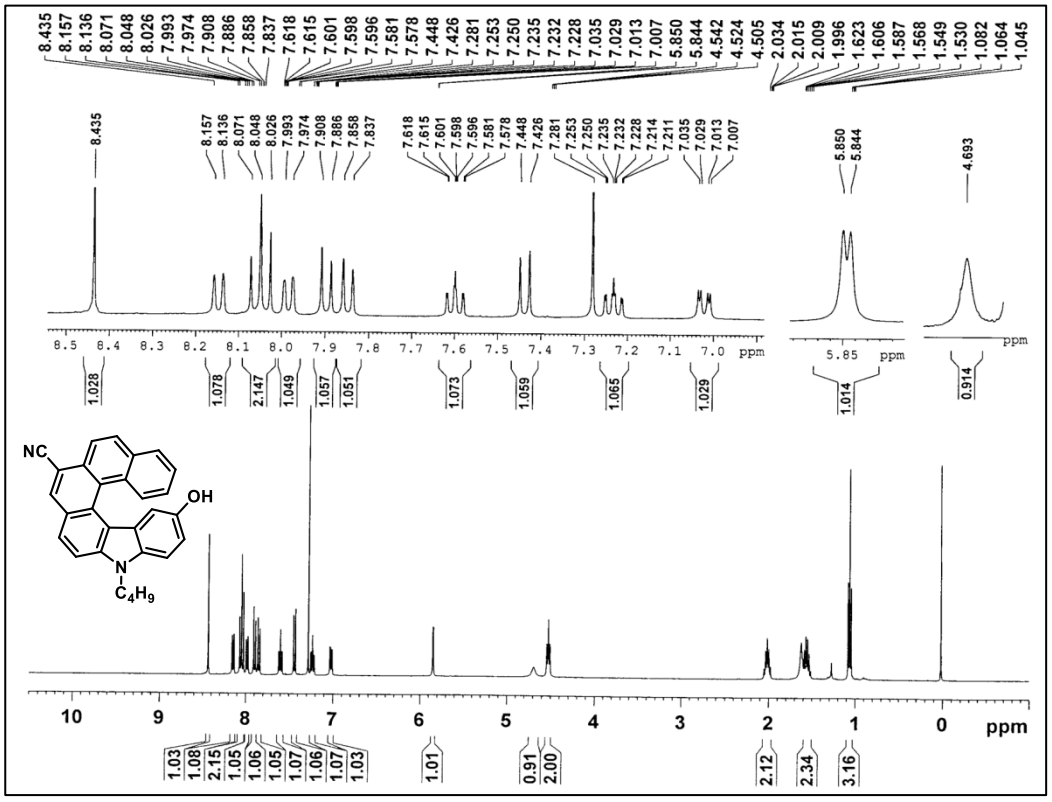

^{1}H-NMR of compound 131 ($CDCl_3$ 400 MHz)

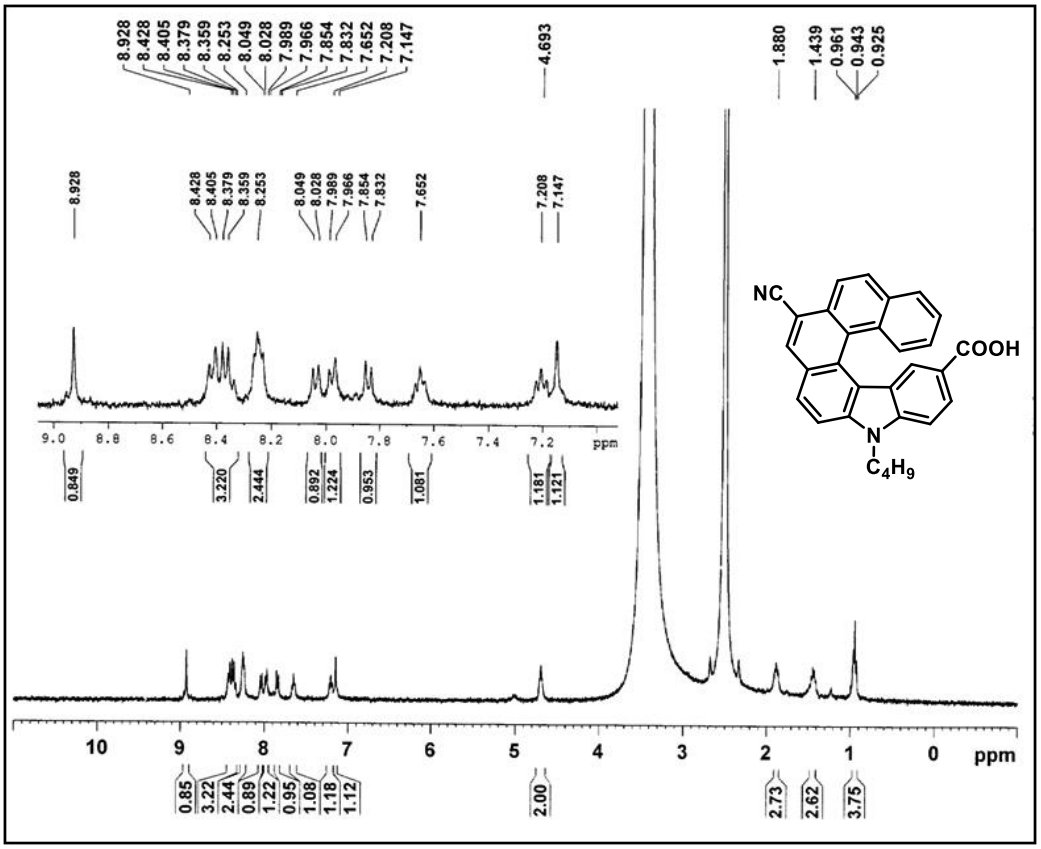

^{1}H-NMR of compound 132 (DMSO-*d6* 400 MHz)

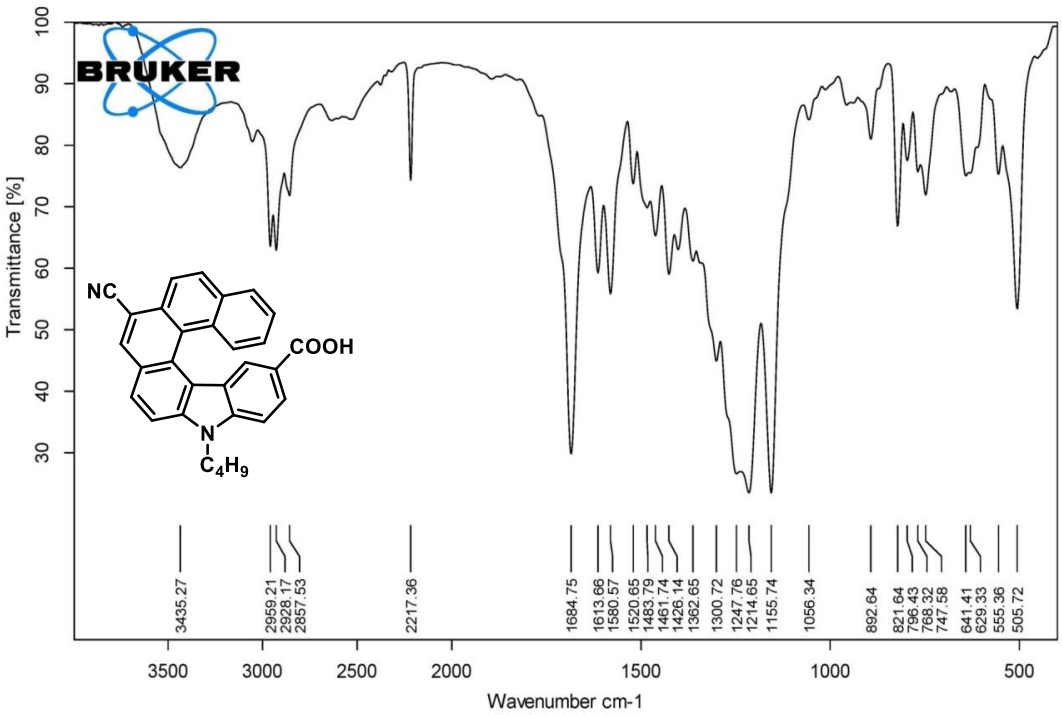

IR spectrum of compound 132

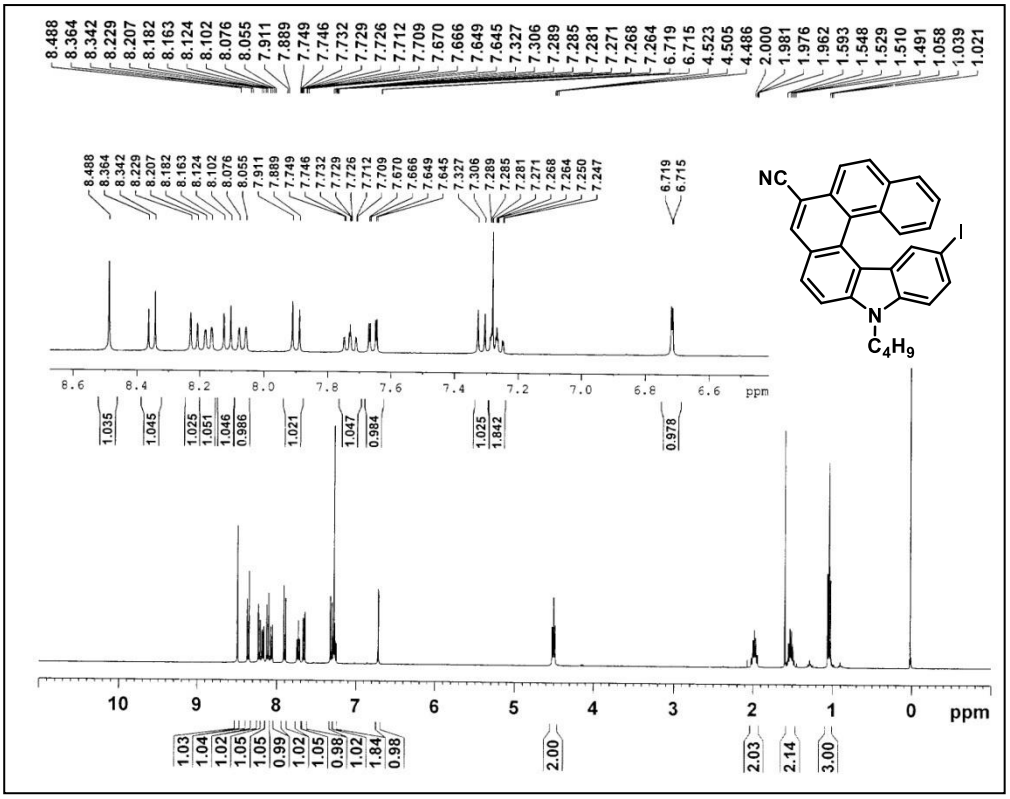

^{1}H-NMR of compound 134 ($CDCl_3$ 400 MHz)

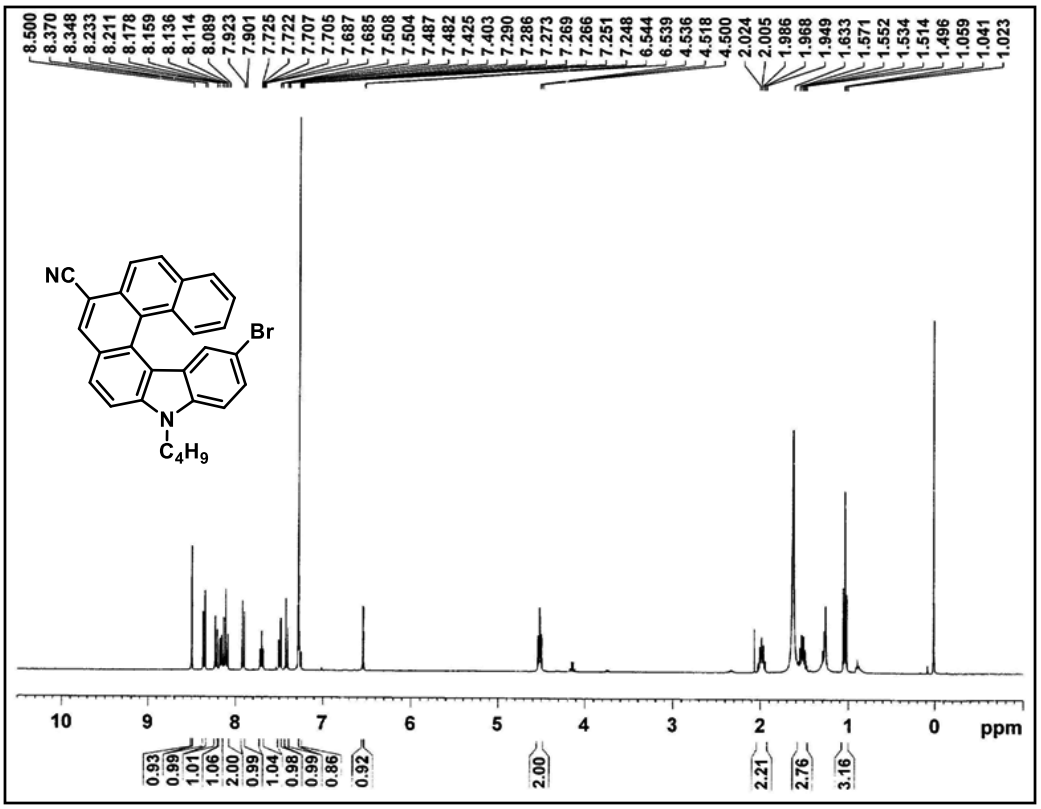

^{1}H-NMR of compound 133 ($CDCl_3$ 400 MHz)

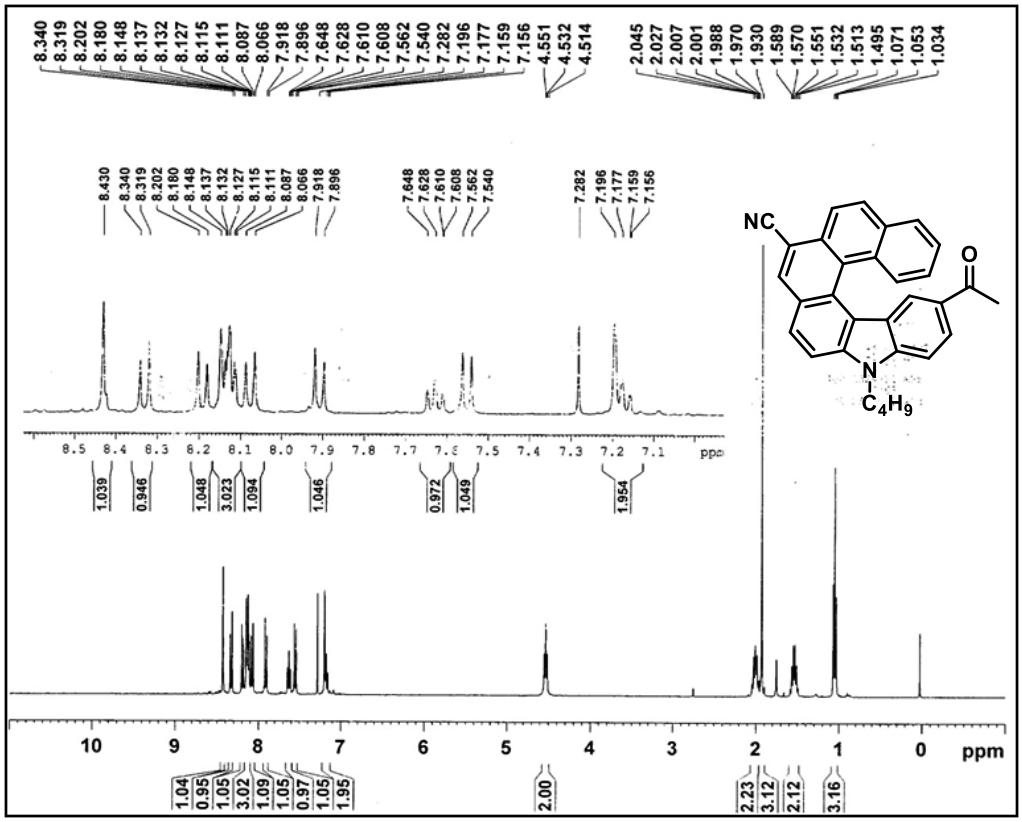

^{1}H-NMR of compound 135 ($CDCl_3$ 400 MHz)

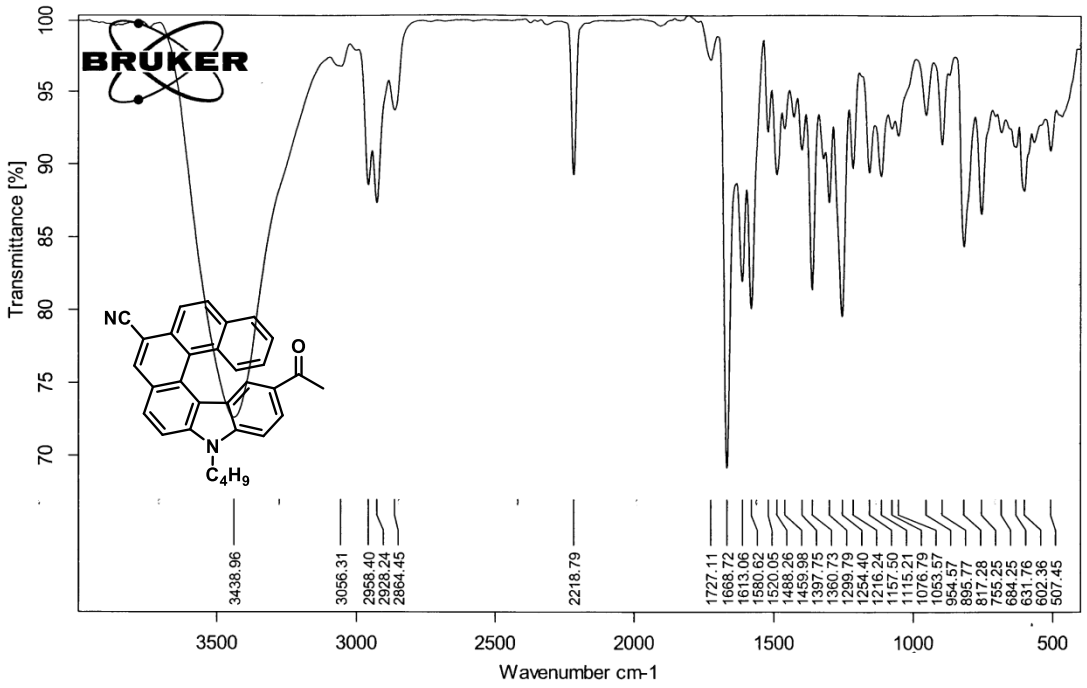

IR spectrum of compound 135

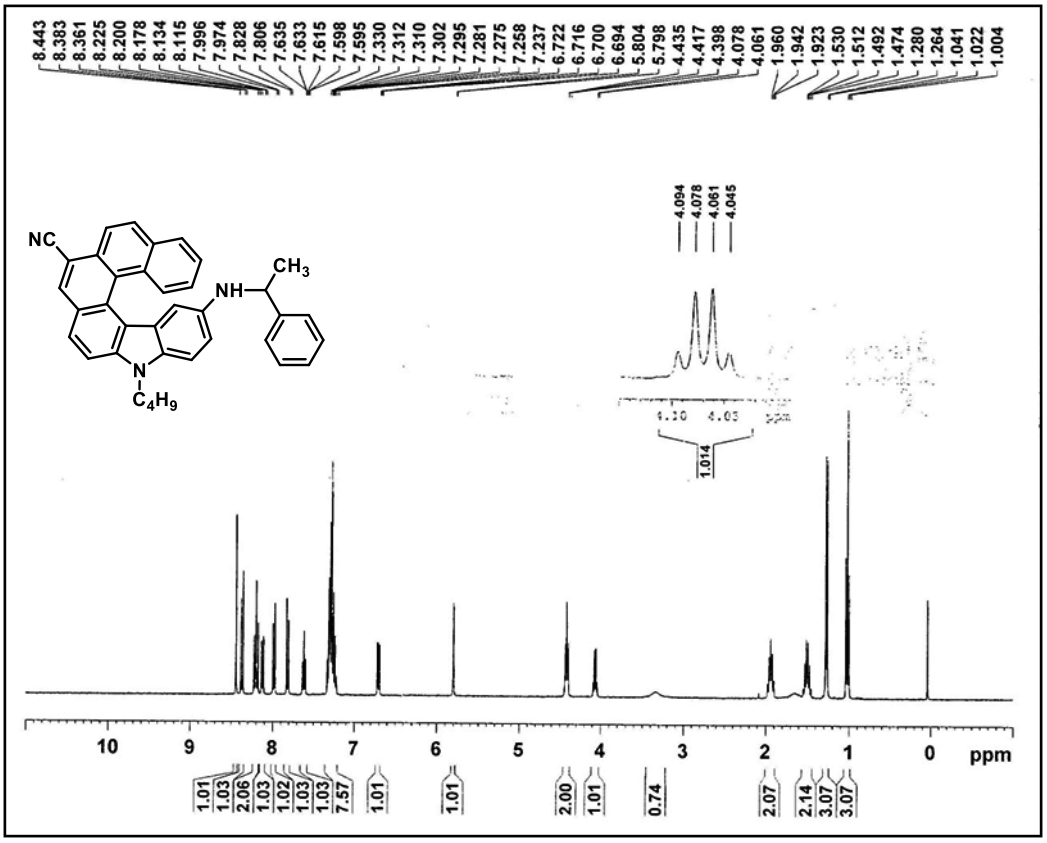

^{1}H-NMR of compound 138 minor diastereomer ($CDCl_3$ 400 MHz)

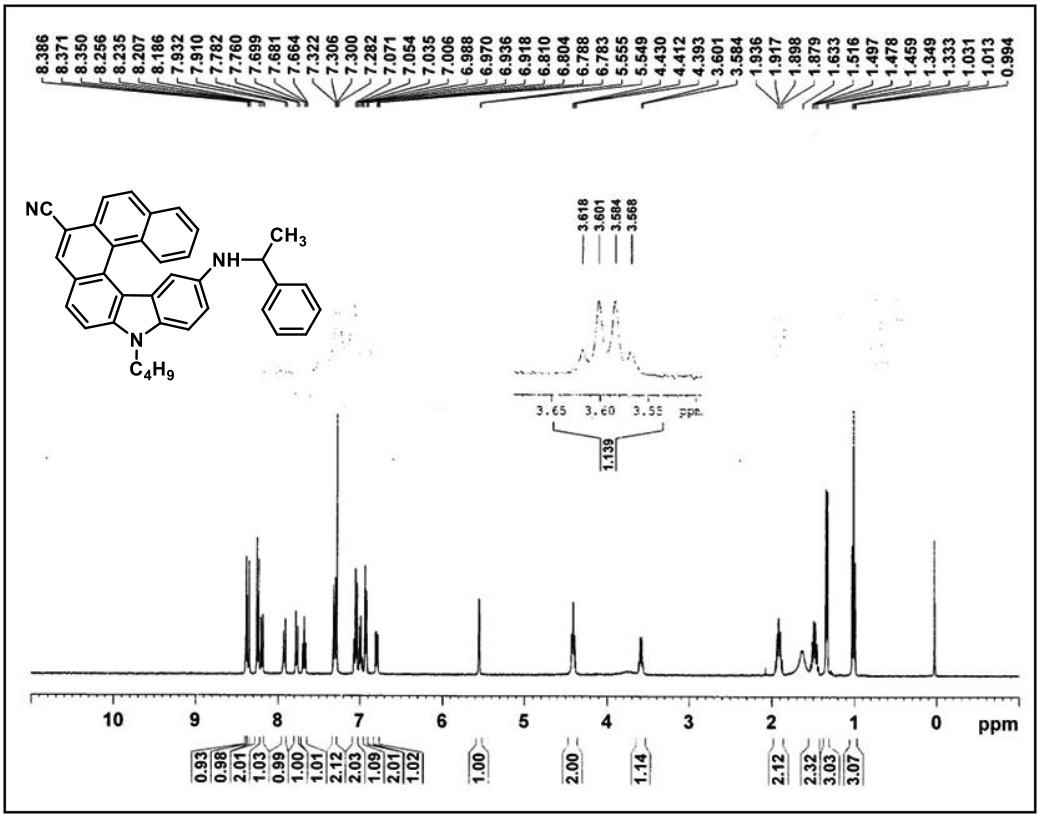

^{1}H-NMR of compound 138 major diastereomer ($CDCl_3$ 400 MHz)

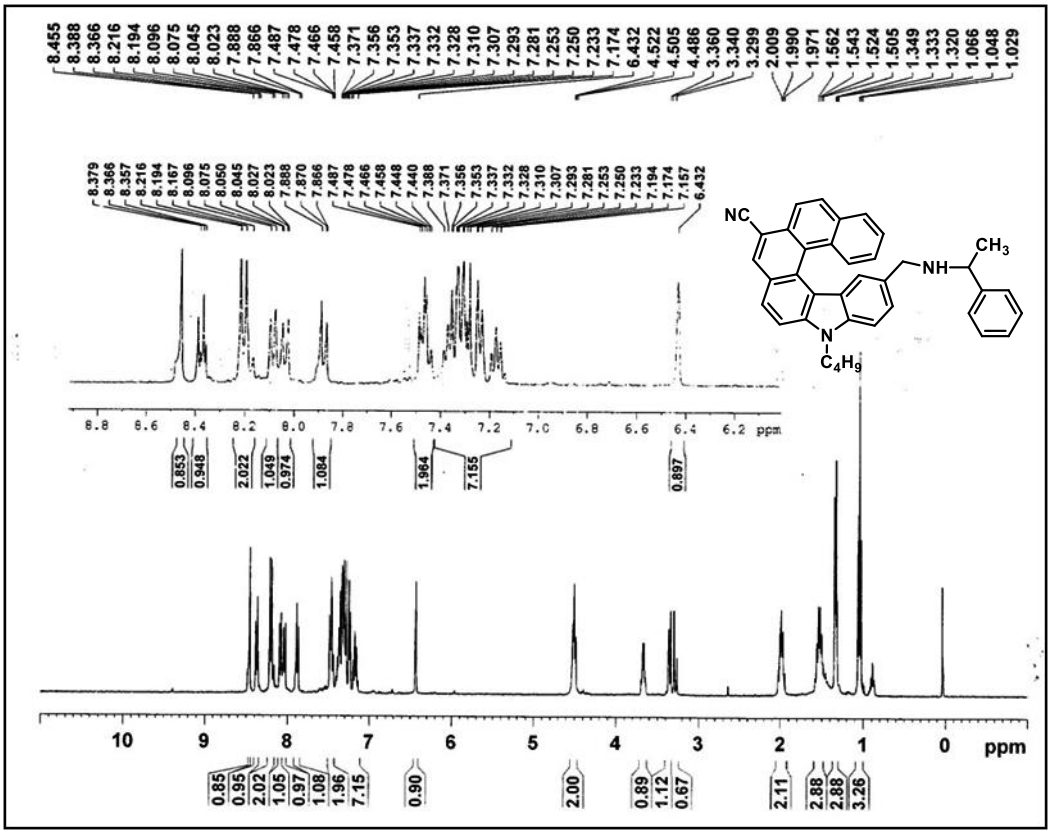

^{1}H-NMR of compound 139 ($CDCl_3$ 400 MHz)

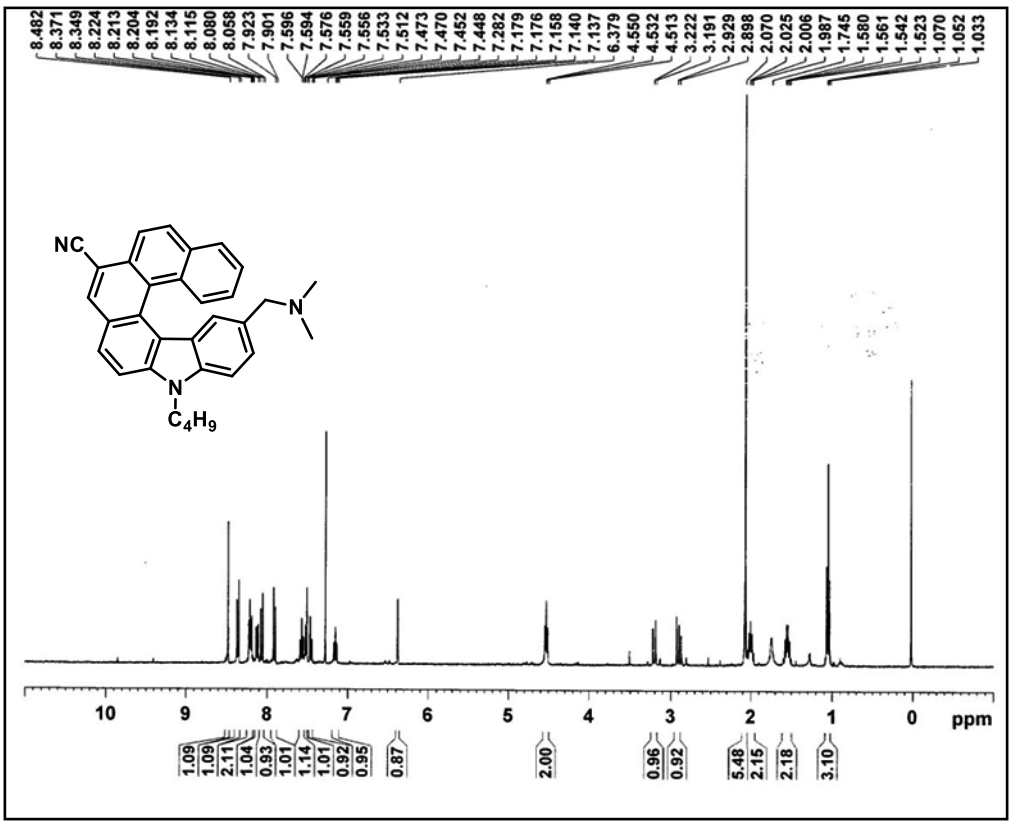

^{1}H-NMR of compound 140 ($CDCl_3$ 400 MHz)

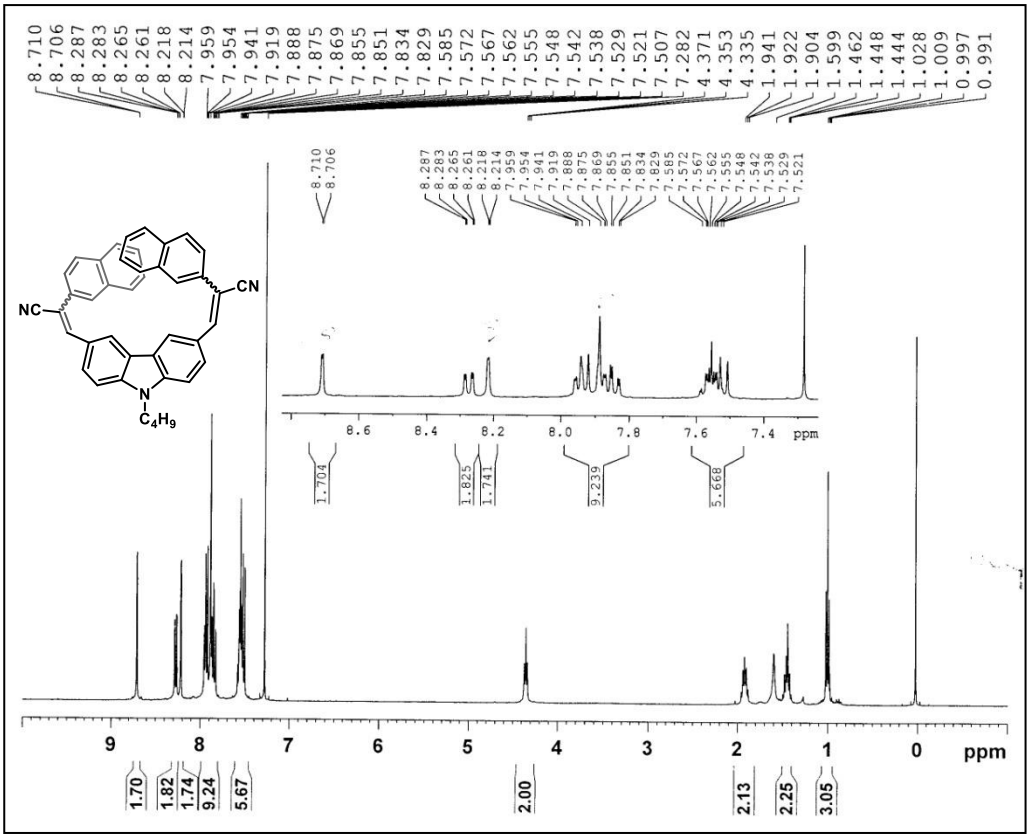

^{1}H-NMR of compound 141 ($CDCl_3$ 400 MHz)

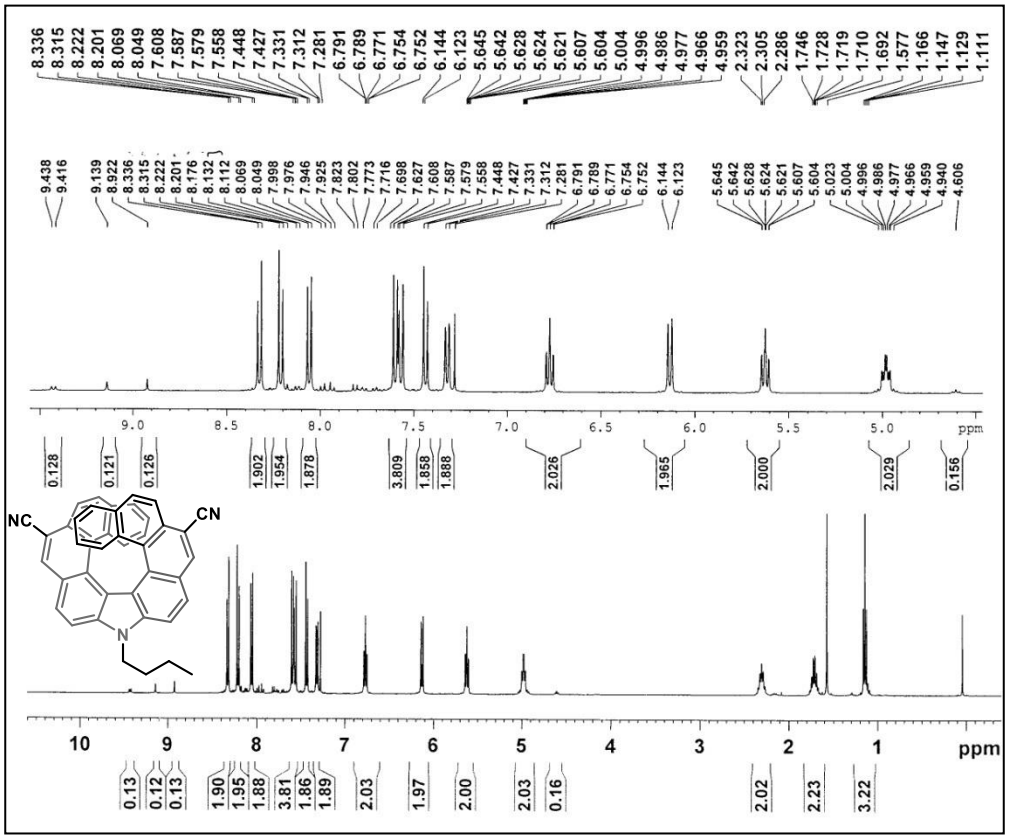

^{1}H-NMR of compound 142 ($CDCl_3$ 400 MHz)

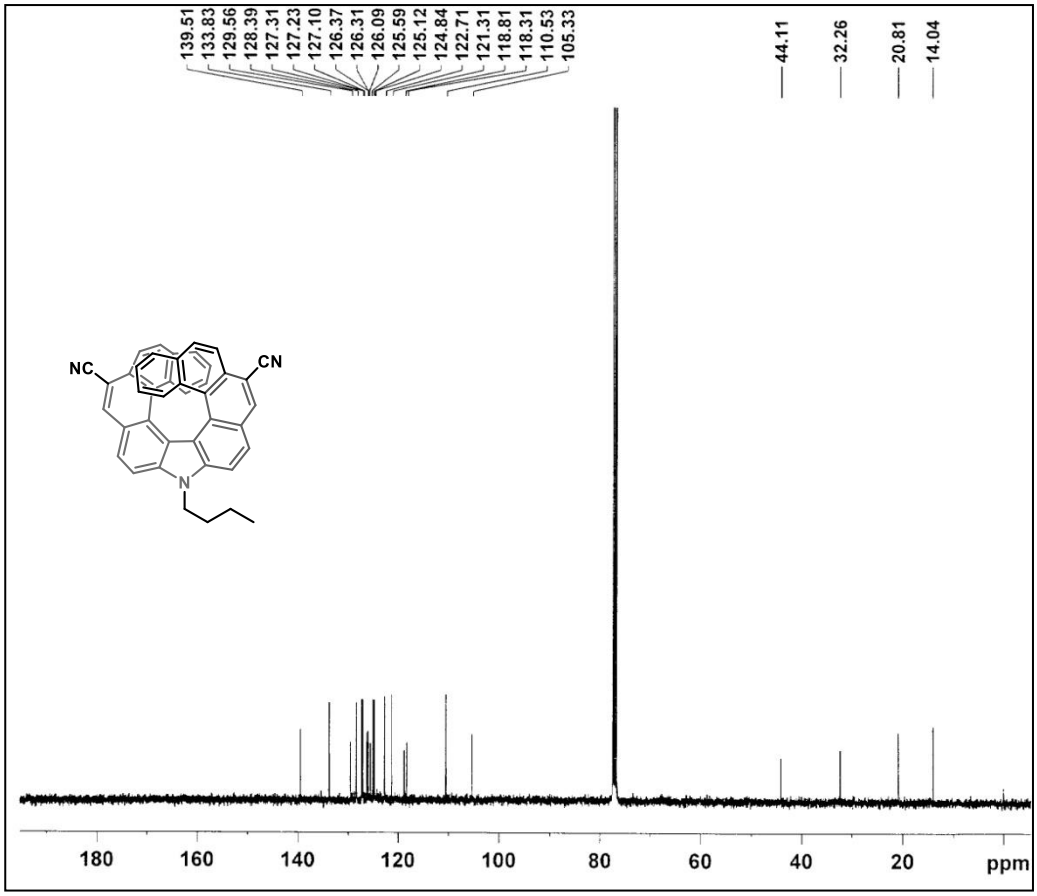

^{13}C-NMR of compound 142 ($CDCl_3$, 100 MHz)

HPLC Chromatogram:

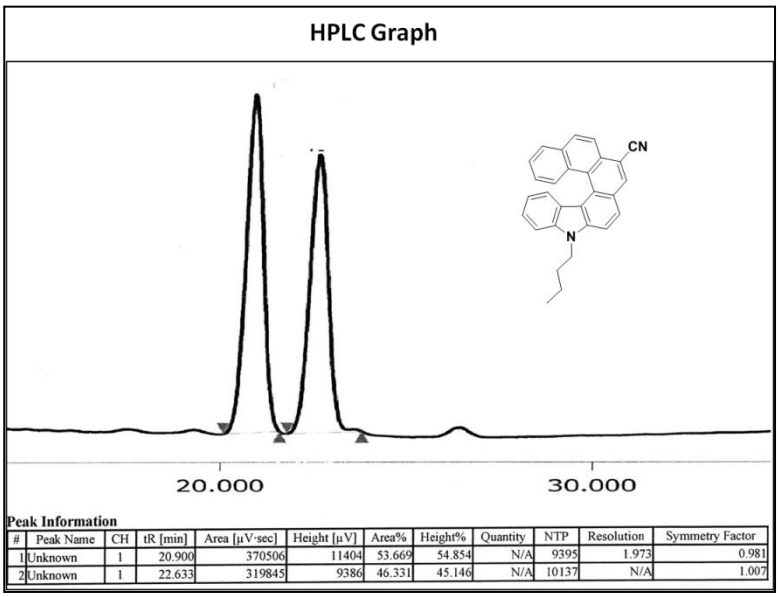

Peak Information

#	Peak Name	CH	tR [min]	Area [μV·sec]	Height [μV]	Area%	Height%	Quantity	NTP	Resolution	Symmetry Factor
1	Unknown	1	20.900	370506	11404	53.669	54.854	N/A	9395	1.973	0.981
2	Unknown	1	22.633	319845	9386	46.331	45.146	N/A	10137	N/A	1.007

HPLC chromatogram of compound 110.

HPLC condition: 20.9 and 22.6 (10 % IPA: hexane, Daicel make Chiralpak IC Column, UV = 254 nm, Flow = 1.0 mL/min)

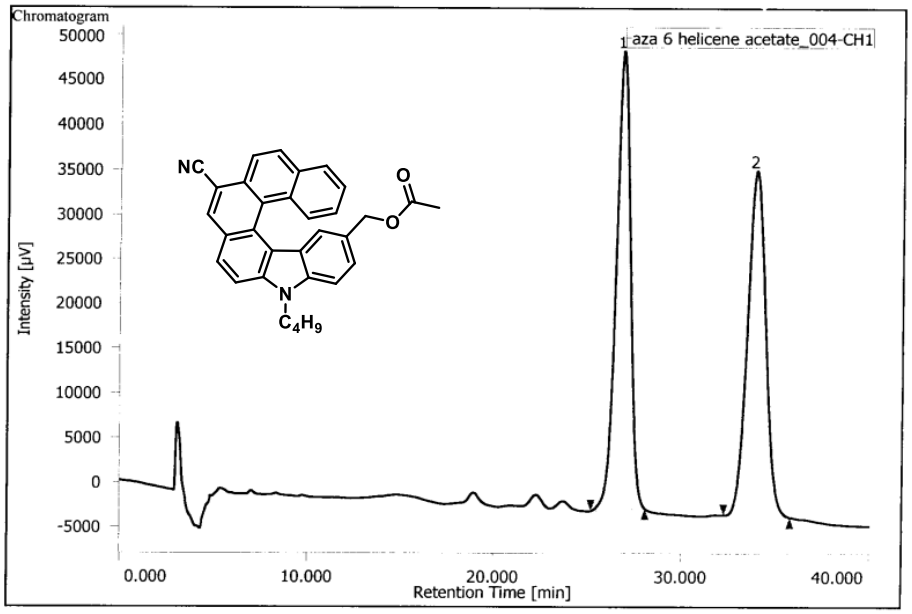

Peak Information

#	Peak Name	CH	tR [min]	Area [μV·sec]	Height [μV]	Area%	Height%	Quantity	NTP	Resolution	Symmetry Factor	Warning
1	Unknown	1	26.842	2672151	51228	50.852	56.946	N/A	6213	4.531	0.988	
2	Unknown	1	33.900	2582581	38730	49.148	43.054	N/A	5922	N/A	1.042	

HPLC chromatogram of compound 137 (racemic)

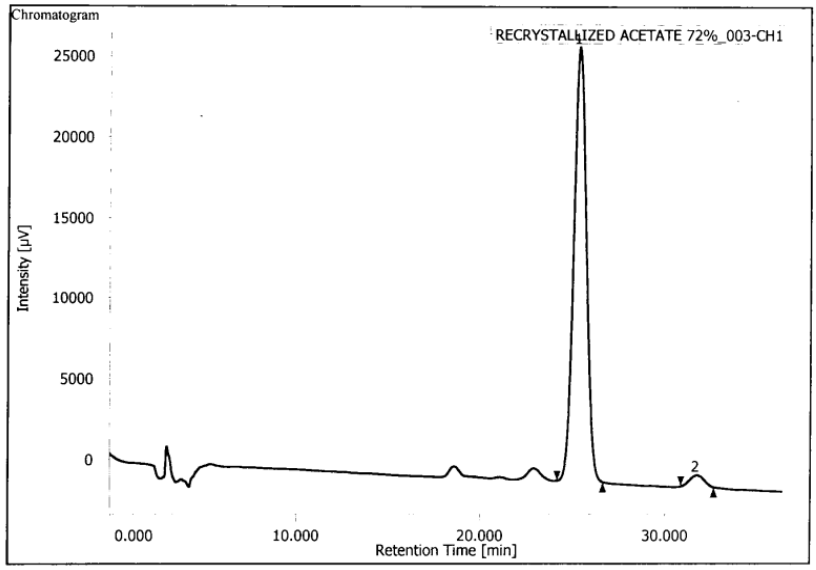

Peak Information

#	Peak Name	CH	tR [min]	Area [μV·sec]	Height [μV]	Area%	Height%	Quantity	NTP	Resolution	Symmetry Factor	Warning
1	Unknown	1	25.375	1272184	26986	96.978	97.299	N/A	6601	4.678	1.021	
2	Unknown	1	31.733	39647	749	3.022	2.701	N/A	7393	N/A	0.996	

HPLC chromatogram of compound 137 (94 % ee)

HPLC condition: (30 % IPA: hexane, Daicel make Chiralpak IC Column, UV = 254 nm, Flow rate = 1.0 mL/min)

2.14 References:

1. (a) Mallory, F. B.; Mallory, C. W. *Org. React*. **1984**, *30*, 1. (b) Jørgensen, K. B. *Molecules* **2010**, *15*, 4334.
2. Smakula, A. *Z. Physik. Chem.* **1934**, *B25*, 90.
3. Parker, C. O.; Spoerri, P. E. *Nature* **1950**, *166*, 603.
4. Mallory, F. B.; Wood, C. S.; Gordon, J. T.; Lindquist, L. C.; Savitz, M. L. *J. Am. Chem. Soc.* **1962**, *84*, 4361. (b) Mallory, F. B.; Wood, C. S.; Gordon, J. T. *J. Am. Chem. Soc.* **1964**, *86*, 3094. (c) Wood, C. S.; Mallory, F. B. *J. Org. Chem.* **1964**, *29*, 3373.
5. (a). Moore, W. M.; Morgan, D. D.; Stermitz, F. R. *J. Am. Chem. Soc.* **1963**, *85*, 829. (b). Doyle, T. D.; Filipescu, N.; Benson, W. R.; Banes, D. *J. Am. Chem. Soc.* **1970**, *92*, 6371. (c). Doyle, T. D.; Benson, W. R.; Filipescu, N. *J. Am. Chem. Soc.* **1976**, *98*, 3262. (d). Cuppen, J. H. M.; Laarhoven, W. H. *J. Am. Chem. Soc.***1972**, *94*, 5914.
6. Liu, L.; Yang, B.; Katz, T. J.; Poindexter, M. K. *J. Org. Chem.* **1991**, *56*, 3769.
7. Talele, H. R.; Gohil, M. J.; Bedekar, A. V. *Bull. Chem. Soc. Jpn.* **2009**, *82*, 1182.
8. Matsushima, T.; Kobayashi, S.; Watanabe, S. *J. Org. Chem.* **2016**, *81*, 7799.
9. Flammang-Barbieux, M.; Nasielski, J.; Martin, R. H. *Tetrahedron Lett.* **1967**, *8*, 743.
10. Mori, K.; Murase, T.; Fujita, M. *Angew. Chem. Int. Ed*. **2015**, *54*, 1.
11. (a) Laarhoven, W. H.; Cuppen, T. J. H. M.; Nivard, R. J. F. *Rec. Trav. Chim.* **1968**, *87*, 687. (b) Laarhoven, W. H.; Cuppen, J. H. M.; Nivard, R. J. F. *Tetrahedron* **1970**, *26*, 4865. (c) Laarhoven, W. H. *Rec. Trav. Chim. J. Roy. Neth. Chem.* **1983**, *102*, 185. (d) Laarhoven, W. H. *Org. Photochem.* **1989**, *10*, 163.
12. Sudhakar, A.; Katz, T. J. *Tetrahedron Lett.* **1986**, *27*, 2231.
13. (a) Sudhakar, A.; Katz, T. J.; Yang, B. *J. Am. Chem. Soc.* **1986**, *108*, 2790. (b) Liu, L.; Katz, T. J. *Tetrahedron Lett.* **1991**, *32*, 6831.
14. Dietz, F.; Scholz, M. *Tetrahedron* **1968**, *24*, 6845.
15. Martin, R. H.; Flammang-Barbieux, M.; Cosyn, J. P.; Gelbcke, M. *Tetrahedron Lett*. **1968**, *9*, 3507.
16. Weber, J.; Clennan, E. L. *J. Org. Chem.* **2019**, *84*, 817.

17. Mallory, F. B.; Mallory, C. W. *Organic Reactions; Wiley: New York* **1984**; *30*, 49.
18. Bazzini, C.; Brovelli, S.; Caronna, T.; Gambarotti, C.; Giannone,M.; Macchi, P.; Meinardi, F.; Mele, A.; Panzeri, W.; Recupero, F. *Eur. J. Org. Chem.* **2005**, *2005*, 1247.
19. Vacek, J.; Andronova, A.; Míšek, J.; Songis, O.; Šámal, M.; Stará, I. G.; Meyer, M.; Bourdillon, M.; Pospíšil, L. *Chem. Eur. J.* **2014**, *20*, 877.
20. Waghray, D.; Zhang, J.; Jacobs, J.; Nulens, W.; Basarić, N.;Meervelt, L. V.; Dehaen, W. *J. Org. Chem.* **2012**, *77*, 10176.
21. Aloui, F.; El Abed, R.; Marinetti, A.; Ben Hassine, B. *Tetrahedron Lett.* **2008**, *49*, 4092.
22. Misek, J.; Teply, F.; Stara, I. G.; Tichy, M.; Saman, D.; Cisarova, I.; Vojtisek, P.; Stary, I. *Angew. Chem. Int. Ed.* **2008**, *47*, 3188.
23. (a) Roithova, J.; Schroeder, D.; Misek, J.; Stara, I. G.; Stary, I. *J. Mass Spectrom.* **2007**, *42*, 1233. (b) Raczynska, E. D.; Gal, J. F.; Maria, P. C. *Int. J. Mass Spectrom.* **2017**, *418*, 130.
24. (a) Jančařík, A.; Rybáček, J.; Cocq, K.; Vacek Chocholoušová, J.; Vacek, J.; Pohl, R.; Bednárová, L.; Fiedler, P.; Císařová, I.; Stará, I. G.; Starý, I. *Angew. Chem. Int. Ed.* **2013**, *52*, 9970. (b) Teplý, F.; Stará, I. G.; Starý, I.; Kollárovič, A.; Šaman, D.; Vyskočil, Š.; Fiedler, P. *J. Org. Chem.* **2003**, *68*, 5193. (c) Teplý, F.; Stará, I. G.; Starý, I.; Kollárovič, A.; Šaman, D.; Rulíšek, L.; Fiedler, P. *J. Am. Chem. Soc*. **2002**, *124*, 9175.
25. Míšek, J.; Teplý, F.; Stará, I. G.; Tichý, M.; Šaman, D.; Císařová, I.; Vojtíšek, P.; Starý, I. *Angew. Chem. Int. Ed.* **2008**, *47*, 3188.
26. (a) Takenaka, N.; Sarangthem, R. S.; Captain, B. *Angew. Chem. Int. Ed*. **2008**, *47*, 9708. (b) Chen, J.; Takenaka, N. *Chem. Eur. J*. **2009**, *15*, 7268.
27. Weimar, M.; Correa da Costa, R.; Lee, F.-H.; Fuchter, M. J. *Org. Lett*. **2013**, *15*, 1706.
28. Yang, Y.; da Costa, R. C.; Smilgies, D.-M.; Campbell, A. J.; Fuchter, M. *J. Adv. Mater.* **2013**, *25*, 2624.
29. Misek, J.; Tichy, M.; Stara, I. G.; Stary, I.; Schroder, D. *Chem. Commun.* **2009**, *74*, 323.
30. Mendola, D.; Saleh, N.; Vanthuyne, N.; Roussel, C.; Toupet, L.; Castiglione, F.; Caronna, T.; Mele, A.; Crassous, J. *Angew. Chem. Int. Ed.* **2014**, *53*, 5786.

31. Matsumoto, A.; Yonemitsu, K.; Ozaki, H.; Míšek, J.; Starý, I.; Stará, I. G.; Soai, K. *Org. Biomol. Chem.* **2017**, *15*, 1321.
32. Nakano, K.; Hidehira, Y.; Takahashi, K.; Hiyama, T.; Nozaki, K. *Angew. Chem. Int. Ed.* **2005**, *44*, 7136.
33. Kaneko, E.; Matsumoto, Y.; Kamikawa, K. *Chem. Eur. J.* **2013**, *19*, 11837.
34. Kötzner, L.; Webber, M. J.; Martínez, A.; De Fusco, C.; List, B. *Angew. Chem Int. Ed.* **2014**, *53*, 4980.
35. (a) Gingras, M. *Chem. Soc. Rev.* **2013**, *42*, 1051. (b) Gingras, M. *Chem. Soc. Rev*. **2013**, *42*, 968. (c) Gingras, M.; Félix, G.; Peresutti, R. *Chem. Soc. Rev*. **2013**, *42*, 1007.
36. Tanaka, K. Transition-Metal-Mediated Aromatic Ring Construction; John Wiley & Sons: Hoboken, NJ, 2013.
37. (a) Alkorta, I.; Blanco, F.; Elguero, J.; Schroder, D. *Tetrahedron Asymmetry* **2010**, *21*, 962. (b) Bell, J. W.; Hext, N. M. *Chem. Soc. Rev.* **2004**, *33*, 589.
38. (a) Chuang, C. N.; Chuang, H. J.; Wang, Y. X.; Chen, S. H.; Huang, J. J.; Leung, M. K.; Hsieh, K. H. *Polymer* **2012**, *53*, 4983.
39. Zhao, T.; Liu, Z.; Song, Y.; Xu, W.; Zhang, D.; Zhu, D. *J. Org. Chem*. **2006**, *71*, 7422.
40. Saiyed, A. S.; Bedekar, A. V. *Tetrahedron Lett.* **2010**, *51*, 6227.
41. Roose, J.; Achermann, S.; Dumele, O.; Diederich, F. *Eur. J. Org. Chem.* **2013**, 3223.
42. Dreher, S. D.; Weix, D. J.; Katz, T. J. *J. Org. Chem.* **1999**, *64*, 3671.
43. (a) Dietz, F.; Scholz, M. *Tetrahedron* **1968**, *24*, 6845. (b) Xue, X.; Scott, L. T. *Org. Lett.* **2007**, *9*, 3937 and references cited there in.
44. Bas, G. L.; Navaza, A.; Knossow, D. R. C. M. *Cryst. Struct. Commun.* **1976**, *5*, 713.
45. Marsh, W.; Dunitz, J. D. *Bull. Soc. Chim. Belg.* **1979**, *88*, 847.
46. (a) Martin, R. H.; Eyndels, C.; Defay, N. *Tetrahedron* **1974**, *30*, 3339. (b) Laarhoven, W. H.; Cuppen, T. J. H. M.; Nivard, R. J. F .*Tetrahedron* **1974**, *30*, 3343.

47. Wismonski-Knittel, T.; Fischer, G.; Fischer, E. J. *J. Chem. Soc., Perkin Trans. 2* **1974**, 1930.

48. Pozo, I.; Cobas, A.; Peña, D.; Guitián, E.; Pérez, D. *Chem. Commun.* **2016**, *52*, 5534.

49. Hua, W.; Liu, Z.; Duan, L.; Dong, G.; Qiu, Y.; Zhang, B.; Cui, D.; Tao, X.; Cheng, N.; Liu, Y. *RSC Adv.* **2015**, *5*, 75.

50. (a) Li, Y.; Ding, J.; Day, M.; Tao, Y.; Lu, J.; D'iorio, M. *Chem. Mater.* **2004**, *16*, 2165. (b) Vander Donckt, E. V.; Nasielski, J.; Greenleaf, J. R.; Birks, J. B. *Chem. Phys. Lett*. **1968**, *2*, 409. (c) Yamamoto, Y.; Sakai, H.; Yuasa, J.; Araki, Y.; Wada, T.; Sakanoue, T.; Takenobu, T.; Kawai, T.; Hasobe, T. *Chem. Eur. J.* **2016**, *22*, 4263. (d) Oyler, K. D.; Coughlin, F. J.; Bernhard, S. *J. Am. Chem. Soc.* **2007**, *129*, 210.

51. Laarhoven, W. H.; Prinsen, W. J. C. *Carbohelicenes and Heterohelicenes. Top Curr. Chem. 125:* **1984**, 63.

52. Chen, J. D.; Lu, H. Y.; Chen, C. F. *Chem. Eur. J.* **2010**, *16*, 11843.

53. (a) Dai, Y. J.; Katz, T. J. *J. Org. Chem.* **1997,** *62*, 1274. (b) Shi, S. H.; Katz, T. J.; Yang, B. W. V.; Liu, L. B. *J. Org. Chem.* **1995,** *60*, 1285.

54. (a) Maiorana, S.; Papagni, A.; Licandro, E.; Annunziata, R.; Paravidino, P.; Perdicchia, D.; Giannini, C.; Bencini, M.; Clays, K.; Persoons, A. *Tetrahedron* **2003**, *59*, 6481. (b) Doulcet, J.; Stephenson, G. R. *Chem. Eur. J.* **2015**, *21*, 13431.

55. Žádný, J.; Velíšek, P.; Jakubec, M.; Sýkora, J.; Církva, V.; Storch, J. *Tetrahedron* **2013**, *69*, 6213.

56. Goretta, S.; Tasciotti, C.; Mathieu, S.; Smet, M.; Maes, W.; Chabre, Y. M.; Dehaen, W.; Giasson, R.; Raimundo, J. M.; Henry, C. R.; Barth, C.; Gingras, M. *Org. Lett.* **2009**, *11*, 3846.

57. Jakubec, M.;Tomas, B.; Jakubík, P.; Sýkora, J.; Jaroslav Žádný, J.; Církva, V.; Storch, J. *J. Org. Chem.* **2018**, *83*, 3607.

58. Hellou, N.; Mace, A.; Martin, C.; Dorcet, V.; Roisnel, T.; Jean, M.; Vanthuyne, N.; Berree, F.; Carboni, B.; Crassous, J. *J. Org. Chem.* **2018**, *83*, 484.

59. Jakubec, M.; Ghosh, I.; Storch, J.; Konig, B. *Chem. Eur. J.* **2019**. *26*, 543.

60. Takenaka, N.; Chen, J.; Captain, B.; Sarangthem, R. S.; Chandrakumar, A. *J. Am. Chem. Soc*. **2010**, *132*, 4536.

61. Ushiyama, A.; Hiroto, S.; Yuasa, J.; Kawai, T.; Shinokubo, H. *Org. Chem. Front.* **2017**, *4*, 664.

62. Ito, N.; Hirose, T.; Matsuda, M. *Org. Lett.* **2014**, *16*, 2502.

63. (a) Chuang, C. N.; Wang, Y. X.; Chen, S.H.; Huang, J. J.; Leung, M.K.; Hsieh, K.H. *Polymer* **2012**, *53*, 4983. (b) Sket, B.; Zupan, M. *J. Org. Chem.* **1986**, *51*, 929. (b) Zhao, T.; Liu, Z.; Song, Y.; Xu, W.; Zhang, D.; Zhu, D. *J. Org. Chem.* **2006**, *71*, 7422. (c) Xu, T. H.; Lu, R.; Tan, C. H.; Qiu, X. P.; Bao, C. V.; Liu, X. L.; Xue, P. C.; Zhao, Y. Y. *Eur. J. Org. Chem.* **2006**, *17*, 4014. (d) Waykole, L.; Rashad, M.; Palermo, S.; Repic, O.; Blacklock, T. *J. SYNTHETIC COMMUNICATIONS* **1997**, *27*, 2159. (e) Velcicky, J.; Soicke, A.; Steiner, R.; Schmalz, H. G. *J. Am. Chem. Soc.* **2011**, *133*, 6948. (f) Abbate, S.; Bazzini, C.; Caronna, T.; Fontana, F.; Gambarotti, C.; Gangemi, F.; Longhi, G.; Mele, A.; Sorab, I. N.; Panzeri, W. *Tetrahedron* **2006**, *62*, 139. (g) Hutten, P. F. V.; Krasnikov, V. V.; Brouwer, H. *J.*; Hadziioannou, G. *Chemical Physics* **1999***, 241*, 139. (h) Mossetig, E.; Kamp, J. V. *J. Am. Chem. Soc.* **1933**, *55*, 2995.